ULTRASTRUCTURAL STUDIES ON TAPETUM AND POLLEN DEVELOPMENT

By

Suresh Chandra Tiwari

A Thesis Submitted for the Degree of
Doctor of Philosophy
At the Australian National University
Canberra, Australia

November, 1985

STATEMENT

All work reported in this thesis
is original and my own,
and has not been submitted
for any other degree.

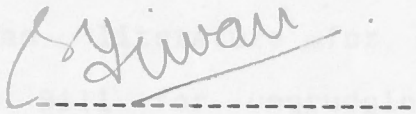

ACKNOWLEDGEMENTS

I express my deepest appreciation and sincere thanks to Professor Brian Gunning for constant encouragement and supervision throughout the course of this work. I have learnt a lot from several people in the Department of Developmental Biology, especially from Adrienne Hardham, Richard Williamson, Eric Hines, Cathy Busby and Jean Perkin and I wish to tell them that it has been a priviledge to work in their midst. I have benefited from numerous discussions with Sue Wick, John Cork, Jan Marc and Sally Blest and I am grateful to them for sharing their experience and wisdom with me. I have also recieved help from Stuart Craig, Frank Sek, Jadwiga Duniec, Janet Gorst, Brenda Ballantyne and Ursula Hurley on numerous occasions and I am indebted to them. Thanks are also due to Marion Gunning and Wolfgang Wernicke for translating french and german literature for me. Special thanks are owed to Bill for ungrudgingly spending umpteen hours in the dark room, printing out thousands of negatives for this work.

I have cherished the friendship offerred by Lok and Uma, Brian Surin, and especially Rina. Life would have been dull without them.

I acknowledge the reciept of a Ph.D. Scholarship from the Australian National University.

ABSTRACT

Ultrastructural, cytochemical and experimental studies on the development of plasmodial tapetum and pollen development were undertaken. The species chosen were Canna indica L. x C. sp. hybrid and Tradescantia virginiana L.

The tapetum in Canna (Chapter 3) was found to be a hitherto undescribed non-syncytial invasive type. During early meiosis the tapetal cell walls broke down, and the protoplasts moved into the loculus but did not form a syncytium. By contrast, the tapetum in Tradescantia (Chapter 4) was of the plasmodial type. After the dissolution of their cell walls, the tapetal cells formed invasion processes that projected into the loculus and eventually fused to form a syncytium. Ultrastructural and cytochemical studies of these two tapetum types revealed that coincident with or after the wall dissolution, the tapetal cells developed a cell coat, approximately 17nm thick. The cell coat was retained through the course of development in Canna, whereas in Tradescantia it disappeared prior to cell fusion. Cell fusion was accomplished by the late tetrad stage of pollen development, and thereby established a true plasmodium. By this time, the plasmodium had also developed a specialized secretory surface in the vicinity of enclosed spore cells.

Evidence is presented that both Canna (Chapter 3) and Tradescantia (Chapters 4,5) tapeta are capable of producing sporopollenin. Employing colchicine treatments, the roles of microtubules in the formation and function of plasmodium were also assessed. It is concluded that the plasmodium does provide exine wall precursors to the developing pollen grains.

Stages of pollen development in Tradescantia (Chapter 6) were monitored by conventional electron microscopy, freeze-substitution and freeze-fracture replication. A variety of cytochemical techniques and colchicine treatments was also employed to augment the data obtained by the above procedures. The data showed that the fibrous primexine which is formed before exine is an artifactual image. Furthermore, microfilaments rather than microtubules may be involved in exine-pattern formation.

Generative cell development in Tradescantia is described in Chapter 7. Here again stages of development have been followed through the application of a range of ultrastructural and cytochemical techniques. Evidence is presented that the position of the generative cell is not predetermined, that the generative cell wall, traversed by channels, persists throughout the course of development, and that microtubules are responsible for its elongation and shape maintenance.

TABLE OF CONTENTS

CHAPTER 1

INTRODUCTION

In some flowering plants the cells of the inner layer of anther wall, the tapetum, fuse to form a syncytium which establishes very close contact with the developing meiocytes and the spore cells. The development of this type of tapetum, the plasmodial type, and the adjacent pollen grains forms the subject of this Thesis.

The Thesis is broadly organized into two major parts, the first three chapters dealing with the tapetum and the last two with pollen development. This division, sometimes transgressed particularly when tapetum-pollen interactions are described (Chapters 2,3), has been retained for the convenience of description, and is inevitably reflected in the Introduction as well. In the Introduction an attempt has been made to furnish relevant background information on these two topics in very general terms, and not as a comprehensive review, for which excellent articles by Heslop-Harrison (1971a,b, 1972, 1975), Buchen and Sievers (1981), Bhandari (1984) and Knox (1984a,b) could be consulted.

1.1. Tapetum

During the formation of pollen grains within the angiospermic anther, cells of the innermost anther wall layer that surrounds the developing spore cells differentiate into the tapetum. Generally consisting of a single cell layer, in some species it may become bi- or even multi-seriate (see examples in Davis, 1966; Bhandari,

1984). Goebel (1905) recognized two types of tapetum. These are: 1. Secretory (also called glandular or parietal) type in which during early ontogeny the tapetal cell walls undergo dissolution, but the cells stay intact in situ until their degeneration. 2. Plasmodial (synonymous with amoeboid, periplasmodial, syncytial, or invasive) type where the cell walls break down and cell fusion occurs, resulting in the formation of a plasmodium which then invades the intermeiocytic spaces of the anther cavity. The timing and sequence of wall dissolution may vary considerably in different species representing both plasmodial (Clausen, 1927) and secretory (see Bhandari, 1984) types, yet distinguishing differences exist between these two types of tapeta. As described in Chapter 3, in Canna, the tapetum does not fall into any of these classes, for, although the tapetal cell walls break down during early meiosis, and the cells migrate into the anther loculus to lie amongst developing meiocytes and spores, they do not fuse with each other, as in the plasmodial type, but remain as discrete cells. This hitherto unrecognized type is intermediate between the secretory and plasmodial tapeta and is referred to as non-syncytial invasive tapetum.

In her classic reference book, Systematic Embryology of the Angiosperms, Davis (1966) recorded that of the 231 families investigated till then, 181 showed secretory, 29 plasmodial, and 21 had cases of both secretory and plasmodial type. Bhandari (1984) updated

this survey and found that subsequent to Davis' book, 17 more families have been investigated and that all of them showed secretory tapetum, making the final tally of secretory tapetum in 198 families. It therefore seems that in at least 227 families the form of the tapetum is a family character. These two surveys also reveal that by and large the secretory tapetum predominates in the dicots and the plasmodial type in the monocots.

Eames (1961) regarded the plasmodial tapetum as a primitive feature because of its occurrence in the sporangium of some lower vascular plants. On the other hand, Sporne (1973) sought a statistical correlation between the type of tapetum and four primitive features including woody habit, actinomorphic flower, polypetalous flower and binucleate pollen, and concluded that secretory tapetum is itself a primitive feature and that the plasmodial tapetum is advanced.

The tapetum has been investigated extensively (see Bhandari, 1984) because of its role in the development of pollen. The following is a brief account of various functions ascribed to the tapetum.

1.1.2. Role of Tapetum in Pollen Development

Tapetal development takes place in close harmony with that of the pollen grain. Recognition of this correlation by early embryologists formed the basis for ideas of pollen being dependent on the tapetum for its development. More recent observations have implicated the

tapetum in a variety of functions ranging from the provision of nutrients, to production of exinic proteins that are involved in recognition-rejection reactions at the time of pollen germination on stigmas.

1.1.2.1. Tapetum and the Nutrition of Meiocytes and Spores

The notion that the tapetum contributes nutrients to the developing spore cells is based on the strategic location of these cells between the anther vascular supply and the developing sporocytes. It is considered that all metabolites must pass through the tapetum before reaching the spore cells (Maheshwari, 1950). The various enzymes, hormones and nutrients present in the locular fluid are all, therefore, viewed as diffusible secretions of the tapetum (Vasil, 1967, 1973).

Ultrastructural and autoradiographic studies have confirmed the early observations that tapetal development is geared to pollen development (Echlin, 1971a,b; Heslop-Harrison, 1972). Generally, premeiotic, meiotic, and post-meiotic phases in the life of the tapetum are recognized, each stage being distinctly related to that in the pollen development. For example, the secretory features in tapetum become fully manifest generally in post-meiotic stage, in accord with the developmental needs of the pollen (Echlin and Godwin, 1968a; Marquardt et al., 1968; Heslop-Harrison and Dickinson, 1969). Williams and Heslop-Harrison (1979) made a comparative study of the incorporation of radioactive uridine in plasmodial tapetum

in Rhoeo and secretory tapetum of Lilium and discovered that in spite of pronounced differences in their behaviour, both types of tapetum phase their overall sequence of RNA and protein synthesis in relation to spore development.

Observations of early tapetal degeneration provide further insights into the role of tapetum. In species where the tapetum degenerates prior to pollen mitosis, or where the pollen is shed at 3-celled stage (the tapetum invariably degenerates long before gametogenesis in most species), it has been noted that following tapetal degeneration, the normal synchrony that exists between the spores of an anther loculus is lost, leading to the suggestion that the synchrony in an anther loculus is controlled by tapetal secretions (Linskens, 1958). Certain environmental conditions are known to cause male sterility (Heslop-Harrison, 1957, 1972) and the behaviour of tapetum in such cases further supports its nutritive function. Heslop-Harrison and Heslop-Harrison (1958) made observations of long-day- and auxin-induced sterility in Silene pendula and noted that failure to produce normal pollen results from early tapetum degeneration and subsequent failure of normal transfer of material to the microspore.

There are several cases of pollen abortion resulting from abnormal behaviour of tapetum, found in the cytoplasmic male sterile (CMS) lines of numerous species. In sterile lines of Beta (Artschwager, 1947) both

plasmodial and secretory tapetum can occur, though not in the same flower, and where secretory tapetum is present, its cells enlarge into the loculus, crushing the microspore tetrads, causing early abortion. However, the degeneration of pollen in the anthers with plasmodial tapetum is delayed, presumably because the plasmodium does not crush the microspores. Cases are also known where tapetum either degenerates too early, as in Triticum (Chauhan and Singh, 1966), or persists beyond its normal time, as in Daucus (Zenkteler, 1962), Linum (Dubey and Singh, 1965), and Sorghum (Brooks et al., 1966), resulting in pollen abortion. The persistent tapetum often becomes hypertrophied (eg., Sorghum, Raj, 1969; Capsicum, Horner and Rogers, 1974), apparently using up nutrients that were destined for the developing microspores (Rick, 1945; Chauhan and Singh, 1966) and consequently pollen abortion takes place. The observation that ^{14}C compounds accumulate to a greater extent in the tapetum of CMS lines than in fertile lines (Nakashima and Hosokawa, 1974), is further testimony to the idea of nutritional blockade and the implicit transmitting role for tapetum (for reviews on CMS, see Edwardson, 1970; Laser and Lersten, 1972; Harvey et al., 1972; Bhandari, 1984).

1.1.2.2. Role of Tapetum in Callose Dissolution

During early meiosis, the meiocytes develop callosic walls which persist until after meiosis.

Stieglits and Stern (1973) studied the dynamics of β-1,3-glucanase (the enzyme that brings about the dissolution of the callose) activity in the anthers of Lilium and reported a sharp increase in the enzyme activity coinciding with post-meiotic dissolution of callose. Interestingly, the enzyme activity was mostly localized in the somatic tissue of the anther, with only 7.3% activity in the microspores themselves. They concluded that the dissolution of the tetrad callosic walls is brought about by the enzymic activity mediated by the surrounding somatic tissue (in all probability the tapetum).

In cytoplasmic and genic male sterile lines of Petunia, Frankel et al (1969), and Izhar and Frankel (1971) related the pollen abortion to the faulty timing of β-1,3-glucanase activity. After establishing that in vitro activity of the enzyme was optimal at pH 5.0 and absent above pH 6.3, they measured the pH at different developmental stages and found that in normal fertile anthers the pH was about 7.0 until the tetrad stage when it dropped to 6.0, followed by callose dissolution. In CMS lines the pH always remained low resulting in a precocious dissolution of callose, whereas in genic MS lines the pH remained high and callose dissolution did not occur. In the light of the work by Stieglits and Stern (1973) it is reasonable to assume that in Petunia, and also in other cases where faulty callose metabolism is implicated in pollen abortion (eg., Warmke and Overman, 1972), the tapetum has a role to play.

1.1.2.3. Tapetum and Exine Proteins

The existence of diffusible proteins in the pollen wall has been known for a long time (Green, 1894). In recent years a variety of substances such as proteins and glycoproteins that may include enzymes, allergens, lectins, carbohydrates, amino acids, pigments, oils, hormones (brassinolides) and an antigen associated with the expression of the S gene, have been recognized in the pollen wall (see Knox, 1971; Knox and Heslop-Harrison, 1969; Knox et al., 1970; Rittscher and Wiermann, 1983; see also reviews by Knox, 1984a,b). Largely due to the pioneering efforts of Knox and Heslop-Harrison, two types of proteins and glycoproteins have been recognized. Those occurring in the cavities of the sculptured part of exine are synthesized in the tapetum and transferred during the final stages of maturation of the pollen; these are accordingly sporophytic in origin. The second type consists of proteins which are embedded between polysaccharide layers of intine, especially in the vicinity of germination apertures; these proteins are incorporated during intine growth and are the product of the spore and, therefore, gametophytic in origin.

The tapetum as the site of synthesis of exine proteins has been demonstrated cytochemically in Iberis and other Cruciferae (Heslop-Harrison et al., 1974; Vithanage and Knox, 1976) and by transmission electron microscopy in Malvaceae (Heslop-Harrison et al., 1973; Heslop-Harrison, 1975) and Cruciferae (Dickinson and

Lewis, 1973a,b). That the proteins responsible for rejection reactions are derived from the tapetum is further evidenced by the observation that typical rejection response (sporophytic incompatibility reaction) are elicited in stigmas in response to the application of isolated tapetal fragments (Heslop-Harrison et al., 1974; for more information, see reviews by Heslop-Harrison, 1975; Knox, 1984a,b).

1.1.2.4. Tapetum, Pollenkitt and Tryphine

The mature pollen grains of many species, mostly entomophilous, are coated with bright coloured, oily or lipoidal substances. These substances have been held responsible for imparting stickiness so that the mature pollen are held in clumps (Knoll, 1930), attracting insect vectors and cementing pollen to these vectors (Heslop-Harrison, 1968a), causing characteristic exine colours (Godwin, 1968) and odours in pollen of certain species (Van der Pijl, 1964) which also serve to attract insects, protecting pollen from harmful ultraviolet radiation (Linskens, 1964) and dehydration (Hesse, 1981), aiding in the adhesion of pollen grains to stigmatic surfaces and carrying factors that are involved in the determination of incompatibility reactions (Dickinson and Lewis, 1973a,b; see Knox, 1984a,b for recent reviews).

Two classes of lipidic materials have been recognized in the literature: tryphine, when the pollen coat lipids contain cytoplasmic fragments, and pollenkitt

when they do not contain cytoplasmic fragments. The term pollenkitt, first used by Troll (1928), has been loosely applied to include both these classes, especially by German workers (see Heslop-Harrison, 1968a; Hesse, 1981), but the distinction may be important in that the tryphine is to be regarded as a degradation product, whereas pollenkitt as a special synthesized product.

It has long been known that these coating materials consist of dissolved carotenoids, probably produced by the tapetum (Steffen, 1953; Pankov, 1957). Godwin (1968) collated early information on pollen colour and concluded that whereas the pigmentation within the pollen protoplast is under haploid control, that of the exine is sporophytically (from the tapetum) derived. Heslop-Harrison (1968a) provided evidence that in Lilium, the pollenkitt consists mainly of lipids and ∝- carotene-5- and 6-epoxides that originate in the tapetum. Ultrastructural investigations by Dickinson (1973) in Lilium showed that during the post-meiotic stages, the tapetal plastids produced large amounts of lipids which, following tapetal degeneration, became deposited on the pollen surface as pollenkitt. This mode of pollenkitt formation and deposition has subsequently been confirmed in several species (Hesse, 1978, 1980). Formation of tryphine, on the other hand, results from the fragmentation of tapetal cells and deposition of the fragments containing endoplasmic reticulum, lipids, pro-orbicular bodies, etc., on the pollen wall (Echlin,

1971a). While in most species the tryphine deposition is a disorderly process (Hesse, 1978, 1980), in Raphanus, according to Dickinson and Lewis (1973b), first a protein, synthesized in the tapetal endoplasmic reticulum and released in the loculus, is applied to the pollen surface followed by a thick layer of tapetally-derived lipoidal material.

Although it is widely accepted that the tapetum contributes to the pollen coat substances (see Bhandari, 1984 for a recent review), Mepham and Lane (1968, 1969a,b) and Mepham (1970) postulated that the lipidic deposits on the pollen surface of Tradescantia bracteata did not originate from the tapetal plasmodium but as an exudate from the pollen cytoplasm. The lipid deposits in Tradescantia are unusual in having parallel stacks of electron-lucent material embedded in the electron-dense lipidic material. The electron-lucent areas according to these authors are the pollen membranes which are extruded to the exterior and 'fossilized' in the lipidic fractions.

1.1.2.5. Tapetum and Pollen Wall Development

Since the beginning of the present century the tapetum has been suspected to be a source of sporopollenin precursors for the growth of the spore wall (see Heslop-Harrison, 1968b). Direct experimental support is lacking, but the idea is based on the following circumstantial evidence:

I. Concomitant with pollen wall development, secretory tapetal cells develop sporopollenin-containing bodies, the tapetal orbicules, on their inner periclinal surfaces (Ubisch, 1927). The presence of these bodies has been considered as the proof of the tapetum's capacity to produce sporopollenin. The orbicules themselves have been regarded by some workers as a transport form of sporopollenin, en route to the pollen wall (Maheshwari, 1950; Madjd and Roland-Heydacker, 1978), or as a by-product of that transport process (Christensen et al., 1972).

II. In a large number of species, the spore cell enlarges considerably while the exine development continues (Echlin, 1971b). It has been considered unlikely that the spore cells themselves carry enough reserve substances to account for this growth, thus implicating the tapetum as the only other feasible source.

III. In sterile pollen grains, exine development can continue even after the degeneration of spore cytoplasm (Beer, 1905; see also later) indicating that the precursors for wall growth must come from the tapetum.

Despite the above observations, controversy, stemming from a more basic question of whether the pollen wall is under sporophytic or gametophytic control (see later), still exists as to whether the tapetum provides wall precursors at all. Arguments that have been marshalled against tapetal participation are:

I. Whereas in most species pollen wall development continues after pollen release from the callosic walls of the tetrad, in some species the entire wall is claimed to develop within the callosic walls, thus denying any possibility of tapetal contribution (*Tradescantia bracteata*, Mepham and Lane, 1968, 1969a,b, 1970; Mepham, 1970; *Mahonia*, Roland-Heydacker, 1979).

II. The function of orbicules as a transport form of sporopollenin has not been conclusively demonstrated although some claims have been made (Gorczynski, 1934; Madjd and Roland-Heydacker, 1978). Besides, as Mepham (1970) has pointed out, it is hard to imagine how the polymerized sporopollenin in the form of orbicules could be transported across the apoplastic gap between tapetum and spore surface and how it could become deposited on the spore surfaces to form species-specific exine patterns.

III. In species with plasmodial tapetum the orbicular bodies have not yet been demonstrated and since some authors consider them to be the transport form of sporopollenin, their absence in plasmodial tapetum has given rise to doubts about the plasmodium's capacity to produce sporopollenin. By extrapolation, the role of the plasmodium, and the tapetum in general, remains in some doubt.

IV. There are no other cases of plant cells whose walls are made by other cells. Is there then any *a priori* reason for spores to be different?

The question of tapetal contribution to the development of pollen wall remains unresolved, though most workers agree that it does contribute. The remaining doubts would be dispelled if it could be shown that plasmodial tapetum has the capacity to produce sporopollenin, and further, if species with plasmodial tapeta show pollen wall growth after the spores are released from their callosic walls. In addition, the plasmodial tapetum is, at least theoretically, better suited for studies of tapetal-spore interactions than the secretory tapetum, because of the closer proximity that develops between it and the spores.

1.1.3. Uniqueness of Plasmodial Tapetum

In higher plants there are only three situations where a syncytium is formed during the course of normal development. These are the developing embryo sac, the Nuclear and Helobial types of endosperms, and the plasmodial tapetum. Unlike the former two which are *ab initio* syncytial, i.e, the syncytium is formed as a result of free nuclear divisions unaccompanied by wall formation, the tapetal syncytium is formed from existing walled cells, i.e., the tapetal walls undergo dissolution and the resultant protoplasts fuse to form the syncytium. The plasmodial tapetum, therefore, provides unparalleled opportunities for studies of cell-cell interaction, and of the behaviour of cytoskeletal elements which must adapt to the change from individual cells to a syncytium.

1.1.4. Brief History of Plasmodial Tapetum

Amongst early cytologists, Tischler (1915) and Clausen (1927) provided considerable information on the organization of plasmodial tapeta. Based on a detailed analysis of several members of the monocots and the Ranales, Clausen recognized four major subtypes of plasmodial tapetum. The subtypes, based on the timing of plasmodium formation and the number of nuclei, are:

A. Sagittaria type: The plasmodium is formed after the liberation of microspores from the callosic walls.

B. Butomus type: The plasmodium is formed at the tetrad stage of microsporogenesis.

C. Sparganium type: Plasmodium formation begins at the tetrad stage, but the tapetal cells are by then multinucleate.

D. Triglochin type: The plasmodium is formed during meiosis.

In some Compositae with plasmodial tapetum, Heslop-Harrison (1969) found an acetolysis-resistant membrane on the outer surface of the tapetum. A similar membrane was earlier demonstrated at the inner tapetal surface in some grasses with secretory tapeta (Banerjee, 1967). Both these observations were later confirmed in additional species by Gupta and Nanda (1972). As yet the significance of this membrane is not clear.

More recently, Nanda and Gupta (1977) have investigated the light microscopic development of plasmodial tapetum in Rhoeo spathacea. Their observations

accord with the Triglochin type of Clausen. Williams and Heslop-Harrison (1979) conducted an autoradiographic study that sought to find similarity between the plasmodial and secretory tapeta of Rhoeo spathacea and Lilium longiflorum, respectively. Their findings are that both the tapeta show similar temporal patterns of incorporation of ^{3}H-uridine, leading them to suggest that the synthetic activity in the tapetum is related to the pollen development rather than to other events such as wall dissolution. In another light microscopic study Ducker et al. (1978) demonstrated that the plasmodial tapetum of Amphibolis antarctica possesses esterase activity.

Ultrastructural investigations of plasmodial tapeta are scanty both in terms of number of species studied as well as the structural and developmental details revealed. The investigated species include Tradescantia bracteata (Mepham and Lane, 1969b), Gentiana (Lombardo and Carraro, 1976), Helianthus (Horner, 1977; Horner and Pearson, 1978), Mahonia (Roland-Heydacker, 1979), Osmanthus, Rhoeo (Cerceau-Larrival et al., 1980-1981), Arum (Pacini and Juniper, 1983), Gibasis (Owens and Dickinson, 1983), and Amphibolis (Pettitt et al., 1984). Except for Tradescantia, Arum and Amphibolis, studies are cursory. The investigations of Mepham and Lane (1969b) on Tradescantia bracteata are by far the most detailed with regard to the development of the plasmodium. Although their account is generally in agreement with investigations on secretory tapeta, some aspects, such as

the role of the tapetum in pollen wall and pollenkitt development, are in disagreement. They did not investigate the cytoskeleton. In Arum, on the other hand, Pacini and Juniper (1983) furnished considerable information on the location and orientation of microtubules during the development of the tapetal plasmodium. During meiotic prophase, microtubules occur parallel to the radial walls of the tapetal cells. By the first meiotic division the tapetal cells form small protrusions into the loculus; microtubules occur in these protrusions, and are considered responsible for pushing or guiding tapetal invasion of the anther loculus. By the tetrad stage the plasmodium has surrounded the tetrads completely, with microtubules occurring at the tapetum-tetrad interface. After liberation of microspores from their callosic walls the plasmodium surrounds the microspores individually. The microtubules again occur at the tapetal-microspore interface. These microtubules are held responsible for keeping the microspores fixed in their position and later to facilitate localized retraction of tapetal plasma membrane from the spore surface so as to allow wall development. In Amphibolis, a sea grass with intine-like composition throughout the entire pollen wall, Pettitt et al. (1984) recorded the occurrence of particulate components and lamellae bearing electron-opaque globuli, possibly sporopollenin, which presumably originate in the plasmodium and subsequently become incorporated in the pollen wall.

However, information on several important aspects of the plasmodial tapetum, such as its precise mode of formation, cell-cell interactions and associated surface events, details of cell fusion, roles of the cytoskeleton, and features that may resolve the persistent question of the role of the plasmodium in secretion of sporopollenin, remains poorly dealt with.

1.2. Pollen

Pollen grains are the carriers of the male genome. Upon germination on stigmas they produce pollen tubes which facilitate transmission of male gametes to their female counterparts. Fertilization takes place resulting eventually in the formation of an embryo and seed. Considering the fact that most higher plants depend on sexual reproduction for their propagation and that the propagation of plants is so innately linked with human survival, it is not surprising that pollen grains and their female counterparts have been subjected to such extensive study (for reviews on pollen development, see Heslop-Harrison, 1971a,b, 1972, 1980; Knox, 1984a,b).

Chapters 6 and 7 deal with aspects of pollen grain development, and in particular with the development of the pollen wall and the generative cell. These topics are introduced at the beginning of the Chapters, and the following account merely outlines the background information on the key concepts that are widely accepted at present.

1.2.1. Pollen Wall Structure

Because of their minute size, it has been inevitable that the developments in pollen morphology have become linked with those in microscopy. Early cytologists, although limited by the resolving power of their microscopes, nevertheless recognized two layers in the pollen wall. The outer sculptured sporopollenin wall was called the exine and the inner cellulosic (presumed) wall was called the intine (see Goebel, 1887). In recent years, particularly after the advent of electron microscopy, a more comprehensive view of the pollen wall has emerged.

Various terminologies are in currency for different wall layers (see Knox, 1984a for an inventory of these terminologies) and the most widely used at present are derived from Erdtman (1966). The sporopollenin-containing exine* consists of two layers, a sculpture external part called the sexine, and a non-sculptured inner layer called the nexine. When the embellishments of the sexine fuse at their outer extremities, the exine is called tectate, and

*Exine consists of a general class of substances called the sporopollenin. Chemically, sporopollenin is a polymer of carotenes (Brooks and Shaw, 1978). Sporopollenin is acetolysis resistant and shares some solubility properties with lignin (Southworth, 1974) although it gives negative results in common cytochemical tests for lignin (Southworth, 1973).

pilate when they are free. Each embellishment itself is called a baculum (pl. bacula). The bases of the bacula may also fuse to form a nexine 1 or foot layer. Nexine 1 is usually separated from an underlying nexine 2 by a 'white line'. The pollen grain surface often shows areas where the full stratification is absent or modified. These are commonly described as apertures, although a wide range of more specific terminologies is applied depending upon the particular structure of this region. The wall layer that occurs between the pollen plasma membrane and the innermost exine layer is called intine. The intine is regarded as cellulosic (Heslop-Harrison and Heslop-Harrison, 1982) although in many electron micrographs the microfibrils are not visible. Chapter 4 deals with this point at some length.

1.2.2. Control of Pollen Wall Pattern

1.2.2.1 Hypotheses

Godwin (1968), Echlin (1968) and Heslop-Harrison, 1968b, 1971c, 1980) have reviewed the various types of control that might initiate and determine pollen morphology, including colour, size and exine patterning. In Sporophytic control, features of pollen morphology are envisaged to develop either through the interaction between haploid spores and the diploid tapetal layers, or through the post-meiotic expression of information bequeathed by the diploid pollen mother cell. By contrast, Gametophytic control, implies that the control

is by the haploid genome of spore cells themselves. Haptophytic control, emphasizes the influence of contact relations between the spores in early tetrad stage.

In the literature there is a consensus that all three influences may operate in the determination of various features of pollen morphology. The tapetum, as discussed before, determines the exine colour and provides precursors for the growth of pollen wall after the liberation of the spores from their callosic walls. Its contribution to the early exine development, while the spores are still enclosed in callose, is generally discounted since callosic walls are considered relatively impermeable (Knox and Heslop-Harrison, 1970). The scheme of sporophytic influence envisages that although the early spore wall is secreted by the haploid spores themselves, the factors responsible for its organization are sporophytic in origin, relics from the diploid pollen mother cell and carried in the cytoplasm. Gametophytic control is accepted for the colour in pollen cytoplasm and for intine development. Haptophytic control has been shown to operate during the siting of pollen apertures. According to Wodehouse (1935) the position of apertures is related to the cleavage planes in the tetrad so that the contact relationships between the spores are directly involved in determining the apertural position. However, controversy exists regarding the mode of control of exine patterning. The bulk of evidence favours sporophytic control of patterning.

1.2.2.2. Evidence for Sporophytic Control

The case for inheritance of sporophytic factors, as opposed to gametophytic determinants, responsible for wall patterning, receives support from observations of genomically unbalanced spores (see Heslop-Harrison, 1971c). Such spores arise from imperfect meiosis and often show a normal exine pattern, although if the exine patterning is under gametophytic control they should be abnormal. Some experimental evidence has also become available in recent years. Heslop-Harrison (1971c) designed experiments involving centrifugation and colchicine treatments with a view to disrupting the polarity of factors that might control exine pattern. Buds of Lilium at pre-determined stages of development were either centrifuged (approximately 30 min) or subjected to 0.1% colchicine treatment (12h) at specific stages of development. Subsequently, they were allowed to grow, in culture conditions, until growth ceased. It was found that the microspores developed abnormal exines when the centrifugation was performed in the interval between diakinesis and early patterned tetrad stages; the abnormalities related to the pattern of sexine and the position of the colpus. In colchicine experiments, exine pattern abnormalities were inducible between diakinesis and metaphase II. Buds treated at the tetrad stage, after the establishment of the pattern, did not show any exine abnormalities. The inescapable conclusion is that the pattern controlling factor(s) exist in the mother cell as

early as the diakinesis stage of meiosis, indicating sporophytic control. A year later, Dover (1972) employed similar procedures to disrupt the polarity in microspore mother cells of Triticum and found that the factor determining the position of the pollen pore could be traced as far back as premeiotic interphase. Sheldon and Dickinson (1983) extended the observations of Heslop-Harrison (1971c) on Lilium and reported that centrifugation could disturb pattern formation as early as pachytene, but that the position of the colpus could not be affected until cytokinesis. It therefore appears that although the experimentally-sensitive period for pattern formation may vary in different species, its sporophytic control is not in doubt.

The factors responsible for controlling wall pattern are believed to reside in the cytoplasm, as evidenced by centrifugation experiments as well as observations of anucleate cytoplasmic masses. In Acanthus (Drahowzal, 1936) these masses, formed after meiosis II, round up within the tetrad wall and eventually develop a normal exine, suggesting that the necessary factors are cytoplasmic. Recently, Sheldon and Dickinson (1983) have made similar observations on centrifugation-induced anucleate spores of Lilium. The ultrastructural correlate of the sporophytic factors has been thought to be the multi-membrane bodies (Heslop-Harrison, 1968b, see also 1980), 'polyvesicular bodies' (Echlin, 1968), some membrane-bound cytoplasmic inclusions (Dickinson and

Andrews, 1977) and coated vesicles (Sheldon and Dickinson, 1983). These inclusions, first detected in pollen mother cells at meiotic prophase, survive through meiosis and are considered to provide "a mechanism for bequeathing short-term morphogenetic information from sporocyte to haploid spore" (Heslop-Harrison, 1968b, see also 1980).

The sporophytic influences from the tapetum on the growth of pollen wall are supposed to be exerted after the spores are released from callosic walls. As mentioned before, among several other contributions, the tapetum is considered to provide exine wall precursors. While the addition of tapetally-derived precursors does not add any new features to the pollen wall patterning, it results in the further growth of the existing patterning. Tapetal contributions to the pollen wall have been described already, the most important piece of evidence being the observations of spores with degenerated cytoplasm which nevertheless develop normal exine (Beer, 1905; Tischler, 1908; Drahowzal, 1936).

1.2.3. Ultrastructural Basis of Pollen Wall Formation

Pollen grains were among the earliest botanical specimens to be studied by electron microscopy (Fernández-Morán and Dahl, 1952). Early ultrastructural investigations were mainly concerned with the structure of the pollen wall. However, in the past 3 decades or so, largely due to the efforts of Heslop-Harrison, much has been learnt about the developmental aspects. Early

observation of Beer (1911) that exine development begins while the spores are still enclosed in callosic walls has been confirmed by ultrastructural studies. Heslop-Harrison (1963) demonstrated that the exine was preceded by a fibrous layer, the primexine. This layer occurs between the callosic wall and the spore plasma membrane, and is asymmetric, being thinner at the presumptive apertural areas than in non-apertural areas. Its asymmetry prompted Heslop-Harrison to suggest that the primexine acts as a template for subsequent exine development and wall patterning. Later (1968c) he showed that this layer was digested by cellulase, confirming its cellulosic composition that was earlier perceived from the electron microscopic images. Subsequent confirmations of the occurrence of primexine in divergent species have been reviewed by Heslop-Harrison (1971a), Dickinson (1976), Buchen and Sievers (1981) and Knox (1984a). Currently, the primexine is regarded as a matrix containing receptors for various wall precursors (Knox, 1984a).

Elements of exine soon begin to appear in the primexine. The spatial distribution of endomembranes is thought to be involved in the development of the exine (see Knox, 1984a). Tubules of endoplasmic reticulum (ER) closely apposed to the spore plasma membrane have been shown to occur beneath the apertural surface and have been considered to block the passage of wall precursors to these regions, so that eventually a weak exine is formed there (Heslop-Harrison, 1963, 1968b, 1971a; Skvarla and

Larson, 1966; Godwin et al., 1967; Dickinson, 1970a, 1976; Dickinson and Potter, 1976; Horner and Pearson, 1978). In some species the site of individual probacula, the forerunner of bacula, is also demarcated by ER tubules (Heslop-Harrison, 1963; Larson and Lewis, 1963). In Zea mays (Skvarla and Larson, 1966) the ER tubules run radially towards the bases of the probacula and are considered to "function in determining exine template form". Membrane-like lamellae are also involved in the actual biosynthesis of exine wall layers. Rowley and Southworth (1967) demonstrated the occurrence of membrane-like lamellae embedded in various exine layers. Rowley and Dunbar (1967) have suggested several possible sources for these structures. Dickinson and Heslop-Harrison (1968) showed that "pleated" membrane-like lamellae, in their view arising from plasma membrane, formed the base of probacula. Both dictyosomes (eg., Lilium) and endoplasmic reticulum (eg., Cosmos) have been implicated in the provision of the material for the build up of exine (see Dickinson, 1976).

While some of these features have been recorded in a number of species, their universal occurrence is not accepted (see Dickinson, 1976). Moreover, most of these studies are based on ultra-thin sections of chemically-fixed anthers. Chemical fixation can cause the loss of cellular components or modify their ultrastructural appearance. Images of ultra-thin sections provide only a partial view. The occurrence of primexine is doubtful,

for example in Tripogandra (Mattsson, 1976) and Gibasis (Owens and Dickinson, 1983). Interestingly, Waterkeyn (1968) working with Ipomoea, was sceptical about the real nature of the primexine. He noted that the primexine becomes birefringent and dichroic (optical properties that are associated with cellulose) only after fixation. He thought that this zone of the wall was filled with a gel-like polysaccharide other than cellulose. The radially placed ER tubules underneath the probacula have not been seen in any other species. The association between the ER tubules and individual bacula and apertural areas was observed in ultra-thin sections and recently Blackmore and Barnes (1985) have illustrated the inadequacy of thin section analysis for such associations. These authors examined the osmium-macerated spores by scanning electron microscope and noted the absence of ER-apertural area association in Cosmos, a species in which such a relationship was established on the basis of images of ultra-thin sections (Dickinson and Potter, 1976). It is obvious that more comprehensive studies are required for elucidating the cellular mechanism of pollen wall formation. It is important that this process be examined by different approaches and alternative techniques.

The role of cytoskeletal elements has generally been discounted in wall pattern formation. Microfilaments have been visualized in mature or germinating pollen, and pollen tubes (Franke et al., 1972; Condeelis, 1974; Zhu et al., 1980), but not in a developing pollen. Microtubules

have been noted in the developing spores of several species (eg., Helleborus, Echlin and Godwin, 1968b; Lilium, Dickinson, 1970a; see also Dickinson, 1976), but their role has been considered unimportant (Heslop-Harrison, 1971c; Dickinson, 1976), or even dismissed (Sheldon and Dickinson, 1983). It must be emphasized that all previous reports of microtubules were based on ultra-thin section images; it is only recently that attempts have been made to visualize microtubules by immunofluorescence procedures (Dickinson and Sheldon, 1984; Van Lammeren et al., 1985). The latter authors made spectrophotometric quantitative analysis of fluorescently labelled microtubules and recorded that during meiosis and development of generative cell the intensity of immunofluorescence was higher than during the tetrad period. Significantly, both these groups of investigators noted the occurrence of a radial system of microtubules running between the nucleus and cell edges at tetrad stage, when the pollen wall is being synthesized. Both ascribe cytoplasmic transport functions to these microtubules.

1.3. Aims of Present Investigation

The paucity of information on plasmodial tapeta was the main reason for undertaking the detailed investigation that is reported here. Particular attention has been paid to aspects of development, tapetal cell surfaces, cell-cell interaction, cell fusion, and the

structure and function of cytoskeletal elements during the formation of the plasmodium. Emphasis has also been toward evaluating, experimentally, the roles of microtubules in various stages of development of tapetum, to gain insights into their function in tapetal development.

It would have been illogical to study the tapetum without also studying pollen development. Accordingly the present work includes observations on the deposition of microspore walls and on the microspore cytoskeleton. The end point of the overall sequence was taken as the completion of microspore mitosis to make bicellular pollen grains.

Datura stramonium, Canna sp., and Tradescantia virginiana were chosen for this study, on the basis that Davis (1966) described all three species as having the plasmodial type of tapetum. Another criterion for their selection was their convenient local availability.

However, early in the investigation it became clear that Datura stramonium has a secretory tapetum and not plasmodial. The observations of this species are therefore outside the scope of this Thesis and have not been included. There was no information on tapetal development in Canna, though Davis (1966) described it as being plasmodial. As described in Chapter 3, this species was in fact discovered to have a hitherto unrecognized invasive but non-syncytial type of tapetum. The novelty of this type warranted an ultrastructural and cytochemical

study with a view to understanding its unique behaviour and possible function.

Studies of Tradescantia virginiana, a member of the Commelinaceae where plasmodial tapetum occurs as a family character, form the major part of this Thesis. Two aspects distinguish the present work from preceding studies of tapetum and pollen development. One is that the complete developmental sequence has been followed from tapetal inception to bicellular pollen. The only comparable portrait concerns another species of Tradescantia, examined in a series of papers by Mepham and Lane. The species used for the present work turned out to be strikingly different and so many new features were found that a complete study was considered worthwhile. The second distinguishing aspect is technical. Unlike previous investigations on pollen development, which were mainly based on analysis of ultra-thin sections of conventionally-processed anthers, the present investigation sought to augment the information gained from the conventional procedures by making use of a variety of approaches such as freeze-substitution, freeze-fracture replicas, light and electron microscopic cytochemistry, immunofluorescence of tubulin and drug administrations. The technique of freeze-substitution has not been used very much for studies of higher plant ultrastructure. It was found to be extremely valuable, and results which have general implications - not just for tapetum and pollen - were obtained. Some of these are introduced in Chapter 6.

CHAPTER 2

GENERAL METHODS AND THE TECHNIQUE OF FREEZE-SUBSTITUTION

The following is a description of some of the common methods employed during this work. Other specialized techniques which were used for particular purposes are described in the relevant chapters. The details of the technique of freeze-substitution also appear in this section.

2.1. Fixation

Unless otherwise mentioned all fixation and post-fixation was carried out at room temperature. The usual fixative in this work was 2% paraformaldehyde and 2.5% glutaraldehyde in 25mM phosphate buffer at pH 7.0. It was prepared as follows: 0.5 g of paraformaldehyde was dissolved in 5 ml of distilled water at 60°C; 1N sodium hydroxide then was added drop by drop until the solution became clear; it was then cooled, and 2.5 ml of 25% glutaraldehyde plus 12.5 ml of 5mM phosphate buffer was added; the pH was then adjusted to 7.0 followed by addition of distilled water to make a total volume of 25 ml.

For transmission electron microscopy the tissue was post-fixed in 1% osmium tetroxide made up in 25 mM phosphate buffer (pH 7.0).

2.2. Dehydration, Infiltration and Embedding

2.2.1. Light Microscopy

Apart from mounting freshly isolated cells in distilled water, observations were also made of embedded

material. For light microscopy, tissue was embedded in glycol methacrylate or Sorvall JB-4 embedding medium. Dehydration for this purpose was performed in a methyl-cellosolve series (O'Brien and McCully 1981). This involved placing the tissue in a sequence of methyl cellosolve, ethanol, n-propanol and n-butanol, two changes of 30 min each. All solvents were at 100% (dried over molecular sieve) and at room temperature.

For GMA embedding, tissue was transferred from n-butanol into complete monomer mixture and infiltrated for 1-2 weeks with daily changes. The monomer mixture was prepared by mixing 95 ml GMA, 5 ml polyethylene glycol 200 and 1.1 gm benzoyl peroxide. During infiltration the specimen vials were wrapped in alfoil to prevent precocious polymerization. Polymerization was achieved using UV radiation under flushing nitrogen at $4^{o}C$ for 2h.

For JB-4 embedding, after 2 changes in n-butanol, anthers were infiltrated with the 'A+B' mixture for 2-3 days and a daily change. Anthers were then embedded in 'A+B+C' mixture and polymerized at $4^{o}C$ overnight.

2.2.2. Electron Microscopy

The tissue was dehydrated in a graded series of 10, 30, 50, 70, 90, and 100% acetone, 30 min each, except for 100% acetone in which two changes were given before infiltration. While in 100% acetone, the tissue was gradually infiltrated over a period of 2-3 days with Spurr's resin (Spurr, 1969). Resin mixture of medium

hardness was prepared by mixing 8 gm vinylcyclohexen dioxide (VCD), 4.8 gm D.E.R., 20.8 gm nonenylsuccinic anhydride (NSA) and 23 drops of dimethylaminoethanol (S_1). Polymerization was accomplished at 60°C overnight.

2.3. Sectioning

2.3.1. Light Microscopy

2-4 µm thick sections were cut of the GMA, JB-4 or Spurr's resin embedded material on dry glass knives for light microscopy or for checking the orientation of the specimens before cutting ultra-thin sections. Sections were placed on a glass slide in a drop of water and air-dried (for GMA or JB-4 sections) or heated at 60°C (for Spurr's resin sections).

2.3.2. Electron Microscopy

Thin sections with interference colours of pale gold to silver were cut on a Diatome diamond knife with LKB ultratome III. While afloat on water the sections were stretched with chloroform vapours, collected on formvar coated copper slot grids, and air-dried.

2.4. Staining

Thick sections of GMA or JB-4 embedded specimens were stained in 0.05% toluidine blue O in benzoate buffer (0.25 gm benzoic acid, 0.29 gm sodium benzoate plus 200 ml of distilled water) at pH 4.4, whereas thick sections of Spurr's resin embedded tissue were stained with 0.5% toluidine blue O in 0.1% sodium carbonate at pH 11.1.

Ultra-thin sections were stained with saturated alcoholic (50% ethanol) uranyl acetate and aqueous lead citrate (Reynolds, 1963) for 15 min each. Lead citrate was prepared by dissolving 1.33 gm of lead nitrate and 1.76 gm of sodium citrate in 30 ml of distilled water in a volumetric flask while stirring for 30 min, mixing 8 ml of 1N sodium hydroxide, and finally adding distilled water to make the total volume to 50 ml.

Staining with uranyl acetate was performed in darkness. Staining times varied between 5 and 15 minutes. Most conventional and freeze-substituted preparations were stained for 15 min. However, when the cells were freeze-substituted in 1% osmium tetroxide in 100% acetone, staining for 5 minutes was adequate. Following staining, sections were rinsed in 50% ethanol and distilled water, and air-dried before staining with lead citrate. The second stain was applied in a carbon dioxide free atmosphere for 5-15 min, following which the sections were washed in distilled water and air-dried before observing in the electron microscope.

2.5. The Technique of freeze-substitution

All histological and cytological studies require fixation at some stage. The connotation of the term fixation has undergone considerable change in recent times. Originally it was used in the sense of rendering the cellular components insoluble, then as coagulation, and now, with the advent of aldehyde fixatives, it means

cross-linking of macromolecules. It is accepted that fixation involves molecular alterations by chemical means and in recent years several publications have emphasized the inadequacy of glutaraldehyde, the most successful and widely used cross-linking agent, for faithful preservation of cellular components. At the ultrastructural level it has been shown to alter properties of biological membranes (Iqbal and Weakley, 1974; Breathnach et al., 1976), cause shrinkage in the surface area (Maul et al., 1972) and in the size of nuclear pores (Willison and Rajaraman, 1977), loss of labile components (Hobot et al., 1984), destruction of F-actin (Lehrer, 1981), and microtubules (Howard and Aist, 1979; McKerracher and Heath, 1985).

It is not surprising, therefore, that the quest continues for other ways of preserving cellular ultrastructure, which may establish independent criteria for the evaluation of fixation procedures. It is in this context that the physical methods of tissue processing become relevant. Such methods generally involve a rapid freezing of the living tissues and cells, thereby avoiding contact with the chemical fixatives. Freeze-substitution is one of such alternative techniques. It was devised by Simpson (1941) who, while exploring the parameters for freezing and drying of tissues, ended up using low temperature substitution media such as methyl cellosolve, absolute ethanol, diethyl ether and chloroform at temperatures in the range of -40^{o} to $-78^{o}C$. Feder and Sidman (1958) further advanced the technique for the light

microscopic level of resolution. They also introduced the use of fixatives in the substitution media; osmium tetroxide was dissolved in acetone, and picric acid and mercuric chloride in ethanol. Essentially, this form of freeze-substitution has been used since then by several workers and few reviews are available (Pease, 1973; Harvey, 1982). However, its use in plant cell ultrastructural studies has been rather limited.

2.5.1. Basic Principle of Freeze-Substitution

The technique essentially consists of two steps: 1. rapid freezing of cells so that all cellular activity will cease and the native state will be preserved; and 2. substitution of cellular water at relatively low temperatures with a suitable solvent that can dissolve the resins employed for electron microscopic ultra-thin sectioning.

2.5.2. Criteria for good Preservation

In the present work the criteria for judging a well preserved freeze-substituted cell were: 1. absence of detectable ice crystals at an intermediate range of resolution (20,000-40,000 times magnification) and 2. the microtubules did not appear collapsed (example shown in Fig. 6.37).

2.5.3. Causes of artifacts

Experience showed that the above-mentioned artifacts could arise at 3 levels: 1. while freezing, i.e., inadequate cooling rates caused the formation of ice crystals as well as damaged the microtubules; 2. rapid thawing; and 3. inadequate substitution. In view of these factors it was essential to freeze the cells quickly, to determine the ideal substitution times (see later) and to thaw them gradually.

Since fast cooling rates are of pivotal importance it puts a definite constraint on the size of the tissue that can be successfully freeze-substituted without any noticeable ultrastructural disruption or damage. Experience with several different tissue types (data not included in thesis) showed that in multicellular tissue the best ultrastructural preservation could only be achieved in the outer most cell layer, no more than 40um deep. In view of this, whole anthers were considered unsuitable for freezing, since the spore or tapetal cells, which were of interest during this work, were situated at least 4-8 cell layers deeper and there was no hope of attaining a good ultrastructural preservation in them. Fortunately, however, these cells exist singly in the species under investigation and it was easy to isolate them, provided, of course, that a suitable technique could be worked out to handle single cells during the entire operation (see later).

2.5.4. Freezing Agent and Substitution Medium

During the course of this work liquid propane was employed as freezing agent and acetone as substitution fluid. Propane at room temperature exists in a gaseous form, but readily liquifies at lower temperature. The advantages of this particular agent are that in liquid state it provides sufficiently low temperature to achieve good tissue freezing, and its rate of evaporation is very slow compared with liquid nitrogen.

2.5.5. Gadgetry

A metal block with 7 holes was especially made for freezing the tissues. A large polystyrene-foam container was filled with liquid nitrogen and the metal block was placed in it. Care was taken so that the level of liquid nitrogen reached almost to the brim of the metal block. When the block had reached the same temperature as liquid nitrogen (the extreme bubbling in liquid nitrogen stops) the propane gas was released into the central hole of the metal block until the entire hole became filled with liquid propane. While liquifying propane gas, care was taken to keep the level of liquid nitrogen in the polystyrene container up to the brim of the metal block. The polystyrene container was then kept covered until further use. The level of liquid nitrogen had to be maintained throughout the operation.

Scintillation vials containing (approximately 1/4 by volume) reactivated molecular sieve (type 4A) and

(approximately 2/3 by volume) 100% acetone (dried over molecular sieve), or 100% acetone plus 1% osmium tetroxide were then dipped in liquid nitrogen until their contents froze. The frozen vials were then placed in the remaining holes of the metal block.

Small baskets were prepared by sawing off the bottom of plastic capsules in which electron microscope grids are commercially sold. A sheet of wire mesh was heated on a flame and when red hot, the sawn off end of the capsule was pressed hard onto the wire mesh so that the two become fused. The wire mesh can then be trimmed around the edges of the capsule. Such baskets are small, handy and provide a sufficient porous area for infiltration by substitution fluids. These baskets and their lids were then placed in the liquid propane.

For handling small samples such as single cells, small wire loops coated with a dry agar film were prepared. Coating was performed by dipping the loops in a warm 2% agar solution, blotting the excess agar on a filter paper so that eventually a thin film is obtained, and allowing the film to dry. The idea of using a thin support film for freezing small specimens was a modification of a procedure communicated by P.K. Hepler and D. Callaham who use a formvar film (see Lancelle et al., 1985). During this investigation the formvar film was considered unsuitable as the cells did not stick to the film. By comparison, the dry agar when hydrated becomes sticky and once the cells become attached to it they stay on the film during subsequent procedures.

2.5.6. Method

After placing the cells on the loops they were quickly immersed in liquid propane with a pair of forceps. A few seconds later they were removed from the liquid propane and transferred to small baskets that were already in liquid propane. These baskets were then quickly closed and placed in scintillation vials in such a way that the wire mesh was sitting on the frozen surface of the substitution fluid. During the transfer of wire loops to the baskets and then to the scintillation vials speed is of the essence.

The vials were then stored in liquid nitrogen until the batches of tissue were frozen. Subsequently, the liquid propane was discarded from the metal block, the block placed back in liquid nitrogen to acclimatize to low temperature again and then the scintillation vials were placed in the holes of the metal block. The metal block was then quickly transferred to an ultrafreezer at -85^{o}C and stored there for 2 days. The duration of 2 days was arrived at after considerable experimentation and experience showed that it was the shortest practicable time for acceptable freeze-substitution. Longer duration (carried out at daily intervals up 7 days) caused extraction of the matrix components whereas shorter duration resulted in inadequate substitution. A few cells became extracted even after 2 days of substitution, but most of them were satisfactory.

After the substitution, the metal block was gradually allowed to come to room temperature. For this purpose it was placed in the ice box of a commercial refrigerator (approximately -20^{o}C) for 2 hr, then in the lower most cabinet of the refrigerator (approximately 4^{o}C) for 1 hr and finally brought to room temperature.

The baskets containing the wire loops were removed from the vials and placed in dry 100% acetone in a petri dish and the loops taken out, while immersed in acetone, the agar film was gently dissected out and transferred to fresh acetone in small specimen vials. The cells that were subjected to substitution in acetone plus osmium tetroxide were immediately processed for infiltration whereas those which were substituted only in acetone were subjected to 1 hr of 1% osmium in acetone, washed in acetone and then infiltrated with Spurr's resin.

For reasons that are not fully understood the sectioning of freeze-substituted material is not easy. Several problems were encountered, the most common of which was the tearing of cells at the plasma membrane-cell wall interface. It was also found that the embedded material if trimmed or cut as thick sections, had the tendency to fall out of the section leaving a gap in its place. However, if handled carefully, ultra-thin sections can be easily obtained from the same samples. Nonetheless, the following precautions helped reduce the problems of sectioning:

1. Infiltration was carried out in the resin mixture without the hardener S-1. At the end, one fresh change and overnight infiltration was performed with resin mixture containing S-1 before the tissue was embedded. It was considered that by omitting the hardner during infiltration, even the slight polymerization that can occur during infiltration would be avoided.

2. To avoid having to trim the block face for thin sectioning, the smallest possible pieces of the agar film were cut before embedding them.

3. While sectioning, no thick sectioning of the tissue was attempted. This increased the amount of work but decreased the chances of cells falling out of the sections.

These precautions helped reduce the problem of section tearing, but by no means eliminated it.

The above-mentioned technique has been successfully applied to a variety of tissues including the epidermal cells of the leaves of Triticum, Lilium, Tradescantia , Chlorophytum, Agrostis, Lemna, and Saccharum, and those of the ovules of Datura and Tradescantia stamen hair (data not shown in the thesis). Results obtained through the application of this technique and with relevance to the thesis are included in Chapters 3,6, and 7.

CHAPTER 3

DEVELOPMENT AND CELL SURFACE OF TAPETUM IN *CANNA* L.

3.1. INTRODUCTION

In angiosperms, the innermost layer(s) of the anther wall differentiates into specialized tapetal cells. Traditionally considered as a nurse tissue (Maheshwari, 1950), the tapetum has been implicated in the development of the pollen wall and determination of sporophytic incompatibility (see Echlin, 1971a,b; Heslop-Harrison, 1972). Two major types of tapetum, secretory and plasmodial, have been distinguished in the literature; in the former there is a partial dissolution of walls but the cells stay intact in situ, whereas in the latter, there is an early breakdown of walls and subsequently the protoplasts move into the loculus and fuse to form a periplasmodium or syncytium. Although the timing and sequence of wall dissolution varies greatly in different species representing both plasmodial (see Clausen, 1927) as well as secretory tapetum (see Bhandari, 1984), yet pronounced differences exist between these two types of tapetum.

As part of a detailed investigation on plasmodial type of tapetum, Canna tapetum was chosen. Canna has been described in the literature as an example of plasmodial tapetum (see Davis, 1966). However, during the course of present investigation it became apparent that in this species the tapetum is a novel type for although early in its ontogeny the cell walls breakdown and the tapetal protoplasts move into the loculus, there is no

plasmodium formation. Hence this type should be described as non-plasmodial invasive tapetum, an intermediate condition between the secretory and the invasive types. Previous ultrastructural studies in this genus deal with the structure of pollen wall (Skvarla and Rowley, 1970; Rowley and Skvarla, 1975; Kress and Stone, 1982), but none on tapetum. To study the unusual behaviour of this tapetum ultrastructural and cytochemical investigations were undertaken. It was found that the cells develop a fibrillar glycocalyx concomitant with the dissolution of their cell walls during early stages of meiosis. This chapter describes properties of the cell coat as well as the results of an ultrastructural survey of the development of this hitherto unreported type of tapetum. Particular attention was paid to the microtubular cytoskeleton of these cells. Preliminary observations, obtained through treatments with colchicine, relating to the function of tapetum in sporopollenin secretion are also included.

3.2. MATERIALS AND METHODS

Young buds and flowers of Canna indica L. x C. sp. hybrid were collected from the Commonwealth Gardens, Canberra.

3.2.1. Light Microscopy

Anthers were dissected from young buds and flowers, rinsed briefly in very dilute detergent (teepol) to render

them wettable, washed in distilled water and fixed overnight in the usual aldehyde fixative. After washing in buffer they were dehydrated in methyl cellosolve series and embedded in Sorvall JB-4 embedding medium or in glycol methacrylate. 2-4um thick sections were cut on dry glass knives stained with 0.05% toluidine blue O in benzoate buffer at pH 4.4 and observed with differential interference contrast optics on a Zeiss Photomicroscope III.

Anther contents were also gently extruded from unfixed anthers, mounted in distilled water and observed as above. Photographs were taken on Kodak Plus X films.

3.2.2. Conventional Electron Microscopy

Anthers were dissected out and fixed in the usual manner. They were then washed and post-fixed for 1h in 1% osmium tetroxide, washed again in buffer, dehydrated in acetone and embedded in Spurr's medium. Because of the high density of the cytoplasm, particularly in the early stages of tapetal development, it was not always easy to visualize microtubules. Tannic acid fixations proved useful in such cases: 0.5%, 1%, and 2% tannic acid (Mallinckrodt) was added to the primary fixative. However, the general ultrastructural preservation was found to be improved when cells were subjected to 1% tannic acid for 1h after post-fixation in OsO4 (see Fujiwara and Link, 1982). Thin sections were cut with a diamond knife, collected on formvar-coated slot grids,

stained with saturated alcoholic uranyl acetate and aqueous lead citrate and viewed on a Hitachi H500 microscope at 75kV.

3.2.3. Scanning Electron Microscopy

Clumps of mature pollen were isolated from dehiscing anthers onto small round cover glasses. The cover glasses were frozen on metal blocks precooled by liquid nitrogen, freeze-dried at -40°C, sputter-coated with gold, and observed using a Cambridge Stereoscan SEM at 30kV for surface features.

3.2.4. Freeze-Substitution

Tapetal cells were gently extruded from freshly isolated unfixed anthers on to wire loops coated with a dry thin film of agar (2%). The wire loops were then quickly frozen in liquid propane precooled by liquid nitrogen. They were then transferred to precooled (in liquid nitrogen) vials containing dry 100% acetone and molecular sieve and stored in an ultrafreezer at -85°C for 2 days. The vials were then gradually brought to room temperature and the loops transferred to new vials containing freshly made 1% osmium tetroxide, or 1% osmium tetroxide plus 0.5% tannic acid (Mallinkrodt) in dry 100% acetone for 1h, washed with acetone for 10 minutes, the agar film bearing the cells dissected out and embedded in Spurr's medium.

3.2.5. Cytochemistry

3.2.5.1. The Thiéry Reaction

The Thiéry reaction was performed on thin sections according to the procedure of Thiéry (1967). Thin sections were collected in plastic loops (see Roland, 1978), treated with saturated aqueous solution of dimedon at 60°C overnight to block any free existing aldehyde groups, washed for 2h in distilled water, oxidized for 1h in 1% periodic acid (PA), washed for 1h in distilled water, incubated in 1% thiocarbohydrazide (TCH) made up in 20% acetic acid for 72h, washed in 20% acetic acid for 1h, in 10% acetic acid for 1h, and in distilled water for 2h, stained for 1h with freshly made 1% aqueous silver proteinate (SP) in dark and washed overnight in distilled water. Sections were then collected on formvar-coated slot grids and viewed. Controls were run by (i) omitting PA oxidation, (ii) by blocking the PA-liberated aldehyde groups with overnight dimedon treatment, and (iii) by omitting TCH incubation.

3.2.5.2. Ruthenium Red and Ferrocyanide Staining

Other cytochemical tests involving ruthenium red and potassium ferrocyanide were performed *en bloc*. The cells were gently extruded from the anthers into a centrifuge tube containing either the fixative or the fixative-reagent mixture. After the treatment the cells were pelletted and most of the supernatant was aspirated. The cells were then put on a millipore filter paper (type

GS, 0.22um pore size) attached to the millipore filtration device and most of the solution was aspirated. In this procedure the cells settle compactly on the filter paper, which can be embedded in 3% agar. Subsequent dehydration and infiltration was carried out while the cells were embedded in agar blocks.

Ruthenium red has been employed extensively in studies of the glycocalyx (see Luft, 1976). The procedure employed was as follows: cells were subjected to 1mg/ml ruthenium red plus the usual fixative in 100mM cacodylate buffer (pH 7.2) overnight, washed in buffered ruthenium red for 30 minutes, and post-fixed in 1% buffered osmium containing ruthenium red and, subsequently, in distilled water, and embedded in agar.

Potassium ferrocyanide in combination with OsO_4 is known to stain the glycocalyx of animal cells (Karnovski, 1971). The procedure employed was as follows: cells were fixed in the usual fixative made up in 100mM cacodylate buffer for 30 minutes, subjected for 1h to freshly made solution of 1% OsO_4 plus 1.5% potassium ferrocyanide in buffer, washed in buffer and embedded in agar and then in Spurr's resin.

3.2.6. ConA and Anti-Tubulin Labelling

For labelling with ConA, isolated tapetal cells were fixed for 1h in freshly made 4% paraformaldehyde plus 0.2% glutaraldehyde in 25mM phosphate buffer (pH 7.0), washed in buffer, and again in phosphate buffered saline

(PBS), treated with 100mM glycine in PBS for 30 minutes, washed in PBS and incubated with FITC-tagged ConA (10ug/ml in PBS) in darkness for 1h, washed in PBS, and mounted in moviol containing 2% n-propylgallate (to reduce fading). Control cells were incubated in α-methyl-D-mannoside (200uM in PBS) before incubation with ConA-FITC. This blocked staining of the type shown in Fig. 3.22.

Microtubules were visualized by indirect immunofluorescence employing a monoclonal antibody raised against β-tubulin. Isolated cells were fixed and washed as above. They were then affixed onto poly-L-lysine (1mg/ml; Mol. Wt. 54,000) coated cover slips by air-drying, rinsed in PBS, permeabilized by 1% triton X-100 in PBS for 1h, and incubated with a mixture of equal volumes of 1% triton X and monoclonal antibody raised against chick brain tubulin (Amersham, cat. no. N.357; 1:500 diluted in PBS) for 1h at 37°C. They were then washed in PBS and incubated in goat-anti-mouse IgG conjugated with FITC (Tago; 1:40 diluted in PBS) for 45 minutes in darkness at 37°C. Afterwards they were washed thoroughly and mounted in moviol. Controls omitting treatment with the first antibody were run concomitantly.

Observations were made on a Zeiss Photomicroscope using epifluorescence and standard fluorescein filters. Photographs were taken on Kodak Tri X film.

3.2.7. Colchicine Treatment

Isolated buds at early tetrad stage were subjected to aqueous solutions of colchicine (5×10^{-3} M) for 12-60h. The details of the procedure have been the same as described in Chapter 5.

3.3. RESULTS

In the following description of tapetal development, stages of the spore cell development are used as reference points.

3.3.1. Premeiotic Phase

Young anthers contain two round locules or microsporangia (Fig. 3.2) which before meiosis acquire a horse-shoe shape (copmare Fig. 3.3 with Fig. 3.2). A group of hypodermal archesporial cells divides in the usual manner to form an outer primary parietal layer and an inner primary sporogenous layer. The former undergoes a few periclinal and anticlinal divisions to form an endothecium, 2-4 middle layers and the tapetum (Fig. 3.1). In a premeiotic anther, the tapetum consists of 1-2 cell layers, but at places it becomes 6-7 layered (Fig. 3.3). The inner outline of the tapetum is highly irregular so that columns of tapetal cells can be seen jutting deep into the spaces between the sporogenous cells. However, they never completely traverse the locular cavity. Numerous plasmodesmata interconnect the various tapetal cells, and pass from the tapetum to cells of the middle

layers on the outside and sporogenous cells on the inner side. The walls between tapetal cells are thin but those between tapetal cells and middle layers or sporogenous cells are thicker and show prominent middle lamellae. The cells are uninucleate and the cytoplasm vacuolate and sparse. Plastids, mitochondria, dictyosomes and smooth endoplasmic reticulum (ER) cisternae occur.

Prior to meiosis, tapetal nuclei undergo divisions without cytokinesis resulting mostly in a binucleate condition (Fig. 3.5) - sometimes, however, as many as 4 nuclei have been observed. By this stage the ER begins to proliferate, its cisternae running close to the walls or the nuclei. Several vesicles can be seen in the vicinity of ER cisternae or the dictyosomes and often some of these appear to be discharging their contents into larger vacuoles showing fibrogranular contents. The population of ribosomes increases - more so than in the sporogenous cells (SCs). There is also an increase in the usual complement of cell organelles. A few spherosomes can also be seen in the cytoplasm, sometimes associated with the ER. Cortical microtubules were few and occurred along tapetum-SC and tapetum-middle layer interfaces. In transverse sections of anthers, their orientation along these walls appeared to be parallel to the long axis of the anther.

3.3.2. Prophase I

Profound changes take place in the tapetal cells with the onset of prophase I. Plasmodesmatal connections become replaced by large cytomictic channels which now interconnect various tapetal cells. Between mid-prophase and late prophase the tapetal cell walls begin to breakdown, commencing at the middle of the horse-shoe shaped loculus and progressing laterally. Also, wall dissolution begins at the inner periclinal walls and gradually extends towards the radial walls. The cytomictic channels persist even after complete dissolution of the radial wall (Figs. 3.6,3.7). Generally, a large number of small vacuoles or vesicles accumulate near the dissolving walls. The spherosomes increase in number, and as the wall dissolution progresses many bodies similar to them become visible outside the plasma membrane, some neatly deposited on the outer periclinal walls adjoining the middle layers (Fig. 3.8). It is noteworthy that this layer of wall is not subjected to dissolution. Putative expelled spherosomes are invariably present at the external edges of the radial walls, which, likewise, do not dissolve. Plasmodesmata between the tapetal cells and sporogenous cells are lost whereas those between the tapetal cells and the middle layers frequently appear occluded by wall material and sometimes by the spherosome globules on the side toward the tapetum. At this stage some vesicles apparently originating from the dictyosomes and containing

fibrogranular material (Fig. 3.8) are also seen so closely associated with the plasma membrane that exocytosis seems probable. Few multivesicular bodies also become visible.

The plastids characteristically show long cylindrical, dumb-bell or cup-shaped profiles (Fig. 3.6). With the advancement of prophase, the tapetal nuclei undergo considerable increase in size, the chromatin condenses and their outlines become lobed. At places their two membranes become distended and some intranuclear vesicles become visible at this stage (Fig. 3.9). There is no obvious association between the intranuclear vesicles and the nuclear membranes.

Prophase I is characterised by a general proliferation of various cell organelles, notable among them are rough ER and ribosomes (compare Fig. 3.6 with Fig. 3.5). Closely packed, parallel cisternae of rough ER are generally spread in the cytoplasm and are conspicuous near the cell surface (Fig. 3.8) or the nuclei. The cytoplasm is very dense because of the accumulation of ribosomes. Vacuoles show a fibrogranular material (Figs. 3.6,3.8). Transectional profiles of cortical microtubules remain (Fig. 3.8) along the inner and outer periclinal surfaces, in spite of the fact that the cell walls are nearly completely dissolved. The cells, however, remain in situ.

The plasma membrane probably undergoes the most dramatic changes during this phase. With the onset of wall dissolution, it starts showing a coat in the form of

fibrillar material (see later) on its exterior surface (Figs. 3.7,3.8). Cells at the middle of the horse-shoe shaped loculus, being at a more advanced stage of development, show the coat material earlier than those at the flanks of the loculus. However, the cell coat develops simultaneously in all those cells which are connected by cytomictic channels, and is found evenly on all the surfaces of a cell. Gradually, all the tapetal cells exhibit the coat.

3.3.3. Meiosis

With the dissolution of the cell wall and the development of cell coat completed, cytomictic channels disappear, tapetal synchrony seen earlier in cells connected by cytomictic channels is nearly completely lost and variations in cell ultrastructure appear. The tapetal cells are released into the locular cavity (Fig. 3.4), but they do not fuse to form a syncytium: they stay intact as individual protoplasts (Fig. 3.10 shows the discrete tapetal cells at a much later stage). By the time the first meiotic division is complete, most of the tapetal cells have migrated into the locular cavity. A typical tapetal cell at this stage is shown in Fig. 3.11. Cell ultrastructure is much the same as in the previous stage, although the intranuclear vesicles have disappeared.

Aspects of tapetal cell surfaces are illustrated by Figs. 3.12-3.16. The fibrils of the cell coat are thin and long and are studded with granules of electron dense

nature. They are more or less evenly spaced - approximately 15-25nm space between the mid-lines of two adjacent fibrils in a given thin section. The space between two granules on the same fibril was found to vary between 10-15nm. The fibrils run tangentially to the cell surface so that in a grazing section their fibrillar nature becomes clearly visible (Figs. 3.12,3.16). In a cross section the granules of the cell coat appear as circular profiles, (average diameter 17nm) adhering to the plasma membrane (Fig. 3.14).

The glycocalyx nature of this coat material was established by its affinity for ruthenium red, potassium ferrocyanide, Thiéry reaction and conA-FITC. Differences were, however, found in the selective binding of these reagents to various components of the cell coat. Whereas the application of potassium ferrocyanide (Figs. 3.18,3.19) and ruthenium red (Figs. 3.20,3.21) revealed a more or less continuous coat intimately associated with the outer leaflet of the plasma membrane (note also the enhanced contrast in the plasma membrane as well as cytoplasmic membranes in cells treated with potassium ferrocyanide), the Thiéry reaction imparted silver aggregates all over the cell surface and particularly on the granules of cell coat fibrils (Fig. 3.17). The general distribution of the silver particles on the cell surface as seen in a grazing section merely reflects the specific affinity of the plasma membrane for this reaction. The Thiéry reaction also stained the contents

of golgi vesicles and the fibrogranular material of the larger vacuoles which give the appearance of having been formed by fusion of several golgi vesicles. ConA-FITC binds specifically to the tapetal surface (Figs. 3.22,3.23), although it has not been possible to determine whether the binding is to the plasma membrane or cell coat or both. So far, attempts to localize conA binding sites at the electron microscopic level have been unsuccessful.

Since the tapetal cells are now lying freely in the loculus, intermingled with the spore cells, it is easy to isolate and examine their ultrastructure by freeze-substitution. Such preparations confirm the presence of a fibrillar extracellular cell coat (Fig. 3.13). However, the distinct nature of each fibril, as seen in conventional preparations, is not always very clear. Also the granules of the coat material seen in conventional preparations can not be visualized by freeze-substitution. The coat material appears denser. Obviously the freeze-substitution technique preserves components of the cell surface which are not retained by conventional procedures, and which partially obscure other details of the cell coat. The cell surface is much smoother following freeze-substitution than conventional processing, but nevertheless there are protrusions suggestive of exocytosis of vesicles. The cell coat does not confer complete rigidity on the tapetal protoplast.

Cortical microtubules can still be seen although more so after freeze-substitution than conventional

processing. They were more easily visualized when tannic acid was used after OsO4 post-fixation. The fibrillar nature of the glycocalyx, the electron-dense granular regions of the fibrils, the microtubules and plasma membrane clearly stand out in this procedure (Figs. 3.15,3.16). Immunofluorescence preparations employing a monoclonal antibody raised against the β-subunit of chick brain tubulin revealed an extensive system of cortical microtubules (Figs. 3.33,3.34). The thick cords of fluorescence no doubt represent bundles of microtubules as seen under the electron microscope. The microtubules appear to maintain a predominant orientation, but with considerable local variation, presumably the same as in premeiotic stages. In grazing thin sections the microtubules are seen to be oriented in the same direction as the nearest cell coat fibrils (Fig. 3.13). Four microtubules seen in this section lie in a range of different orientations, yet the cell coat fibrils adjacent to each of them closely follow their orientation.

The reduction in tapetal synchrony is manifest in the development of amoeboid processes by some cells while meiosis is still in progress. However, this becomes more common after the tetrad stage. Also a few of the tapetal cells progress to a cytoplasmic configuration which characterises the immediate post-meiotic phase.

3.3.4. Post-Meiotic Stages

Notwithstanding the fact that variations in cellular ultrastructure and the development of amoeboid processes become more pronounced, a typical healthy tapetal cell at the tetrad stage is shown in Fig. 3.24. One of the conspicuous features is that mitochondria and (especially) dictyosomes are grouped in clusters (Figs. 3.24,3.25). The cell coat appears thinner then before, but can still be visualized by the Thiéry reaction (Figs. 3.26,3.27). Larger dictyosome vesicles continue to show a reaction product formed by the Thiéry reaction (Fig. 3.27). The population of plastids declines sharply in these cells, but they could still be identified by their characteristic shape. Unlike the conventional preparations, in freeze-substituted cells, plastids invariably showed microtubules associated with their envelope (Fig. 3.31). The amount of lipid bodies, vesicles filled with fibrogranular material, dictyosomes and mitochondria increases dramatically. Numerous electron dense globules, presumably lipidic, are discharged from the tapetal cells (Figs. 3.24,3.25). Some of these cells also showed cytoplasmic accumulations of lipid bodies and occasionally bundles of filaments in the vicinity of the lipid bodies (Fig. 3.32).

The ER becomes much more elaborate and mostly peripheral (Figs. 3.24,3.25). Their intra-cisternal spaces become distended, obviously interconnected, and carry flocculent material. The outermost cisternae and

the plasma membrane approach and come in contact with one another at numerous locations on the cell surface, raising the possibility of a transient direct discharge of material from the ER to the exterior (Fig. 3.25). Such association persists till quite late after meiosis, even when the apparent discharge of lipids from these cells has ceased. Freeze-substitution was employed to validate this association and although such preparations confirmed the close relationship between the plasma membrane and the elements of ER (Fig. 3.28) no continuity between these two membranes was ever recorded. The technique proved excellent for the general preservation of cellular ultrastructure. For example, Fig. 3.29, in contrast to Fig. 3.30 (conventional), shows undistorted dictyosomal vesicles with electron dense contents and inter-cisternal rods. Fig. 3.28 illustrates the smooth contours and the bilayer construction of the plasma membrane.

The frequency of microtubules increases but the residue of a preferred orientation is lost, except in localized domains (Figs. 3.35,3.36). As the cells gradually develop amoeboid processes the frequency of microtubules remains high but their order becomes further reduced, initially in the amoeboid process and later in the entire cell (Figs. 3.35,3.40).

At the late microspore stage, a few tapetal cells continue to show the ultrastructure described above: their cell coat is sparse and the frequency of cortical microtubules remains high, although the ER becomes more

extensive, highly branched and vesiculate (Fig. 3.43). However, increasingly the ER becomes less clearly organized and large empty vacuoles dominate the general appearance of the cells (Figs. 3.42,3.44). The population of various cell organelles including the microtubules (Figs. 3.41,3.42) eventually declines; the mitochondria remain grouped; some myelin-like figures, multivesicular bodies and microbodies (with crystalloids) are also present in the cytoplasm. The outline of the cell becomes highly irregular. These cells are considered to be progressing into their degeneration phase.

During further degeneration certain amorphous, densely osmiophilic (presumably lipidic) materials accumulate in the cytoplasm and apparently occlude many organelles (Fig. 3.45). Similar material also becomes deposited on the cell surface obscuring the plasma membrane and cell coat. A gradual increase in the amount of dense osmiophilic substance accompanies the complete degeneration of the tapetal cells (Fig. 3.46). Eventually, the cells fragment into smaller pieces, many of which can be seen in close association with pollen surface (Fig. 3.47). Microtubules have completely disappeared by this stage. By the time of anther dehiscence there is no trace of tapetum, but the pollen grain surfaces show numerous deposits of an oily nature (Fig. 3.48) - the pollenkitt.

3.3.5. Colchicine Treatment

Since the tapetum in Canna does not show any manifestation of sporopollenin secretion such as tapetal orbicules, it was decided to perturb the cellular machinery by employing colchicine and investigate if any visible manifestation of sporopollenin secretion could be obtained. The possibility of using colchicine in this way arose from an investigation on the plasmodial tapetum of Tradescantia where colchicine treatments disrupted the pathway of sporopollenin secretion (see Chapter 5). It was decided to administer colchicine at early tetrad stage because it is from this stage onward that the tapetum is likely to produce sporopollenin. Preliminary results show that colchicine probably does interfere with sporopollenin secretion and polymerization in Canna. 12 hours of treatment removed microtubules from the tapetal cells and anther wall layers. Prolonged treatments resulted in development of a massive granular deposition (Fig. 3.49) in all extracellular spaces of the anther cavity. The amount of granules increased with the duration of treatment. These granules were too small to be subjected to acetolysis in semi-thin sections, but they resembled tapetal orbicules of secretory tapeta in their electron-lucent central area and thick electron-dense coating. They were mostly solitary, but occasionally occurred in aggregates. Similar granules were sometimes encountered in the larger dictyosomal vesicles and vacuoles of tapetal cells.

3.4. DISCUSSION

Contrary to previous descriptions (see Davis, 1966), the tapetum in Canna is invasive but non-plasmodial, a type hitherto unreported in the literature. Because of its unusual behaviour it can be considered as an intermediate type between secretory and plasmodial tapeta. In common with the secretory type of tapetum, the cells in Canna stay discrete although not in their original sites. With the plasmodial tapetum it shares features such as migration into the anther loculus and absence of tapetal orbicules. The existence of this type of tapetum demands care in applying terms such as invasive, amoeboid, plasmodial or syncytial - all commonly considered synonymous in embryological parlance.

Features of Canna tapetum, perhaps related to its novel behaviour, include the presence of an unusual cell coat and the complete symplastic isolation during its secretory phase. These aspects are discussed below, along with a comparison with other tapeta and comments on the role of this type of tapetum in pollen development.

As in all the species investigated so far, tapetal cells of Canna in premeiotic stages are symplastically connected to each other as well as to the middle layer on the outside and to sporogenous cells on the inner side. However, with the onset of meiosis the connections between the tapetal cells and sporogenous cells are lost, whereas the plasmodesmata present between the tapetal cells are replaced by large cytomictic channels. The presence of

cytomictic channels has been considered to bring about synchrony in tapetal behaviour (Heslop-Harrison, 1964). This is also manifest in Canna, for the cells connected by cytomictic channels show more or less similar features, the simultaneous development of cell coat being an example. Whether the tapetum is secretory or plasmodial, the trend is toward the establishment of a syncytium of some sort; in the secretory type the presence of cytomictic channels makes the tapetum a hollow, cylindrical, partial syncytium and in the plasmodial type the plasmodium is itself an extreme example of a syncytium (see Heslop-Harrison, 1972). However, in both these types, the syncytial or synchronous phase is maintained until after meiosis i.e., until the end of the tapetal secretory phase. By contrast, in Canna the cytomictic channels are lost by the end of prophase I when the tapetal cells migrate into the loculus, where they stay as discrete cells, without forming a plasmodium. It seems that a consequence of this symplastic isolation is loss of synchrony, leading to the appearance of variations in cell ultrastructure which become particularly pronounced after meiosis I, when all the tapetal cells have migrated into the loculus.

Cells in complete symplastic isolation are rare in higher plants. The isolation of Canna tapetal cells is not as extreme as in the case of spore cells which develop a special relatively impermeable callosic wall (Knox and Heslop-Harrison 1970) around themselves, but it must

nevertheless limit their functional capacities. They do not contain much reserve material when released into the loculus and yet they engage in massive synthesis, secretion and internal reorganization (see later). The peak secretory activity at a given region in the anther loculus appears short-lived, since the number of apparently healthy tapetal cells declines sharply at the late microspore stage; indeed a few degenerating cells can be seen as early as meiosis I.

Unlike most other genera (eg. Helleborus, Echlin and Godwin, 1968a; Lilium, Heslop-Harrison, 1968a; Reznikova and Dickinson, 1982; Tradescantia, see Chapter 4) where the major secretory activity of the tapetum occurs at the tetrad stage or later, Canna tapetal cells accumulate ribosomes and cytoplasmic membranes in the late premeiotic period until they acquire aspects of a secretory tissue by the time of prophase I, although maximum activity is expressed after the second meiotic divison. As also noted in several other species (for example, Avena, Steer, 1977), the rough ER is the most prominent feature, occupying a peripheral position, often extremely close to the plasma membrane. However, no continuity between ER and plasma membrane of the kind claimed for the tapetum of Ulex (Misset and Gourret, 1984) was recorded in Canna.

Of the various functions ascribed to tapetum, its role in the secretion of sporopollenin for the development of spore exine after the dissolution of

callosic walls has been investigated most extensively. In species such as Helleborus (Echlin and Godwin, 1968a), Allium (Risueno et al., 1969), Pinus (Dickinson and Bell, 1976) Sorghum (Christensen et al., 1972) and Lilium (Heslop-Harrison, 1968a; Reznikova and Dickinson, 1982) tapetal cells are known to synthesize lipids which, it is believed, are required for synthesis of sporopollenin coats of both tapetal orbicules and microspores. Tapetal cells in Canna also produce a large amount of lipidic substances. However, unlike other species where this is first detected at the microspore stage, in Canna the tapetal cells produce lipids from the time of dissolution of their walls and continue to do so until their degeneration. Nevertheless the quantity of lipid production in Canna does not appear to be as high as in other species such as Lilium, judging from the published micrographs. This may perhaps be related to the rather unusual type of wall of pollen grains in Canna. Skvarla and Rowley (1970) have demonstrated that in this species the sporopollenin-containing exine is mainly limited to the spinules (spine like ornamentations of the wall) and a few pockets included in the intine, the remaining pollen wall being an extremely thick intine. Hence the pollen wall of Canna may not require large quantities of substrate for its exine development. The short life-span of the tapetal cells, the relatively low amounts of lipids produced by them and the paucity of pollen exine are perhaps inter-related. In later stages the tapetal cells

fragment and densely osmiophilic lipids become deposited on the pollen wall in the form of tryphine.

The preliminary results of colchicine treatments, however, throw new light on the function of this tapetum. While it can not be claimed with certainty that the colchicine-induced deposition of granular material in the locular cavity is of sporopollenin nature, the structure and electron density of the granules makes this likely. Moreover, a close parallel exists in Tradescantia (see Chapter 5) where similar deposits are acetolysis resistant. The structure of these granules, with an electron-lucent central area surrounded by electron-dense exterior (presumably sporopollenin) is reminiscent of tapetal orbicules seen characteristically in secretory tapeta (see Christensen et al., 1972; Abadie and Hideaux, 1979). The experimental induction of such deposits is an indication that the Canna tapetum can produce sporopollenin even though it does not show obvious signs of this activity during the normal course of development. In Tradescantia (Chapter 4) during normal development a specialized secretory surface develops at the plasmodial interface with developing spores. Colchicine treatments disrupt the formation of this surface, resulting in the occurrence of abnormally-placed sporopollenin deposits. By contrast, in Canna the tapetum is non-plasmodial and does not show any particular surface specializations in terms of polar secretion of sporopollenin. Yet colchicine treatment induces much the same response as in

Tradescantia. How colchicine brings about this effect in Canna is not clearly understood. It could be that colchicine merely hastens the polymerization of soluble precursors of sporopollenin that may be present in the locular fluid.

Important questions also remain as to why differences are seen in the morphology of colchicine-induced extracellular deposits in Tradescantia and Canna In Tradescantia the free deposits were globular whereas those attached to lipidic surfaces were ordered and resembled the early pollen exine (before the fusion of bacular heads). In Canna, which does not have bacula, and whose exine has only very sparse sporopollenin contents, the colchicine-induced deposits occurred in the form of small granules, much smaller than the free globules seen in Tradescantia and certainly unlike any structures seen in Canna itself during normal development. No ordered lipid-bound deposits occurred in Canna. The size of the granules was very uniform in Canna, suggesting that a species-specific mechanism, which normally controls the deposition of sporopollenin in pollen exines may remain operative (though modified) during colchicine treatment so that polymerization still occurs in a definite manner.

Aspects of the tapetal cell coat warrant further discussion. The coat develops coincident with tapetal wall dissolution. Its image varies according to the procedure employed for its visualization. ConA-FITC binds

to the cell surface, but since the labelling could not be performed at the EM level it is not known which component(s) of the coat are labelled. The coat consists of granule-studded fibrils running tangential to the cell surface, plus a matrix that is partially lost during conventional processing but is retained by freeze-substitution to the extent that the granules can scarcely be discerned and the fibrils themselves become indistinct. With potassium ferrocyanide and ruthenium red staining it was difficult to visualize the fibrillar nature of the coat, presumably because the matrix component present in the spaces between the fibrils was also stained by these reagents. The Thiéry reaction, however, imparted electron density to the fibrils and particularly to the granules.

The particular efficacy of freeze-substitution in retaining labile substances is well documented (Fisher and Housley, 1972; Hobot et al., 1984). In the present material this is amply demonstrated when a comparison is made of dictyosomes and their vesicles in the tapetal cells processed conventionally and with freeze-substitution. Whereas in the former these vesicles invariably appear empty and distended, in the latter they are compact, spherical and filled with an electron-dense material. The fibrogranular material of larger golgi vesicles, as seen in conventional preparations, appears homogenous and electron-dense in freeze-substituted cells. These contents as well as the granules of the coat fibrils stain with the Thiéry reaction, indicating the presence of

carbohydrates in both locations. In Canna these vesicles are often seen so close to the plasma membrane that exocytosis seems probable. If the dictyosomal vesicles do indeed carry material for the cell surface and if the morphology of their contents is modified by conventional procedures, then it is not surprising that similar matrix substances at the cell surface also become modified. Nevertheless, the results of all the different procedures employed during this investigation establish the presence of a form of glycocalyx on the cell surface of Canna tapetal cells.

Freeze-substituted preparations of Canna tapetum also show superior preservation of cytoskeletal elements, as also found for other cells by Howard and Aist (1979), Tiwari et al. (1984) and McKerracher and Heath (1985). Plastid-associated microtubules were not seen in conventional preparations but were regularly present in freeze-substituted cells. Their significance is unknown.

The orientation of the cell coat fibrils, tangential to the cell surface, varies by up to 45^{o}, even within quite small expanses of cell surface (eg., Figs. 3.13,3.14,3.16). The fibrils far outnumber the cortical microtubules but the latter run parallel to the former, also varying in their orientation. This correlation is highly reminiscent of the congruent orientation of microtubules and cellulose microfibrils commonly seen in plant cells (see Gunning and Hardham, 1982; Robinson and Quader, 1982) and raises the possibilities of microtubular

involvement in cell coat deposition and linkage of cell coat fibrils to the microtubules across the plasma membrane.

The cell coat does not seem to provide structural rigidity to the tapetal cells, which acquire variable shapes, particularly in post-meiotic stages. The high density of microtubules after the migration of tapetal cells into the loculus until the time of their degeneration suggests that they could themselves have a structural role. Variations in cell coat as seen in the later stages of meiosis apparently represent a genuine developmental change, for the cell ultrastructure undergoes simultaneous change. In animal cells it is well known that the cell coat is a product of the cell on which it is situated and that the variations reflect the degree of maturity and functional state of the cell (Ito, 1974; Luft, 1976).

It is by no means clear what biological roles are played by the cell coat. It is not structurally rigid; it does not adhere to the microspores (or not until very late in development); it apparently does not block secretion. One possibility is that it prevents the tapetal cells from fusing, but this in turn poses the question of the possible biological role of an invasive but non-plasmodial tapetum. As seen in Canna, there is a gradual progression of developmental stages in tapetal cells from the flanks to the middle of the loculus (seen clearly in a transverse section of the anther), leading to a degree of asynchrony.

Moreover, in a large elongate anther such as that of Canna, microspore maturation takes place in an acropetal manner (Heslop-Harrison, 1972), so that there is variation in developmental stages of both sporogenous and tapetal cells from base to tip. It may be that a population of discrete tapetal cells can better match the varying nutritional requirements of a developmental gradient of spores than would a continuous and therefore more synchronous plasmodium.

Figs.3.1-3.4. Transverse sections of young anthers showing the development of anther wall. (ep, epidermis; en, endothecium; ml, middle layers; t, tapetum; mmc, microspore mother cells).

Fig. 3.1. High magnification photomicrograph showing the wall layers and sporogenous tissue. x 400.

Fig. 3.2. A round loculus shows a multilayered anther wall enclosing a group of microspore mother cells. Arrows indicate the areas where the tapetum intrudes between microspore mother cells. x 170.

Fig. 3.3. Before meiosis the loculus acquires a horse-shoe shape. Arrows indicate the tapetal intrusion between the microspore mother cells. x 190.

Fig. 3.4. During prophase I the tapetal walls breakdown and the protoplasts (arrows) then migrate into the loculus as discrete entities. x 190.

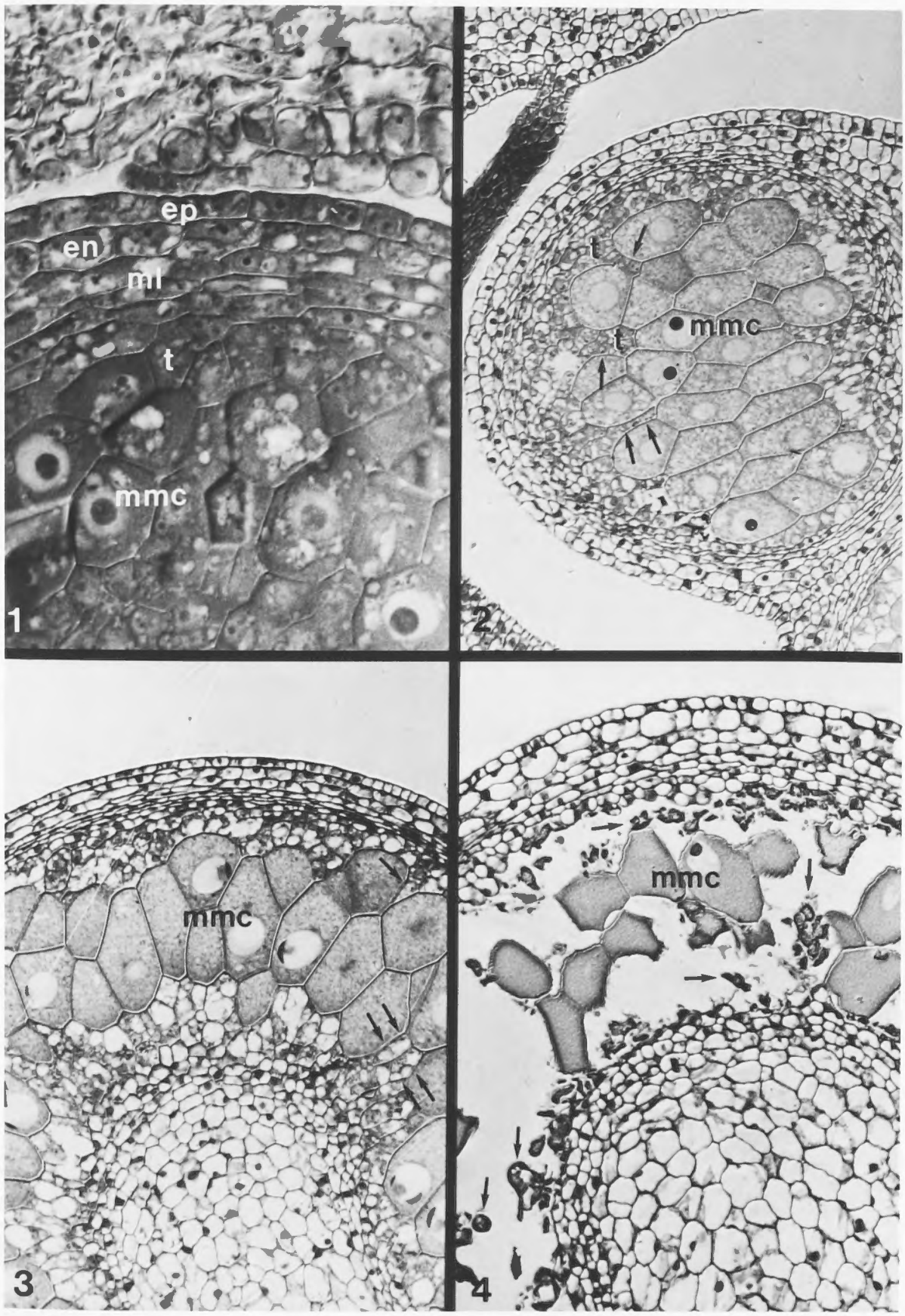
ep
en
ml
t
mmc
1
t
mmc
t
2
mmc
3
mmc
4

Fig. 3.5. General ultrastructure of a premeiotic tapetal cell as seen in a transection of the anther (mmc, microspore mother cells). x 4,500.

Fig. 3.6. A tapetal cell at the time of prophase I. The radial (stars) and inner periclinal walls (asterisk) have dissolved by this time, but the cells remain in situ. Cytomictic channels can be seen in the lower right corner (ml, middle layer of the anther wall). x 5,700.

Fig. 3.7. High magnification view of a cytomictic channel traversing a partially dissolved wall, connecting two tapetal cells at their radial surfaces. Cell coat granules are already visible on the outer face of the plasma membrane. x 72,000.

Fig. 3.8. A part of the tapetal cell at prophase I to show aspects of cortical cytoplasm and cell surface. Note the microtubules (arrowheads) and the cell coat (arrows). Dictyosomes (D) and their vesicles are present. Similar, though enlarged, vesicles occur near the cell surface (1,2) and profiles suggestive of exocytosis are seen (3). The topologically external face of the membranes of the vesicles does not have a cell coat, though the granules in the vesicles are not like those of the cell coat. Asterisk near the wall shows a presumed lipidic deposit. x 71,500.

Fig. 3.9. A part of tapetal cell nucleus to show an aggregate of intranuclear vesicles (arrowheads) and the distention of the membranes of nuclear envelope (arrow). x 42,000.

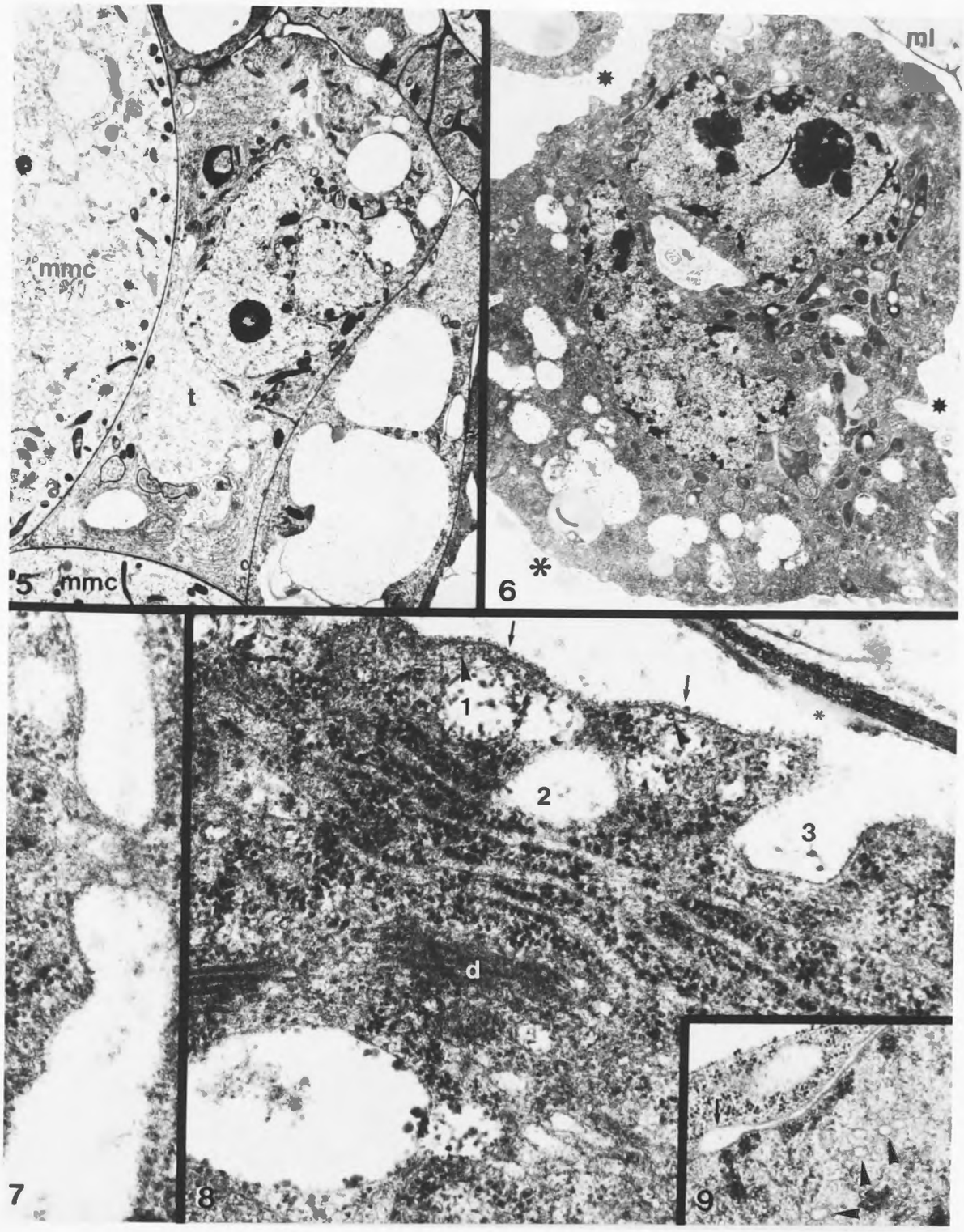
mmc
t
5 mmc
ml
6
1
2
3
d
7
8
9

Fig. 3.10. Interference contrast image of tapetal cells and microspores (m). The tapetal cells remain discrete (n, nucleus; v, vacuole). x 1550.

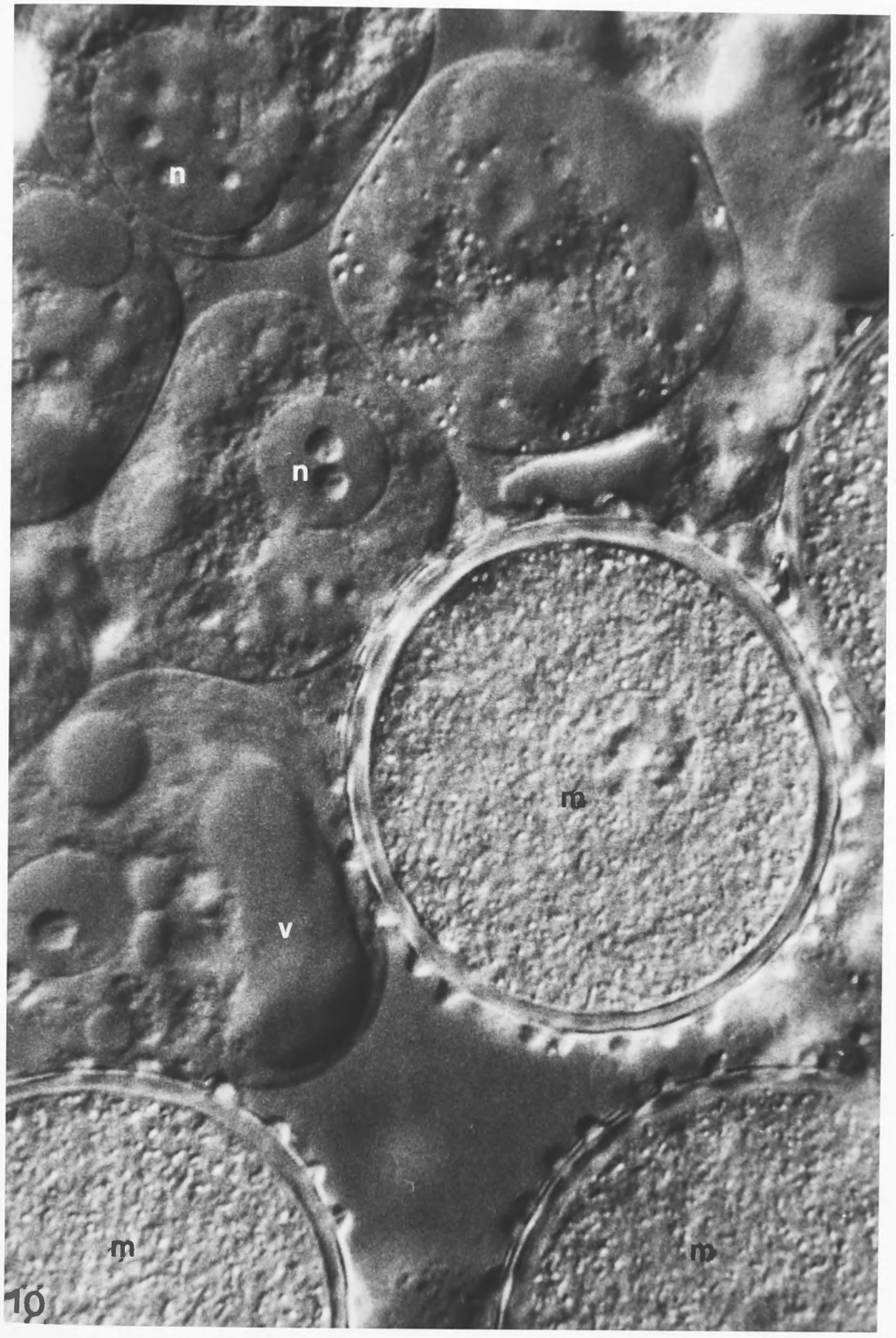
n
n
m
v
m
m

Fig. 3.11. A tapetal cell after its migration into the anther cavity, containing numerous dictyosomes, mitochondria, and plastids (densely stained). x 6450.

Figs. 3.12-3.16. Grazing and median sections of the tapetal cells to show aspects of granulo-fibrillar extracellular cell coat.

Figs. 3.12, 3.16 are conventional preparations. Cell coat fibrils are shown by arrows. x 47,250 and 75,000, respectively; Fig. 3.13, freeze-substituted in acetone and contrasted in 1% acetone plus 0.5% tannic acid. Note the congruent orientation of microtubules (arrows) and cell coat fibrils (double headed arrows). x 72,000.

Figs. 3.15, 3.16 show cells treated with 0.5% tannic acid after osmication. Microtubules are shown by arrowheads and cell coat fibrils by arrows. x 81,000.

Fig. 3.17. A section subjected to the Thiéry reaction reveals the deposition of silver grains, particularly in the electron dense granules of the cell coat. x 102,900.

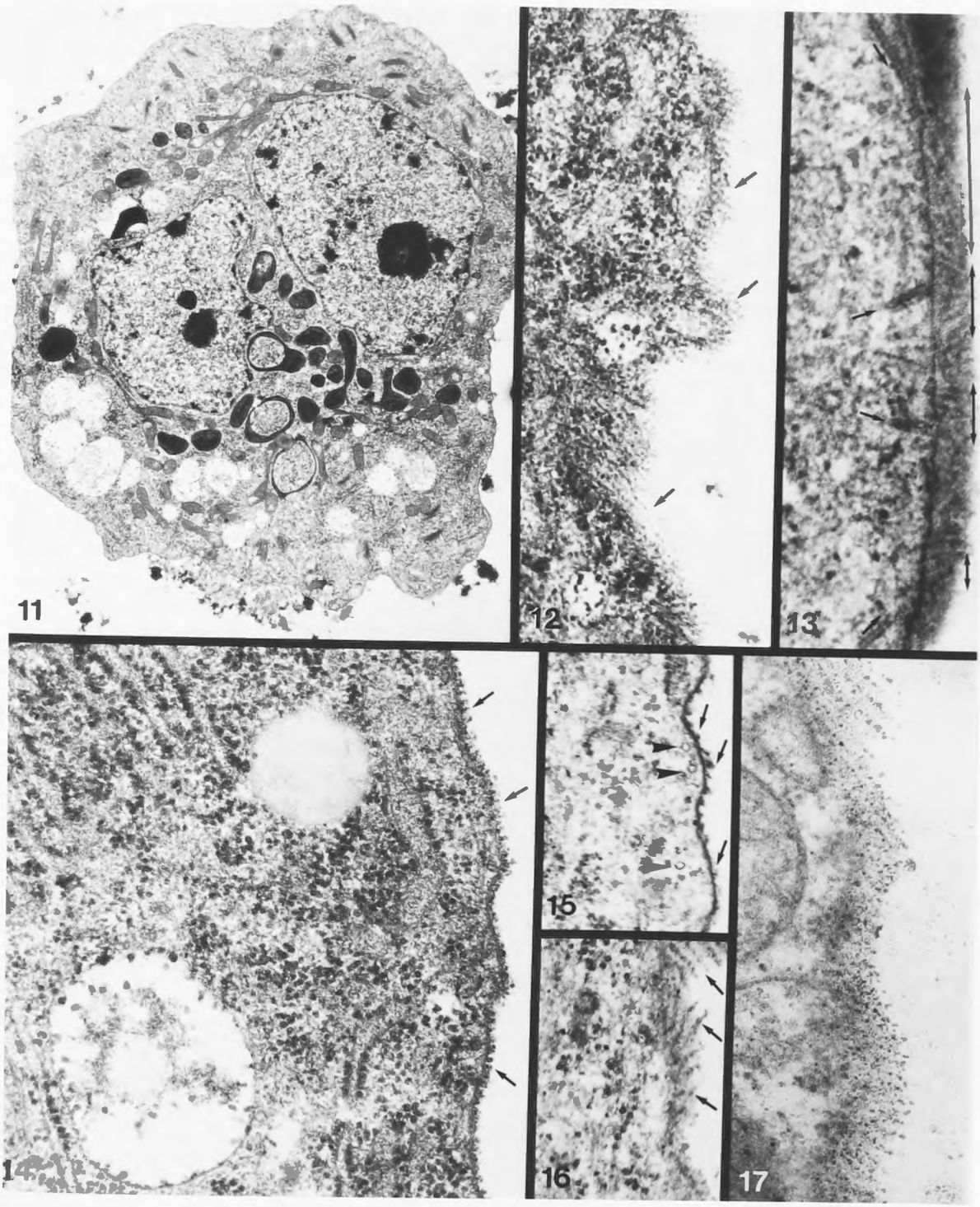
11
12
13
14
15
16
17

Figs. 3.18,3.19. Tapetal cell treated with potassium ferrocyanide. Fig. 3.18 unstained and Fig. 3.19 post-stained with uranyl acetate and lead citrate, showing plastid, mitochondria, and vesicular and cisternal endoplasmic reticulum with luminal contents. x 90,350 and 54,500, respectively.

Figs. 3.20,3.21. Cells treated with ruthenium red. Fig. 3.20 unstained and Fig. 3.21 post-stained with uranyl acetate and lead citrate. Note the interconnected cisternae of ER, filled with flocculent contents (as in Fig. 3.19). x 64,000 and 44,800, respectively.

Figs. 3.22,3.23. Fluorescence and bright field micrographs of a tapetal cell showing the ConA-FITC binding at the cell surface. x 1,100.

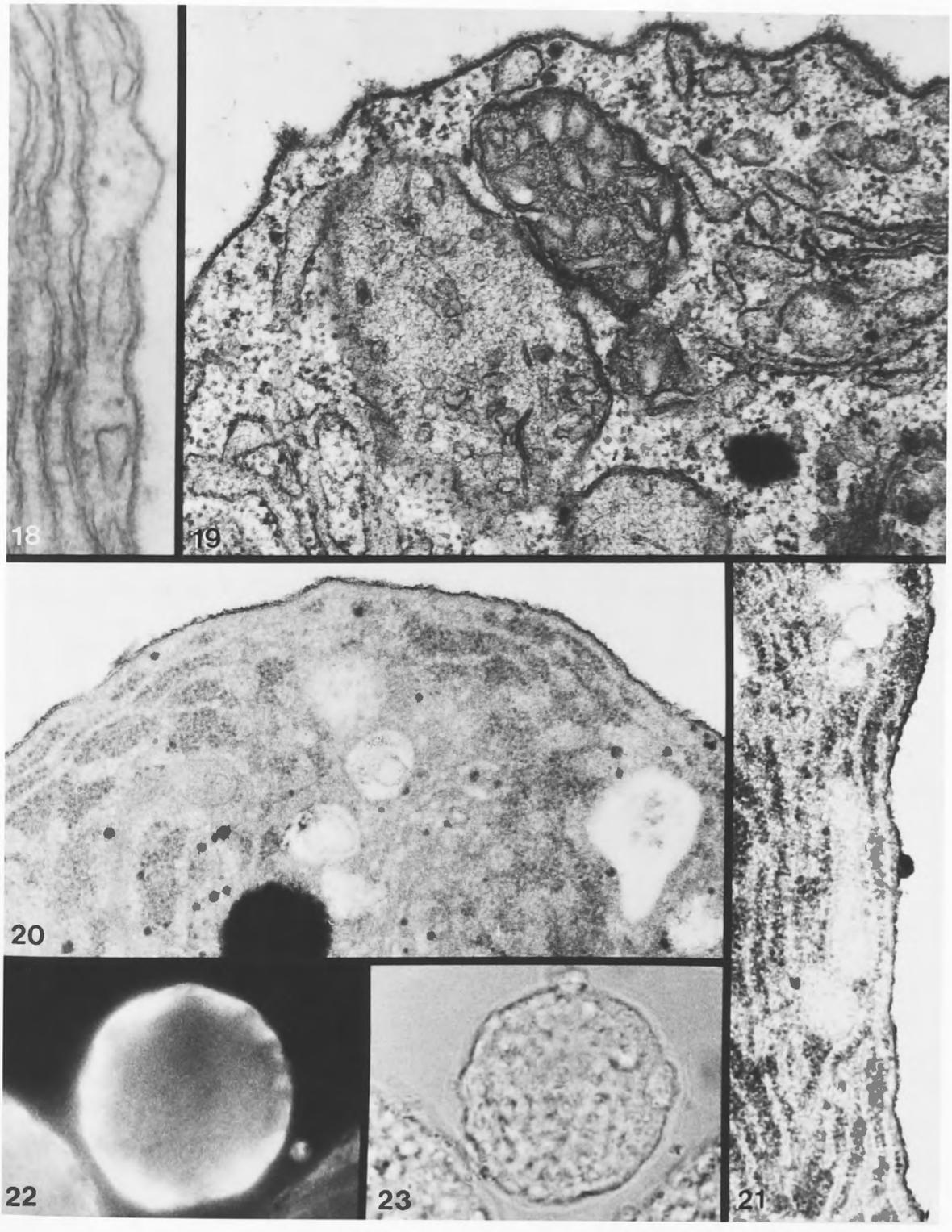
18
19
20
21
22
23

Fig. 3.24. A tapetal cell seen at the tetrad stage. Note the lipid droplets at the cell surface, the extensive peripheral ER with distended lumen, and the clusters of mitochondria and dictyosomes. The area within the broken lines is magnified in Fig. 3.25. x 7,450.

Fig. 3.25. Magnified view of a part of the cell shown by broken lines in Fig. 3.24. The outermost cisternae of the ER sometimes approach the plasma membrane and appear to touch it. x 21,800.

Fig. 3.26. Section subjected to Thiéry reaction reveal silver aggregates at the plasma membrane indicating the presence of a glycocalyx at this stage of development. The flocculent contents of the ER do not react. x 64,400.

Fig. 3.27. A part of tapetal cell stained with Thiéry reaction showing the reaction product in the cell coat and the dictyosomal vesicles (arrows; d, dictyosome). x 56,000.

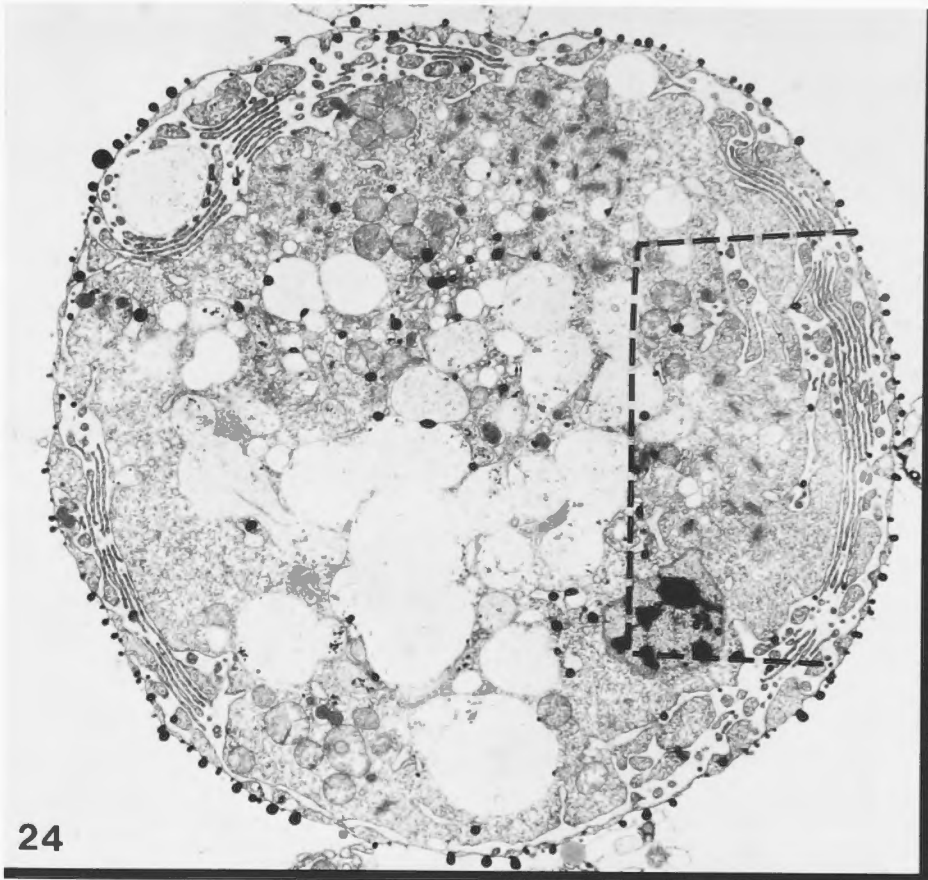
24

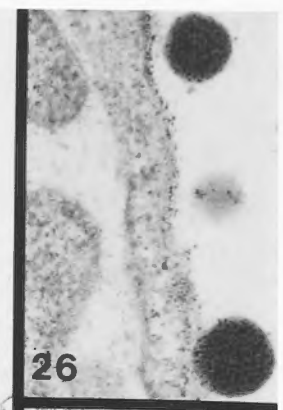
26


d
27

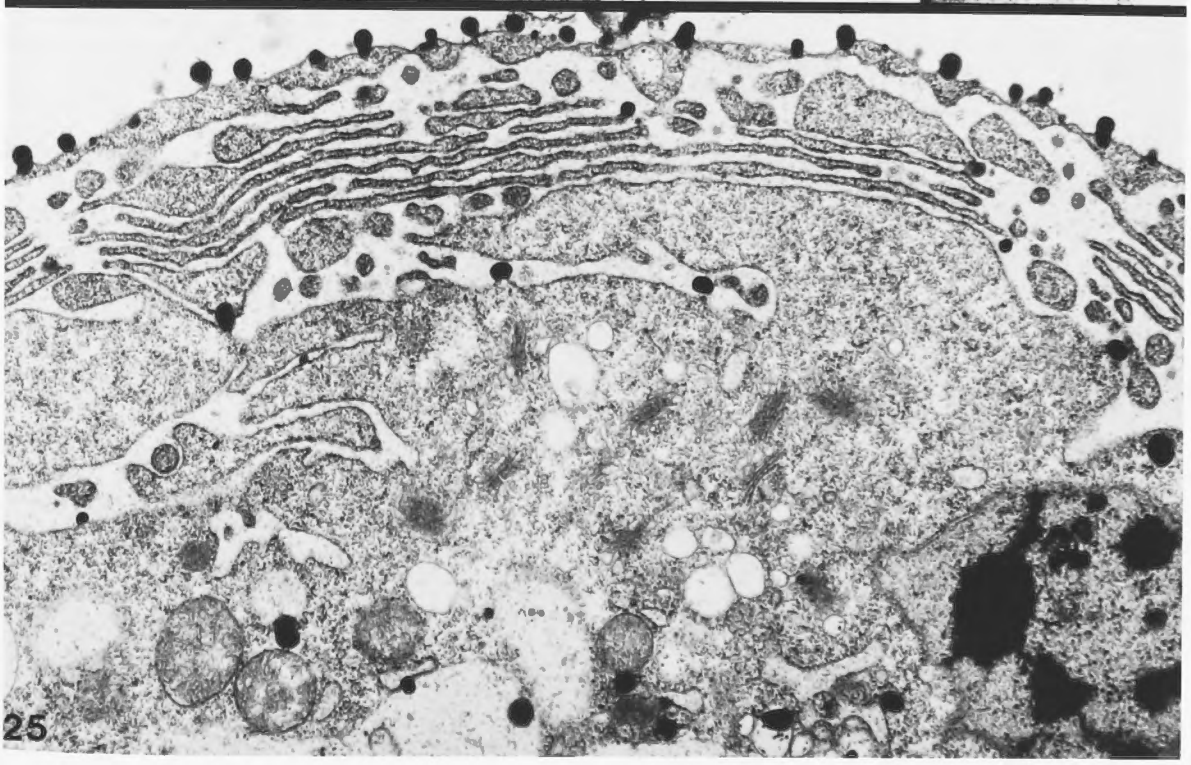
25

Fig. 3.28. Part of a tapetal cell freeze-substituted in acetone plus osmium. Note the close association between the ER cisternae and the plasma membrane (arrowheads), but no continuity of these two membranes is evident. The electron dense material outside the plasma membrane is the agar of the film on which cells were placed before freezing (arrows, microtubules). x 60,350.

Fig. 3.29. Part of a tapetal cell freeze-substituted in acetone and osmium to show aspects of dictyosomes. The vesicles have uniform contents and are not distended (cf. Fig. 3.30). The upper dictyosome shows structural elements between the cisternae. x 51,000.

Fig. 3.30. Dictyosomes from a tapetal cell at the same stage as in Fig. 3.29, prepared in conventional manner. x 3,000.

Fig. 3.31. A plastid from a freeze-substituted tapetal cell showing the associated microtubules (arrowheads). x 39,430.

Fig. 3.32. Cytoplasmic lipid bodies (l) occasionally show bundles of filamentous material (arrows) in their vicinity. x 81,430.

Fig. 3.33,3.34. Immunofluorescence and phase contrast micrographs of a tapetal cell soon after its release, to show the microtubules stained by a monoclonal antibody raised against β-subunit of chick brain tubulin. Microtubules at prophase I are not as abundant as later, and show a polarised orientation, running transverse to the long axis of the cell. x 1,500.

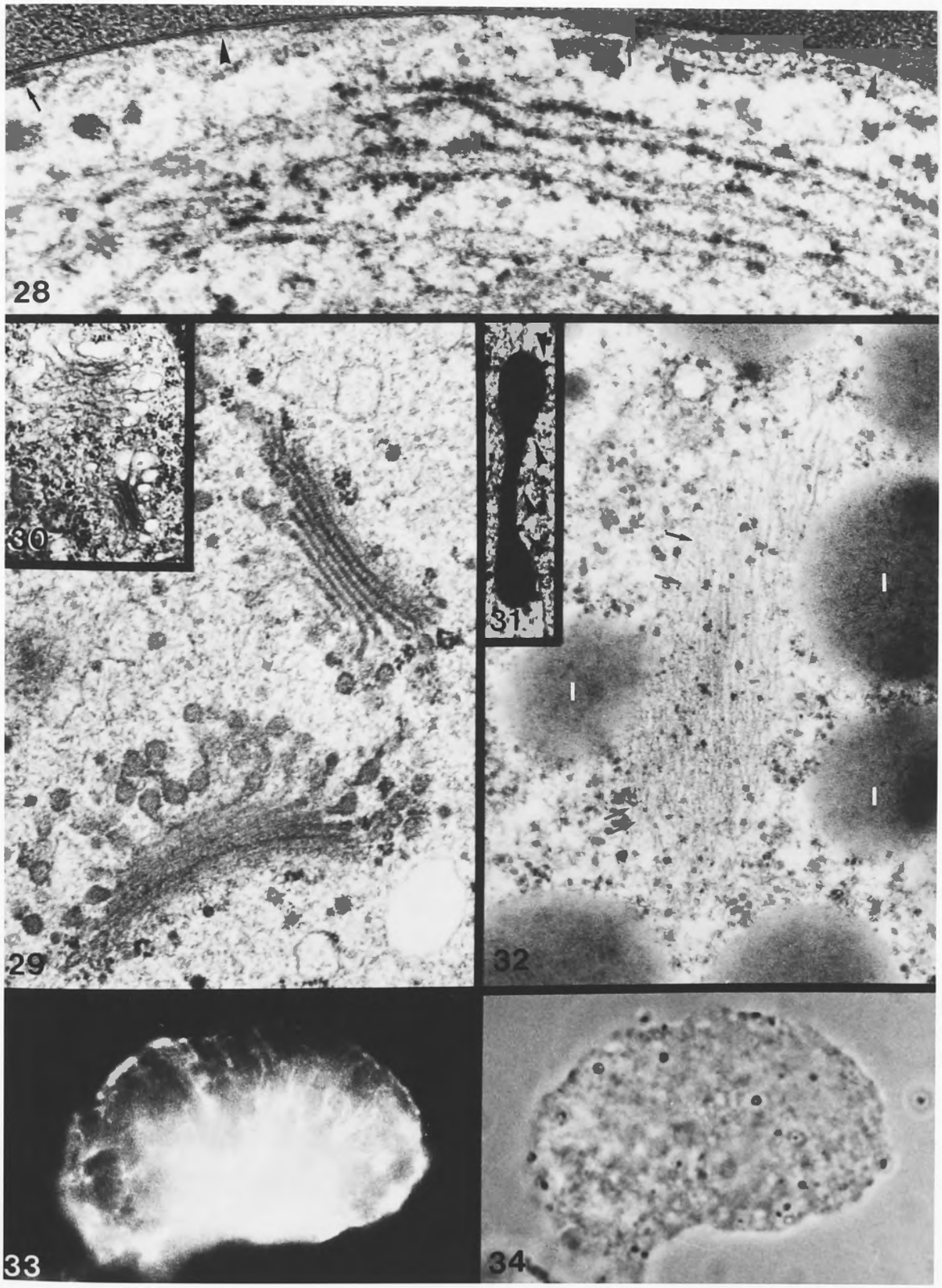
28
30
29
31
32
33
34

Fig. 3.43. Part of a tapetal cell in the early stages of degeneration. The ER becomes highly branched and vesiculate, though microtubules (arrowheads) remain. Note the beginning of the accumulation of electron-dense material. x 41,800.

Fig. 3.44. A tapetal cell that has progressed further toward degeneration, with apparently empty ER lumina and numerous distended vesicles or vacuoles. x 6,000.

Fig. 3.45. Tapetal cytoplasm showing advanced features of degeneration. The densely osmiophilic material appears to occlude many organelles and even becomes deposited on the plasma membrane (arrows). x 93,000.

Fig. 3.46. A nearly degenerate tapetal cell. Note the massive increase in electron dense material and vacuoles. x 6,900.

Fig. 3.47. A fragment of tapetal cell seen in close association with a spinule (pw) of the pollen wall (arrowheads). x 2,850.

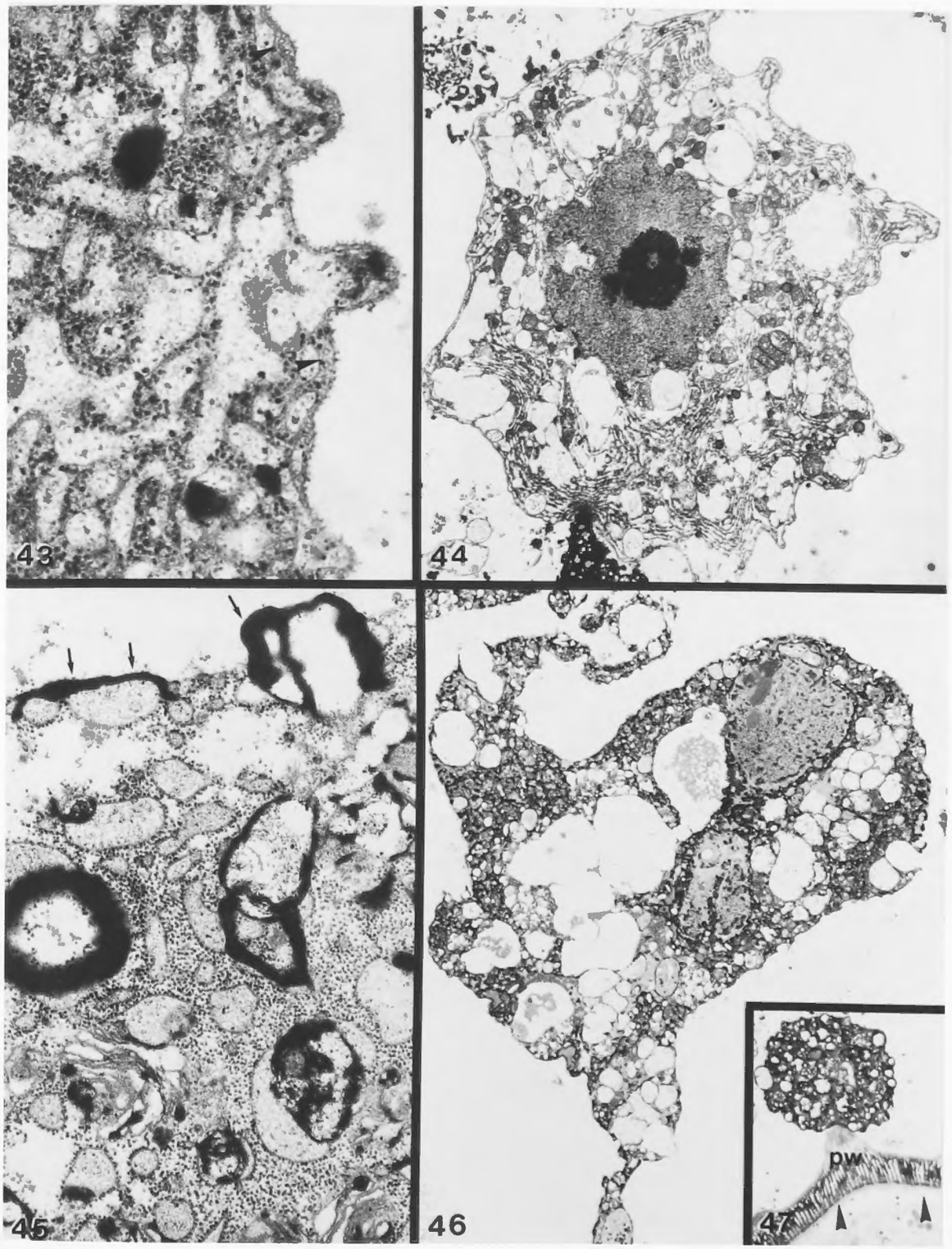
43
44
45
46
47
pw

Fig. 3.48. Scanning electron micrograph of mature pollen grains at the time of dehiscence showing tryphine deposits (arrows) on their surfaces. x 900.

Fig. 3.49. Granular deposits seen in the anther cavity after 36h of colchicine treatment. Note the central electron-lucent areas and the electron-dense coating (sw, spore wall). x 96,000.

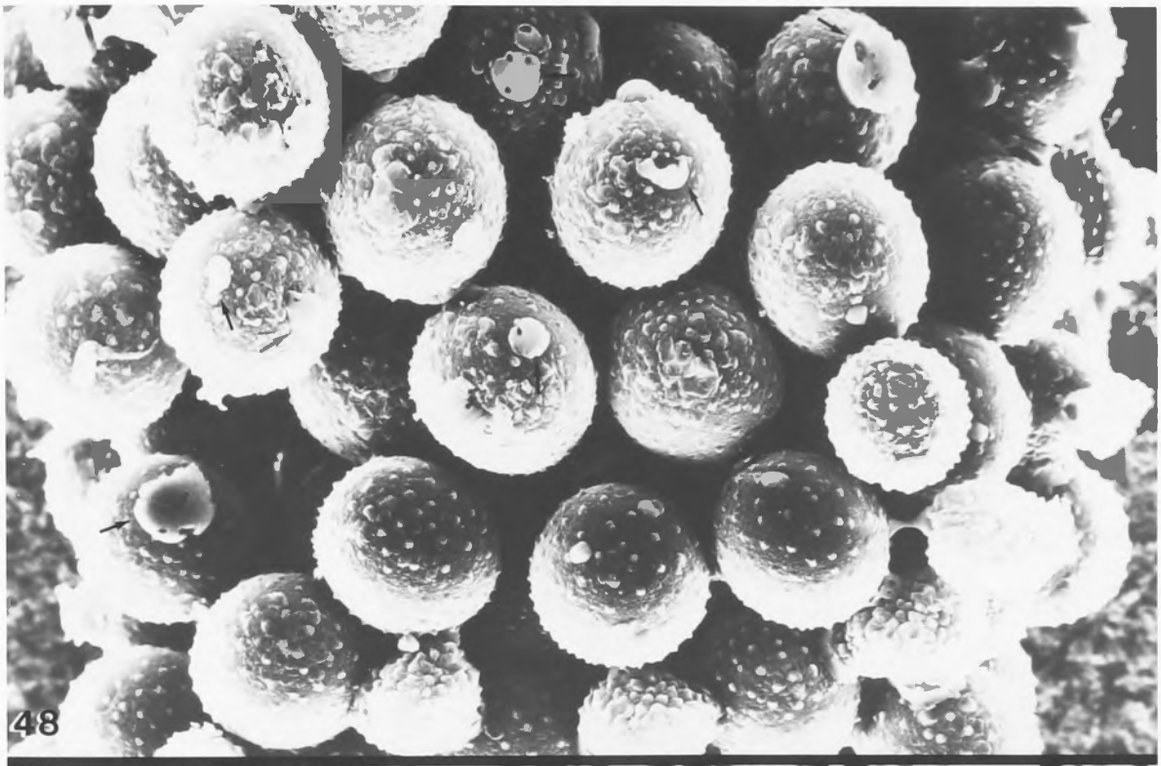

48

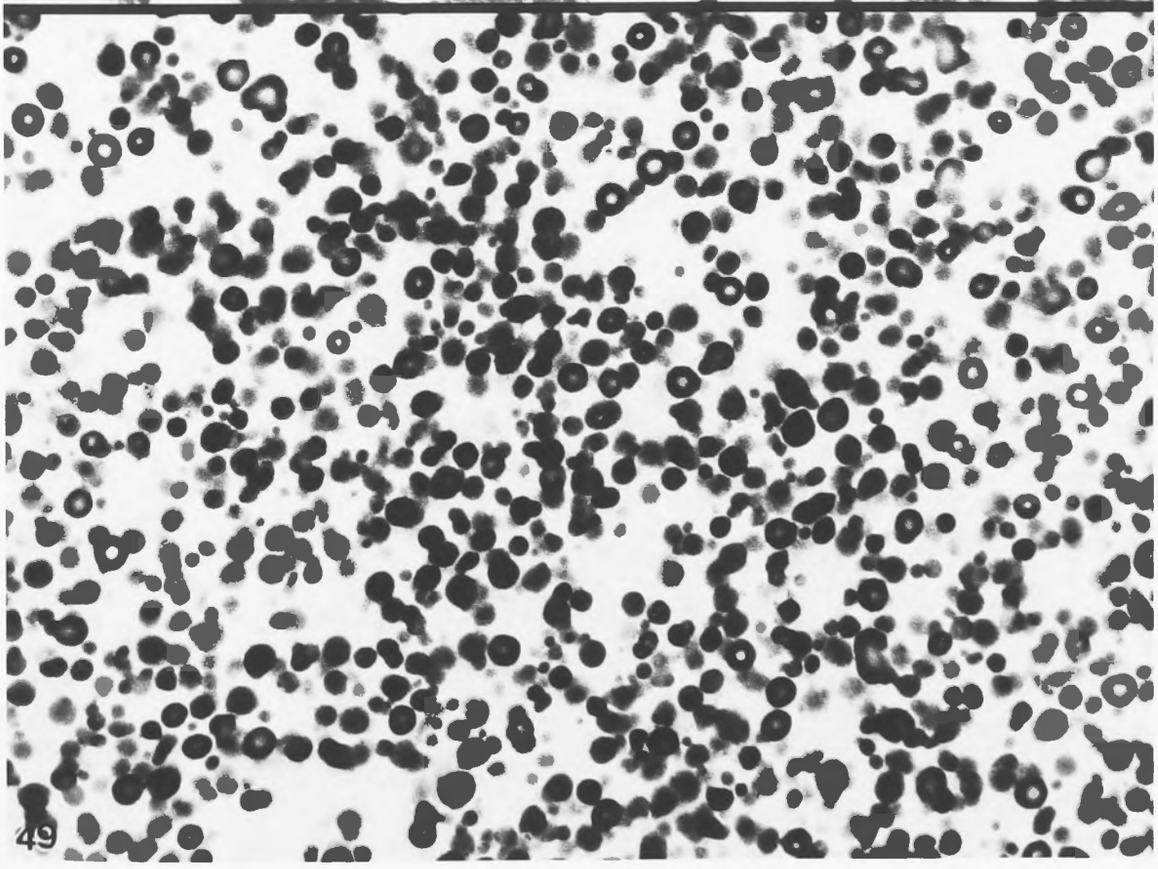

49

CHAPTER 4

DEVELOPMENT OF PLASMODIAL TAPETUM IN *TRADESCANTIA VIRGINIANA* L.

4.1. INTRODUCTION

Developmental details of the plasmodial type of tapetum are less well known than in the case of secretory tapeta. Only three species with plasmodial tapetum have been studied in some details: *Tradescantia bracteata* (Mepham and Lane, 1969a,b), *Arum italicum* (Pacini and Juniper, 1983), and *Amphibolis* (Pettitt *et al.*, 1984), although there are less full descriptions of several other species (Owens and Dickinson, 1983; see also the literature cited in Pacini and Juniper, 1983). It has been suggested that in *Arum*, microtubules are responsible either for bringing about the invasion of the anther loculus by the tapetal cytoplasm, or to "guide an otherwise initiated flow in the right direction". The investigations reported in this Chapter were started as an extension of the work of Pacini and Juniper (1983), and aimed at elucidating the organization and aspects of the cytoskeleton and the cell surface during plasmodium formation, and to gain an insight into the sporophyte-gametophyte interactions, especially the provision of sporopollenin by the plasmodium.

The idea that the tapetum provides spore cells with sporopollenin precursors after the dissolution of callosic walls of young tetrads has been in currency from the beginning of this century (see Heslop-Harrison, 1968b). Definitive experimental evidence is lacking, but support is found in the following observations: (i) In the secretory type of tapetum, concomitant with the pollen

wall growth, the inner face of the tapetum develops a granular deposition of sporopollenin known as orbicules or Ubisch bodies. These bodies have been considered to be a transport form of sporopollenin to be deposited on the spore wall (see Echlin, 1971a,b) or a by-product of that transport process. (ii) In a large number of species the spore cells enlarge (sometimes as much as 30 fold, see Echlin, 1971a), with concomitant spore wall growth and deposition. It has been considered unlikely that the spore cells would carry enough reserve metabolites to account for this growth and that the tapetum must, therefore, supply precursors. (iii) In sterile spores, exine development has been known to continue even after the degeneration of spore cytoplasm indicating that the precursors for spore wall growth must come from elsewhere. Several questions, however, remain unresolved. These concern the cellular mechanism of synthesis of sporopollenin in the tapetum, its secretion from the tapetum and transfer across the apoplastic gap between tapetum and the spore wall, and its assembly on the pollen wall to generate species-specific patterns of spore wall. Clearly, the transfer of sporopollenin from the tapetum in the form of orbicules seems unsatisfactory since orbicules are not of universal occurrence, even in secretory tapeta (for example, see Misset and Gourret, 1984); they certainly have not been reported for any plasmodial tapetum. Besides, as pointed out by Mepham (1970), it is difficult to imagine how polymerized sporopollenin of the

orbicules could migrate and be incorporated in the spore wall to form specific ornamentations of the exine. Indeed, controversy has arisen about whether tapetum contributes to the growth of the spore wall at all (Mepham, 1970; Mepham and Lane, 1968, 1969a,b, 1970). It is held that the spore wall can develop completely while the spores are still enclosed in the callosic wall, implying thereby that the tapetum does not contribute (Mattsson, 1976; Roland-Heydacker, 1979; Audran, 1981; Zavada, 1983), since the callosic wall would pose a barrier to precursors.

The investigations reported here focus on these problems. This Chapter describes hitherto unreported details of tapetal invasion into the anther loculus followed by establishment of a syncytium, the post-meiotic structural and developmental details with relevance to the plasmodium's secretory functions. Further insights obtained through the use of colchicine treatments have been reported in Chapter 5.

4.2.MATERIAL AND METHODS

Plants of Tradescantia virginiana L. "Sydney hybrid" were grown and maintained under natural lighting and day-length in a glasshouse.

4.2.1. Conventional Electron Microscopy

Buds were harvested at different stages of spore development, and the anthers dissected out while immersed

in the fixative, fixed for 2h to overnight in 2.5% glutaraldehyde plus 3% paraformaldehyde in 0.025M phosphate buffer at pH 7.0, washed in the buffer, post-fixed for one hour in 1% buffered osmium tetroxide, dehydrated in a graded series of acetone solutions and then embedded in Spurr's resin. Ultra-thin sections were cut on a diamond knife, collected on formvar-coated slot grids, stained with saturated uranyl acetate in 50% ethanol and aqueous lead citrate, and observed using a Hitachi H500 or H600 transmission electron microscope at 75kV.

4.2.2. Cytochemistry

4.2.2.1. The Thiéry Reaction

To localize polysaccharides at the ultrastructural level, the Thiéry reaction (Thiéry, 1967) was employed. Thin sections were collected in plastic loops (see Roland, 1978) and processed as described in Chapter 3.

4.2.2.2. ZnIO-Impregnation

The zinc-iodide-osmium tetroxide impregnation method of Harris and Chrispeels (1980) was employed to study the conformation of the ER. Anthers were fixed in the usual aldehyde fixative (buffered) for 2h at room temperature, washed in buffer and post-fixed in zinc-iodide-osmium tetroxide (ZnIO) complex for 4-16h at $4^{o}C$. The complex was prepared freshly by mixing equal volumes of 2% osmium tetroxide and zinc iodide solutions. Zinc

iodide was prepared by adding 3gm zinc powder to 20ml of water, sonicating for 2 minutes and later adding 1gm of iodine, stirring for 5 minutes and filtering. The filtrate was mixed immediately with an equal volume of 2% osmium tetroxide and used. Repeated changes with fresh ZnIO complex in the first 1-2h were found to improve the impregnation quality. After the impregnation, the anthers were washed in distilled water, dehydrated in a graded series of acetone solutions and embedded in Spurr's medium. Thick (0.25-1μm) and ultra-thin sections were cut. Thin sections were lightly stained with alcoholic uranyl acetate and lead citrate whereas thick sections were observed unstained with a Hitachi H600 TEM at an accelerating voltage of 75kV.

4.2.3. Immunofluorescence of Tubulin

Microtubules were visualized by indirect immunofluorescence employing a monoclonal antibody raised against α-tubulin. Whole anthers were fixed in 4% paraformaldehyde plus 0.2% glutaraldehyde made up in phosphate buffer (25mM, pH 7.0) for 1h, washed in buffer for 15 minutes and again in phosphate buffered saline (PBS) for 15 minutes. For visualizing microtubules in the plasmodium, antibody was applied to thick sections. For this purpose, anthers (after the PBS wash) were embedded in Tissue Tek II O.C.T. compound embedding medium for frozen tissue specimens (Miles Labs, U.S.A.), frozen in liquid nitrogen and cut in a cryostat at -20^{o}C to produce

sections of approximately 6-10um thickness. Sections were collected on cover slips coated with poly-L-lysine (1mg/ml; Mol. Wt. 54,000), air dried and later flooded with PBS for 15 minutes. Sections were then permeabilized with 1% triton X-100 in PBS for 1h. The excess detergent was then drained and without washing, the sections were incubated in 1:1 mixture of 1% triton X-100 and a monoclonal antibody raised against chick brain tubulin (Amersham, cat. no. N.356; diluted in PBS 1:500) for 45 minutes at 37^{o}C. Sections were then washed thoroughly in PBS and incubated in goat-anti-mouse-IgG conjugated with FITC (Tago; diluted in PBS 1:40) for 45 minutes at 37^{o}C in darkness. Sections were then washed thoroughly in PBS and mounted in moviol containing 2% n-propylgallate (to reduce fading). Observations were made on a Zeiss Photomicroscope using epifluorescence and standard fluorescein filters. Photographs were taken on Kodak Tri X film. Controls included the use of goat-anti-mouse-IgG-FITC alone and replacing anti-tubulin with an irrelevant monoclonal anti-actin antibody (Amersham, cat. no. N.350; diluted in PBS 1:500). The two control procedures gave no staining of structures that resembled those which stained with anti-tubulin.

4.2.4. Osmium Maceration

To visualize the 3-dimensional disposition of the endoplasmic reticulum (ER), the PSM and the spore tetrads, an osmium maceration procedure was employed. After trying

out several variations described in the literature which produced unsatisfactory results, the following protocol was developed. Anthers were fixed in buffered glutaraldehyde-paraformaldehyde for 1h at room temperature, washed in buffer (15 minutes) and frozen in liquid propane cooled by liquid nitrogen. They were then transferred onto a metal block which was precooled by liquid nitrogen, and fractured with a razor blade. Pieces of anther were then transferred in frozen condition to vials containing 1% osmium tetroxide in acetone and dry molecular sieve (precooled by liquid nitrogen), and left at -85^{o}C. After 3 days the samples were transferred to fresh osmium in acetone (precooled to -85^{o}C) and the vials left in the ultrafreezer for 25 days. Vials were then gradually brought to room temperature, the specimens transferred to fresh dry acetone and washed overnight in two changes of acetone. The samples were then critical point dried employing liquid carbon dioxide, sputter-coated with gold and observed in a Jeol 100C STEM at an accelerating voltage of 80kV.

4.3. OBSERVATIONS

In the following description of tapetal development, developmental stages of the sporogenous cells are used as reference points.

4.3.1. Premeiotic Stage

Tradescantia anthers are tetrasporangiate with an epidermis, endothecial layer, two middle layers and a single-layered tapetum which in places becomes bilayered. Tapetal cell nuclei are large and highly lobed with condensed chromatin.

The tapetal cytoplasm is richer in ribosomes than are sporogenous cells. The rough endoplasmic reticulum (ER) contains some flocculent material; mitochondria are elongated or round, plastids are mostly dumbbell shaped, and there are a few large vacuoles. Dictyosomes are few with associated electron translucent vesicles, many of which are seen close to the radial and periclinal walls. Calcium oxalate crystals are abundant.

Tapetal cell walls are thin and exhibit loose microfibrillar arrangement at the premeiotic stage. Cortical microtubules, few in number, lie mostly (in transverse sections of anthers) longitudinally with respect to the anther along the tapetal-sporogenous and tapetal-middle layer interfaces. Occasionally, they can also be seen in oblique profiles along the radial walls. Microfilaments could not be visualized.

The tapetal cells are connected to each other and to the inner middle and outer sporogenous layers by plasmodesmata. Prior to meiosis, however, tapetal plasmodesmata are replaced by large cytomictic channels which can be seen along the radial walls, and connections between the tapetum and sporogenous tissue are lost.

4.3.2. Prophase I

With the onset of prophase I in sporogenous cells, the inner periclinal walls (and even the outer periclinal walls of the inner tapetal cells in areas where the tapetum is bilayered) of tapetal cells start undergoing dissolution (Fig. 4.1), this process later extending to the lateral walls. The cytomictic channels become enlarged. Dissolution of radial walls takes place relatively slowly (Fig. 4.7) and many cells retain partially dissolved walls until as late as the dyad stage of meiosis. Moreover, the bases of the radial walls (towards the middle layers) persist and show a deposit of (presumed) lipidic material on them. In places where the radial walls have dissolved completely, the plasma membranes of the adjoining tapetal cells do not fuse at this stage (Fig. 4.7).

Concomitant with dissolution of the tapetal walls, the sporogenous cells (SCs) start separating and rounding up, and large spaces develop between them (Figs. 4.1,4.3) as the anther grows.

When dissolution of inner periclinal walls of tapetum and separation of SCs has progressed, the tapetal protoplasts start forming large invasion processes (Fig. 4.3) which invade the spaces between the SCs. In spite of the presence of cytomictic channels, the formation of invasion processes is not synchronous in all tapetal cells. Some of the tapetal cells, probably where the tapetum is bilayered, migrate as a whole between the SCs

(Fig. 4.11). Concurrently, the population of ribosomes (free or attached to ER), mitochondria, plastids and dictyosomes increases in the main body of the tapetal cells. A few multivesicular bodies and lipid bodies can also be seen at this stage. Often some of these organelles are encircled by ER cisternae.

The ER is mostly rough and occupies sites near the cell surface or nuclei and in the invasion processes (Fig. 4.6). Often, the cisternae seem to focus upon a region in the cytoplasm close to the nucleus. Cisternal, tubular and vesicular forms are seen, all carrying flocculent contents.

The dictyosomes appear hypertrophied at this stage and are associated with two kinds of vesicles: small ones with electron-opaque contents and other larger ones with smooth intensely osmiophilic membranes and mostly electron-lucent contents. The former type is seen close to the plasma membrane. The electron-lucent vesicles, on the other hand, apparently coalesce to form much larger complexes containing some fibrous material, possibly a mucilage or slime (Figs. 4.7,4.11). These organelles, and most conspicuously the parallel stacks of ER, migrate as components of the invasion processes (Fig. 4.6).

At this stage a few aggregates of large membrane sacs, distinct from ER, also become apparent. The origin of these sacs could not be determined with certainty even after serial sectioning. Their initial location in the cytoplasm is highly variable. Microtubules and coated

vesicles are commonly associated with them. The staining properties of the membranes of these sacs are exactly the same as that of the plasma membrane if it is assumed that the lumen of the sac is topologically equivalent to the exterior of the cell: on this basis the outer layer of their membrane is the more densely osmiophilic (Fig. 4.15, compare with Fig. 4.2). Also, the membranes of these sacs react positively in the Thiéry reaction (Fig. 4.14), just as the plasma membrane.

Some of the invasion processes reach far inside the loculus, but those originating from different cells do not fuse (Fig. 4.10). When invasion processes from different cells meet they form apposition areas at which the membranes appear smooth with no cell coat. However, the free surfaces of tapetal cells show a thick, amorphous, irregularly placed, patchy coat, particularly prominent at the apices of the invasion processes and thinner on their lateral surfaces (Fig. 4.6). The plasma membrane on the outer periclinal side maintains firm adherence to the wall. However, in areas where the plasma membrane had withdrawn from the wall during preparation for electron microscopy, there was no extracellular cell coat (Fig. 4.20), in spite of the fact that some vesicles containing the fibrillar component were apparently fusing with the membrane in that region. A sparse cell coat was also present on the radial surfaces where the wall dissolution was more or less complete (Fig. 4.21). The Thiéry reaction, when applied to the ultra-thin sections,

revealed essentially the same features as those obtained by conventional preparations. The outer leaflet of the tapetal plasma membrane appeared highly electron-dense throughout the course of development. The extracellular cell coat present on the radial surfaces (Fig. 4.21) and the invasion processes (Fig. 4.22) reacted positively. Reaction product was also found on the fibrous contents of large dictyosomal vesicles.

The microtubules become frequent. After the inner periclinal walls have disappeared but the invasion has not commenced, most of the microtubules in a cross section of anther show transectional profiles along the inner and outer periclinal surfaces of the tapetal cells (Fig. 4.2). At this stage the tapetal cells bulge into the spaces between the SCs, where the invasion processes will later form. Microtubules were never seen in the bulges, but occasionally could be seen at their boundaries. Later, in addition to their transectional profiles along the original outer and inner periclinal walls, microtubules could be seen at a much higher frequency in transectional or oblique profiles all along the lateral surfaces of the invasion processes (Figs. 4.4,4.5,4.8). No microfilaments were ever recorded in the cytoplasm before the invasion, or even in the bulge region. Special attention was focussed on looking for microfilaments in the tapetal cytoplasm after the tapetum invaded the loculus (see later). So far, only the images shown in Fig. 4.9, where a possible microfilament bundle is seen

running parallel to the long axis of the invasion process, have been recorded. The image, however, is by no means conclusive (see later). If such bundles are present they must be labile.

4.3.3. Meiosis

Invasion by the tapetal cells continues during the subsequent stages of meiosis. Some invasion processes branch in the spaces between the meiocytes. Sometime between the prophase I and dyad stages the tapetal nuclei undergo division; most cells become binucleate, but occasionally as many as four nuclei are formed. Some of the nuclei begin moving into the invasion processes. The cells still remain more or less intact and separated along their invasion processes (Figs. 4.12,4.18) and often along the site of the original radial walls.

The earliest events of cell fusion are seen at this time (Fig. 4.18). Fusion appears to take place at the sites referred to as apposition areas in the description of the prophase I stage of tapetal development. Microtubules become more prominent at these areas (Figs. 4.16,4.17), aligned along the membranes in criss-crossed bundles (Fig. 4.19). The cell coat is absent along these surfaces, but membrane sacs lie nearby (Fig. 4.18). Free surfaces of the invasion processes retain their extracellular coats up to the dyad stage. Subsequently, the coat thins out and eventually disappears during the second meiotic division or early post-meiotic stages when

a large number of the tapetal cells have fused more or less completely to form a true plasmodium (Fig. 4.23).

At the dyad stage the cytoplasm shows increased amounts of rough ER, crystals, polyribosomes, plastids, mitochondria, dictyosomes and vesicles containing fibrous material (Fig. 4.12). A few microbodies become visible; plastids continue to show starch grains, and some lipid bodies lie scattered in the cytoplasm.

By far the most conspicuous development at the dyad stage is a large increase in the population of membrane sacs (Figs. 4.12,4.13). Their location is still variable. Coated vesicles and microtubules (Fig. 4.15) are still associated with them. Often the sacs are seen in continuity with the plasma membrane, particularly at the free cell surfaces (Fig. 4.14) and where two invasion processes meet (Fig. 4.18). The sacs often contain single (or aggregates of) membrane-bound granules, especially in those sacs which are at or close to the plasma membranes. Such granules, first detected at prophase I, increase in amount so as to reach their peak frequency at post-meiotic stages. The plasma membrane continues to show a high frequency of coated or smooth vesicles and coated pits. Cortical microtubules still occur all along the inner surface of the plasma membrane, running more or less transverse to the long axis of the invasion process as well as the main body of the cell. They are by no means restricted to the apposition areas.

Although quantitative studies were not undertaken, it appears that the proliferation of various cell organelles continues even after the formation of a true plasmodium - an event which begins during the second meiotic division and is more or less finished by the late tetrad stage. The fusion of plasma membranes of two or more tapetal cells around a developing tetrad results in the formation of a membrane-limited compartment in which the tetrads are lodged (Fig. 4.23). After plasmodium formation the fibrillar component of the cell coat can no longer be visualized at this surface, even with the Thiery reaction, although the membrane of the compartment itself stains positively. Since this membrane is derived from the original plasma membranes of the tapetal invasion processes and still shows the Thiéry-positive characteristics of plasma membrane (unlike the tonoplasts), it will henceforth be referred to as perispore membrane (PSM).

4.3.4. Tapetum at Tetrad Stages

As mentioned before, the fusion of tapetal extensions during late meiosis and early post-meiotic stages results in the formation of a membrane-bound compartment around the developing tetrads (Figs. 4.23,4.24). Cell fusion is slow, spanning the period from early second meiosis to late tetrad stages, and asynchronous so that while some early tetrads appear completely surrounded by compartments consisting of single

membrane expanses, others within the same loculus appear invested by compartments consisting of closely appressed, but discrete, plasma membrane expanses of two or more tapetal invasion processes. Cell fusion is largely accomplished by the late tetrad stage and certainly by the time the plasmodium comes to surround individual microspores, no discrete plasma membranes are seen in the plasmodial mass other than at the tapetum-spore interfaces.

The membrane of this compartment, designated perispore membrane (PSM), is a composite of the plasma membranes of various tapetal invasion processes that fuse to form it. It continues to show the characteristic features of plasma membrane such as its affinity for silver proteinate in the Thiéry reaction (Figs. 4.23,4.24). The extracellular Thiéry-positive cell coat seen on the plasma membranes of tapetal invasion processes prior to cell fusion and during meiosis could not be visualized in post-meiotic stages (Figs. 4.25,4.29, 4.30,4.32).

During meiosis certain membrane sacs associated with microtubules and coated vesicles were found to originate in the tapetal cytoplasm and migrate in a polarized fashion to the plasma membranes of tapetal invasion processes. A partial incorporation of the sacs in the plasma membranes gives the latter a convoluted appearance. In early post-meiotic stages the cytoplasmic accumulations of the membrane sacs persist and large areas

of nascent PSM are devoid of convolutions (Figs. 4.40-4.42). Thus, migration and incorporation of sacs continues even in early post-meiotic stages. In areas of the PSM where membrane sacs have not yet become adjoined, the membrane occasionally shows extensive coating of clathrin-like cages (Fig. 4.41). Migration of the sacs to the PSM is completed by the late tetrad stage, and no cytoplasmic accumulations of them remain by then (Figs. 4.23,4.24). The frequency of the convolutions reaches its maximum around the late tetrad stage. Both parts of the PSM, i.e. the tapetal plasma membranes and the membrane sacs, display an affinity for the Thiéry reagent (Figs. 4.24,4.25), unlike the tonoplasts in the plasmodium. The ZnIO-impregnation method clearly distinguishes between the sacs and ER tubules which lie amongst them (Figs. 4.26,4.27, see also later).

In a gently prepared squash of anthers at the tetrad stage, it is sometimes possible to isolate a tetrad along with its intact PSM. This procedure was employed to use freeze-substitution as a means of checking that the convolutions are not caused by conventional fixation methods. Freeze-substitution confirmed their presence although other PSM-associated features could not be identified. However, the extrusion method employed in freeze-substitution (see Chapter 2) disturbs organelle distributions in the tapetum, and so freeze-substitution of such preparations was only used for detailed studies of spore development.

After dissolution of the callosic wall around the tetrads (referred to as late tetrad stage), the plasmodium does not immediately invade the intermicrosporal spaces. There is a transient stage when all four microspores are still enclosed within a common PSM of the tapetum (Figs. 4.23,4.24). The sacs and convolutions of the PSM in general lie at a rough tangent to the tetrad surface. In median sections the convolutions were rarely seen opening up into the lumen bounded by the PSM whereas in grazing tangential sections openings were seen quite commonly. They were also seen in scanning electron micrographs of anthers subjected to freeze-fracture followed by osmium maceration (Fig. 4.28).

The convolutions of the PSM carry some membrane-bound granules of variable dimensions and intermediate electron opacity (Figs. 4.29-4.32). The membrane around the granules may be either a single layer or made up of multiple concentric layers. The granules have never been recorded in any other part of the tapetal cytoplasm or on any tapetal surface where the sacs had not become incorporated. They have a tendency to aggregate with each other. Their number, like those of the sacs which contain them, reaches its peak coincident with the dissolution of callosic walls around the tetrads. During the formation of the granules, some surfaces of the sacs or PSM convolutions form small projections into the lumen (Fig. 4.31). The projections have swollen heads with one or more granules of electron-opaque material, probably

lipidic, contained within. Conceivably, a simple pinching off of the swollen heads would result in the formation of single or composite membrane-bound granules. The membrane surrounding the granules, as well as the PSM, is Thiéry-positive (Fig. 4.25), consistent with an origin of the former from the PSM. Many granules, particularly the ones which are detached from the PSM surface show a thin electron-dense deposition on their exterior surface. At late tetrad stage a few convolutions also contain an electron-dense amorphous material (Figs. 4.29,4.30). Many granules are also present in the lumen bounded by the PSM and in the intermicrosporal spaces of late tetrads (Figs. 4.23,4.24), often close to the spore wall. However, no physical continuity was ever recorded between the granules and the spore wall.

A consistent feature of the PSM at post-meiotic stages is its association with numerous microtubules and coated or smooth vesicles. Application of a monoclonal antibody which reacts with the α-subunit of the tubulin molecule to frozen sections revealed microtubules underlying and tangential to the PSM at the later part of tetrad stage (Figs. 4.34-4.37). Ultra-thin sections cut normal or tangential to the PSM also reveal these microtubules (Figs. 4.30,4.32,4.38). Analysis of adjacent serial thin sections showed that most of them are short.

At the early tetrad stage some of the PSMs, particularly those formed as a result of apparently complete fusion of tapetal extensions, begin to show

massive accumulations of tubular ER in their vicinity (Fig. 4.40). There are, however, still a large number of PSMs or 'pseudo-compartments' which do not show this feature; in such cases rough ER continues to be abundant (Fig. 4.41). By the late tetrad stage, however, the tubular ER system develops in the vicinity of almost all the PSMs of a loculus. Thin (Fig. 4.26) or thick sections (0.25-1 μm; Fig. 4.27) of ZnIO impregnated specimens when viewed stereoscopically revealed that these tubules of ER form a complex branched and often interconnected network interdigitating with the convolutions of the PSM. The membranes in the deeper parts of the plasmodium were found to be more ribbon-like sheets which frequently showed connections with the PSM-associated ER and occasional continuities with the nuclear envelope. In conventionally prepared thin sections the tubular ER in the vicinity of the PSM appears filled with flocculent material and seemingly engenders vesicles which accumulate near the PSM (Fig. 4.29), some of them in profiles suggestive of exocytosis. The tubular ER and its vesicles are hardly seen at the outer tapetal face (close to the anther wall layers) although rough ER is abundant throughout the plasmodium. Stereopairs of scanning electron micrographs of anthers subjected to osmium maceration reveal the 3-dimensional relationship of the ER, the PSM and its convolutions and the lumen of the PSM where the spore cells are lodged (Fig. 4.28). Unfortunately, the procedure adopted did not preserve the PSM-associated

microtubules, although it proved excellent for other cytoplasmic features such as endoplasmic reticulum and Fig. 4.33 has been included to illustrate this point. This figure shows the endoplasmic reticulum from the vicinity of the PSM. The flat ribbon-like profiles gradually becoming tubular are clearly shown in the figure.

Many vacuoles are present in the plasmodium and they contain a fibrous Thiéry-positive polysaccharidic material in which a crystalline structure can occasionally be seen. Dictyosomes, mitochondria and plastids are abundant in the plasmodium.

4.3.5. Tapetum at Microspore Stage

After dissolution of the callose wall, the plasmodium invades the intermicrosporal spaces of a late tetrad by protruding secondary invasion processes, in which cortical microtubules are aligned more or less perpendicular to the long axis (Fig. 4.39). This phase of invasion is relatively faster, for although the early invasion processes could be visualized, stages of fusion of these invasion processes in the intermicrosporal spaces could not be seen. When this phase of tapetal invasion is completed, the PSM surrounds each microspore individually (Fig. 4.43). The convolutions of the PSM seen in earlier stages disappear completely, apparently having been utilized for surface expansion during this phase of invasion. At the same time there is no trace of membrane-

bound putative sporopollenin granules between the PSM and the spore wall. However, the PSM itself appears intact and assumes very close contact with the exine of the microspore enclosed within it (Fig. 4.45). On its outer surface the PSM develops a 20nm thick granulo-fibrillar coat (Fig. 4.45). The Thiéry reaction stains both the membrane and the coat material, indicating the presence of polysaccharides in them. This coat appears morphologically distinct from the coat seen on tapetal surfaces in early stages of development. Microtubules are still associated with the PSM although they are less frequent. There were fewer coated vesicles. ER and numerous vesicles remain concentrated near the PSM initially, but gradually this correlation was lost and by mid-microspore stage the tubular ER can only be seen in a few pockets distributed randomly in the plasmodium.

From early microspore stage onwards the tapetum starts synthesizing massive amounts of pigment, presumably carotenes, which imparts a yellowish colour to the anthers. A squash made at this stage shows the pigment located exclusively in the plasmodial mass and the ultrastructural correlate appears to be accumulation of globules in both plastids and the general cytoplasm, although there is a striking difference in the electron density of lipid globules at the two sites (Figs. 4.43-4.45). It is likely that the globules in both locations are lipidic since they are not stained by the Thiery reaction and those in the cytoplasm are strongly osmiophilic in unstained ultra-thin sections.

In subsequent stages of development the plasmodial cytoplasm starts appearing vacuolate, yet there is no sign of degeneration. The vacuoles are frequent and carry fibrous Thiéry-positive polysaccharidic material. Some of them, close to the PSM, show myelin-like multiple layers of membrane. There is an overall decline in the population of ER tubules and cisternae. The tubular ER shows the greater diminuition and by the time of pollen mitosis there is hardly any trace of it left. Free ribosomes, multivesicular bodies, dictyosomes, mitochondria and plastids remain prominent throughout this phase of development. Rough ER gradually establishes a close relationship with various cytoplasmic organelles, particularly plastids, encircling them completely. Dictyosomes continue to appear active, producing numerous vesicles (Fig. 4.45). The granulo-fibrillar coat decorating the external surface of the PSM remains.

By the late microspore stage, when the spores have attained their full size, the PSM has established even more intimate contact with the spore wall, penetrating the interbacular spaces and following the contours of the exine. Recognizable by its positive Thiéry reaction (Fig. 4.46), the PSM still maintains its integrity and retains its granulo-fibrillar coat.

4.3.6. Tapetum at Binucleate Pollen Grain Stage

The amount of lipid and the number of vacuoles increases considerably, although other features are

retained for some time. The morphology of the lipid globules changes from spherical to more amorphous shapes which often appear to occlude various membranous organelles. At the same time the anthers begin to appear yellowish-orange. The PSM retains its prominent coat and associated microtubules (Fig. 4.47) and maintains firm adherence to the pollen wall. Plasmodia from anthers close to the time of anthesis show large apparently empty vesicles (Fig. 4.48) bounded by multiple layers of clear tripartite membranes (Fig. 4.49) often close to the spore wall. Sometimes lipid complexes appear in close association with these vesicles, and this becomes more common as the anthers desiccate. With further desiccation, the lipid bodies tend to cluster around the pollen grains and the PSM starts losing its integrity; discontinuities can be seen in it. The PSM disintegration is slow and asynchronous. As a result the spore wall establishes direct contact with tapetal cytoplasm. However, wherever the PSM is still intact it shows its associated microtubules.

A dehisced anther shows no trace of plasmodium. The pollen wall in these anthers shows a deposition of a densely osmiophilic nature which is traversed by stacks of electron-translucent lamellae (Fig. 4.50). This material, described as pollenkitt in the literature, seems to be of plasmodial origin. It not only covers the exine, but also occurs in the interbacular spaces and under the tegillate roof of the exine. However, it was never recorded in the

pollen cytoplasm or the inner layers of the pollen wall. No features of this material were seen which could suggest that it was a secretion of the pollen.

4.4. DISCUSSION

The available ultrastructural studies of invasive and plasmodial tapeta, although few (Mepham and Lane, 1969b; Owens and Dickinson, 1983; Pacini and Juniper, 1983; Pettitt *et al.*, 1984), reveal considerable diversity in the timing of wall dissolution and plasmodium formation. In *Arum* (Pacini and Juniper, 1983) the radial walls of the tapetum break down, the cells fuse laterally, and only then is the inner periclinal wall removed, prior to invasion of the anther loculus. In *T. virginiana*, as described here, the walls show coincident dissolution with loss of the inner periclinal wall permitting formation of invasion processes before the radial walls finally disappear late in meiosis. The consequence is that invasion precedes plasmodium formation, i.e. the reverse of the sequence in *Arum*. Plasmodium formation was reported to occur during prophase I in *Tradescantia bracteata* (Mepham and Lane, 1969b), whereas in *T. virginiana* cell fusion is delayed and consequently the plasmodium is formed somewhere between the second meiotic divison and late tetrad stage, so that by the time the plasmodium comes to surround each microspore individually there is no trace of discrete plasma membrane expanses in it, except the PSM around the spores. The observations

reported here regarding the time of plasmodium formation are in accord with those of Clausen (1927).

In T. virginiana tapetal invasion of the loculus takes place in two distinct phases although temporal synchrony within an individual anther is not marked. In the early meiotic phase, the invasion processes, each with a patchy extracellular cell coat, reach and surround the meiocytes; labyrinthine reservoirs of future plasma membrane (PSM) are accumulated intracellularly; cell fusion follows, having previously only taken the form of enlarged cytomictic connections in the remnants of the radial walls of the tapetal cell layer. These events seem related to the establishment of a plasmodium. Phase two consists of postmeiotic invasion of the intermicrosporal spaces that are opened up by breakdown of the callose wall in the young tetrads.

The observed differences between Arum and T. virginiana extend to the level of the tapetal cell cytoskeleton. Aggregations of microtubules at the inner periclinal cell cortex led Pacini and Juniper (1983) to suggest that they might function in invasion "to push the tapetal cytoplasm between the meiocytes, or to guide an otherwise initiated flow in the right direction". There is no evidence for this in T. virginiana; the intrusive zone of the tapetum where future invasion processes are likely to form do not show any microtubular aggregates. However, microtubules do occur in the invasion processes, in their cortical regions or in the cytoplasm associated

with the membrane sacs and may have roles in maintaining their shape and - especially evident in colchicine treatments - transport of membrane sacs along them (Chapter 5). Microtubules are also associated with the second phase of invasion in a very different manner (see later).

While approaching and investing the meiocytes, the invasion processes carry an extracellular coat, distributed unevenly as Thiéry-positive patches over their surfaces. The coat material is so widespread that it is most unlikely to be merely a remnant of the original inner periclinal walls of the tapetum. Moreover, it is absent from the tapetal plasma membrane lying against the original outer periclinal walls and only sparsely present on the radial walls of the tapetum. It is very different in morphology from the parallel fibrils of the corresponding cell coat in invasive non-syncytial tapetal cells of Canna (Chapter 3), and unlike Canna, where the cells retain their coat and do not form a plasmodium, the coat of Tradescantia invasive processes disappears prior to the fusion process. As discussed in Chapter 5, colchicine treatments alter both the cell coat and cell fusion in T. virginiana. Roles in mediating the timing of plasmodium formation seem to be indicated.

In T. bracteata, Mepham and Lane (1969b) reported that a reorganization of plasmodial cytoplasm takes place towards the end of meiosis and is characterized by the "reappearance of 'rough' ER profiles, dictyosomes and

microtubules, absent during the streaming phase". In T. virginiana, although a reorganization of the cytoplasm does take place towards the end of meiosis and seems related to the spatial regulation of sporopollenin secretion by the plasmodium, none of these organelles appeared to diminish during the first phase of invasion.

The first phase of invasion culminates in the complete investment of the meiocytes with extensions of tapetal cells. At this stage it is quite clear that the investing membrane around the meiocytes is a composite of the tapetal cell plasma membranes. The spore cells are not "enclosed within the vacuoles of the tapetal cytoplasm" and the terms "pollen vacuole" (Mepham and Lane, 1969b) and "pollen vesicle" (Pettitt et al., 1984) seem inappropriate. There is apparently no agreed terminology for this bounding membrane, which must be very important in many aspects of sporophyte-gametophyte interaction (see later). It is proposed that, by analogy with the "peri-bacteroid membrane" of Rhizobium-infected cells in legume root nodules, it be called the "perispore membrane" (PSM). The asymmetry of the layers of this membrane, the positive staining in the Thiéry reaction (unlike the tonoplasts of the periplasmodium), and the morphological aspects of its origin, combine to make its plasma membrane nature unequivocal.

Several features of the membrane sacs are noteworthy. They are consistently associated with microtubules, which are not present as extensive arrays

but as individuals lying close to the cytoplasmic face of their membrane. The microtubules have been tracked by serial sectioning and appear to be quite short. The consistency of the association suggests that the microtubules help in the polarized migration of the membrane sacs to the plasma membranes of the invasion processes thus forming an extremely labyrinthine membrane reservoir at the PSM towards the end of meiosis. This idea receives support from the outcome of treatments with colchicine, which inhibit the migration of membrane sacs, and disrupt the formation of the labyrinth and its addition to the plasma membrane during the second phase of invasion. Another consistently seen feature of the membrane sacs is the presence of a population of coated vesicles which are of unknown significance. Within the lumen of the membrane sacs (i.e. the compartment that will become extracellular after the incorporation of the sacs into the tapetal plasma membrane) there are several small membrane-bound granules. These granules, or indeed the sacs which contain them, appear at late prophase and proliferate in subsequent stages of meiosis. The timing of the appearance and the morphology of these granules suggests that they are a modified or rudimentary form of orbicule, seen characteristically in secretory tapetum (see later for fuller description).

The PSM remains composite, in the sense that it is contributed to by the still incompletely fused mass of tapetal cells, until the early post-meiotic stage.

Several aspects of the fusion process that finally generates a true plasmodium warrant discussion. Before fusion takes place there are regions where the plasma membranes of the adjacent tapetal processes lie closely appressed, each face lined with arrays of microtubules. These could be interpreted either as regions that are specialised for initiating fusion, or alternatively as part of a system that postpones fusion until this relatively late stage in development. After fusion there is a great decrease in surface to volume ratio of the tapetal mass, indeed the fusion process could probably have contributed ample plasma membrane area to surround the separating microspores. However, as already described, a reservoir of membrane is instead prepared and drawn upon, suggesting that special attributes are given to the final form of the PSM. Certainly exine development in T. virginiana continues after release of the microspores from the callosic walls (Chapter 6), just as in Gibasis (Owens and Dickinson, 1983), another member of the family Commelinaceae with a plasmodial tapetum, and colchicine treatments reveal that the PSM is involved in the spatial regulation of sporopollenin secretion (Chapter 5). Observations of late stages of pollen development further substantiate the view that the PSM is specialised, for it can be seen, especially when the Thiéry reaction is employed, to become so closely appressed to the sculptured exine that there can be little doubt that at least some of its molecular constituents become retained there to be

dispersed with the pollen, conceivably to have a role in later surface recognition events.

Until the tetrad stage the tapetum of Tradescantia is dominated by features leading to the establishment of the plasmodium. By early post-meiotic stages, the major features of the plasmodium relate to the organization of its polarized secretory surfaces which are fully manifest by the late tetrad stage. These features include the development of the PSM with a labyrinthine outline, intimate relationship of the tubular ER with the convolutions of the PSM and restriction of microtubules to the cortical regions underlying the PSM. Later, when the PSM comes to surround each microspore individually, the labyrinthine outline of the PSM is lost, the frequency of the microtubules apparently declines and the associations between the PSM and tubular ER become infrequent. Significantly, the pollen wall undergoes almost 100% increase in its thickness (Chapter 6) during the interval between the late tetrad and early microspore stages. This is consistent with a relationship between the peak secretory phase of the plasmodium and the synthesis of sporopollenin for spore wall growth. Yet another indication of the peak secretory phase of the tapetum is the fact that colchicine induces abnormal deposition of sporopollenin (Chapter 5) when the treatments encompass the tetrad stage. Features such as proliferation of ER or dictyosomal activity coincident with sporopollenin synthesis have been described for several other species

(see Echlin and Godwin, 1968a; Steer, 1977; Misset and Gourret, 1984), which, however, lack the cellular mechanism for synthesis and polar secretion described here for Tradescantia.

Two features of the tapetum at the late tetrad stage need further discussion. One relates to the membrane-bound granules seen in the convolutions of the PSM and the other to the role of tapetum in pollen wall development.

Membrane-bound granules seemingly arise from the PSM during early and late tetrad stages. Their numbers reach their peak at the late tetrad stage and they could not be identified after the plasmodium invaded the intermicrosporal spaces. It has not been possible to conduct an acetolysis test on these granules because of their small size, but they are Thiéry-negative (although their bounding membranes are Thiéry-positive) and show the same electron density as the spore wall. In this work, they are considered to be analogous to the tapetal pro-orbicules, the forerunners of orbicules that characterise the secretory tapetum. Thus, the granules and pro-orbicules are both formed on specialized surfaces of the tapetum and they arise as bodies of intermediate electron opacity which in extracellular spaces gradually develop an electron-dense exterior known to be composed of sporopollenin in the case of secretory tapeta (see Christensen et al., 1972; Rowley and Skvarla, 1974; Abadie and Hideaux, 1979; Bhandari, 1984 for fuller descriptions

of tapetal orbicules). It should, however, be emphasized at this point that sporopollenin accretion on the pro-orbicules of T. virginiana, or indeed the amount and dimensions of the pro-orbicules, are not as obvious as in secretory tapeta, perhaps indicating that in the plasmodial tapetum the machinery for transferring tapetally-synthesized sporopollenin to the spore wall is efficient enough to limit the extent of orbicular polymerization. As evident from colchicine experiments (Chapter 5), availability of an extracellular space favours sporopollenin polymerization and in this regard the plasmodial tapetum offers a considerably reduced extracellular space when compared with that in anthers with secretory tapeta. No evidence was found to suggest that these granules contribute to spore wall growth, although they were sometimes seen close to the spore wall in the lumen bounded by the PSM. The fate of these putative sporopollenin granules remains unclear, since they could not be seen in later stages when the plasmodium invaded the intermicrosporal spaces. The question remains whether they might be a manifestation of the plasmodial tapetum's capacity to overproduce sporopollenin, or an evolutionary relic of the secretory tapetum (if plasmodial type is to be considered more evolved than the secretory type, see Sporne, 1973). No other plasmodial tapetum has yet been shown to produce comparable structures.

That the tapetum contributes to sporopollenin, pollenkitt, and exine protein contents of the spore wall

has often been emphasized (for reviews see Echlin, 1971a,b; Heslop-Harrison, 1971a,b, 1972, 1975; Bhandari, 1984). However, the lack of orbicules in plasmodial tapeta has given rise to doubts about the role of plasmodial forms (and indeed the tapetum in general) in pollen wall development (Mepham, 1970; Mattsson, 1976; Roland-Heydacker, 1979). Interpretations based on the available ultrastructural studies addressing the question of the role of plasmodium in spore wall development of flowering plants differ. Mepham and Lane (1968, 1969a,b) and Mepham (1970) rejected the idea that the plasmodium in Tradescantia bracteata is involved in pollen wall development because: (i) it lacks orbicules; (ii) exine development in this species is claimed to be completed before the microspores are released from the callosic wall. On the other hand, Owens and Dickinson (1983) in their study on pollen development in Gibasis (another member of the family Commelinaceae with plasmodial tapetum) recorded that "the close contact of the tapetal plasma membrane and the exine surface, the occurrence of fusion of vesicles with the plasma membrane, the increase in droplets of a lipidic and osmiophilic content in the tapetal cytoplasm and the association of microtubules with the plasma membrane all strongly endorse a tapetal involvement in the deposition of exine". In a more recent study on spore wall development in Anemia (a fern with plasmodial type of tapetum), Schraudolf (1984) also concluded that the plasmodium provides precursors for wall

growth. In this context it is relevant that T. virginiana (present investigation) seems to differ from T. bracteata (Mepham, 1970). In T. virginiana pollen wall development continues after removal of callose from the tetrads (see Chapter 6), and the plasmodium does synthesize granules which, as discussed above, are comparable to the orbicules seen in secretory tapeta.

The PSM is clearly part of a highly specialized assembly of cellular components organized to form a localized secretory surface adjacent to the developing spores. Its convolutions offer an amplified surface area characteristic of secretory surfaces where the plasma membrane amplification is known to facilitate transmembrane transport processes (Gunning, 1977; Harris et al., 1982). The PSM convolutions, and associated microtubules, ER tubules and coated and smooth vesicles are presumably all related to its secretory functions. In the light of observations presented here and those from colchicine treatments (Chapter 5), it can be envisaged that the endomembrane system, particularly tubular ER, supplies precursors which are expelled at the PSM into its lumen and then, in the extracellular space, accreted upon specialized surfaces of pro-orbicule-like bodies or the spore wall.

The main role for the PSM-associated microtubules in Tradescantia may be to stabilize the 3-dimensional organization of the complex secretory pathway, including the ER, membrane sacs, and PSM. Microtubules are also

associated with the membranous sacs both before and after migration of the sacs to the PSM, and migration is blocked by colchicine treatment. Colchicine also induces abnormality in the spore wall (see Chapter 6), but no evidence has been found in Tradescantia for correspondence between microtubule localization at the PSM and sites where ornamentations develop in the exine, as claimed for Anemia by Schraudolf (1984). Similarly there was no indication of localized retraction of PSM to facilitate pollen wall development as proposed for Arum (Pacini and Juniper, 1983). Earlier, microtubules have been recorded in association with plasmodial membranes adjacent to the developing spores in T. bracteata (Mepham and Lane, 1969b), Arum (Pacini and Juniper, 1983), and Gibasis (Owens and Dickinson, 1983), and, for species with secretory tapetum such as Helleborus (Echlin and Godwin, 1968a), Avena (Steer, 1977), Olea (Pacini and Juniper, 1979) and Datura (unpublished observations), although in secretory tapeta they occur at a much lower frequency, perhaps commensurate with the smaller size of the cells and a simpler secretory zone, with no convolutions and hence a reduced requirement for a stabilizing cytoskeletal system at the orbicule-bearing surfaces.

The microtubules found at the PSM and its associated membranous sacs appear to be different in function from those present in the cortex of the invasion processes that introduce the tapetal plasmodium to the spaces within tetrads after dissolution of the callose

wall. The latter are directly comparable to those in primary invasion processes in being aligned more or less perpendicular to the long axis of the process. They do not seem to guide this phase of invasion (Chapter 5) which can at least commence despite their removal by colchicine.

After the plasmodium surrounds each microspore individually, the specialized features of the PSM diminish. The frequency of PSM-associated microtubules declines, PSM convolutions disappear, having been utilized for surface expansion during the second phase of invasion, and the spatial distribution of PSM-associated tubular ER is gradually lost. A few pockets of randomly dispersed tubular ER, however, survive for some time in the plasmodium. Henceforth, the tapetum appears to embark on a lipid-carotene synthesis as there is a gradual increase of these complexes in the plasmodium during subsequent development. In Lilium, a species with secretory tapetum, the spectrophotometric study of Heslop-Harrison (1968a) indicated that the carotenes were exclusively synthesized in the tapetum. The observations reported here demonstrate that in this regard the behaviour of plasmodial tapetum in Tradescantia is similar. The lipids are apparently synthesized in the plastids and released into the plasmodial cytoplasm, as has also been recorded in T. bracteata (Mepham and Lane, 1969a,b) and Lilium (Dickinson, 1973; Reznikova and Dickinson, 1983) among other taxa.

Mepham and Lane (1968, 1969a,b) and Mepham (1970), as part of their argument that the tapetal plasmodium of T. bracteata does not contribute to pollen wall development, noted that lipid droplets around the pollen did not become coated with sporopollenin: they viewed lipidic deposits on the pollen surface as an "exudate" from the pollen cytoplasm, and that the electron-lucent portions of the deposits could in fact be "fossilized" pollen membranes, also extruded to the exterior. The observations reported here on T. virginiana support a quite different interpretation. There is abundant lipid in the plasmodium after it has surrounded each microspore individually. After the PSM has become very closely appressed to the pollen wall, the plasmodial cytoplasm develops numerous vesicles or vacuoles with two or more membranes. Later, pollenkitt deposits which include membrane-like profiles are found on the exine and under its tegillate roof. Although freeze-substitution does reveal channels through the intine (Chapter 6), there is no evidence to suggest that the pollenkitt is a product of the pollen. Rather, the lipid droplets and the membrane-bound vesicles seem much more likely to be the precursors of the pollenkitt, with the morphological changes representing alterations in the physical state of the lipid induced by progressive dehydration. In spite of the presence of pollenkitt, the dehisced pollen grains do not tend to stick in clumps and, as argued by Heslop-Harrison (1968a), this must be related to the paucity of

pollenkitt. In T. virginiana pollenkitt was not found in the spaces of a dehisced anther; it only occurred on or in the cavities of exine.

4.5. Microfilaments in the Plasmodium: Some Techniques and Results

It is evident from the previous account that the development of a syncytium involves massive synthesis and movement of organelles and reorganization of cytoplasm within the plasmodium, especially in its formative phase. The participation of microtubules in this polarized migration is documented in Chapter 5. A careful search was also undertaken for microfilaments, using a two-pronged approach: (i) the anti-microfilament drug, cytochalasin B, was applied, and (ii) attempts were made to visualize microfilaments at light or electron microscopic level. The following description is an account of these approaches. Unless otherwise stated, the search was restricted to the early meiotic phase of tapetal invasion since the probability of encountering microfilaments during this phase appeared to be higher.

Cytochalasin B was administered to isolated buds at concentrations of 50-200ug/ml in 1% DMSO (drug concentrations modified from Bradley, 1973) for 12, 24 and 36h. Buds were isolated, employing bud length-spore stage correlation, at the pre-invasion phase of tapetal development. They were cut while immersed in distilled water and then dipped in drug solution for the above-

mentioned durations. Simultaneously, controls were run in 1% DMSO alone for similar durations. The pre-invasion phase of tapetal development was chosen for beginning the treatment because within 24h of further development, the tapetal cells form invasion processes (see Chapter 5). It was anticipated that cytochalasin B might inhibit this movement. After the treatment, anthers were processed for electron microscopy in the usual manner. Contrary to expectation, it was found that tapetal invasion progressed in the normal fashion in the presence of cytochalasin B. Unfortunately, these negative results did not exclude a role for microfilaments in tapetal invasion and movement of organelles, since there was no information on whether the drug was taken up by the anthers and, if so, whether it was metabolized.

To determine whether the drug reached into or close to the anthers in a form that could express its effect, the well-established effect of inhibition of cytoplasmic streaming in response to cytochalasin (see Thomas, 1978) was exploited. Older buds, in which cells of the stamen hair showed cytoplasmic streaming, were subjected to drug treatments as described above for 12,24,36 and 50h. The stamen hairs were then isolated, mounted in distilled water and observed with differential interference contrast optics for signs of cytoplasmic streaming. The time between the removal of the buds from drug solutions and observation was less than 5 minutes. No evidence for inhibition of streaming was found. However, in buds

treated for more than 36h with drug concentrations greater than 100ug/ml, a large number of stamen hairs appeared unhealthy, shrivelled and sometimes plasmolysed, indicating degeneration. A few of the healthy cells, however, still continued to show streaming.

To summarize, treatments with cytochalasin B gave no positive results concerning the possible role of microfilaments in tapetal morphogenesis. Therefore, efforts were directed toward visualizing microfilaments at light or electron microscopic level.

A squash made of the tapetal plasmodium in premeiotic (Fig. 4.54) as well as post-meiotic (Fig. 4.55) stages often shows fine strands. Several different procedures were employed on these and other preparations. Phallotoxins such as phalloidin and phallacidin have been shown to bind selectively to actin filaments (Wieland, 1977) and, if tagged with a fluorescent marker, can be located by fluorescence microscopy (Barak and Yocum, 1981). Rhodamine-labelled phalloidin was used here. Anthers were fixed in 4% paraformaldehyde in phosphate buffer (25mM; pH 7.0) for 1h, washed in buffer for 10 min and again in phosphate buffer saline for 10 min. Some of these anthers were squashed onto a poly-L-lysine coated cover slip in a drop of PBS. The cover slip was then allowed to air dry. Some other anthers were embedded in Tissue Tek O.C.T. compound for frozen tissue specimens, frozen in liquid nitrogen and cut with a cryostat at -20^{o}C to produce sections of 6-10um thickness. Sections were

collected on poly-L-lysine coated coverslips and affixed by air drying. Cover slips bearing cut sections or squashed tissue were then processed identically. They were washed in PBS and subjected to the protocol described in Gunning and Wick (1985). This involves taking the specimens gradually to 50% methanol followed by incubation in rhodamine-labelled phalloidin (in 50% methanol) for 1h at room temperature. Afterwards coverslips were gradually brought back to PBS, mounted in distilled water and observed on a Zeiss Photomicroscope III employing epifluorescence and standard rhodamine filters. No microfilaments were visualized by this procedure. To check the efficacy of the procedure, intact stamen hairs showing cytoplasmic streaming were fixed and stained with rhodamine-phalloidin in a similar manner. These revealed cables of actin filaments running along the length of the cells similar to the ones shown by NBD-phallacidin in Tiwari et al. (1984).

At the electron microscopic level the results were again ambiguous. Apart from the image shown in Fig. 4.9, the invasion processes fixed in standard aldehyde-osmium combination frequently showed images exemplified by Figs. 4.51-4.53. These images could either be damaged membranes or poorly-preserved microfilaments; it must be pointed out that good ultrastructural preservation of the early stages of tapetal development was not always achievable. However, the possibility of their being membranes is less likely in that elements of normal endoplasmic reticulum

are present in the neighbouring cytoplasm (see Figs. 4.51,4.52). Nevertheless, these images were inconclusive.

A negative staining procedure was also employed. Plasmodial material from anthers showing early stages of invasion was extracted with a round-tipped glass rod into an Eppendorf tube and diluted with 70mM KCl and 1mM $MgCl_2$ at pH 7.0. A drop of the extract was then placed on formvar-coated slot grid and allowed to settle. Excess solution was then drawn off with a filter paper and washed repeatedly with 70mM KCl. Grids were then stained with 1% aqueous uranyl acetate for 1 minute, air-dried and observed immediately in the electron microscope. This procedure revealed an abundance of fibrillar structures as shown in Fig. 4.56, but decoration with meromyosin would be needed to identify these fibrils as F-actin.

Alternative fixation regimes were also employed. Addition of tannic acid during fixation has been claimed to result in improved preservation of microfilaments (LaFountain et al., 1977; Goldman et al., 1979; Seagull and Heath, 1979). In the present work tannic acid was employed in two different ways: i) anthers were fixed in the standard aldehyde fixative containing 1-2% tannic acid (Mallinkrodt); and, ii) anthers were fixed in aldehyde fixative, washed in buffer and then treated with 1-2% tannic acid in buffer for 1h. Subsequently, anthers were osmicated for both the procedures and processed for electron microscopy in the usual manner. Microfilaments were not observed in either of the procedures. Closer

examination revealed that tannic acid did not penetrate the tissue deep enough. A cell well-penetrated by tannic acid usually shows an excellent preservation of its membranes such as ER, golgi, nuclear envelope, etc. (see Maupin and Pollard, 1983); both faces of the membranes can be easily identified. In Tradescantia anthers it was found that tannic acid penetration, identifiable by the contrast in membranes, was confined to the anther wall layers. Hardly any penetrated to the tapetum. Increasing the duration or concentration of tannic acid treatments resulted in extraction of cytoplasmic matrix components.

The problem of poor penetration of tannic acid has been faced by many workers and it has been suggested that addition of 0.5mg/ml of the detergent saponin, along with tannic acid, to the primary fixative overcomes the problem (Maupin and Pollard, 1983). Application of this procedure involved fixation of anthers in 2% glutaraldehyde plus 0.5mg/ml saponin and 0.2% tannic acid in 25mM phosphate buffer containing 50mM KCl and 5mM $MgCl_2$ at pH 7.0 for 2h, rinsing in buffer and post-fixation in 1% osmium tetroxide in the same buffer. Addition of saponin did result in a better infiltration of tannic acid, but microfilaments still could not be visualized.

Recently, Boyles (1983) reported that addition of primary amines to the primary fixative resulted in improved preservation of actin filaments in vivo as well as in vitro. Accordingly, anthers were fixed in 3% glutaraldehyde plus 50mM lysine in 5mM cacodylate

buffer at pH 7.0 for 2h, rinsed in buffer and post-fixed for 1h in 1% buffered osmium. No microfilaments were seen using this method. However, it revealed the occurrence of some wispy filamentous structures in the plasmodium, sometimes associated with cytoplasmic membranes (Fig. 4.57). Such structures had never been seen in conventionally-prepared tissue. The question of their artifactual or real nature remains open.

Based on the idea that phallotoxins stabilize the microfilaments and counteract the destructive effects of fixatives (Wieland, 1977; Gicquaud et al., 1980; Gicquaud and Loranger, 1981), a procedure was developed employing phalloidin. Anthers were immersed in buffered (25mM phosphate buffer, pH 7.0) phalloidin (500ug/ml) for 1h and then fixed in the usual manner (phalloidin, being a peptide, could not be used in the fixative), washed, post-fixed and processed for electron microscopy. This procedure resulted in poor preservation of cytoplasm (Fig. 4.58). Alternatively, anthers were fixed in 2.5% glutaraldehyde plus 0.3mM phenylmethyl sulfonyl fluoride (PMSF, a protease inhibitor) made up in 25mM phosphate buffer at pH 7.0, for 2h at 4^{o}C. After washing in buffer containing PMSF, anthers were treated with phalloidin (500ug/ml) in buffer for 1h at room temperature, washed thoroughly and post-fixed at 4^{o}C and processed for electron microscopy in the routine manner. This protocol resulted in improved preservation (Fig. 4.59) but neither method revealed microfilaments, although in the latter preparation some wispy structures did occur.

In brief, the attempts to localize microfilaments in the plasmodium have so far failed. The images obtained by conventional procedures or negative staining are the closest to the suggestion of the presence of microfilaments. The inclination nevertheless is to believe that the filaments in the plasmodium are destroyed by the various fiaxatives employed in this work. The destructive effect of osmium on the microfilaments is well documented. Maupin-Szamier and Pollard (1978) demonstrated that osmium could destroy microfilaments even after they had been cross-linked with glutaraldehyde. Damage to actin filaments by aldehydes has also been recorded by Lehrer (1981). In view of this it seems reasonable to assume that all fixatives used were unsuitable for preserving microfilaments in the plasmodium.

To confirm the destructive influence of conventional procedures it was decided to compare conventional procedures and freeze-substitution, since contact with chemical fixatives is avoided or minimized in the latter. Freeze-substitution involves freeze-fixation (see Chapter 2) followed by substitution with alcohol or acetone before the tissue is embedded for electron microscopy. Successful freezing requires a fast cooling rate, otherwise large ice crystals develop in the tissue which could destroy the ultrastructural preservation. In view of this, plasmodial tapetum was considered unsuitable for freezing because of its location deep in the anther.

Stamen hairs, on the other hand, provided a good system to freeze easily. Stamen hairs were isolated from anthers showing tetrad stages of microsporogenesis and freeze-substituted as described in Chapter 2. Briefly, they were frozen in liquid propane and substituted for 2 days in dry 100% acetone at -85^{o}C, brought to room temperature, osmicated for 1h, and flat embedded in Spurr's resin. For comparison, stamen hairs were isolated while immersed under the standard aldehyde fixative, fixed for 1h, washed and post-fixed for 1h in 1% buffered osmium, dehydrated in acetone and flat embedded. Fig. 4.60 shows part of a stamen hair cell processed in conventional manner, whereas Fig. 4.61 shows a comparable area in a freeze-substituted preparation. Note the presence of a delicate system of 'microfilaments' in the cell cortex of the freeze-substituted hair, while in the conventionally processed hair this system is absent. These filaments may traverse the cortical cytoplasm on their own, or they may lie alongside microtubules. Both procedures employed acetone dehydration and osmium tetroxide treatments, so the destruction of microfilaments in conventionally processed tissue may have been due to aldehyde fixation This does not necessarily mean that no microfilaments will survive aldehyde fixation. Indeed robust cables of microfilaments have been studied in many plant systems employing aldehyde fixation (for example, see Gunning and Wick, 1985; Williamson, 1985). It is, however, apparent that delicate microfilaments can be destroyed by aldehyde fixation. It

is not known whether these 'microfilaments' consist of F-actin. Note also some remarkable features of microtubule terminations in Fig. 4.61; one microtubule shows abrupt dilated termination (see Chapter 6 for fuller discussion).

To summarize, negative staining and conventional preparations revealed some images suggestive, though inconclusive, of microfilaments in the plasmodium and the possibility is considered that they are either destroyed or considerably distorted by the various procedures employed. The results of freeze-substituted stamen hairs, though not exactly applicable to the plasmodium, are indicative of this possibility.

Fig. 4.1. A tapetal cell (t) after the dissolution of walls. Remnants of a radial wall (arrows) can still be seen in the right hand corner of this bilayered tapetum (sc, sporogenous cell). Prophase I. x 2,950.

Fig. 4.2. Transectional profiles of microtubules (arrowheads) can be seen along the inner periclinal surface of a tapetal cell. Prophase I. x 72,000.

Fig. 4.3. Soon after the wall dissolution, the tapetal cells form long invasion processes (ip) which grow in the spaces between the sporogenous cells (sc). Note that the radial walls (arrows) have dissolved, yet no cell fusion has taken place. Late prophase I. x 9,500.

Figs. 4.4,4.5. Immunofluorescence and phase contrast micrographs of a tapetal invasion process showing the distribution of microtubules. x 675.

Fig. 4.6. Invasion process (ip) is heavily covered by an extracellular cell coat (arrows) particularly at its apex. Among the various cytoplasmic organelles, parallel stacks of ER form the most conspicuous feature of the invasion process (sc, sporogenous cells). Late prophase I. x 13,550.

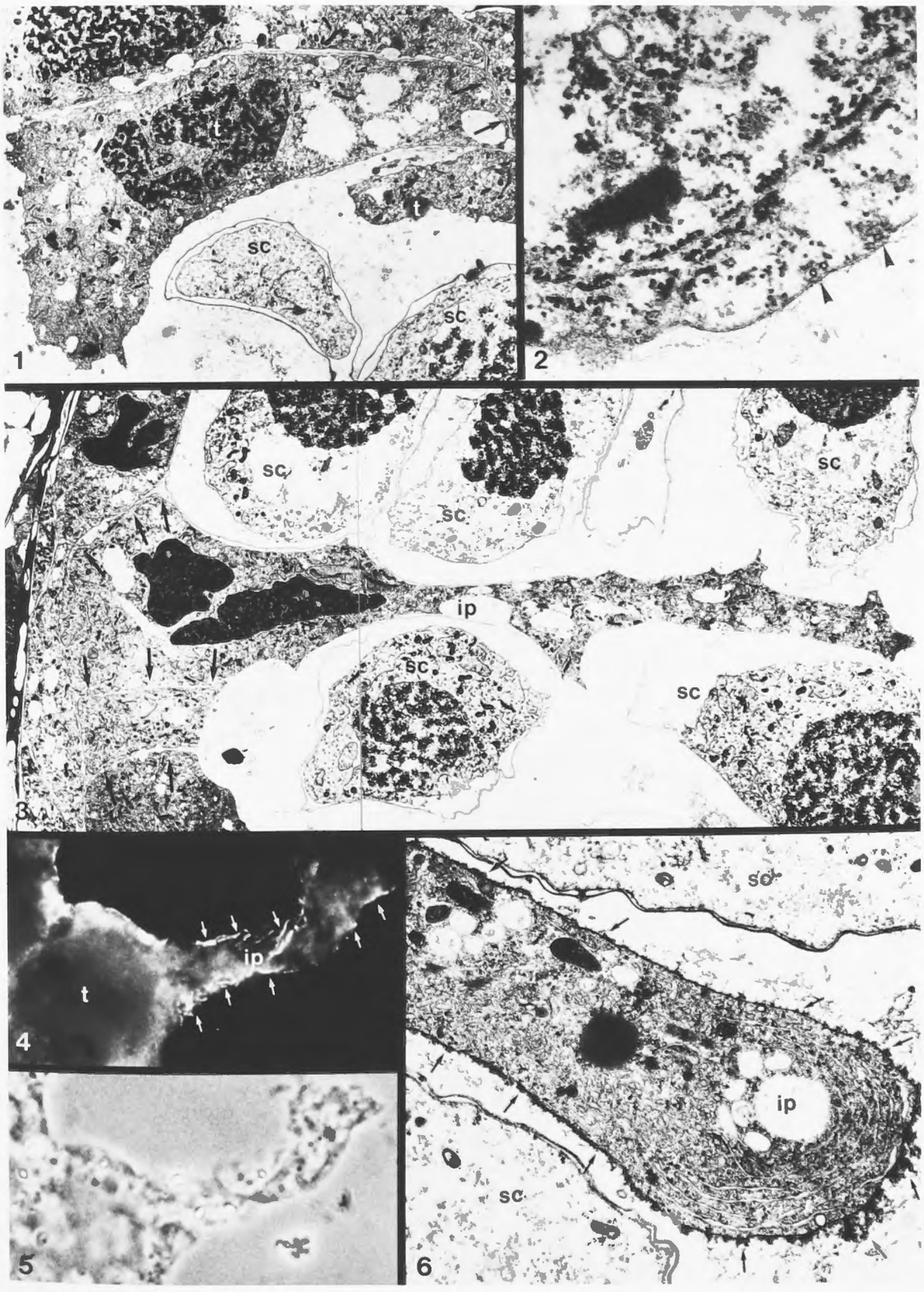
t
t
sc
sc
1
2
sc
sc
sc
ip
sc
sc
3
ip
t
4
5
sc
ip
sc
6

Fig. 4.7. Tapetal cells (t) showing incomplete dissolution of radial walls (arrows), the cytomictic channels and the invasion processes (ip). Note the appositions area (arrowheads) between two invasion processes (sc, sporogenous cells). Late prophase I. x 2,450.

Fig. 4.8. Cortical microtubules (arrowheads) present along the plasma membrane of a tapetal invasion process. The wall of the sporogenous cell (sc) can also be seen. Late prophase I. x 65,630.

Fig. 4.9. Putative microfilaments (arrowheads) seen in the cytoplasm of an invasion process. Late prophase I. x 51,430.

Fig. 4.10. Invasion processes (ip) from different tapetal cells do not fuse at this stage, but form apposition areas (arrowheads; sc, sporogenous cells). Late prophase I. x 2,700.

Fig. 4.11. Some of the tapetal cells (t) probably where it is bilayered migrate discretely into the spaces between the sporogenous cells (sc). Late prophase I. x 3,000.

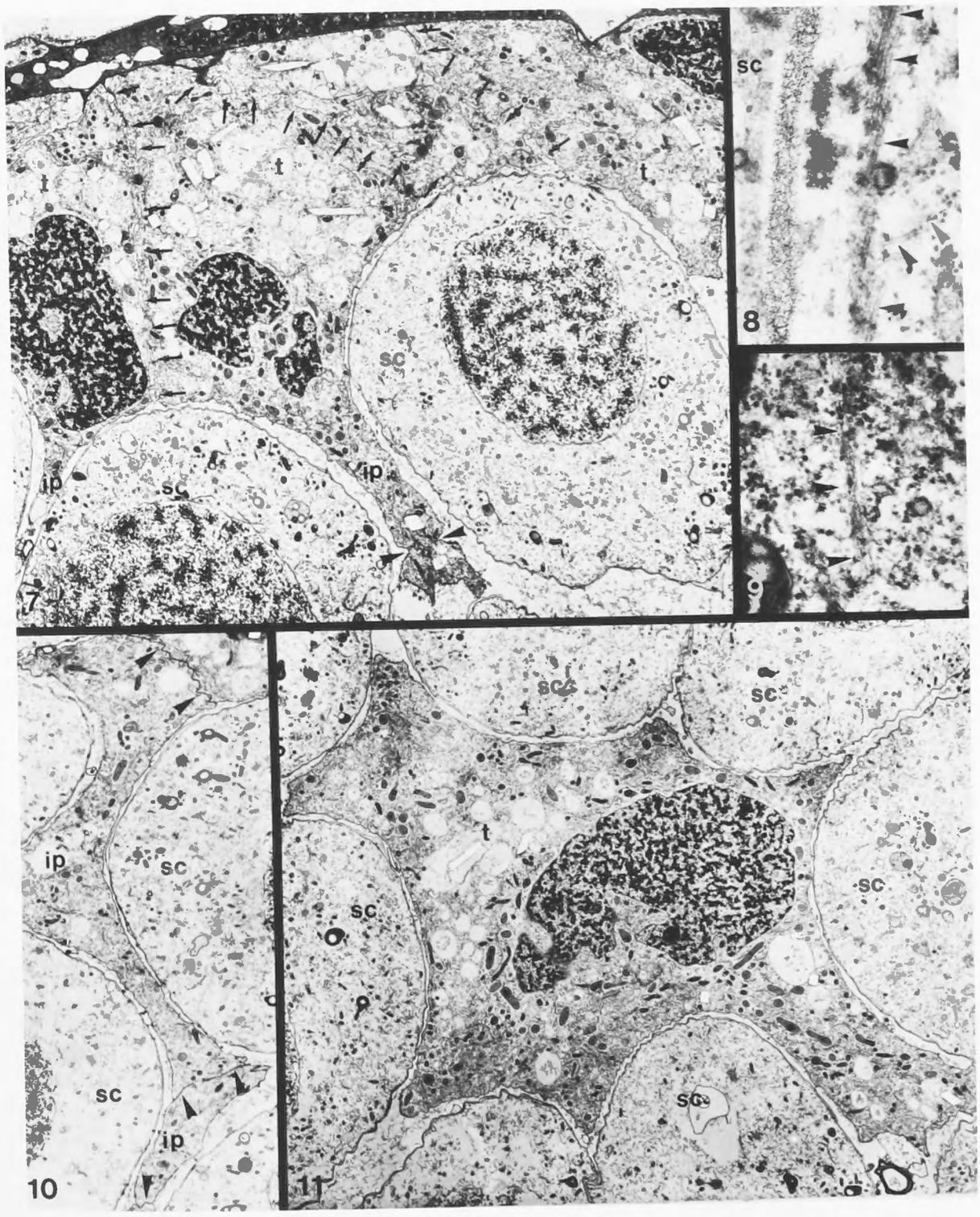
t
t
t
sc
ip
ip
sc
7
sc
8
9
ip
sc
sc
ip
10
sc
sc
t
sc
sc
11

Fig. 4.12. Tapetum at dyad stage of meiosis to show the aggregations of membrane sacs (arrows). Invasion processes by this stage have become highly branched, but still maintain more or less discrete boundaries as seen along the arrowheads. x 2,240.

Fig. 4.13. High magnification photograph of a part of Fig. 4.12 to show the general distribution of membrane sacs in the tapetal cytoplasm. x 7,680.

Fig. 4.14. The Thiéry reaction imparts electron density to the membranes of the sacs, same as in plasma membrane. The micrograph also illustrates the continuity between some sacs and the plasma membrane. x 20,000.

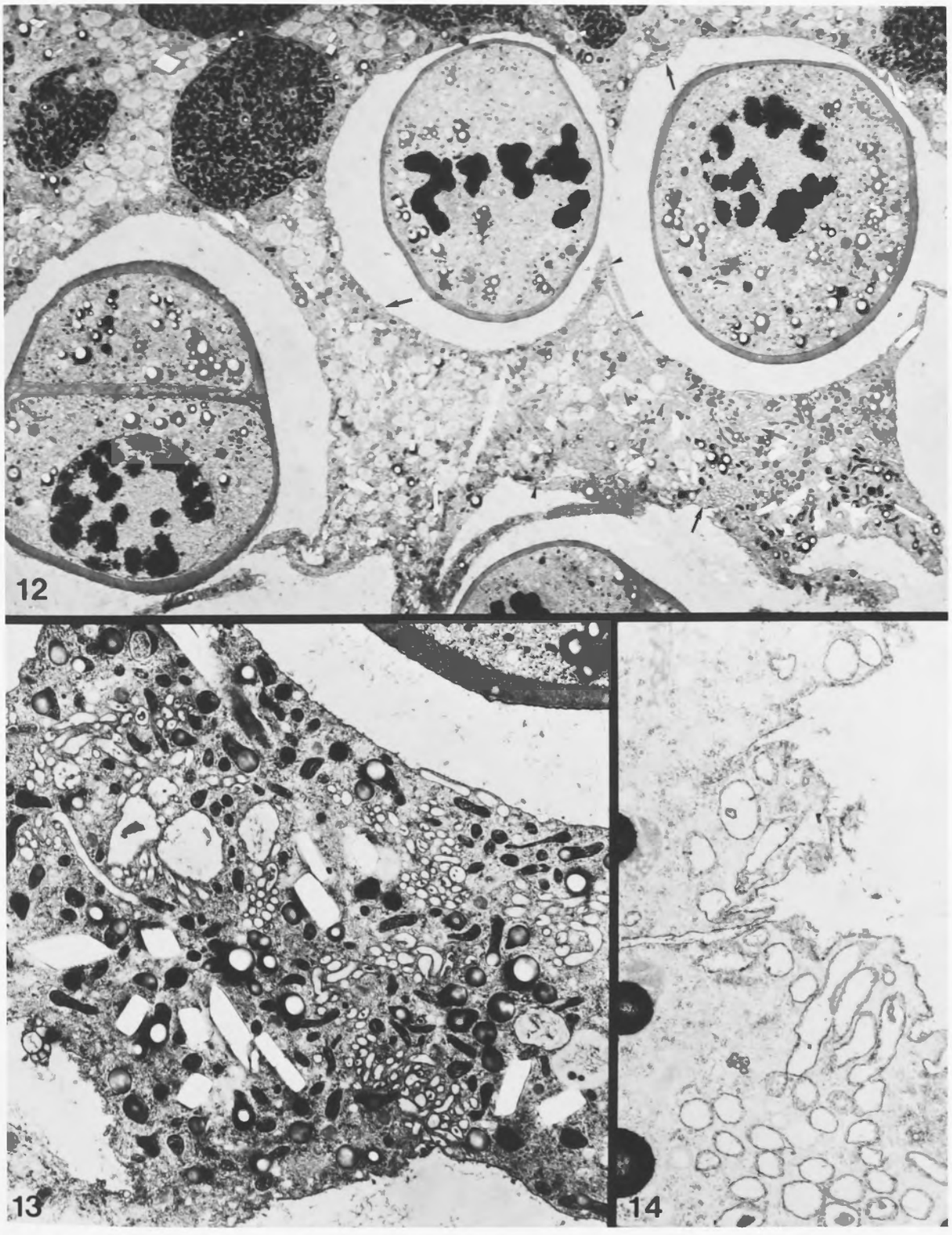
12
13
14

Fig. 4.15. Coated vesicles (arrowheads) and microtubules (arrows) are seen in close association with the membrane sacs. Note also the occurrence of granules in the lumen of some sacs. x 56,570.

Fig. 4.16,4.17. Immunofluorescence and phase contrast micrographs to show the tubulin fluorescence at a putative fusion site (arrowheads) as well as at the plasma membranes (arrows). The intensity of fluorescence is much higher at the possible fusion site. Early tetrad stage (t, tapetum; s, spore). x 1,460.

Fig. 4.18. An apposition area (arrowheads) between two tapetal processes. Compare it with the area at prophase I in Fig. 4.10. Note the accumulation of membrane sacs at or close to the fusing membranes. Dyad stage. x 6,300.

Fig. 4.19. A part of the apposition area to show the microtubules at the putative fusion sites. Dyad stage. x 41,870.

Fig. 4.20. The Thiéry reaction reveals the absence of a cell coat at the outer periclinal surface of the tapetal cells. Dyad stage. x 41,780.

Fig. 4.21. The Thiéry reaction reveals the presence of a rather sparse cell coat on the radial tapetal walls. Dyad stage. x 61,500.

Fig. 4.22. Invasion processes (ip) of two tapetal cells at dyad stage showing their prominent cell coats as stained by the Thiéry reaction. Note that the invasion processes are discrete at this stage. Few electron-dense starch grains can also be seen. x 12,500.

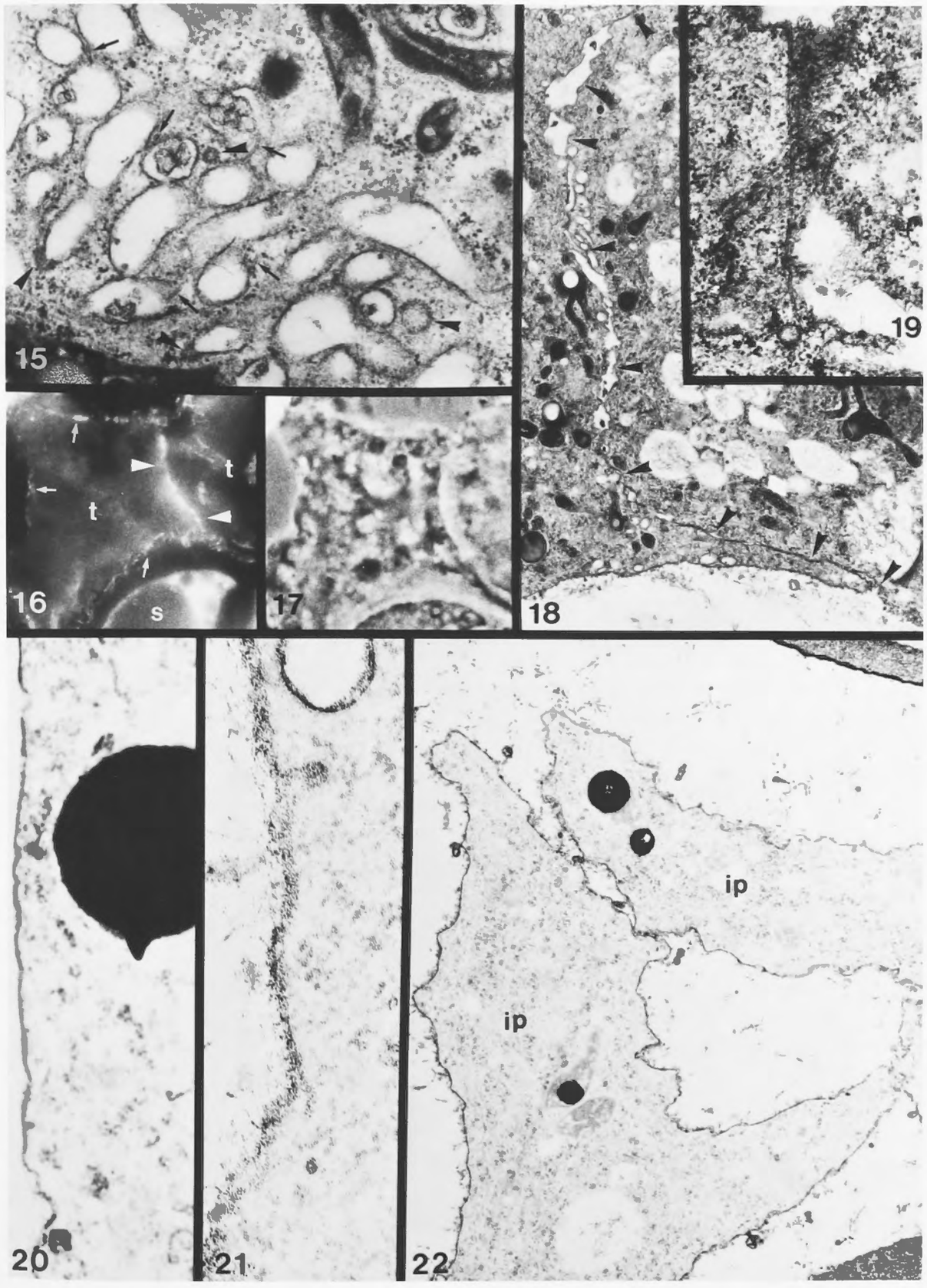
15
16
t
t
s
17
18
19
20
21
22
ip
ip

Fig. 4.23. Median section of a late tetrad with the remnants of callosic wall material between the microspores (ms). The perispore membrane (psm) is convoluted (small arrows) by preceding partial incorporation of membrane sacs. Note the granules (arrowheads) in the lumen bounded by PSM. x 2,870.

Fig. 4.24. Median section of a late tetrad stained with the Thiéry reaction. The PSM and its convolutions (arrows) are stained, unlike the tonoplast of the vacuoles (v). The electron density of the chromatin is not caused by silver deposits, but is due to incomplete deosmication by periodic acid (arrowheads, putative sporopollenin granules; ms, microspore). x 3,000.

Fig. 4.25. High magnification micrograph of a part of the PSM at late tetrad stage, stained with the Thiéry reaction and showing the convolutions (sw, spore wall). Serial sections of this type of material demonstrate luminal continuity among many sacs, and between them and the main spore compartment. x 12,450.

Fig. 4.26. Section of the PSM from ZnIO-post-fixed anthers to show the relationship between tubular ER (electron dense areas) and the PSM convolutions (asterisks). Ultra-thin section, post-stained with uranyl acetate and lead citrate (arrows, microtubules). x 33,340.

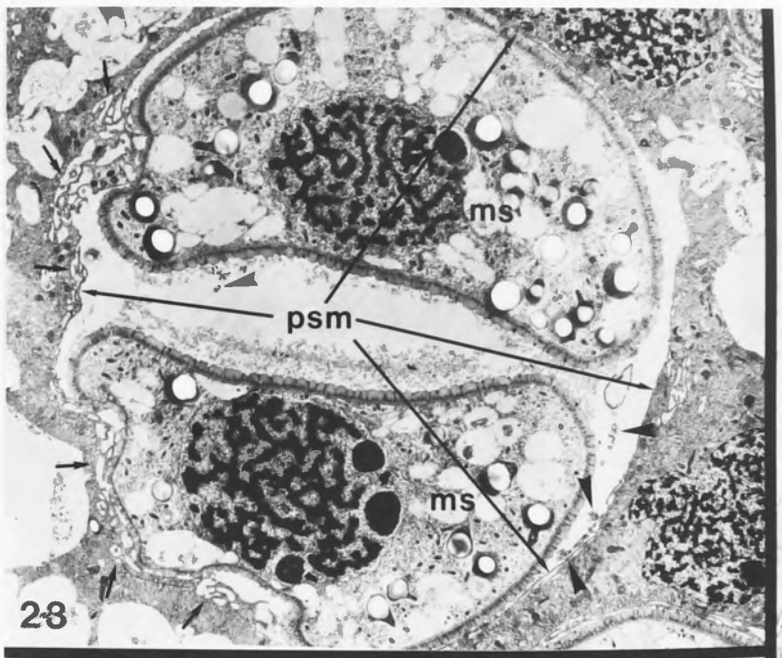
ms
psm
ms
28

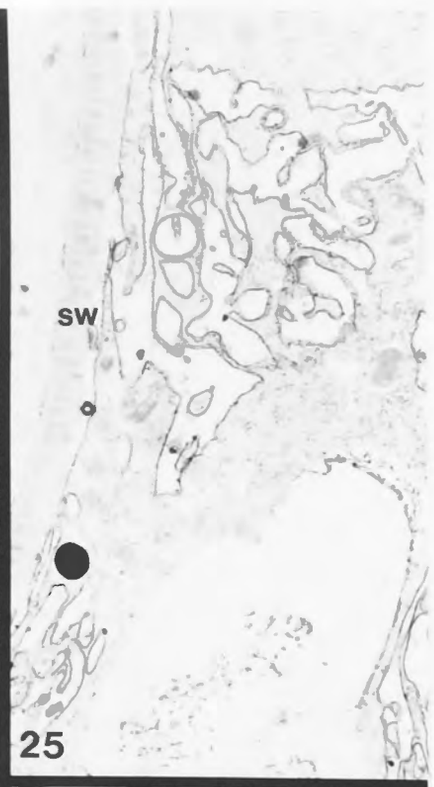
sw
25

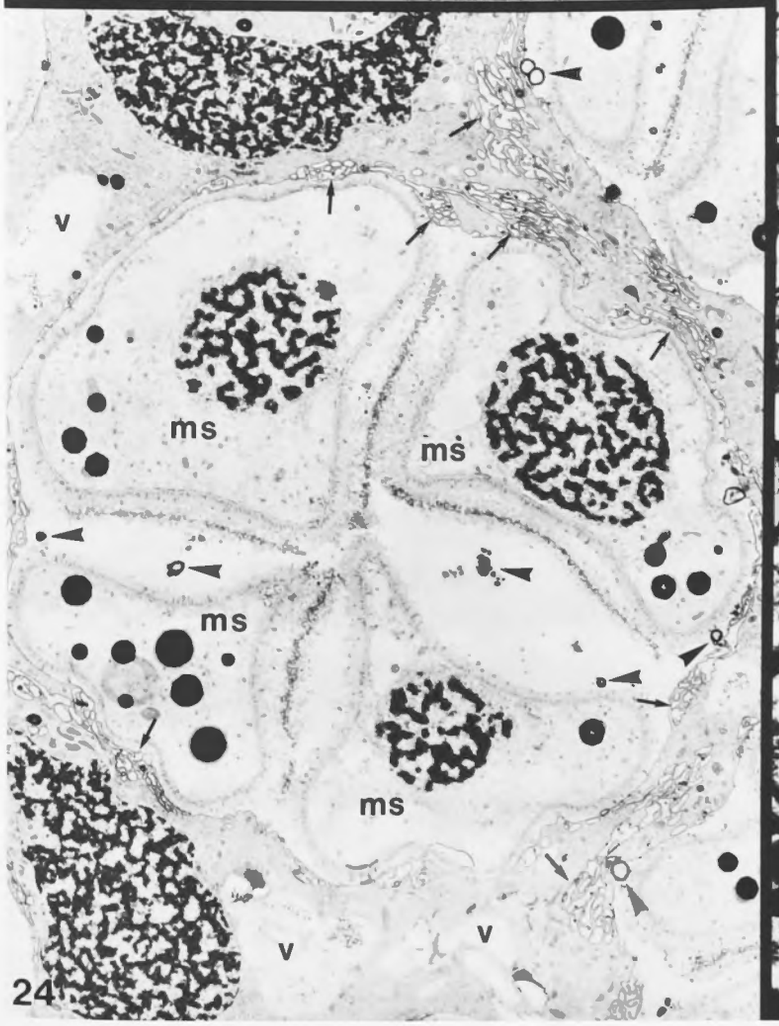
v
ms
ms
ms
ms
v
v
24

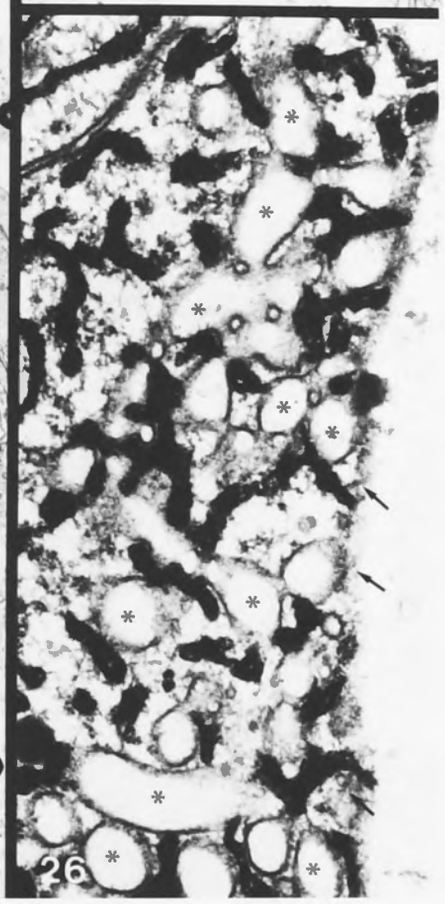
26

Fig. 4.27. Stereopair of a 1µm thick section of ZnIO-post-fixed anther showing the electron-dense ER tubules in the vicinity of the PSM and its convolutions (asterisks) at late tetrad stage. Tilt angle 12^{o}. x 28,370.

Fig. 4.28. Stereopair of the PSM at late tetrad stage from an anther which was subjected to osmium maceration and viewed with scanning electron microscope. White triangles show PSM convolutions and their openings into the main spore-containing compartment. Tilt angle 2^{o}. x 16,000.

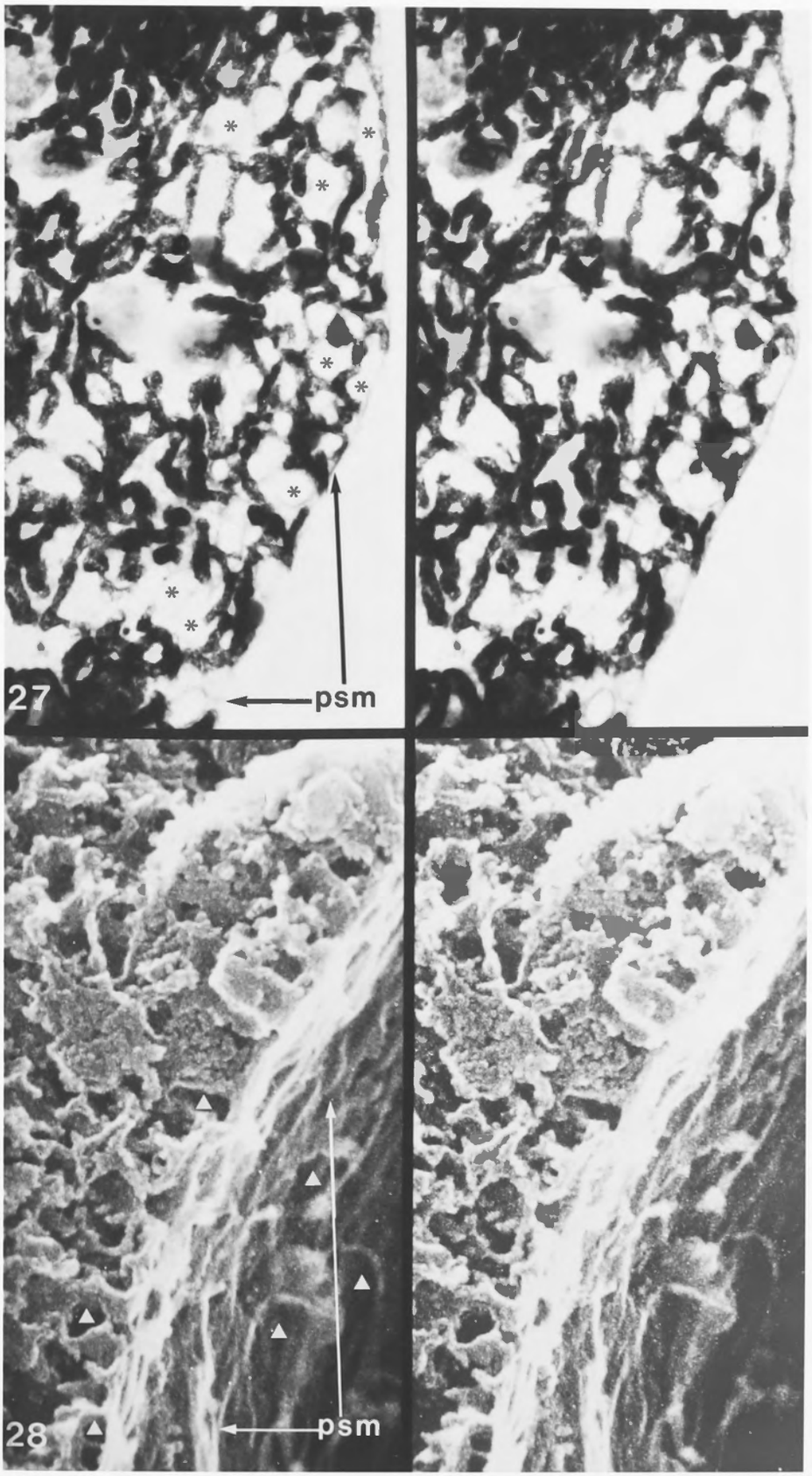
27
psm
28
psm

Fig. 4.29. Ultrastructure of the PSM and its associated features at late tetrad stage. Note the tubular ER (ter) and its vesicles in close proximity with the convolutions of the PSM. The cisternal rough ER (rer) seems relatively distant to the PSM. Note also the amorphous electron dense material (arrowheads) in some of the convolutions (sw, spore wall). x 21,180.

Fig. 4.30. High magnification micrograph of the PSM at late tetrad stage to show the poorly delineated tubular ER (arrows), microtubules (arrowheads) and granular or amorphous contents (stars) in the membrane convolutions. Many regions of the sac membranes are "coated" (white arrows). x 48,000.

Fig. 4.31. A part of the PSM illustrating the likely mode of formation of the putative sporopollenin granules (arrows). x 43,710.

Fig. 4.32. A part of the PSM showing putative sporopollenin granules (arrows; arrowheads, microtubules; sw, spore wall). x 36,000.

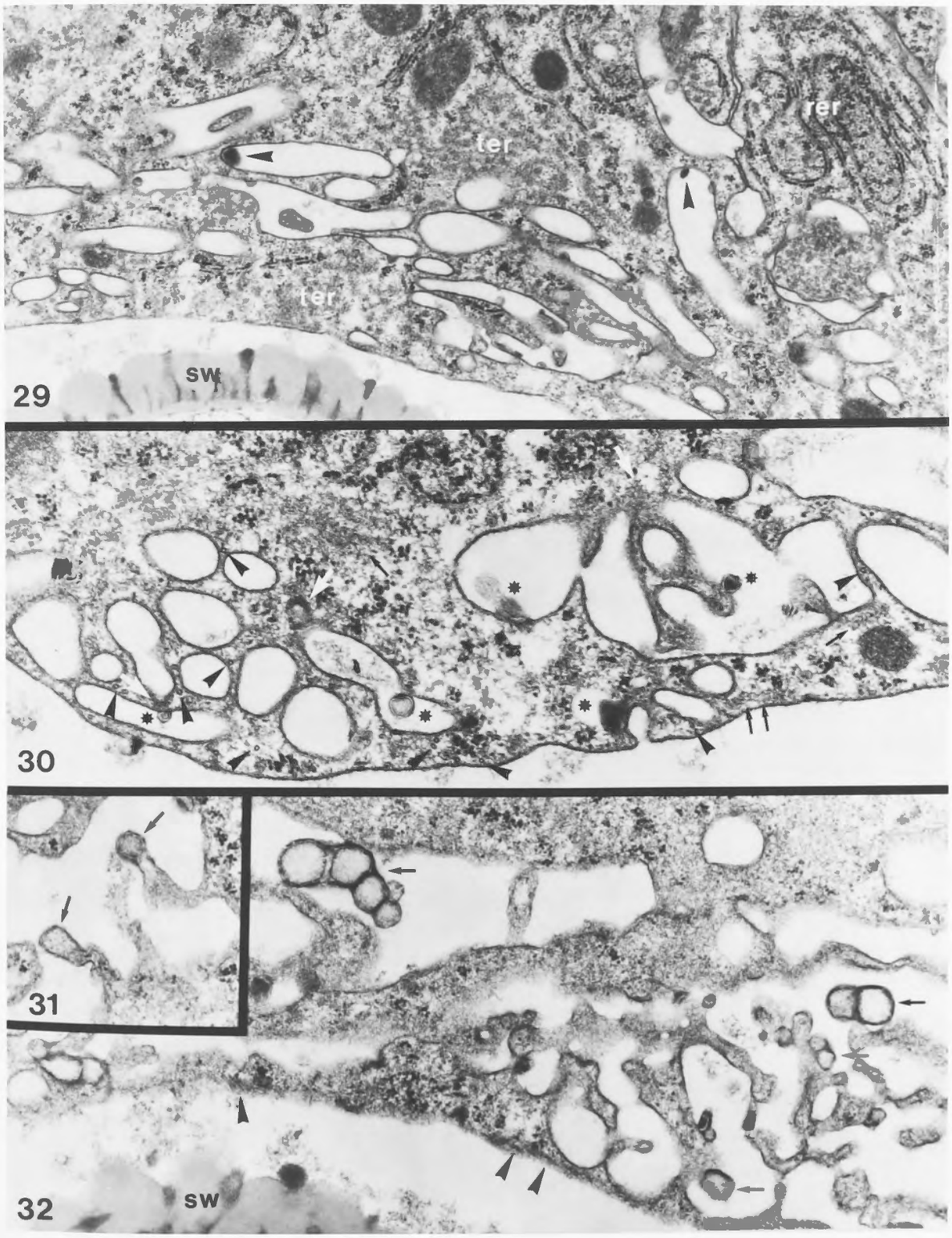
rer
rer
rer
sw
29
30
31
32
sw

Fig. 4.33. Scanning electron micrograph of endoplasmic reticulum (er) from the tapetum of an osmium macerated anther. x 10,000.

Fig. 4.34,4.35. Fluorescence and phase contrast pair of a thick section of tapetal plasmodium at early tetrad stage showing immunofluorescence of microtubules which are associated with the PSM (arrows). The PSM has been cut in a median plane. Note that the fluorescence is restricted to the PSM (sc, spore cells). x 1,500.

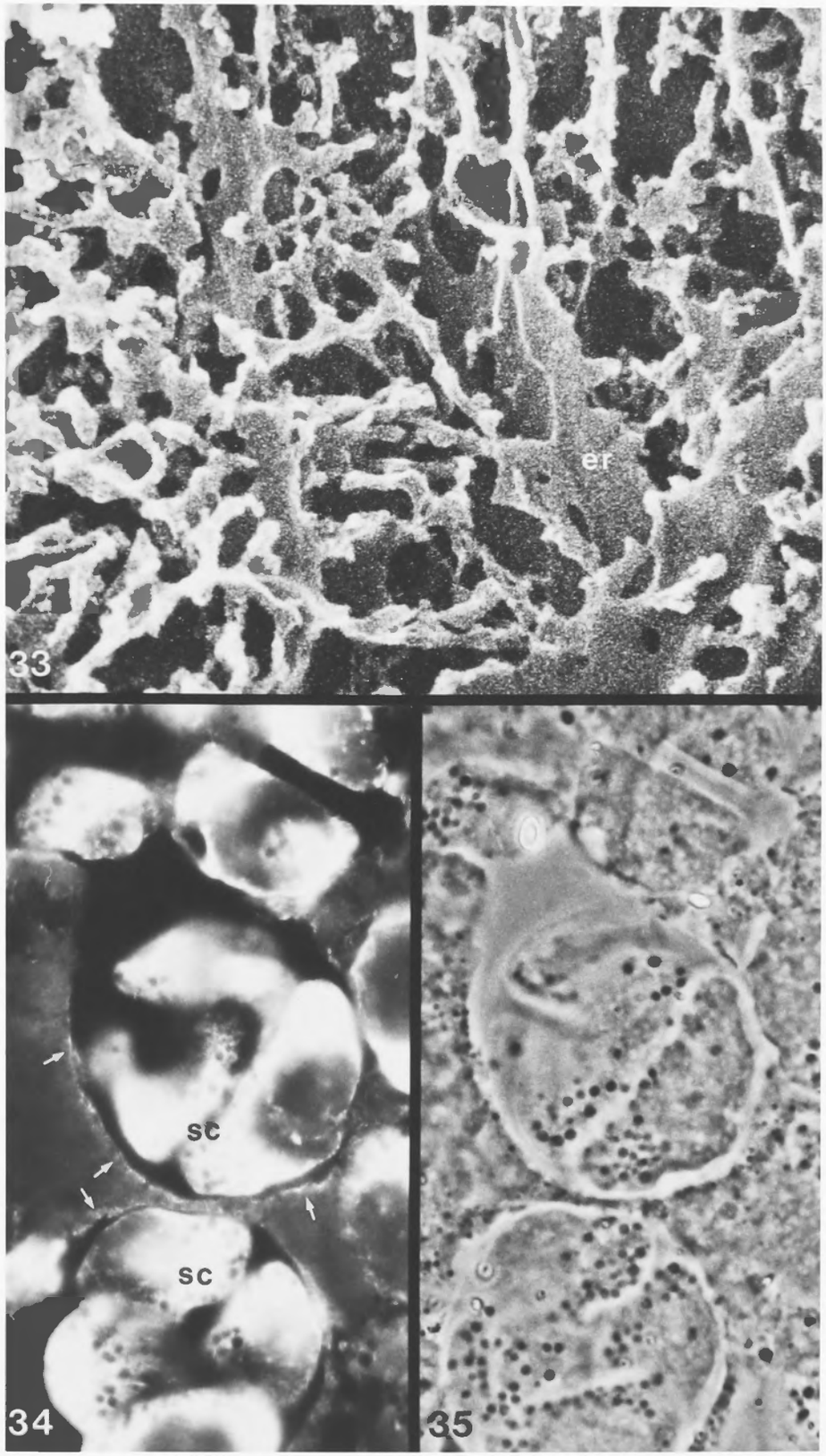
er
33
sc
sc
34
35

Fig. 4.36,4.37. Fluorescence and phase contrast pair of a thick cryostat section of tapetal plasmodium and spores at early tetrad stage. The PSM has been cut in oblique profile. Immuno-fluorescence of microtubules can be seen associated with the PSM. The bright fluorescence in the microspores (s) is considered in detail in Chapter 6. x 1650.

Fig. 4.38. Grazing section of a part of the PSM, remote from membrane sacs, at late tetrad stage showing the underlying microtubules (arrows; sw, spore wall). x 42,350.

Fig. 4.39. A secondary invasion process (ip) invading the intermicrosporal spaces of a late tetrad. Note the presence of microtubules (arrowheads) oriented approximately transverse to the long axis of the process (sw, spore wall). x 39,190.

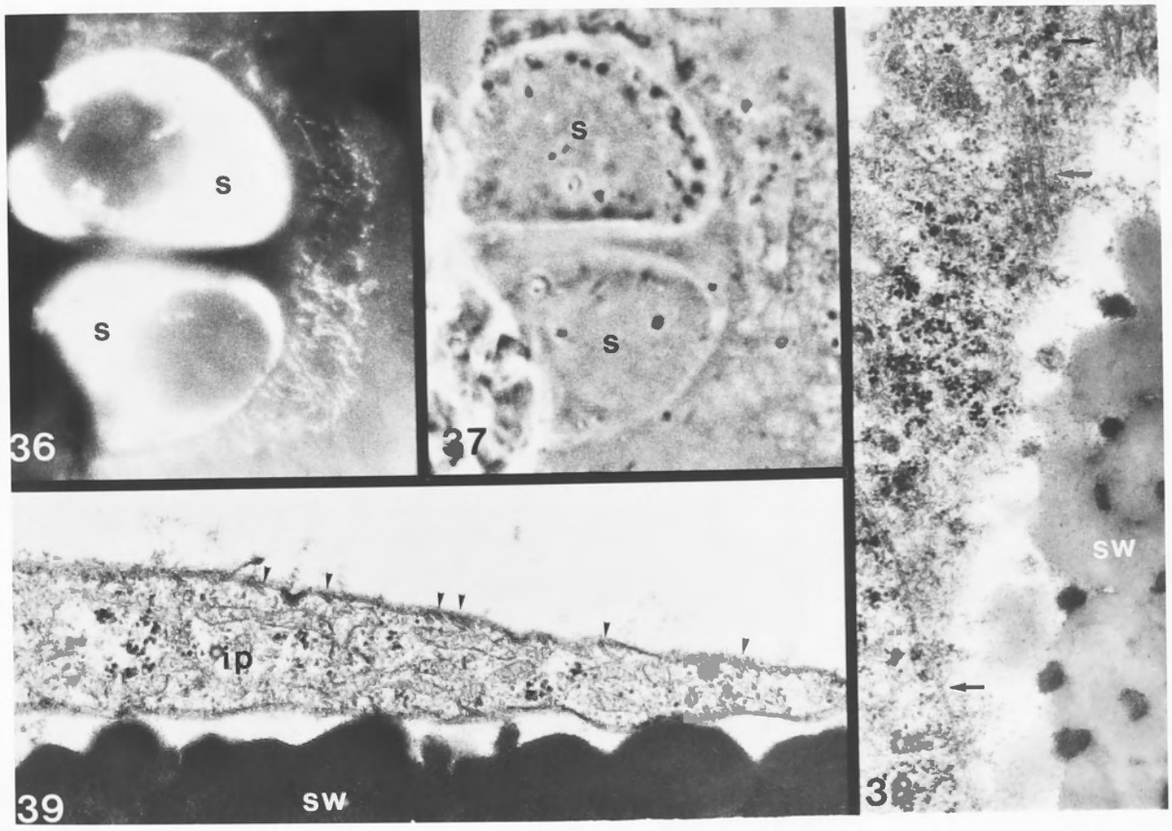
s
s
36
s
s
37
sw
38
ip
sw
39

Fig. 4.40. The PSM and its associated cytoplasmic features at early tetrad stage, with the edge of the partially dissolved callose wall (asterisks) just visible at the bottom of the picture. Note the accumulation of tubular endoplasmic reticulum (ter) in the vicinity of the PSM, abundant cisternal ER deeper in the cytoplasm, and absence of cell coat. A few membrane sacs (ms) can also be seen at the PSM. Arrowheads trace the course of apposed plasma membranes of as yet unfused portions of tapetal invasion processes. x 30,000.

Fig. 4.41. Wherever the PSM is not yet organized into the mature secretory conformation with tubular ER and membrane sacs, the tapetal plasma membrane (pm) is underlain by small vesicles and abundant rough ER (rer); clear areas at upper and lower left are vacuoles. Early tetrad stage. x 42,350.

Fig. 4.42. Grazing section of a part of PSM at early tetrad stage to show extensive coating with clathrin-like cages(arrows). Part of a starch-containing plastid (p) is included. x 72,000.

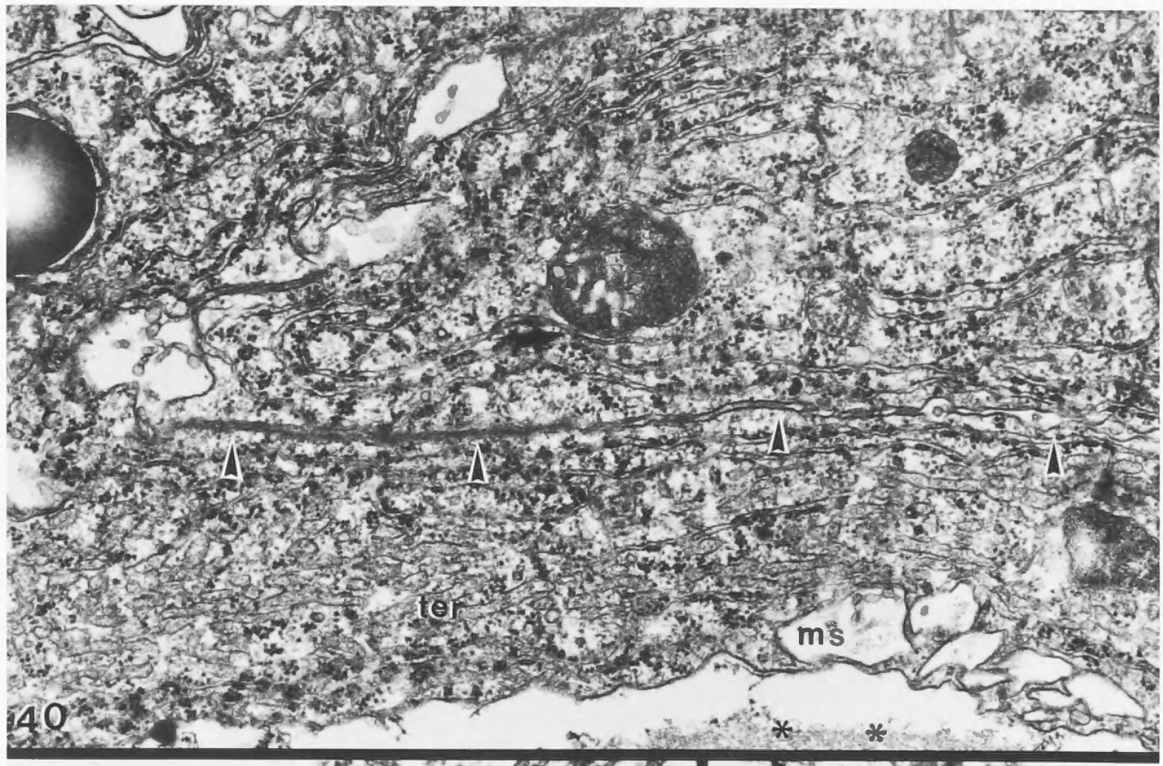
ter
ms
40

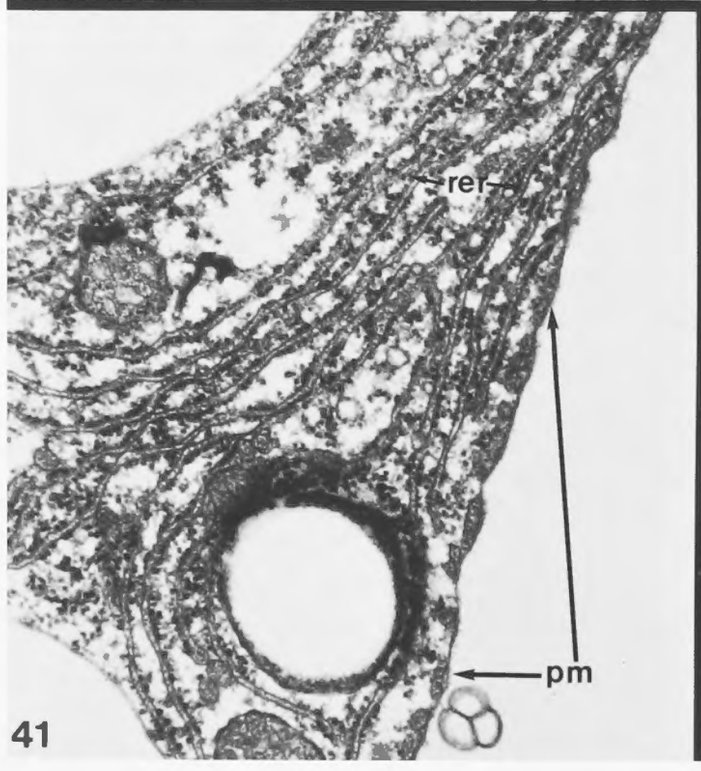
rer
pm
41

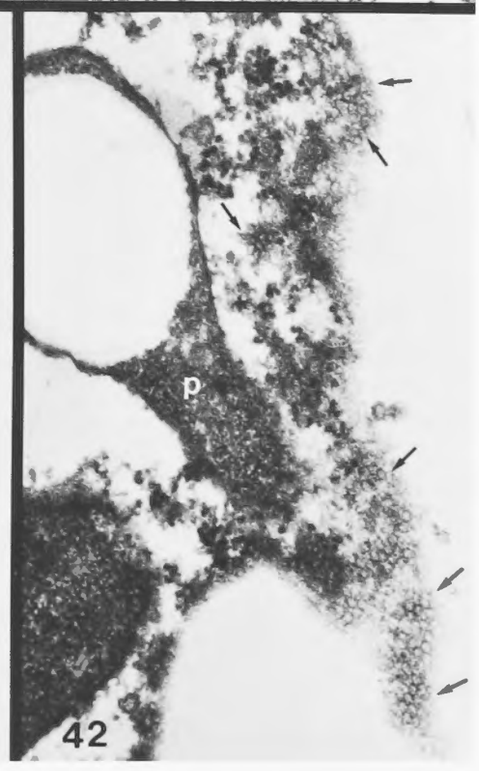
p
42

Fig. 4.43. Plasmodium during the interval between young-late microspore stages. The PSM has surrounded each microspore (ms) individually and its convolutions disappear. Note the presence of numerous lipid bodies in the plasmodium. x 3,350.

Fig. 4.44. A pocket of tubular ER and lipid bodies in the plasmodium (ms, microspore). x 10,910.

Fig. 4.45. PSM (arrows) at late microspore stage showing the granulo-fibrillar coat on its external face adjacent to the pollen wall (sw). Note the absence of tubular ER close to the PSM and presence of numerous lipid bodies. One lipid body appears to be occluding a multivesicular body (mvb). The frequency of the PSM-associated microtubules has declined considerably by this stage (d, dictyosome; m, mitochondrion). x 50,000.

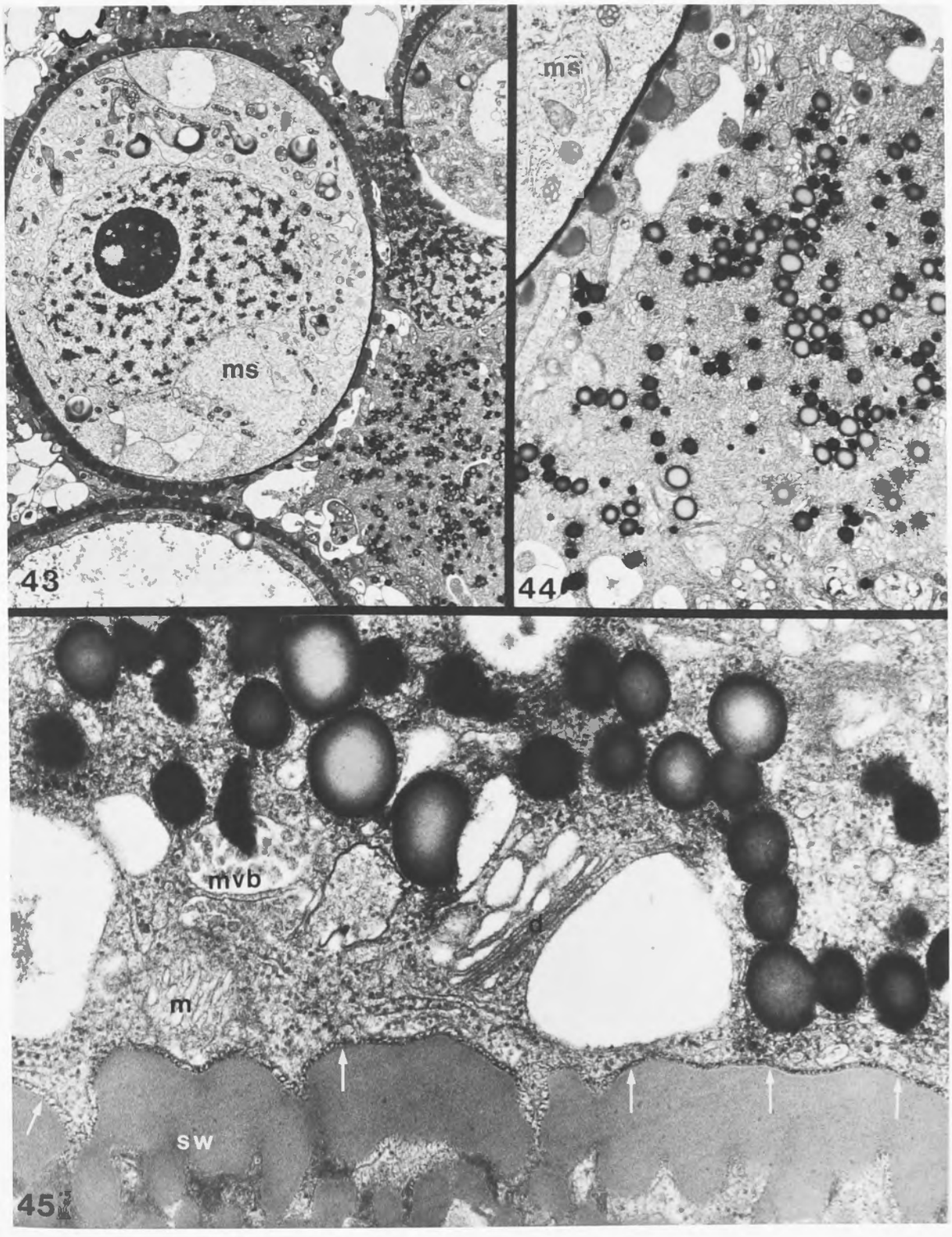
ms
43
ms
44
mvb
m
sw
45

Fig. 4.46. The PSM and its fibrillar coat (arrowheads) stain positively with the Thiéry reaction, as does the intine (i). The lipid bodies seen in Figs 18-20 do not stain with the Thiéry reagent (not illustrated), unlike the starch grains (se, spore exine; t, tapetal plasmodium). x 17,500.

Fig. 4.47. Microtubules (arrows) can still be seen at the PSM. Binucleate pollen grain stage (sw, pollen wall). x 68,570.

Fig. 4.48. Apparently empty vesicles with prominent tripartite membranes accumulate in the plasmodium close to the PSM (s, pollen grain). x 18,000.

Fig. 4.49. A high magnification micrograph to show the tripartite membranes of the vesicles as seen in Fig. 4.48. Often the membranes are in double or multiple layers (arrowheads). x 120,000

Fig. 4.50. A median section of the pollen wall from a dehisced anther to show the deposition of densely-osmiophilic pollenkitt (tp) material on the spore exine (se) and under the tectate roof of the exine. Note the discontinuities (arrowheads) in the nexine layers of the exine, yet no continuity can be seen between the electron-dense material and the interior of the pollen cytoplasm. x 68,570.

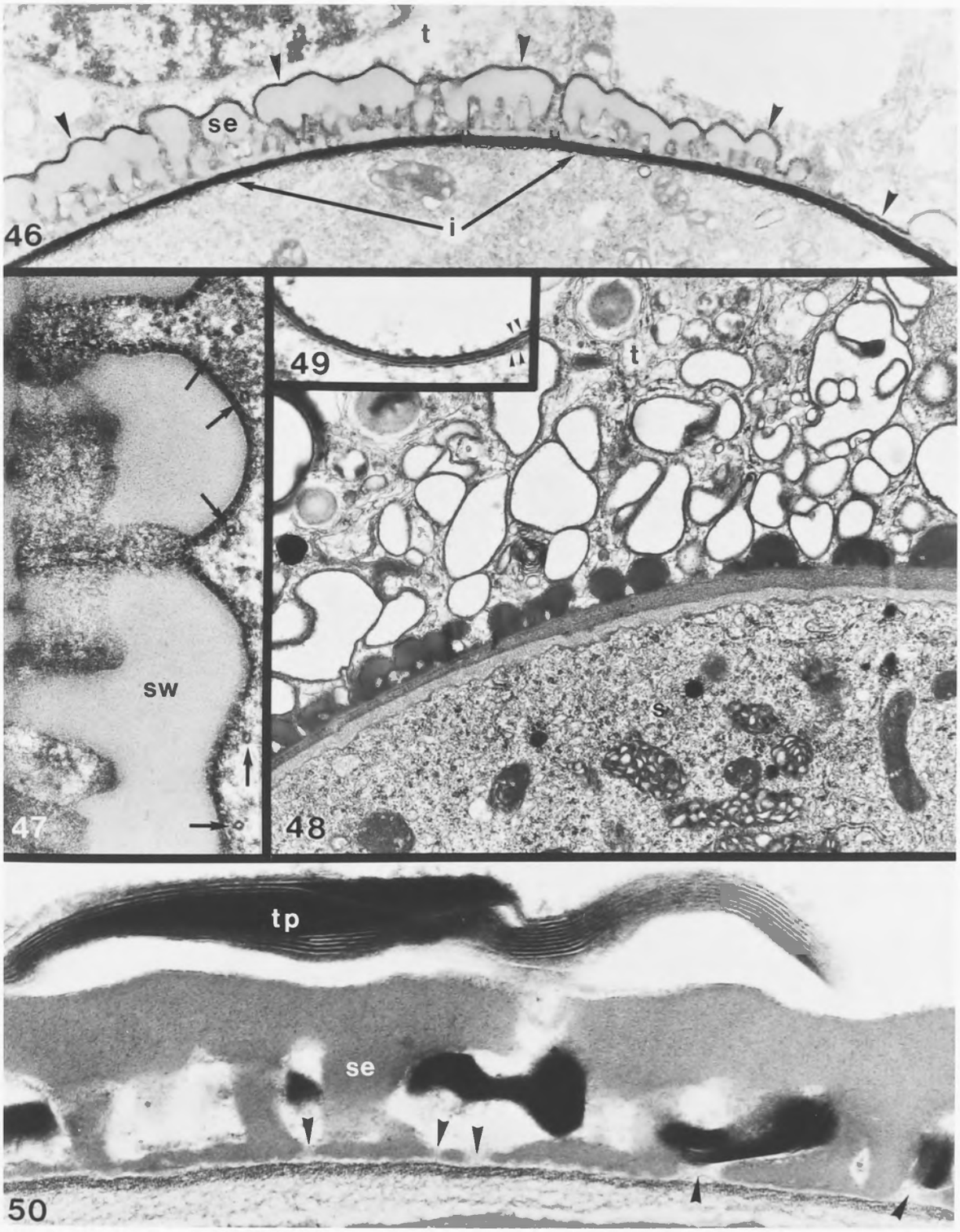
t
se
i
46
sw
47
49
t
s
48
tp
se
50

Figs. 4.51-4.53. Parts of tapetal invasion process showing elements of endoplasmic reticulum (arrows) and some other profiles (arrowheads) of doubtful identity. x 18,000; 45,000 and 42,000, respectively.

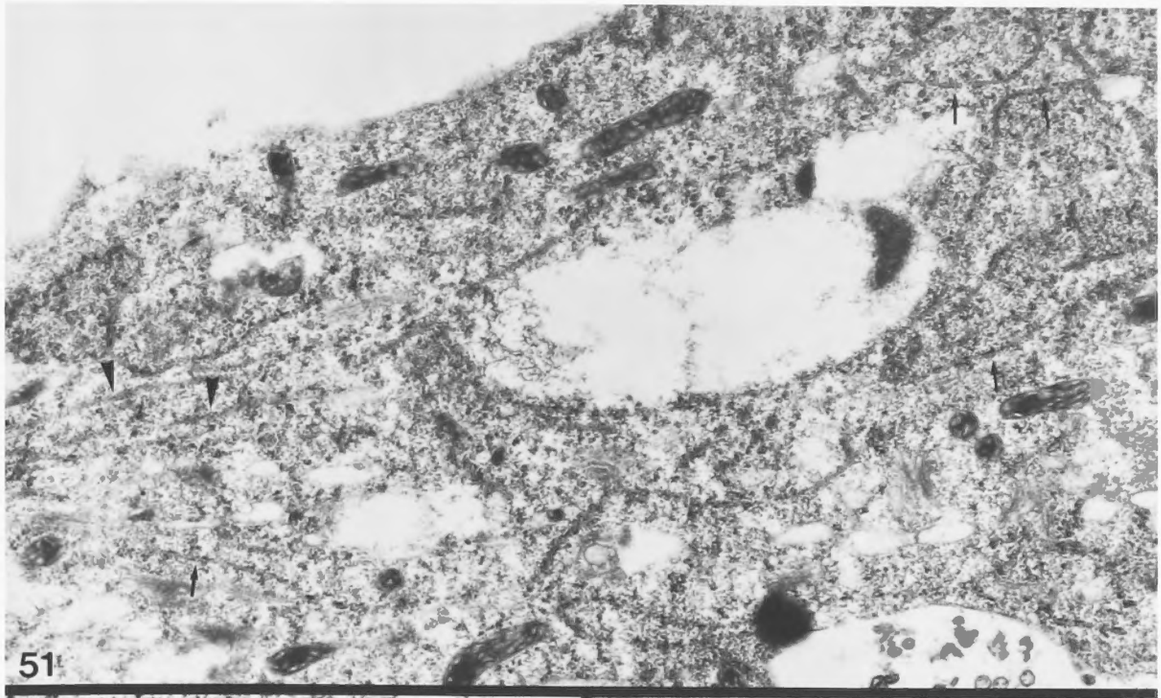

51

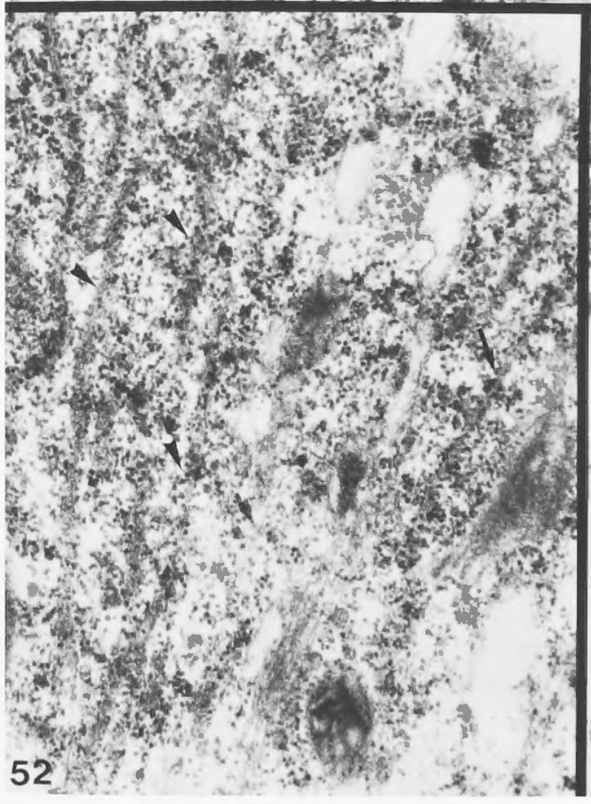

52

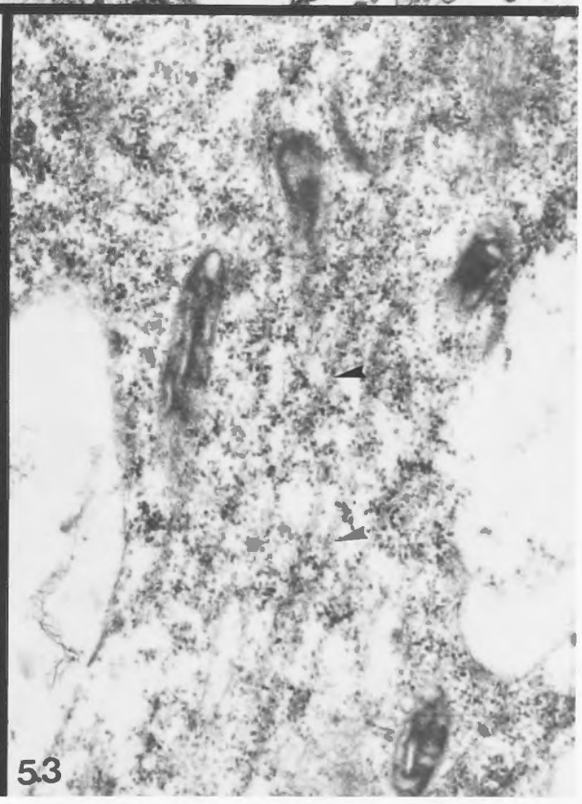

53

Figs. 4.54,4.55. Squashes made from tapetum both at early meiosis (Fig. 4.54) and postmeiotic (Fig. 4.55) stages show strands of fibrillar material (arrows). x 700 and 750, respectively.

Fig. 4.56. Negatively stained preparation of filamentous structure from the plasmodium. x 89,750.

Fig. 4.57. A part of plasmodium from an anther which was fixed in the presence of 50mM lysine, showing wispy structures in the cytoplasm. x 41,650.

Fig. 4.58,4.59. Parts of the plasmodium from an anther which was treated with phalloidin before fixation (Fig. 4.58) and from an anther which was treated with phalloidin after fixation (Fig. 4.59). Note the improved preservation of cytoplasm in Fig. 4.59. x 41,140 and 46,150, respectively.

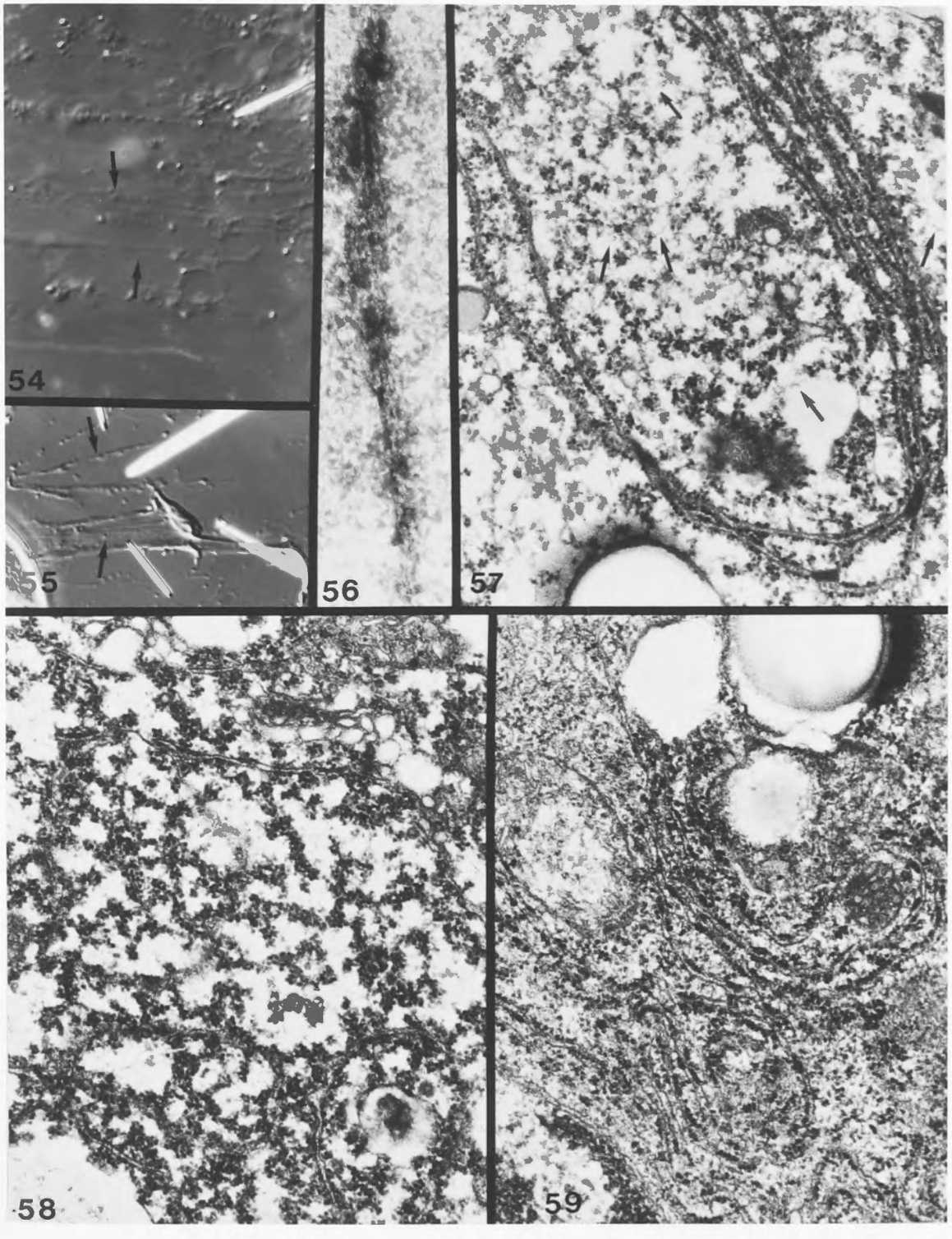
54
55
56
57
58
59

Figs. 4.60,4.61. Parts of conventionally-processed (Fig. 4.60) and freeze-substituted (Fig. 4.61) cells of the stamen hair showing aspects of cortical cytoskeleton. Conventionally-processed cells do not show any microfilaments (arrowheads) and the microtubules (arrows) appear distorted. In freeze-substituted cells, however, the microfilaments, arranged parallel to the cortical microtubules, can be clearly visualized. One microtubule profile placed perpendicular to other microtubules, shows the closed termination (see Chapter 6 for further discussion on such terminations). Double-headed arrows indicate the direction of the long axis of these cells. x 64,800 and 74,770, respectively.

60

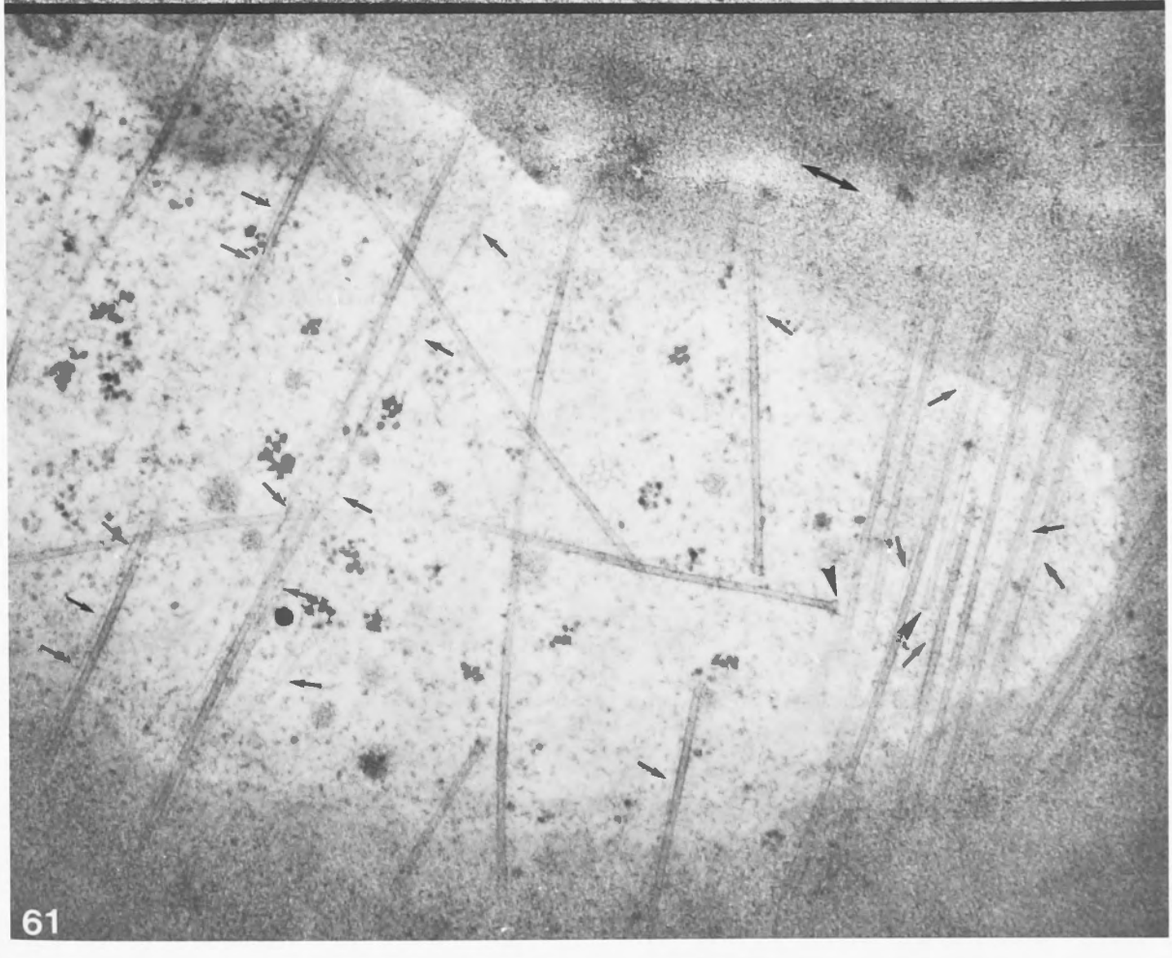

61

CHAPTER 5

EFFECTS OF COLCHICINE ON THE TAPETUM OF *TRADESCANTIA VIRGINIANA* L.

5.1. INTRODUCTION

The host side of the sporophyte-gametophyte interface in angiosperm anthers consists of the tapetum, a tissue layer whose morphology can vary widely in different taxa from a secretory epithelium to an invasive plasmodium. The tapetum contributes to the nutrition of the meiocytes and pollen cells that develop in symplastic isolation in the anther loculus, and among these contributions one specific role - provision of sporopollenin - is widely accepted (for reviews see Echlin, 1971a,b; Heslop-Harrison, 1971a,b, 1972, 1975). However, the precise mode of tapetal function in sporopollenin deposition in the pollen cell wall has not been established. Questions remain concerning the nature of the precursor(s), their site of synthesis and pathway through the tapetal cytoplasm, their exocytosis and movement across the apoplastic gap to the spores, their assembly and deposition, and whether the tapetum is their sole source.

Chapter 4 describes an invasive plasmodial type of tapetum in Tradescantia virginiana L. Features that seem relevant to some of the above questions include: the development of specialised membranes in the form of membrane sacs associated with cytoplasmic microtubules; incorporation of the sac membrane into the perispore membrane (PSM) during and after the dissolution of the callosic wall in the tetrads; the presence of putative sporopollenin granules within these sacs; exclusive

occurrence of microtubules in the cortical regions underlying the PSM at the late tetrad stage; spatial relationship of abundant tubular ER with the PSM; and subsequent very close association between the PSM and the developing sporopollenin exine. Cytoplasmic microtubules were also seen in the invasion processes that form when the original tapetal cell walls break down, and also at the apparently specialised contact zones between invasion processes before cell fusion creates a true tapetal plasmodium.

The experiments reported here were originally planned as an extension of the work of Pacini and Juniper (1983), whose observations on the plasmodial tapetum of Arum suggested that microtubules might aid in mobilising tapetal cytoplasm and guiding its invasion of the anther locule. However, Tradescantia and Arum were found to differ in a number of respects (see Chapter 4), and while the experiments reported here, using colchicine, did not confirm a role for microtubules in tapetal invasion, they did throw new light on the process of sporopollenin deposition and antecedent intracellular transport systems in tapetum. These topics are described here.

5.2. MATERIAL AND METHODS

5.2.1. Colchicine Treatment

Plants were grown and maintained as described in Chapter 4. Colchicine was applied in aqueous solution at a concentration of 5×10^{-3} M to isolated buds of known

developmental stages. Buds were excised while immersed in distilled water and dipped in vials wrapped in aluminium foil and containing colchicine solution for 8-60 hours in glasshouse conditions. The treatment duration was largely determined on the basis of the time required for colchicine to penetrate to the anther locule, and the times taken for transitions from one developmental stage of interest to another. After the treatment, anthers were dissected out and processed for electron microscopy as described previously (Chapter 4). Controls were run in distilled water under identical conditions.

5.2.2. Acetolysis Test

Sporopollenin was identified in semi-thin sections according to the procedure of Dickinson and Bell (1973). 2-4 μm thick sections of plastic-embedded anthers were dried onto glass slides, stained with toluidine blue O in 0.1% sodium carbonate (pH 11.1), mounted in distilled water and photographed using differential interference contrast optics on a Zeiss Photomicroscope III. Later, freshly made acetolysis mixture (1 ml concentrated sulfuric acid + 9 ml acetic anhydride) was introduced under the cover glass and the slide heated on a small flame for 5 minutes, while constantly irrigating the preparation with fresh acetolysis mixture. The preparation was then sealed with wax and observed with interference contrast optics.

5.3. RESULTS

During the course of this investigation the disappearance of microtubules from the tapetal cells and anther wall layers served as the primary indicator that colchicine had penetrated and taken its effect. Some of the treatment periods needed to obtain desirable effects were long when compared with other investigations using the drug, nevertheless reproducible results were obtained. Short duration treatments were also monitored to establish effective treatment durations.

5.3.1. First Phase of Tapetal Invasion

Buds at pre-invasion stages of development were subjected to colchicine treatment in order to study the effect of colchicine on tapetal invasion of the loculus. After 8h treatment, the tapetal cells showed normal features. Their radial wall and inner periclinal walls appeared more or less dissolved (Fig. 5.1); they maintained their uniform outlines toward the inner side of the loculus with no sign of invasion; and microtubules remained (Fig. 5.2). However, it would appear that some time between 8 and 12 hours sufficed for colchicine to penetrate and have its first discernible effects. Microtubules disappeared from the tapetal and other cells of the anther wall when the buds were given 12h of treatment. Nevertheless the 12h treated tapetal cells had developed projections into the loculus, between the sporogenous cells (Fig. 5.3). In untreated controls these

projections develop into long invasion processes during normal tapetal development. Still longer treatments, observed at regular intervals up to 60h, did not seem to hinder the growth of the tapetal projections. Figs. 5.4 and 5.5 are from buds treated for 22 and 60h, respectively; the tapetal invasion process in Fig. 5.5 has reached far inside the loculus, branched, and partially surrounded the developing meiocytes, although its cytoplasmic organisation is abnormal (see later).

A fibrous extracellular cell coat, which reacts positively with the Thiéry reaction, develops on the free surfaces of the tapetal cells and their invasion processes soon after the dissolution of tapetal cell walls and persists until the cells fuse (Chapter 4). Colchicine treatment interferes with the deposition of this cell coat. Depending upon the duration of the drug treatment, the plasma membrane was found to be smooth or smoother than in the controls. Fig 5.6 shows a completely smooth inner tapetal surface at the dyad stage of meiosis, in material treated for 60h, and Fig. 5.7 represents the normal cell coat in a control.

5.3.2. Second Phase of Tapetal Invasion

One of the most conspicuous features of tapetal invasion processes in Tradescantia is the development of membrane sacs which migrate toward the free inner surfaces of the tapetal cells. They accumulate where the plasma membrane of one tapetal invasion process meets another

process, or where it comes into contact with sporogenous cells, eventually forming a labyrinthine reservoir of membranes around the tetrads. Microtubules are so consistently associated with these membrane sacs that it may be conjectured that they function in the polarized migration of the sacs to the inner regions of the tapetal extensions, or in stabilising the labyrinth. Results of colchicine treatments accord with this hypothesis. 12h of colchicine treatment removed the microtubules, though not the coated vesicles, that are associated with the membrane sacs (Fig. 5.8).

To further investigate the inhibition of migration of these sacs in response to colchicine it was necessary to start the treatment when the sacs were still being synthesized but before completion of their intracellular movement. Early stages of the second meiotic division were appropriate for beginning the colchicine treatment, and the callose-free late tetrad stage for cessation. By the latter stage all of the sacs have become incorporated in the PSM and no cytoplasmic accumulations remain. However, this developmental interval is relatively long and therefore longer exposures to colchicine (60h) than are usually employed in this type of drug treatment were necessary. Notwithstanding this limitation, colchicine was observed to inhibit the polarised migration of the sacs. Fig. 5.10 shows a part of the plasmodium, the PSM and the callose-free late tetrad from an anther which had been treated with the drug for 60h. Unlike the control

(Fig. 5.11), where the PSMs surround all of the tetrads, and are always underlain by many membrane convolutions, in the drug-treated anthers, many PSMs fail to form, but of those that do develop, most have either no associated membrane sacs or few sacs which, in these latter cases, could have reached the PSM before the colchicine took its effect. Additionally, the colchicine-treated plasmodia showed massive accumulations of anastomosed or free sacs in the deeper parts of the cytoplasm (Fig. 5.9). The controls do not show any such cytoplasmic accumulations at the late tetrad stage. In drug-treated plasmodia a few sacs were even recorded at or close to the outer face of the tapetum, a feature never seen in controls. In Fig. 5.10 note also that the colchicine-treated tapetum has formed small invasion processes into the intermicrosporal spaces just as in the controls, indicating thereby that microtubules are not required to initiate the post-meiotic tapetal invasion of the intermicrosporal spaces (see also later).

The results do not distinguish between a possible specific effect of colchicine upon the microtubules that are associated with the membrane sacs, or a possible more general effect upon the polarity of the invasion processes. The latter cannot be excluded as colchicine also interferes with the movement and release of golgi vesicles which can be seen to accumulate in massive quantities in the tapetal cytoplasm, even in pre-invasion stages (Figs. 5.3-5.5). However, the microtubules

associated with the membrane sacs are largely removed by short-term (12h) treatments with colchicine.

5.3.3. Tapetal Cell Fusion

During cell fusion, two cells or their invasion processes come close to each other, their plasma membranes show accumulations of membrane sacs, shed their cell coats, and form appressed junctions with arrays of microtubules lying parallel to and just underneath the plasma membrane. To investigate the possible role of microtubules in cell fusion, it was, once again, important to select the right stages for treatment with colchicine. The transition from callose-bound tetrads to the free microspore stage when, normally, cell fusion is complete, takes approximately 20h. The colchicine was therefore applied for 24h.

Colchicine was found to have an inhibitory effect on cell fusion. Fig. 5.13 is from a drug-treated anther and Fig. 5.12 represents a control showing complete cell fusion and invasion of the intermicrosporal spaces (seen in Figs. 5.10,5.11), so that each microspore is individually surrounded by a PSM. Figs. 5.13 and 5.14, by contrast, show that there are many 'unfused' expanses of discrete plasma membranes. It should, however, be pointed out that in drug-treated plasmodia there were a few PSMs which had been formed as a result of a preceding cell fusion (Fig. 5.10 shows a PSM in a plasmodium that was subjected to much longer colchicine treatment), but since

cell fusion is slow and asynchronous (see Chapter 4) it is likely that these might have been formed before the drug began to act. Although 24h of treatment removed most microtubules from the syncytium, the anther wall, or even from these discrete cells (Fig. 5.15), a few microtubule profiles remained subjacent to some of these unfused membranes (Fig. 5.16).

5.3.4. Sporopollenin Deposition

As mentioned in Chapter 4, there were some indications in the form of a high population of microtubules underlying the PSM, spatial relationship between the ER and the PSM and putative sporopollenin granules in the membrane labyrinths of the PSM, that it might be possible to produce visible perturbations of tapetal function in sporopollenin deposition. Colchicine treatment does in fact disrupt the directed transport of material for pollen wall growth. The treatment was started when tetrads were still enclosed in callose and terminated at later stages of free microspore development because it was in this interval that the pollen wall exine attained its full growth. This entire transition took approximately 60h and colchicine was applied for the same duration.

The most conspicuous effect of this colchicine treatment was deposition of sporopollenin in all the extracellular spaces of the plasmodium. As described above, many tapetal cells remain 'unfused' under the

influence of colchicine, and it was in the intercellular spaces between these 'unfused' tapetal protoplasts that sporopollenin deposits were found in the form of electron-dense globules which had a tendency to fuse (Figs. 5.18, 5.21-5.24). The largest and most conspicuous deposits occurred on the outer periclinal surface of the tapetum (Figs. 5.18-5.20) where sporopollenin accumulated in the form of a continuous layer of uneven thickness between the inner face of the wall of the middle cell layer (of the anther wall) and the tapetal plasma membrane (Fig. 5.20, cf. control Fig. 5.17). An electron opaque layer of lipidic material was often found interpolated between the sporopollenin layer and the cell wall (Fig. 5.20). Even the occasional remnants of the original radial walls of the tapetal cells showed this feature (Fig. 5.21). Upon acetolysis this deposit was found to show the same resistance as the spore exine (Figs. 5.25,5.26), thus confirming its sporopollenin nature. In the intercellular spaces between the 'unfused' cells the deposits existed as aggregations of apparently loose electron-dense globules of variable dimensions (Figs. 5.18,5.22). Often these globules were seen attached to electron-opaque lipidic surfaces (Figs. 5.22,5.24) or short tripartite membrane-like profiles (Fig. 5.23) which are possibly formed from the lipidic material (Fig. 5.24 is suggestive of this), and, then, assume the 'ordered' deposition seen in the peritapetal location. There were, however, many larger solitary deposits in which the lipidic or membrane

component could not be identified (Fig. 5.21), perhaps having been occluded by accretion of sporopollenin. After treatment with colchicine numerous deposits of densely osmiophilic material were also seen associated with many of the organelles (Figs. 5.19). These deposits were usually smaller but otherwise resembled the extracellular deposits of sporopollenin. Interestingly, the tapetal plasma membrane never shows any adherent sporopollenin deposits, unlike the membrane lamellae in the extracellular spaces, though it does have a few cup-shaped depressions in which lie sporopollenin deposits (Figs. 5.23,5.24), suggestive of reverse pinocytosis.

As described in Chapter 4, a prominent feature of the tapetum-spore interface at the time of sporopollenin deposition is an elaborate system of tubular ER underlying the PSM. Under the influence of colchicine the PSM does not receive membranes from the sacs which in normal conditions accumulate as a labyrinth near the tetrads. As well as disrupting migration of membrane sacs, colchicine treatment results in failure to locate the ER near the PSM. Instead, the ER tubules are found more or less throughout the tapetal cytoplasm (Fig. 5.19). The surfaces which receive abnormally-placed sporopollenin deposits, i.e. the "unfused" regions of the tapetal invasion processes and the outer face of the tapetum are commonly underlain by tubular ER (Fig. 5.20).

The disordered deposition of sporopollenin in response to colchicine was seen only if the treatments

encompassed the tetrad stages. Treatments terminated before or begun after the tetrad stages did not produce the results described above.

5.4. DISCUSSION

Some of the colchicine treatments used in the present work were prolonged, and there is no means of knowing how much breakdown or exclusion the drug sustained en route to the tapetum. In view of this, and the knowledge that colchicine is by no means a specific anti-microtubule drug (see Hart and Sabnis, 1976), it cannot be claimed that the responses seen in the present material are all direct consequences of removal of tapetal microtubules. There was a lag of 8-12h before any effects could be found, and even after 60h some tapetal regions retained a few microtubules, though by then they had been completely removed from the cells of the anther wall. Accordingly, microtubule destruction is probably responsible, directly or indirectly, for at least some of the perturbations, although the exact role of the tapetal microtubules must await further elucidation. Nevertheless the perturbations themselves reveal a considerable amount of new information about the functioning of the plasmodial type of tapetum which has not previously been examined by this type of experiment.

The first point to be emphasized is that tapetal invasion does proceed in the presence of colchicine, both into the inter-meiocyte spaces and later into the inter-

microsporal spaces opened up by dissolution of the callose wall of the tetrads. It is possible that cytoskeletal elements are not required for the tapetal cytoplasm to invade the anther locule once the restraining cell walls are removed, but if guidance or shaping systems are necessary, it would appear that they do not include microtubules, at least in Tradescantia, although microtubules are present in the cortex of the invasion processes in both phases of invasion, running approximately transverse to the long axis of the processes. Neither do the arrays of microtubules that have been postulated to guide invasion in Arum plasmodial tapetum (Pacini and Juniper, 1983) occur in Tradescantia (Chapter 4).

However, several processes within the tapetal cytoplasm are strongly influenced by colchicine. One concerns migration of membrane sacs to form a labyrinth where the invasion processes contact the meiocytes. A second concerns junctions between separate invasion processes, where their plasma membranes become closely appressed. Both of these have associated microtubules; in the former case sparse but clearly alongside the membrane sacs, and in the latter case taking the form of more extensive arrays underlying the opposed plasma membranes. A third process concerns spatial control of sporopollenin deposition: this is disrupted, perhaps secondarily by effects of colchicine upon the first two processes, though more direct effects are also possible.

Tapetal investment of the young microspores in Tradescantia anthers has been described as a two-phase process (see Chapter 4), although temporal synchrony within the individual anther is not marked. In the first phase, membrane sacs arise and congregate at sites close to meiocytes. In the presence of colchicine the microtubules associated with the sacs are removed relatively quickly, and prolonged treatments inhibit their polarized migration, leading instead to aggregations of anastomosed sacs remote from the reproductive cells. In phase two the membrane of the labyrinth of sacs is incorporated into the PSM as the tapetum infiltrates the intermicrosporal spaces of tetrads. In the treated anthers the PSM does form small secondary invasion processes into the spaces of a tetrad, indicating that microtubules do not initiate even this phase of invasion. However, since longer treatments were not performed, it is not known whether further tapetal infiltration (so as to surround each microspore individually) is eventually inhibited either directly or secondarily by the absence of membrane sacs.

It it noticeable that following colchicine treatment, golgi vesicles likewise do not follow their normal pathway of exocytosis in the invasive processes (Figs. 5.3-5.5). Such phenomena are more familiar as the outcome of treatment with anti-microfilament drugs (Mollenhauer and Morré, 1976; Picton and Steer, 1981, Volkmann and Czaja, 1981), so it may be that the

cytoskeleton of the tapetum has suffered a wholesale influence from the colchicine treatment. Microtubules are quite commonly associated with membranous organelles, e.g. nuclei (McKerracher and Heath, 1985), mitochondria (see Gunning and Hardham, 1982), endoplasmic reticulum (e.g. Ryan, 1984 and literature cited therein), and involuted plasma membrane (Oross and Thomson, 1982), but none of these, except perhaps the first two, offer a close parallel to colchicine-sensitive transport of membranous material of the sort seen here in Tradescantia tapetum.

Sites where tapetal cell fusion first occurs cannot be identified with certainty. Relevant observations are that colchicine inhibits cell fusion, and that in controls local expanses of appressed plasma membranes have subjacent arrays of microtubules. Incorporation of the membrane sacs into the apposed plasma membranes usually precedes, and possibly triggers fusion, so the action of colchicine could be either primary, on the cortical microtubules, or secondary, as a delayed outcome of its effect on migration of the components of the membrane labyrinth. At any event, expanses of unfused tapetal plasma membrane persist in the loculus. This then becomes highlighted by a subsequent phenomenon.

Most studies of sporopollenin deposition have been made on species with secretory tapeta (see Echlin 1971a,b; Heslop-Harrison, 1971a,b, 1972; Bhandari, 1984), where concomitant with exine development, sporopollenin is also deposited in the form of a layer of orbicules on the

thecal face of the tapetal plasma membrane. The presence of tapetal orbicules in secretory tapetum has been considered as proof of the tapetum's capacity to produce sporopollenin. By contrast, orbicules are not found in species with plasmodial tapeta and this, together with the finding that exine deposition is apparently complete before the microspores are released from the callosic walls, led Mepham and Lane (1969b), and Mepham (1970) to conclude that the plasmodial tapetum of Tradescantia bracteata does not contribute to the growth of the sporopollenin wall of pollen.

The effect of colchicine on Tradescantia virginiana anthers provides convincing evidence that the plasmodial tapetum does participate in the synthesis and secretion of sporopollenin, even though it may not show any marked manifestations of this activity unless experimentally disturbed. It is true that much of the microspore exine is laid down within the enveloping callosic wall of the tetrads, but at the time of spore release the spores still have relatively thin walls (see Chapter 6). Under normal conditions sporopollenin deposition continues and the spore wall shows almost 100% increase in its thickness during the interval between late tetrad and early microspore stages. Colchicine treatments disrupt the spatial regulation so that sporopollenin (identified as such by resistance to acetolysis) is laid down (a) in patches outside the "unfused" plasma membranes of tapetal invasion processes, the effect being similar to the

colchicine-induced deposition of sporopollenin granules in the anther cavity of Canna (which has a non-syncytial invasive tapetum that normally does not show orbicules, Chapter 3); and (b) in a substantial layer on the outer periclinal face of the tapetum, abutting the middle layer of the anther wall and thus resembling the peri-tapetal deposit produced normally in Ulex (Misset and Gourret, 1984), some compositae (Heslop-Harrison, 1969) and gymnosperms (Pettitt, 1966; Dickinson, 1970b).

The fact that sporopollenin deposition is normally restricted to the microspore wall in contact with the PSM (excluding earlier exine formation within the callosic walls) suggests that this membrane has special properties. It acquires highly specialized features in the form of its convolutions, association with microtubules and intimate relationship with ER and coated and smooth vesicles. Drug treatments prevented migration and consequently incorporation of the membrane sacs in to the plasma membranes, inhibited cell fusion and consequently the formation of a structurally organized PSM, depolymerized the microtubules, and disturbed the spatial distribution of ER which became randomly dispersed and often found close to the tapetal surfaces on which sporopollenin deposits became abnormally placed. Because sporopollenin can be laid down on all available extracellular lipidic surfaces under the influence of colchicine, it may be that the role of the PSM in normal development is to localize the availability of precursors to the maturing pollen

grains. In the invasive plasmodial tapetum of T. virginiana, cell fusion normally removes all surfaces other than the PSM, and accordingly, deposition occurs only on the exine. In species with secretory tapeta the large separation between the analogous membrane and the pollen wall provides an opportunity for large scale extraneous polymerisation (orbicule formation) to take place, much as in colchicine-treated Tradescantia where there is abnormal continuity to the exterior via gaps between unfused tapetal processes.

Since in treated anthers sporopollenin polymerized in an 'ordered' form only when it came in contact with an extracellular lipidic surface, it seems that availability of lipidic surfaces and extracellular space imposes physical constraints on the amount of sporopollenin deposited at any particular site. To the best of my knowledge this is the first time such an effect has been observed and provides an experimental basis for the observations of Rowley and Southworth (Anthurium and Scapania, 1967), Godwin et al. (Ipomoea, 1967), Dickinson and Heslop-Harrison (Lilium, 1968; see also Dickinson, 1976), Atkinson et at. (Chlorella, 1972) and my own (Stenoglotis, unpublished) relating to the polymerization of sporopollenin on trilaminar lamellae during normal development.

Figs. 5.1-5.5. Transverse sections of anthers from drug-treated buds. The treatments were started before the commencement of premeiotic tapetal invasion of the loculus.

Fig. 5.1. Tapetal cells (t) after 8 hours of treatment. Invasion has not yet commenced (sc, sporogenous cells). x 1,950.

Fig. 5.2. 8 hours of treatment was insufficient to remove the microtubules. Figure shows microtubules (arrowheads) present at the inner periclinal wall of the tapetum after the treatment. x 59,400.

Figs. 5.3,5.4. Tapetal cells (t) after 12 and 22 hours of treatment, respectively. Note that they have formed small protrusions in the spaces between the sporogenous cells (sc). Microtubules had disappeared between 8-12 hours of treatment. x 3,940 and 2,700, respectively.

Fig. 5.5. After 60 hours of treatment a well-developed tapetal invasion process (t) has formed. The sporogenous cells (sc) have produced a thick callosic wall. Dictyosomal vesicles have accumulated in the tapetal cytoplasm during the treatment. x 2,150.

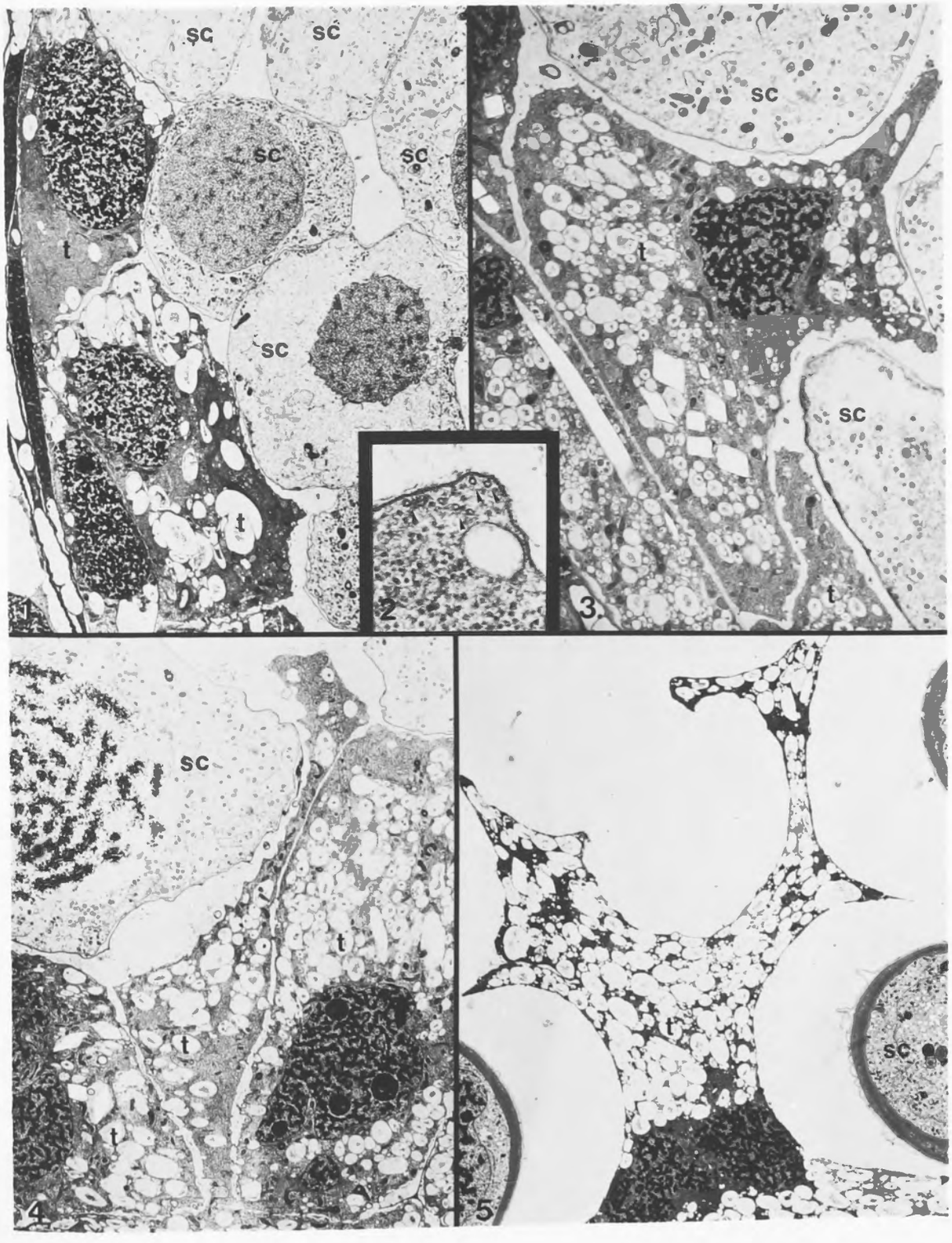
sc
sc
sc
sc
sc
t
t
1
2
sc
t
sc
t
3
sc
t
t
t
4
t
sc
5

Figs. 5.6.,5.7. Tapetal cell surfaces from drug-treated and control buds, respectively. Unlike the control, where the cell coat is prominent, the treated cells have lost their cell coat after 60 hours of treatment. x 48,000 and 26,000, respectively.

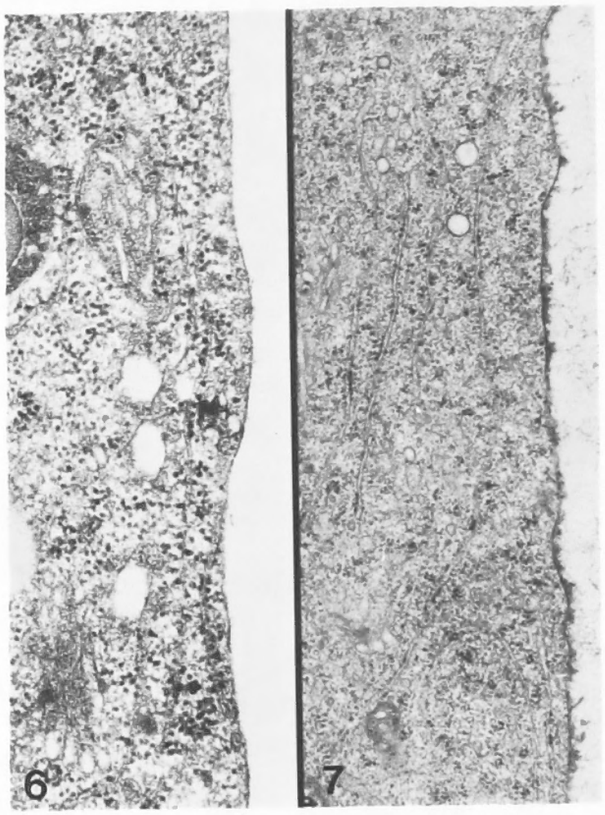
6
7

Figs. 5.8-5.11. Parts of tapetal cells to show the behaviour of membrane sacs in response to colchicine.

Fig. 5.8. Colchicine treatment of 12 hours removed the microtubules associated with the membrane sacs (ms). This figure is from dyad stage. Arrows indicate the coated vesicles. x 41,540.

Fig. 5.9. Accumulations of coalesced sacs in the plasmodium at late tetrad stage in response to 60 hours of treatment. Adjacent serial sections of this material negated the possibility of this being a grazing section of the perispore membrane. x 12,000.

Figs.5.10,5.11. Drug-treated and control microspore tetrads, respectively, after 60 hours of exposure. The treated plasmodium show very few membrane convolutions (arrowheads) as compared with the PSM in the control. Note also that in both these micrographs the plasmodium has formed small invasion processes into the intermicrosporal spaces (arrows). x 2,680 and 2,920, respectively.

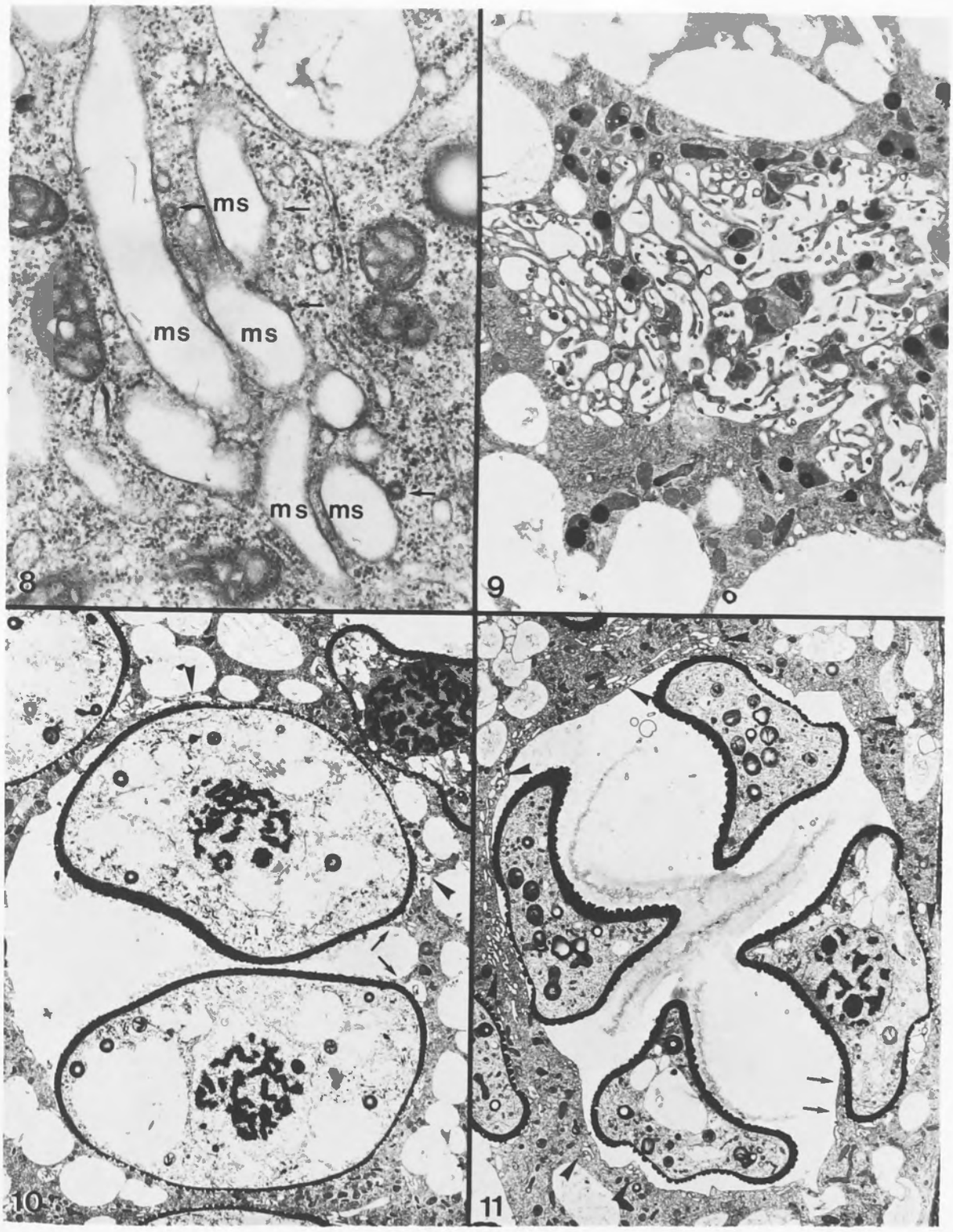
ms
ms
ms
ms
ms
8
9
10
11

Figs. 5.12-5.16. Electron micrographs to illustrate the effect of colchicine on tapetal cell fusion.

Fig. 5.12. The control for this experiment shows a uniform syncytium with no 'unfused' tapetal cells at the early microspore stage (ms, microspore). x 2,000.

Figs. 5.13,5.14. Plasmodium treated for 24 hours, also at the early microspore stage. There are many 'unfused' tapetal cells (apposed plasma membranes are traced by arrowheads; ms, microspores). x 2,430 and 5,070, respectively.

Fig. 5.15. Contiguous surfaces of discrete tapetal cell from which microtubules have been removed by colchicine. The apposed plasma membranes have undergone vesiculation in some places. x 52,500.

Fig. 5.16. Surface of a still discrete tapetal cell which shows the presence of microtubules in spite of 24 hours of treatment. x 42,000.

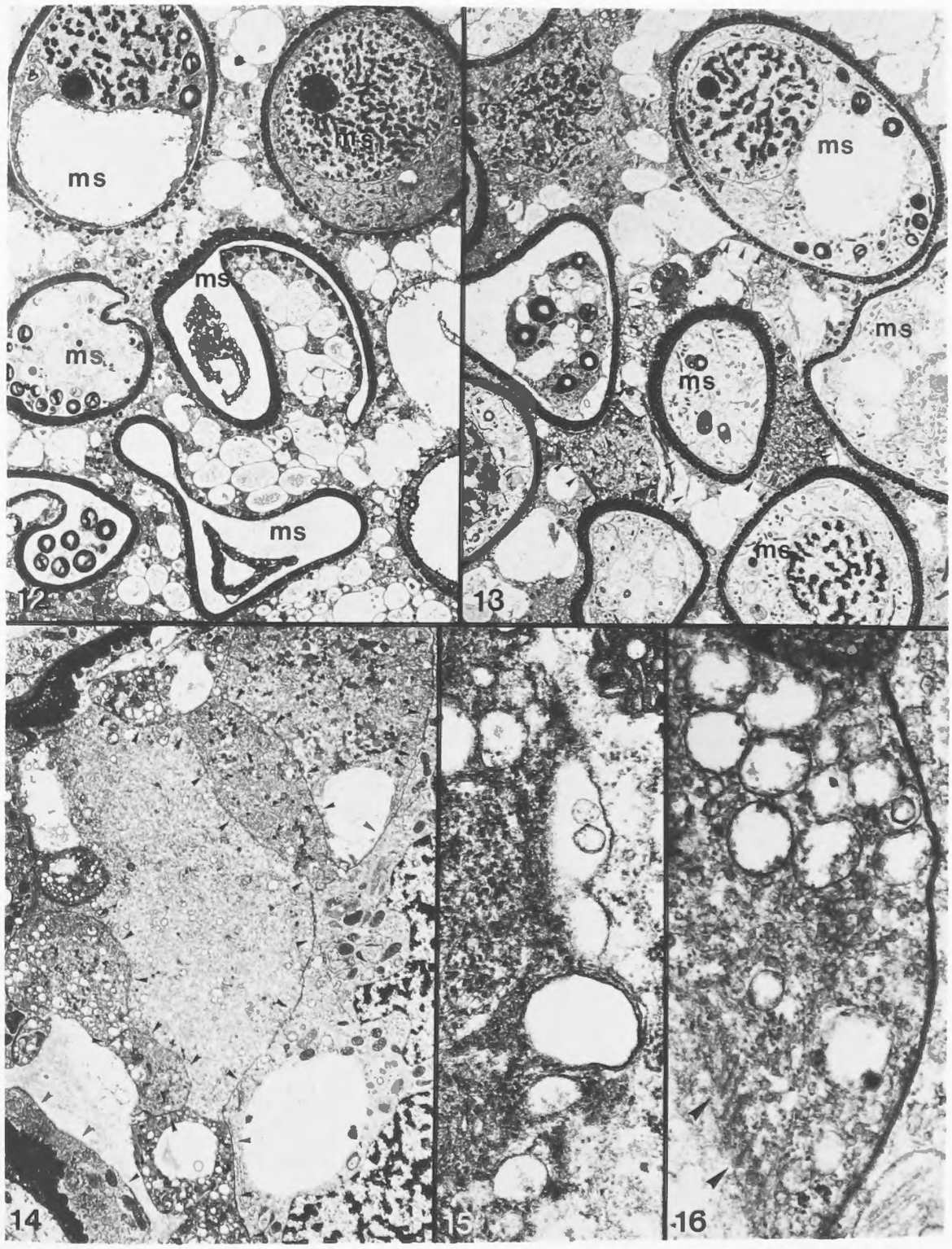
ms
ms
ms
ms
ms
12
ms
ms
ms
ms
13
14
15
16

Figs. 5.17-5.19. Electron micrographs to show the effect of colchicine on the deposition of sporopollenin.

Fig. 5.17. Tapetal-middle layer interface from the control anthers at microspore stage. x 14,400.

Fig. 5.18. 60 hours of treatment results in the deposition of sporopollenin in the spaces between 'unfused' cells (arrows) and on the outer periclinal face of tapetum (arrowheads) where it adjoins the middle layer (ml) of the anther wall. Microspore stage. Compare this photograph with Fig. 5.17. x 3,770.

Fig. 5.19. A part of tapetal cytoplasm to show the general ultrastructure of the colchicine-treated plasmodium. Many cytoplasmic organelles show electron-dense material. The peritapetal deposit can be seen at the bottom of the photograph (d, dictyosome; m, mitochondrion; n, nucleus; p, plastid). x 35,160.

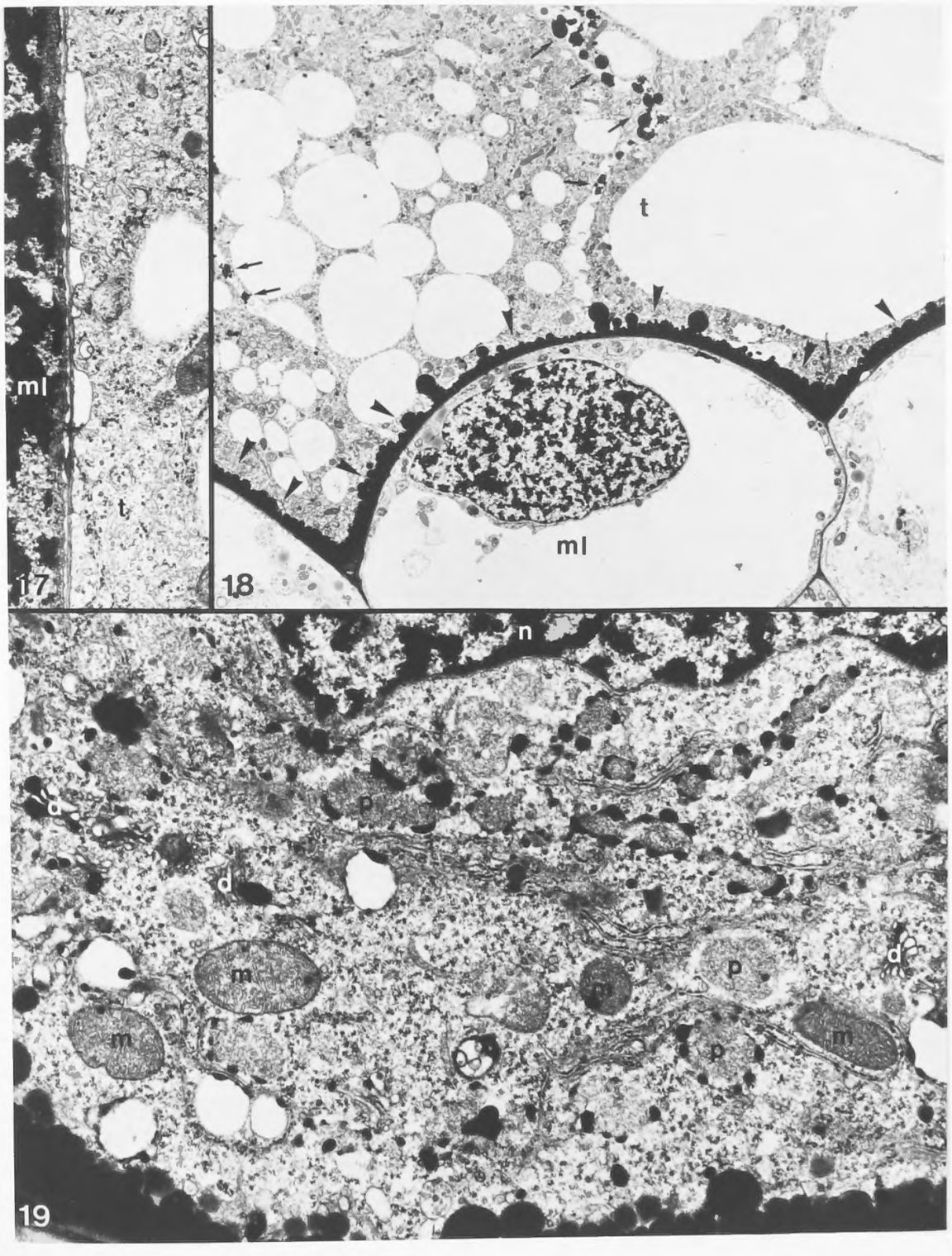
ml
t
17
t
ml
18
n
d
p
d
m
m
p
d
p
m
19

Figs. 5.20-5.24. Electron micrographs to show aspects of abnormally-placed deposits of sporopollenin which are formed in response to colchicine treatment.

Fig. 5.20. Plasmodial cytoplasm adjacent to the middle layer (ml) of the anther wall. Peritapetal deposit of sporopollenin (ptl) is outside the tapetal plasma membrane (black arrows). A thin layer of electron opaque lipidic material (white arrows) is interpolated between the cell wall and the peritapetal deposit. Note the abundance of tubular ER vesicles. x 42,000.

Fig. 5.21. Deposition of electron-dense sporopollenin globules on the remnants of original radial wall (rw) and the lipidic material (arrows). A large sporopollenin (sp) deposit is also seen between the withdrawn plasma membrane and the cell wall. Deposits such as this do not reveal lipidic surfaces. x 16,000.

Fig. 5.22. Sporopollenin deposits on electron-opaque lipidic surfaces (arrows) to produce characteristic patterns. x 12,000.

Fig. 5.23. Tripartite membrane lamellae (arrows) are often seen embedded in the sporopollenin deposits. Arrowheads indicate the cup-shaped depressions in the tapetal plasma membrane that seemingly accommodate sporopollenin globules. x 46,300.

Fig. 5.24. Lipidic surfaces embedded in the sporopollenin deposits. The lipid material at the bottom of the micrograph assumes a flat lamellate configuration towards the middle of the photograph. Arrowheads indicate the cup-shaped depressions in the plasma membrane. x 31,960.

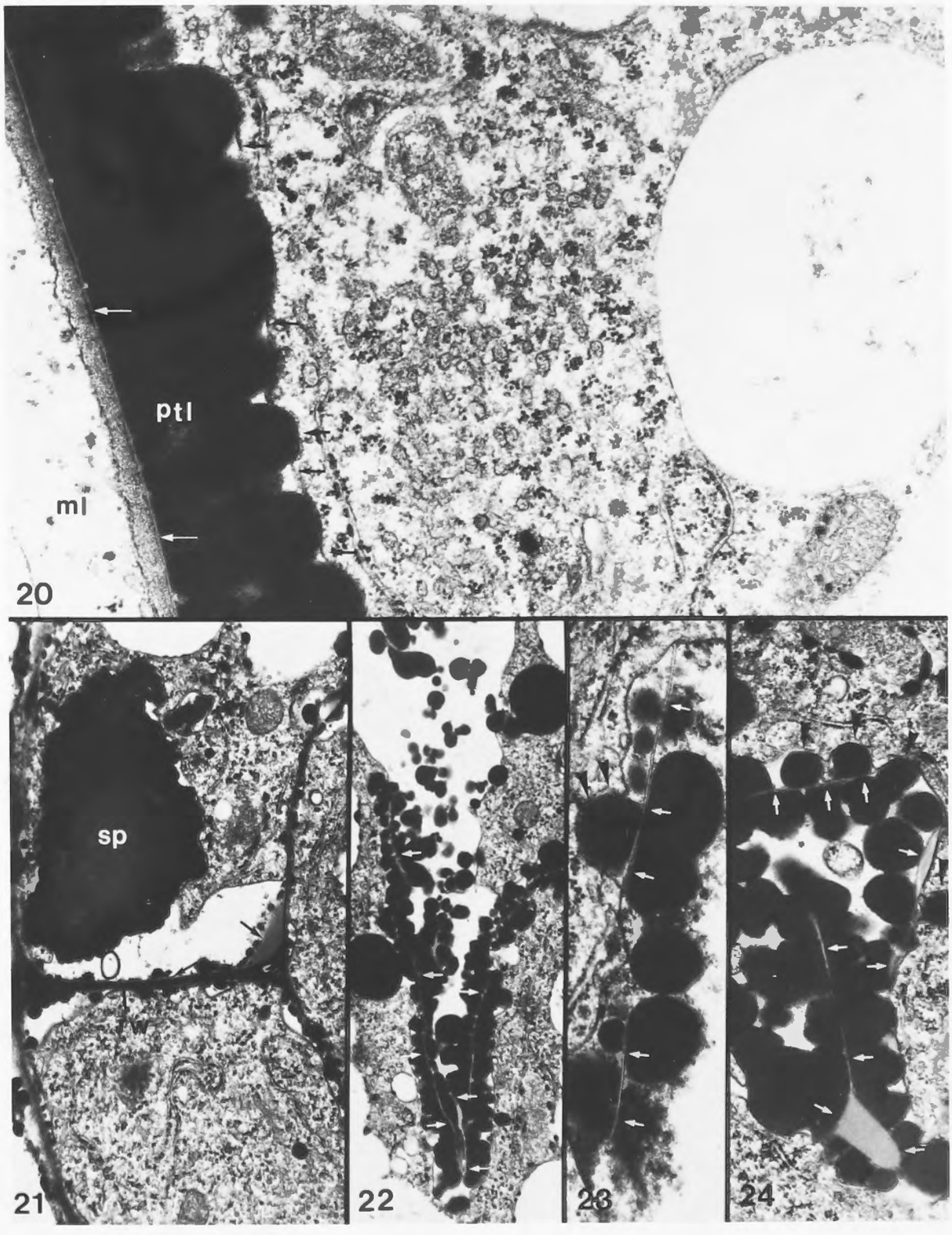
ptl
ml
20
sp
21
22
23
24

Figs. 5.25,5.26. Light micrographs of 4 µm thick sections of a part of anther treated with colchicine for 60 hours.

Fig. 5.25. Section stained with toluidine blue. Note the sporopollenin-rich peritapetal layer (ptl). The middle layer (ml) of the anther wall can also be seen outside the tapetum (t). x 700.

Fig. 5.26. Sporopollenin-containing peritapetal layer after acetolysis. During the preparation, some microspores become detached from their position and move about. The sporopollenin-containing microspore-shells (ms) seen in the photograph are examples of this. Note that only the microspore exine shells and the peritapetal layer (ptl) survive acetolysis. x 880.

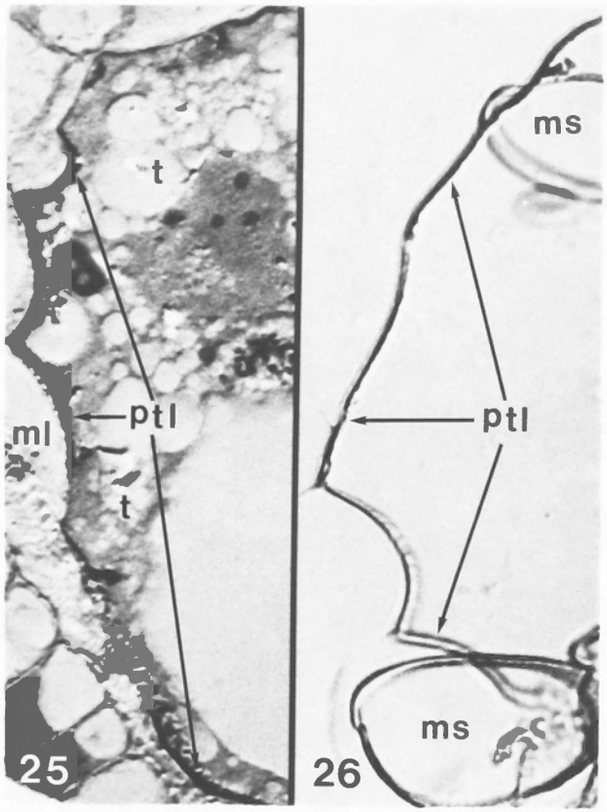
t
ml
ptl
t
25
ms
ptl
ms
26

CHAPTER 6

DEVELOPMENT OF POLLEN IN *TRADESCANTIA VIRGINIANA* L.

6.1. INTRODUCTION

Ultrastructural investigations of pollen development are not new and have been conducted in numerous species (see Knox, 1984a for a recent review), including Tradescantia (T. paludosa, Rowley, 1959; Horvat, 1966; T. bracteata, Mepham, 1970; Mepham and Lane, 1970). These studies have shown that in spite of species-specificity of pollen wall pattern, there is the prevalence of a basic system of wall construction which is only faintly perceived by light microscopy.

Much has also been learned about the subcellular mechanism of pollen wall pattern development in higher plants. A cellulosic primexine has been shown to be laid down by the spore protoplast prior to exine formation (Heslop-Harrison, 1963; see also Buchen and Sievers, 1981; Knox, 1984a) that presumably serves as the template for the latter's development. A 'stencil' of endoplasmic reticulum apposed to the spore plasma membrane in the presumptive apertural areas during primexine formation (Heslop-Harrison, 1963, see for reviews Dickinson, 1976; Buchen and Sievers, 1981), has been suggested to block the passage of precursors so that a weak exine results at these sites. Ribosome aggregates have been shown to occupy sites beneath the bacula (Heslop-Harrison, 1968b) and membrane profiles to form the basis of bacula and nexine layers (Rowley and Southworth, 1967; Dickinson and Heslop-Harrison, 1968).

All these observations have been made on the basis of thin sections of conventionally prepared spores and while their contributions have been outstanding, few attempts have been made to employ additional techniques. In the present investigation a coordinated effort has been made to investigate pollen wall development in Tradescantia virginiana L. with the use of techniques of freeze-substitution, freeze-fracture replica, immuno-fluorescence (of tubulin) and electron microscopic cytochemistry. Information gained from colchicine treatments (see Chapter 5) with relevance to pollen development is also included.

6.2. MATERIAL AND METHODS

Plants of Tradescantia virginiana L. 'Sydney hybrid' were grown and maintained as described in Chapter 4.

6.2.1. Light Microscopy

For light microscopic observations, anthers were isolated from young buds and flowers at different developmental stages, cut at their apical ends with a sharp razor blade and their contents gently extruded in distilled water on a clean glass slide, mounted with a cover slip and observed and photographed on a Zeiss Photomicroscope III fitted with Nomarski interference contrast optics.

6.2.2. Conventional Electron Microscopy

The procedure for conventional transmission electron microscopy was as described in Chapter 4. Observations were made on Hitachi H500 or H600 TEMs at an accelerating voltage of 75kV.

6.2.3. Scanning Electron Microscopy

Some unfixed dehisced anthers and their pollen were air-dried, sputter-coated with gold and observed with an Hitachi HHS2R scanning electron microscope at an accelerating voltage of 15 kV.

6.2.4. Freeze-Substitution

Spore cells were extruded from freshly isolated unfixed anthers onto wire loops coated with a dry thin film of agar (2%). The wire loops were then quickly frozen in liquid propane (precooled by liquid nitrogen) and processed as described in Chapter 3.

6.2.5. Cytochemistry

6.2.5.1. Fluorescence Microscopy

Callose was identified by mounting cells in a drop of 0.05% aqueous aniline blue and observing in a Zeiss photomicroscope using mercury vapour lamp and UG1 as exciter and 51 as barrier filters. Controls were mounted in distilled water and observed. Some spores were also mounted in aqueous 0.1% calcofluor white M2R and observed under the fluorescence microscope using UG1 as exciter and 43 as barrier filters.

6.2.5.2. Acetolysis Test

Controlled acetolysis procedure of Dickinson and Bell (1973) was applied for the identification of sporopollenin. The details of this have been mentioned in Chapter 5.

6.2.5.3. Thiéry Reaction

To localize polysaccharides at the ultrastructural level, the Thiéry reaction (Thiéry, 1967) was employed. Thin sections were collected in plastic loops and processed as described in Chapter 3.

6.2.5.4. ZnIO-Impregnation

To study the conformation of endoplasmic reticulum, the zinc-iodide-osmium tetroxide impregnation method of Harris and Chrispeels (1980) was employed. Spore cells were gently extruded into Eppendorf tubes containing the usual aldehyde fixative, fixed for 1h, washed in buffer (25mM phosphate buffer, pH 7.0), and post-fixed in freshly made zinc-iodide-osmium tetroxide (ZnIO) complex for 4-16h at $4^{o}C$. After impregnation the cells were pelletted and embedded in 3% agar and the agar blocks processed for electron microscopy. Thick (0.25-1μm) and ultra-thin sections were cut. Ultra-thin sections were lightly stained with alcoholic uranyl acetate and lead citrate whereas thick sections were observed unstained with Hitachi H600 TEM at an accelerating voltage of 75 kV.

6.2.6. Immunofluorescence of Tubulin

Microtubules were visualized by indirect immunofluorescence employing a monoclonal antibody (Amersham) raised against the α-subunit of chick brain tubulin. Whole anthers were fixed as described in Chapter 4, washed in buffer and again in phosphate buffered saline and sectioned in a cryostat, before incubation with the antibodies (see Chapter 4 for details). Spore cells were also extruded from the fixed anthers on to cover slips coated with poly-L-lysine, air-dried and subjected to the same protocol as described in Chapter 3.

6.2.7. Freeze-Fracture Replicas

To obtain information about the spore cell surface freeze-fracture replicas were prepared. Spore cells were extruded from freshly isolated anthers into a drop of distilled water onto gold stubs for preparing complementary replicas. A mesh grid placed between the two stubs prevented the cells from becoming squashed. The stubs were then quickly frozen in liquid propane (precooled by liquid nitrogen) and stored in liquid nitrogen until the time of fracturing. The stage of each preparation was determined beforehand by preparing a squash of one anther from every bud and observing under a phase-contrast microscope. To make a comparison as well as to assess the extent of ice damage, some replicas were also made of the fixed spore cell. For

this purpose whole anthers from buds of known developmental stages were fixed in the usual fixative for 1h, washed in buffer for 10 minutes and gradually cryoprotected by exposure to 10, 20 and 25% buffered glycerol for 30 minutes each. Spore cells were then extruded from these anthers onto gold stubs in a small drop of 25% buffered glycerol. The subsequent procedure remained the same as above.

Cells were fractured in a Balzer freeze-fracture unit at -110^{o}C and immediately replicated by coating with carbon and platinum. Sometimes the cells were etched (for 1 minutes) before replication. The replicas were cleaned overnight in chromic acid plus sulphuric acid which removed most of the organic debris although sporopollenin continued to contaminate some replicas. They were gradually transferred to distilled water, washed thoroughly, mounted on formvar-coated grids and observed.

6.2.8. Colchicine Treatment

The procedure for colchicine treatment was as described in Chapter 5.

6.3. OBSERVATIONS

In this investigation the terms spores and microspores have been employed to describe stages before pollen mitosis, and the term pollen grain to describe the stages after pollen mitosis. Also, the terms

primexine, primary exine, and exine are used to distinguish between fibrous pre-pattern spore wall, the sporopollenin-containing patterned wall formed within the callosic wall of the tetrad, and the sporopollenin-containing patterned wall after the spore release from the callose, respectively. The latter two terms are used merely for distinguishing stages, and are not meant to denote any structural dissimilarity. Mature pollen grains have an elongate shape and the term 'polar axis' refers to the axis of elongation.

Early features of spore development in Tradescantia have been described by Sax and Edmonds (1933) at the light microscopic level. As is common in monocots, meiotic cytokinesis is successive.

6.3.1. Tetrad

Spores in a tetrad are commonly arranged in a two-by-two isobilateral symmetry, so that all four spores are seen in an optical plane (Fig. 6.1); sometimes, however, one cell plate is placed at right angles (Fig. 6.2) or at approximately 45^{o} angle to the other (Fig. 6.3). Whatever be the geometrical arrangement of tetrads, a polar axis (see Fig. 6.2) is well defined in the individual spores.

6.3.1.1. Pre-Pattern Nascent Tetrad

A nascent tetrad is enclosed in a thick callosic wall, identifiable by the characteristic aniline blue-

induced yellowish fluorescence (Fig. 6.4). In conventionally-fixed (CF) spores, callose appears homogeneous with no stratification (Fig. 6.7). As also noted by other workers, in CF preparations the cellular ultrastructure of early tetrads was generally not well-preserved, presumably due to the reduced permeability of the thick callosic wall. However, a few well-preserved spores showed the usual ultrastructure with a large nucleus containing highly condensed chromatin, abundant ribosomes, dictyosomes, plastids with starch, and mitochondria. The spore cytoplasm appeared dense, and the endoplasmic reticulum (ER) was sparse. A few myelin-like figures and multivesicular bodies were also present. The plasma membrane was retracted from the callose at several locations (Fig. 6.7). The cortical microtubules, not always visualized, were few. No microfilaments were ever seen in conventionally-prepared thin sections of any stage.

Barring the spores that developed ice damage or freezing injuries at the resolution of the present observations, the general ultrastructure was found to be better preserved in freeze-substituted (FS) spores than in CF preparations. This was manifest in many ways and will be described subsequently, but some of the common differences are mentioned here. Firstly, in FS spores the cytoplasm did not appear as dense as in CF (compare Figs. 6.32,6.35,6.37,6.38 with Figs. 6.28,6.29). The ribosomes in the FS preparations appeared well spaced

and arranged in small clusters of polyribosomes, whereas in the CF preparations, fewer polyribosomes were recognizable, and the spacing between the single ribosomes had been lost, thus imparting a dense appearance to the cytoplasm. Occasionally in FS spores, polyribosome profiles suggestive of a helical arrangement of ribosomes were also seen (eg., in Fig. 6.37). These differences between CF and FS preparations were noted at all stages.

The FS nascent spores consistently showed numerous closely spaced microtubules (25-30um^{-1}) running transverse to the polar axis of the spores (Fig. 6.32). A quantitative comparison of microtubule frequency between the two types of preparations at this stage was not undertaken since in CF preparations many spores showed no microtubules. In addition, the FS spores showed a delicate system of sub-plasma membrane microfilaments (Fig. 6.33). Occasionally these microfilaments could be seen in association with cortical microtubules. In the cytoplasm, microtubules were sometimes seen in the vicinity of mitochondria. The FS spores also showed several pockets of a component of the endomembrane system, with partially coated membranes (Figs. 6.32,6.37). Vesicles occurred in the vicinity of such membrane profiles. A few multivesicular bodies (Fig. 6.36) also occur.

6.3.1.2. Late Pre-Pattern Tetrad

CF spores at a slightly older stage showed two major developments. Firstly, plates of short tripartite membrane lamellae appeared outside the plasma membrane, running tangential to the spore surface (Figs. 6.8,6.9). The lamellae development gradually became extensive (compare Fig. 6.8 with Fig. 6.9) and surrounded the entire non-apertural surface. The lamellae were absent in the presumptive apertural areas. They had indistinct terminations and in the initial stages they occurred generally adpressed against the plasma membrane (Figs. 6.8,6.9). In some places the two were separated (Fig. 6.29) by vesicular structures or plates of electron-dense material (presumably, the earliest form of polymerized sporopollenin) that was more electron dense than the primexine. But such structures became more common in subsequent stages of development (see Fig. 6.11). The origin of these lamellae could not be determined with certainty. Unlike the plasma membrane, the lamellae did not show affinity for the Thiéry reaction (Fig. 6.10).

The second development concerned the appearance of an electron-dense fibrous layer, the primexine, outside the plasma membrane or the plates of membrane lamellae (Figs. 6.8,6.9). In some preparations, the primexine appeared thinner at the presumptive apertural surfaces, but such a distinction was not common. The primexine reacted only slightly with the Thiéry

reaction, just as in the case of the callose wall outside, and disappeared after controlled acetolysis. At this stage, generally, the callosic wall appeared further separated from the spore surface and the intervening space often contained some loose fibrous material (Figs. 6.8,6.9, 6.11).

The appearance of primexine coincided with a proliferation of endomembranes. In ZnIO-impregnated thick sections (1µm thick) the endomembranes appeared distributed randomly throughout the cell (Fig. 6.30). When viewed stereoscopically, such preparations failed to reveal any definite and consistent relationship between the ER and the presumptive apertural area. In thick sections, ER appeared both sheet-like and tubular. The flat sheet-like profiles occasionally showed pore-like structures (Fig. 6.31) which morphologically resembled the nuclear pore complexes. Continuities were seen frequently between the ER, nuclear envelope and dictyosomes in stereopairs of thick sections.

The peripheral spore cytoplasm continued to show some multivesicular bodies (Fig. 6.29). Vesicles similar to those in the multivesicular bodies were encountered at the spore surface between the plasma membrane and the membrane lamellae (Fig. 6.29). Myelin-like figures continued to occur in the cortical cytoplasm (Fig. 6.28); occasionally, continuities were seen between these membranes and the plasma membrane. The cortical microtubules remained rare in CF.

A major drawback of the technique of freeze-substitution (especially when acetone alone or in combination with osmium tetroxide is used as substitution fluid) is that the trilaminar structure of membranes (excepting the plasma membrane) is not always clear. Consequently, in FS spores at comparable stages a clear membrane-like profile could not be recognized, but such spores did show an electron-dense continuous layer outside the plasma membrane that corresponded with the membrane lamella of CF spores. The lamella has a wavy outline, sometimes closely appressed against the plasma membrane and other times widely spaced from the latter (Fig. 6.20,6.21). In CF spores the spacing between the lamella and the plasma membrane was not as pronounced as in FS spores. Fig. 6.20 also shows a few electron-dense globules at the spore surface, in association with the membrane lamellae. The globules are thought to represent the earliest stages of probacula development. The FS spores further revealed a distinct stratification in the callose wall; there was a thin layer of callose close to the plasma membrane which showed a lighter electron density and loose texture as compared to the rest of the callose wall. These spores lacked an empty space between the callose and the spore surface (cf. Figs. 6.8,6.9,6.11). Also, the fibrous primexine was absent. The myelin-like figures could not be seen in FS (cf. Fig. 6.35), but the plasma membrane did show an occasional infolding into the cortical cytoplasm.

Partially coated membranes are less common in late pre-pattern tetrads than in earlier ones. Eventually, in later stages, they could not be seen. The population of cortical microtubules also declined substantially. Immunofluorescence of tubulin as seen in frozen sections (Figs. 6.42-6.45) as well as in permeabilized whole spore cells (Figs. 6.46,6.47), revealed a general diffuse fluorescence indicative of high amounts of unpolymerized tubulin. A few microtubules could sometimes be seen in sectioned immunofluorescent preparations (Fig. 6.43) but largely they were masked by the fluorescence of unpolymerized tubulin. The delicate network of sub-plasma membrane microfilaments (Fig. 6.34) remained.

Freeze-fracture replicas of unfixed spores at this stage showed a homogeneous wall layer, corresponding with callose. Neither the stratification of the callose that was seen in FS preparations, nor the primexine layer seen in conventional thin sections between the callose and spore plasma membrane, could be distinguished in the replicas of spores that were cross-fractured. Callose, being non-fibrillar, appeared homogeneous in the replicas. Replicated spore surfaces revealed a pattern of surface architecture in the form of lobed elevated areas (Fig. 6.39), presumably corresponding with the 3-dimensional pattern of the lamella that was seen outside the plasma membrane in thin sections, i.e., the elevations representing the

areas where the lamella was spaced from the plasma membrane, as seen in thin secions of FS spores. The elevated areas seem to undergo a gentle curvature and then abruptly merge with the background, consistent with thin section images in which the lamella touches the plasma membrane at certain places. That these images were not an artifactual form of freezing damage was evidenced by the observation that even fixed and cryoprotected spores showed this pattern. However, the elevations were not so pronounced and this was consistent with thin section images of CF spores where the spaces between the lamella and plasma membrane also appeared reduced.

6.3.1.3. Early Pattern Tetrad

In CF spores, establishment of an exinous pattern is first seen as electron-dense patches, presumably the early probacula, in the primexine (Fig. 6.11), marking the early stages of primary exine development. It was difficult to ascertain whether the probacula appeared first at any particular surfaces of the spore, or if there was any difference in their dimensions at any particular surface, because they were not easy to distinguish from the primexine which, at this stage, remains as a matrix filling up the spaces between the probacula. The probacula grow further within the primexine matrix (Fig. 6.12).

The probacula are more or less uniform on all spore surfaces, except the presumptive apertural areas where they appear shorter, sparse and dome-shaped. Analysis of intermediate stages between those shown in Figs. 6.11 and 6.12 reveal that the membrane lamellae develop into a more or less continuous layer (except in apertural areas) with a wavy outline that sometimes touches the plasma membrane and other times is separated from it by small electron-lucent spaces. It was also apparent that in the non-apertural area, the probacula emerge radially outwards from the lamella, whereas in the apertural areas they arise directly on the plasma membrane. Membrane-bound, electron-dense vesicular aggregates seen in previous stages (Fig. 6.29) continue to occur between the plasma membrane and the lamella, especially in areas where the two are distant. The spore wall continues to be Thiery-negative and with the appearance of primary exine, becomes acetolysis resistant.

In freeze-substituted spores, this was the first stage when any recognizable spore wall could be seen (Fig. 6.22). Electron-dense primexine is noticeably absent in such preparations, hence the earliest stages of the development of individual probacula are clearer than in CF preparations. The stratification of the callose continues to be visible in FS spores and after the appearance of probacula, the inner zone of callose fills up the spaces between the probacula. FS spore

surfaces in Figs. 6.22,6.23 are very different in appearance from CF spore surfaces in Figs. 6.11-6.13. The tiny electron-dense blebs seen at the membrane lamella in previous stage (Fig. 6.20) grow further to appear columnar and more extensive (Fig. 6.22,6.23). These structures, the probacula, arise directly on the plasma membrane in apertural areas, unlike in non-apertural areas where they are mostly located on lamella (Figs. 6.22,6.23). However, at this stage no differences were found in the dimensions of probacula at the apertural or non-apertural surfaces. The spaces between the plasma membrane and the lamella show few electron-dense vesicular aggregates (Figs. 6.22,6.23), some apparently in the process of fusion with the membrane above or sometimes with the probacula. However, with further growth of probacula (Fig.6.24) the vesicular structures become more common. The probacula-bearing lamella shows irregular thickness of its leaflets (Fig. 6.23), presumably due to uneven accretion of sporopollenin on its faces. The increase in the thickness of the lamella marks the first stage of the formation of nexine. These stages of nexine formation could not be visualized in CF spores (see Fig. 6.12). Probacula of differing heights are found in close proximity on the same surface (Figs. 6.22,6.23), so their development seems to be asynchronous.

The sub-plasma membrane network of microfilaments remains. Oblique sections of spores reveal these

filaments in the cell cortex (Fig. 6.38) underlying the spore plasma membrane. They occur only in the early stages of probacula formation. It has not been possible to visualize the filaments in median thin sections, suggesting that they run in the plane of the membrane, parallel to it. Since they could not be discerned in median sections it is difficult to attempt any correlation between their location and that of the probacula.

Cortical microtubules still underlie the plasma membrane (Fig. 6.38) and, as in the previous stage, their frequency remains low. Immunofluorescence of tubulin in frozen sections or whole cells continues to show the diffuse fluorescence of unpolymerized tubulin.

Freeze-fracture replicas of spores at this stage continued to show the surface pattern (Fig. 6.40) that was seen in pre-pattern stages (Fig. 6.39). Such preparations also confirmed the results obtained from thin sections: development of probacula on the lamella outside the plasma membrane (Fig. 41), the frequent occurrence of spaces between the plasma membrane and the probacula-bearing lamella, and the occurrence of granular objects in the space between the two. There was no correlation between the siting of probaculum and the surface architectural features, which spanned larger areas than individual probaculum. Also, there was complete absence of any fibrous matrix between the probacula (Figs. 6.40,6.41). Figs. 6.40 and 6.41 show

replicas of spores that roughly correspond with that in Fig. 6.23 (FS) and slightly later than in Fig. 6.11 (CF); in CF spores the primexine matrix was visible at this stage between the probacula, and in FS spores callose of lighter density occurred at these sites. The corresponding sites in freeze-fracture replicas do not show any material distinguishable from the callosic wall; the callose continues to appear homogeneous.

6.3.1.4. Late Pattern Tetrad

Continued accretion of sporopollenin on the probacula increases their height. They remain compact (Fig. 6.13). They appear discrete, at least at their bases, in FS (Fig. 6.24), but not in CF (Fig. 6.13). Also, in FS spores at this stage, the heads of some neighbouring probacula appear fused resulting in a partially tectate exine (Figs. 6.24, compare Fig. 6.13). Accretion of sporopollenin on either surface of the probacula-bearing lamella, in the spaces between the probacula, has by this stage resulted in the formation of nexine 1 on its outer surface and nexine 2 on its inner surface (Figs. 6.13,6.24). The lamella itself, embedded between the two nexine layers appears as an electron-opaque 'white line'. It continues to be wavy and its undulations appear correlated with the uneven thickness of the nexine layers (see Fig. 6.13). In CF spores (Fig. 6.13), the electron-opaque probacula-bearing lamella is clearly visible as a 'white line',

but nexine 1 can not be distinguished from the sexine and the nexine 2 can only be seen in some places underneath the probacula-bearing lamella. By contrast, in FS spores well-developed nexine 1 and 2 layers can be clearly seen (Fig. 6.24). The electron-dense granular elements continue to occur between the probacula bearing lamella and the plasma membrane in the spaces between the two (Figs. 6.13,6.24), and presumably participate in the formation of nexine layers. In FS preparations at this stage, the spaces also appeared filled with less dense flocculent material of medium electron density (Fig. 6.24). The dense granules sometimes appeared fixed in images suggestive of their migration across the probacula bearing lamella and, thus, of their contribution to the growth of nexine 1. However, they were never recorded intact outside the probacula bearing lamella even in the early stages when the lamella does not show substantial sporopollenin deposition (eg., Figs. 6.22,6.23).

The population of cortical microtubules remains low and the cortical system of microfilaments could not be visualized at this stage. The distinction between the dimensions of probacula at the non-apertural and apertural spore surfaces becomes more pronounced.

Gradually, the callose wall surrounding the spores shows signs of dissolution, more so at the periphery around the tetrads than the cell plate regions (Figs. 6.5,6.50). Eventually, by the late tetrad stage, callose could not be seen.

6.3.1.5. Late Tetrad

By this stage the spore exine, with its apertural and non-apertural areas, has become completely established, although its growth continues until the early microspore stage (see Table 1). The apertural zone develops at the surfaces away from the cell plates, i.e., facing the peripheral wall (spore mother cell callose wall), in spores arranged in a two-by-two isobilateral fashion (see Fig. 6.50). However, in spores arranged other than isobilaterally, the apertural area develops commonly at the lateral surfaces, although some variation may occur. The probacula at the apertural area continue to be relatively shorter (Fig. 6.26) and generally sparse when compared with the non-apertural area (see Fig. 6.50). The exine now shows a fairly well developed sexine with columnar bacula, and nexine layers (Fig. 6.25). By this stage, several bacular heads have fused (Fig. 6.25) so as to form a more or less regular roof or, in other words, a tectate exine. Due to further consolidation of sporopollenin in the form of nexine layers, the probacula-bearing lamella has become completely embedded in nexine, still appearing as a wavy 'white line', but it no longer has a membrane-like appearance. Nexine 2 continues to show small dense granular aggregates embedded at its base in some places, indicating that its development is still continuing. The apertural spore wall consists of a sparse and thin sexine and a poorly

developed, irregular nexine 1 (Fig. 6.26). Nexine 2 is non-existent at this region. There was still no sign of intine.

The thick sections of ZnIO-impregnated spores at this stage (Fig. 6.51) still gave no evidence of any preferential association of endoplasmic reticulum with the apertural area. There was a general decline in the population of endomembranes (compare Fig. 6.51 with Fig. 6.30).

In FS preparations the cortical microtubules became more frequent once again (Fig. 6.25) but without the cortical microfilaments. Freeze-fracture replicas at comparable stages do not show the surface lamella, presumably because it has become embedded in sporopollenin and thereby lost its propensity to fracture. The fracture in late tetrads invariably occurs in the plasma membrane, which appears smooth.

Thin sections of CF spores at this stage, frequently show large, apparently empty spaces between the spore plasma membrane and the spore wall at regions of greatest curvature. Comparable regions in FS spores contain electron-dense flocculent material (Figs 6.50, 6.52). This interfacial zone persists until the early microspore stage, when the wall expands, producing an elongated spore from the quadrant shape found in the tetrad.

By the late tetrad stage a few vacuoles begin to appear at the poles (Fig. 6.5). The spore size

increases (Table 1) nearly 100% during the interval between pre-pattern or early pattern tetrad and late tetrad stages. After spore release from the callose, growth takes place predominantly along the polar axis.

Table 1

Stage	Size	Total Thickness of the Exine
Early Tetrad	35 um	NA
Late Tetrad	35 um	0.3 um
Young Microspore	40 um	0.7 um
Late Microspore	70 um	0.7 um
Bicelled Pollen	70 um	0.7 um

These values represent averages taken from several micrographs. Spore size (along polar axis) was determined from whole mount preparations and exine thickness from electron micrographs of median sections of spore wall (NA, not applicable).

6.3.2. Microspore

After their release from the callosic walls, the microspores gradually become invested by the tapetal perispore membrane and establish a direct contact with the tapetal plasmodium (see Chapter 4 for details).

Microspores were studied at two distinct stages: (i) immediately after the tapetal investment of the individual microspores, the stage being referred to as young microspore (Fig. 6.6) in this work; and (ii) late

microspore stage which refers to the stage just before pollen mitosis.

From Table 1 it is evident that the maximum growth of the spores takes place in the interval between young microspore and late microspore stages. However, the exine growth is accomplished primarily between the late tetrad and young microspore stages, although the basic features are established while the spores are still enclosed within the callose. The most obvious correlate of cell expansion was the gradual development of vacuole/s at the pole/s (Fig. 6.6; see also Chapter 7). The spores become slightly asymmetrical prolate ellipsoids. As the exine stretches, the distinct nature of each baculum becomes more manifest, even in CF preparations. The accompanying nexine 1 stretching results in the appearance of wide discontinuities (or channels) in this layer. Since the edges of these channels do not appear rough or irregular they probably exist as narrow apposition areas in previous stages. The channels do not occur between individual bacula but between groups or islands of bacula, so that with further widening of the channels, small islands of bacular groups become apparent (eg., Figs. 6.14,6.16, 6.18). However, within an individual island all the bacula remain joined by the continuous nexine 1 at the base and more or less completely fused bacular heads at the top. Sometimes, however, the heads of the bordering bacula of neighbouring islands were also fused, as for

example in Fig. 6.18. Because of the comparatively thin and sparse exine on the apertural side, the stretching appears maximum in this area, and hence the bacula become widely spaced (eg., Figs. 6.17,6.19).

A dense population of microtubules was recorded at the young microspore stage. Tubulin immunofluorescence reveals that a young microspore contains an extensive system of microtubules (Figs. 6.48,6.49). In immunofluorescence preparations these microtubules can clearly be seen running perpendicular to the polar axis (axis of maximum growth) of the spore, as in the spores at early pre-pattern stages (Fig. 6.32). The unpolymerized tubulin seen in previous stages (Figs. 6.42-6.47), could not be visualized at this stage, presumably having been utilized for polymerization.

ZnIO-impregnated spores continue to show sparse endomembranes in young microspores, but in subsequent stages there is some increase in the population of membranes, eventually reaching moderate levels in a premitotic pollen (Fig. 6.54).

During the interval between the early and late microspore stages, another spore wall, the intine, is laid down between the exine and the plasma membrane. It was difficult to determine the precise stage when intine synthesis commences, but there certainly was no evidence of intine in a young microspore in either FS or CF preparations, or freeze-fracture replicas (Fig. 6.48). Late premitotic spores, however, showed a relatively

well-developed intine (Figs. 6.14,6.27). The intine is developed asymmetrically, almost twice as thick in the apertural areas as in non-apertural areas (compare Figs. 6.17,6.19,6.27 with Figs. 6.14,6.16,6.18). In CF preparations it either appears as an empty space between the spore plasma membrane and the exine or it occurs as poorly-preserved homogeneous layer in which the fibrillar nature is difficult to ascertain (figs. 6.14,6.16-6.19,6.55). In FS preparations, however, it appears clearly fibrillar (Figs. 6.27,6.56,6.65,6.67). The fibrillar nature of the intine was also confirmed by freeze-fracture replicas of cross fractured spores (eg., Fig. 6.66). The microfibrils run transverse to the polar axis of the spore. The Thiéry reaction imparts electron density to this layer confirming its polysaccharidic nature (Fig. 6.15). The intine also fluoresces when stained with calcofluor.

Unlike CF spores, the FS showed radially directed cylindrical channels traversing the entire thickness of the intine (Figs. 6.27,6.57,6.59). Freeze-fracture replicas also confirmed their presence (see in Fig. 6.68). Neither procedure gave conclusive evidence as to whether the channels are bounded by a membrane. They appear as an abrupt local drop in electron density in the intine, with a denser core.

Grazing tangential sections of freeze-substituted premitotic microspores, when the spores have more or less attained their full size and the intine synthesis

is well underway, continue to show numerous closely spaced cortical microtubules, congruent with the wall microfibrils of the intine (Figs. 6.56,6.58). The frequency of microtubules was considerably lower in CF preparations than in FS preparations. Analysis of 25 random samples of thin sections of FS spores showed the frequency of microtubules in the range of 7-12um^{-1}. Similar analysis of CF spores at this stage showed 2-4 microtubules um^{-1}. In the FS spores an occasional microfilament associated with these microtubules may also be visualized, but such associations become more frequent in later stages (Figs. 6.62,6.65).

In a normal longitudinal profile of microtubules, because of their hollow cylindrical nature, the terminations appear flat and 'open' (Fig. 6.56). It is often difficult to know whether a microtubule ends within the thickness of the section, or whether it leaves at an angle at one or the other surface. However, in FS spores a large number of terminations were seen which appeared 'closed' by a hemispherical termination (Fig. 6.59). Fig. 6.58 shows an area with several longitudinal profiles of microtubules and at higher magnification (photographs not provided) this preparation showed 6 microtubules with closed terminations, indicating that this type of termination is quite frequent. That both ends of a microtubule show such terminations is illustrated by Fig. 6.59 and the stereopair in Fig. 6.60. Figure 6.60 also shows that

microtubules with 'closed' terminations may abut end on, thus giving the impression that they combine to make a circumferential hoop around the cell periphery. Cross bridges between adjacent microtubules are also visible.

Late microspores show increased amounts of vesicular ER, free ribosomes, dictyosomes and mitochondria (Fig. 6.53). Smooth and coated vesicles, and a few multivesicular bodies are seen aligned along or close to the spore plasma membrane. The exine is fully developed at this stage. At the apertural area it appears pilate whereas the non-apertural area shows a partially tectate texture due to the fusion of bacular heads (Fig. 6.14). Also, at the apertural area it now rests directly over the thick intine, and consists solely of sexine and a very thin, discontinuous nexine (Fig. 6.27). The rest of the spore wall consists of an outer thick and patterned sexine and an inner unpatterned nexine. The distinction between nexine 1 and 2 is lost by this stage, as the intervening 'white line' can no longer be distinguished (Fig. 6.14). The exine growth apparently ceases after the development of intine, since the increase in thickness of the exine, or the occurrence of granular structures in the wall region corresponding with nexine 2, could not be found, even in FS spores. Channels continue to traverse both the exine and intine.

6.3.3. Bicelled Pollen Grain

Features with relevance to pollen mitosis and the generative cell are described in Chapter 7.

At the bicelled pollen grain stage the exine (Figs. 6.16-6.19) continues to show the same features as in premitotic mature microspores, but tapetally-derived pollenkitt is deposited close to the time of dehiscence (Figs. 6.18,6.19).

In post-mitotic stages, the intine is clearly bilayered (Figs. 6.16-6.19), and it continues to be thicker in the apertural region (Fig. 6.17) than in the non-apertural areas (Fig. 6.16). At the early bicelled pollen grain stage the intine wall microfibrils remain predominantly transverse to the polar axis of the pollen (Figs. 6.65,6.66), but their synthesis continues until the time of pollen dehiscence (compare Figs. 6.18,6.19 with Figs. 6.16,6.17) by which time the microfibrils show variable orientations (Figs. 6.67,6.68). In FS preparations the intine wall channels could be seen even in dehisced pollen.

Unlike CF spores, FS spores at late post-mitotic stages, when the generative cell is undergoing elongation, show an extensive cortical system of microfilaments in the vegetative cell (Figs. 6.61,6.62). These microfilaments sometimes run in the same direction as the microtubules (which also may have associated parallel microfilaments), but generally they do not display any preferred orientation and occur scattered in

the peripheral cytoplasm. Microfilament bundles were also consistently seen associated with the vegetative nuclear envelope (Figs. 63,64) and in the vicinity of dictyosomal vesicles.

In dehisced pollen the vegetative cell cytoplasm accumulates lipid bodies, most of which are ensheathed by ER (Figs. 6.69,6.70). The dictyosomes appear highly active, producing numerous vesicles. The population of the endomembranes in the vegetative cell also increases markedly to reach its maximum density at the time of pollen dehiscence. Rough ER is conspicuous occurring either in close association with lipid bodies (Fig. 6.69) or in localized aggregates of cisternae (Fig. 6.70). Cortical microtubules remain (Fig. 6.67), although they are not as frequent as in early bicelled pollen, and their co-orientation with intine wall microfibrils is no longer marked.

Dehisced pollen shows pollenkitt deposits in the cavities of the exine (Figs. 6.19,6.20). As a result of gradual desiccation, the pollen wall undergoes infolding at the apertural zone. The dry pollen thus shows a deep furrow running between the poles (Fig. 6.71). The exine is now completely tectate, but with perforations.

6.3.4. Colchicine Treatment

While investigating the role of plasmodial tapetum in the secretion of sporopollenin by disrupting the specialized secretory surface through treatments

with colchicine (Chapter 5), it was noticed that colchicine also affected spore morphology and exine patterning. The buds grown in 5 x 10^{-3}M aqueous solutions of colchicine from early tetrad to late microspore stage - the period during which most of the spore wall developed - showed anomalies of spore exine and shape. The majority of the spores appeared healthy, albeit with an abnormal exine. The apertural region of such spores showed much more compact bacula (Figs. 6.72,6.73) than in the controls (Fig. 6.74,6.75). Unlike the controls, where the spore wall underwent stretching during the interval between the late tetrad and early microspore stage to develop from a 3-sided spore into an elongated ellipsoid (Fig. 6.74,6.75), in drug treated anthers many spores failed to acquire the normal shape and remained 3-sided (Figs. 6.72,6.73).

6.4. DISCUSSION

Development of Tradescantia pollen can be discussed in terms of a succession of phases. The phases are not absolutely discrete, but may be defined as follows:

1. Early pre-pattern: precedes primexine and exine deposition; numerous microtubules, microfilaments, and partially coated membranes present.

2. Late pre-pattern: extracellular tripartite lamellae appear and coalasce to a single lamella upon which exine will be deposited; callose becomes

stratified; partially-coated membranes and microtubule population reduced, but microfilaments present.

3. Early exine pattern: deposition of bacula on the lamella; few microtubules present, but cortical microfilaments remain; partially-coated membranes not seen.

4. Late exine pattern: nexine 1 and 2 present under bacula; microtubules reduced and cortical microfilaments not seen.

5. Late tetrad: callose dissolved and cell expansion begins; basic features of exine well-developed; microtubules return, normal to polar axis.

6. Young microspore: exine completely developed; spore now elongated; no intine as yet, but abundant microtubules in cell cortex.

7. Late microspore: single-layered intine present; premitotic stage; cell expansion accomplished between this and previous stage; microtubules remain.

8. Bicelled pollen: intine bilayered; microtubules still present; generative cell detaches and undergoes elongation (see Chapter 7).

9. Late bicelled pollen: microfilaments traverse cytoplasm; microtubules decline and disordered microfibril deposition in intine.

10. Maturity: pollenkitt deposition; dehydration and unfolding of apertural area.

These events, and some topics of special significance are now discussed in more detail.

Current views on pollen exine pattern formation envisage the development of a cellulosic primexine preceding the exine, and al least some regulation exerted via specific spatial arrangements of ER membranes. Employing conventional procedures of electron microscopy, Heslop-Harrison (1963) discovered that a fibrous primexine preceded the exine. The primexine was found to be asymmetric, thinner at the apertural surfaces. He regarded the primexine as a template for subsequent exine development. He also demonstrated (1968c) that the primexine was degraded in the presence of cellulase, leading him to conclude that primexine is cellulosic in nature. The occurrence of primexine is now known in several species (see Knox, 1984a for a list).

All these investigations relied on conventionally processed cells, and, as shown here, such procedures can result in the loss or modification of cellular ultrastructure.

In Tradescantia a comparison of CF and FS spores indicates that the electron-dense, fibrous wall that precedes primary exine formation is an artifact of conventional procedures. In FS spores at the corresponding stage, the callose wall is stratified. A comparison of freeze-substituted, newly-formed callose at the cell plate region at dyad stage of meiosis (observations not reported here) with the inner layer of callose at late pre-pattern stage of spore development

failed to reveal any similarity, thus precluding the possibility that the inner layer of callose may be newly-formed callose. It may be that the inner layer of callose becomes modified during conventional processing to appear as a fibrous wall. It is significant that while in CF spores the callose wall appeared far removed from the primexine, in FS spores no such gaps occur. Freeze-fracture replicas of unfixed spores also failed to show any fibrous component at the spore surface. The Thiéry reaction (on CF preparations) stained the fibrous material only slightly, as in the case of the outer callose wall. These points constitute evidence that in Tradescantia the primexine is an artifactual image produced by degradation of the inner layer of the callosic wall which breaks away from the outer callose and precipitates as the layer known as primexine.

The inner layer seen in FS spores may be partially dissolved callose. This view would imply that the hydrolytic enzyme for the degradation must come from within the spore. In this context the observation of Stieglits and Stern (1973) that 7.3% of the total activity of β-1,3 glucanase was localized in the spores themselves, becomes significant. Interestingly, the presence of partially-coated membranes coincides with the dissolution of callose and their transient development may be somehow related to secretion or synthesis of the enzyme.

The concept that the spatial distribution of membranes determines exine pattern requires discussion in the light of the results presented here.

In species such as Silene (Heslop-Harrison, 1963), Lilium (Heslop-Harrison, 1968b,c), Helleborus (Echlin and Godwin, 1968b; see Knox, 1984a for more examples) early in spore development, sheets of ER have been seen to appose the plasma membrane in the apertural areas, and it is believed that such apposition could block the supply of material for wall development at the apertures. Skvarla and Larson (1966) observed an association between bacula formation and strands of ER, oriented perpendicular to the spore surface, and considered that ER determined the site of probacula. All such associations have been observed in thin sections which give only a partial view, as demonstrated in a recent investigation by Blackmore and Barnes (1985) who viewed the osmium-macerated spores with the scanning electron microscope and reported an absence of spatial ER-plasma membrane relationship in the apertural regions of Cosmos where such relationship was previously claimed on the basis of thin section images (Dickinson and Potter, 1976). In the present investigation, an attempt has been made to visualize ZnIO-impregnated endomembranes in thick sections. The stereopairs of thick sections of ZnIO-impregnated spores of T. virginiana failed to reveal any spatial relationship between the cytoplasmic membranes and the apertural

areas at any stage of spore wall development. Also, radially placed ER tubules beneath the site of probacula could not be detected (cf. Skvarla and Larson, 1966), and in this regard T. virginiana resembles T. paludosa (Horvat, 1966). It is concluded that neither macro- nor micro-scale features of the pollen wall in T. virginiana derive in any simple way from the distribution of endoplasmic reticulum in the young spore.

Trilaminar profiles, often described as 'membrane lamellae', occur embedded in the exine layers of several species (see Gupta and Nanda, 1983 for an inventory). Rowley and Southworth (1967) showed that during the formation of nexine 2 near the apertures of microspores in Anthurium, sporopollenin was deposited on lamellae of 'unit-membrane dimensions'. Gradual superimposition and compaction of the lamellae and sporopollenin eventually produced the nexine 2 layer in this region. Later, Dickinson and Heslop-Harrison (1968) were able to show the occurrence of lamellae in nexine 1 and sexine of Lilium spores. According to them 'pleated' lamellae placed radially at the spore surface, formed the basis of probacula. In Tradescantia the observations of CF and FS spores and freeze-fracture replicas (the only other freeze-fracture study has been restricted to the mature microspores of Lilium, Southworth and Branton, 1971), allow the role of the role of lamellae in exine pattern formation to be assessed. These observations along with the results of colchicine treatments reported

in Chapters 3 and 5 provide a basis for a working hypothesis for pattern formation in Tradescantia pollen grains.

The lamellae arise as short tripartite profiles placed tangentially to the spore surface, much as in Chlorella (Atkinson et al., 1972). Soon they develop into a single continuous lamella that covers the entire spore surface, except in the apertural region. A 'pellicle' (corresponding with this lamella) has also been described in the nexine 1 of developing spores of T. paludosa by Horvat (1966), but he neither provides any details nor attaches any significance to its appearance. In the present species the development of the lamella slightly precedes the appearance of the earliest form of probacula, since tiny electron-dense blebs can be seen at the lamella in FS spores, only after the lamella becomes continuous. The occurrence of the lamella exclusively in the non-apertural areas marks the earliest stages of exine formation. Subsequently, all the exine layers in the non-apertural areas arise at the lamella. Its absence in non-apertural areas appears correlated with poor development of nexine 1 and absence of nexine 2 in such regions. It is as if the lamella provides a stabilizing, skeletal surface for the subsequent exine formation.

Large expanses of the lamella are spatially separated from the spore plasma membrane, as evidenced by the thin section images and the matching areas of

elevations in freeze-fracture replicas. It is possible that the surface features seen in freeze-fracture images are also related to another character of exine pattern in mature pollen grains. The islands of elevations and depressions may mark the position of future exine channels; during cell expansion, it may be that groups of bacula situated on one island become separated from those on another island, thus creating the channels in the underlying layers. Certainly, the apposition of lamella with plasma membrane in certain regions would result in poor development of nexine 2 in such regions, making them potential sites of separation during cell expansion.

Radially placed lamellae that have been noted to form the basis of bacula in Lilium (Dickinson and Heslop-Harrison, 1968) could not be visualized in FS or freeze-fracture preparations of Tradescantia spores. The probacula arise as electron-dense blebs that gradually grow to become columnar; later many of them become fused at their outer extremities to form a tectate exine at the non-apertural areas.

While the presence or absence, and the wavy outline, of the lamella may account for some differences in the structure of exine at apertural and non-apertural areas and the location of nexine channels, it cannot be correlated with the determination of the site of apertures or with the particular morphology of the sexine. In this regard, Wodehouse (1935) has emphasized

the importance of geometrical arrangement of spores in the tetrad. Dover (1972) has shown how meiotic spindle poles determine the position of the aperture in Triticum. In Tradescantia the spores that are arranged in isobilateral tetrads, with second set of meiotic cell plates parallel to each other, develop apertures at the surfaces that are in contact with the peripheral callosic wall, whereas spores from tetrads other than isobilateral develop the apertures mostly at the lateral surfaces. The consistency of these features indicates that both contact geometry and the meiotic spindles may be related to the siting of apertural areas in this species as well.

It is in the context of the specific morphology of the sexine that observations of colchicine treatments reported in Chapters 3 and 5 become relevant.

It was found that both in Canna (Chapter 3) and Tradescantia (Chapter 5) colchicine treatments induced abnormally-placed sporopollenin deposits in the anther cavity. Striking differences were noted in the morphology of these deposits between the two species. In Canna, where the pollen wall does not have an organized exine and sporopollenin occurs in patches that are embedded in the intine (Skvarla and Rowley, 1970; Rowley and Skvarla, 1975; Krebs and Stone, 1982, 1984), the colchicine-induced sporopollenin deposits occurred mostly as small, single granules. In Tradescantia, on the other hand, the deposts were much larger and when in

contact with a lipidic surface, they developed into granular masses that at least partially resembled bacula. Many of these deposits, for example those in a peritapetal location, were not very different from the early sexine. In both the species the deposits occurred in extracellular spaces; indeed in Tradescantia the size of the deposits seemed to depend on the availability of extracellular space. These observations are suggestive of the possibilities that: 1. the information for the species-specific order is inherent in the molecular constitution of sporopollenin; 2. that there are species-specific differences in the constitution of sporopollenin in different species, for if the constitution was the same then pronounced differences should not be seen in these two species (in Canna even the size of the colchicine-induced granules was quite uniform); and that 3. the lipidic surfaces merely provide a surface on which sporopollenin can express its intrinsic order through polymerization.

The exine pattern in Tradescantia can be partially interpreted on this basis. The differences in the morphology of sexine and nexine layers can be explained on the basis of limited availability of extracellular space on either surface of the lamella, which may prevent the nexine layers from depositing sporopollenin in the same form as in the sexine. The sexine develops columnar deposits because it has large extracellular spaces made available by dissolution of

the inner region of the callose wall. The fusion of bacular heads may also be explained on the basis of availability of extracellular spaces: the bacula initially develop as discrete columnar deposits; the fusion of their heads does not take place until the bacula have become long enough to touch the callose wall (the outer callose); it may be that once they touch the callose wall further elongation cannot take place, but tangential growth can still occur, resulting in the fusion of their heads. A major drawback of all these suppositions is that the differences in the morphology of bacula at the apertural and non-apertural regions can not be fully explained.

The origin of the lamella could not be determined. Rowley and Dunbar (1967) have suggested four possible ways in which exinic lamellae could arise. They could arise from microvillus-like extensions of plasma membrane; from vesicles of sporal or tapetal origin; and by de novo synthesis at the spore surface. Dickinson and Heslop-Harrison (1968) and Dickinson (1976) believe that the lamellae of Lilium arise from the plasma membrane. The observations of FS and CF spores in Tradescantia rule out the origin of lamella from: 1. microvillus-like plasma membrane extensions since such elaborations do not occur; 2. vesicles of tapetal origin since the callose wall could effectively prevent their movement from the plasmodium to the surface of a young spore; and 3. vesicles of sporal

origin since although vesicles were seen at the spore surface, resembling those in multivesicular bodies, they occur more frequently after the formation of a continuous lamella and are more likely to provide wall precursors. It may be that in T. virginiana there is de novo synthesis at the plasma membrane. Certainly, no cytoplasmic structure in the spores could be linked with the synthesis of lamella in FS spores. In this context it is significant that misplaced colchicine-induced sporopollenin deposits also sometimes show lamellae embedded in them. De novo synthesis in the extracellular spaces was also suggested for autospores in Chlorella (Atkinson et al., 1972).

As is common in higher plants, exine development takes place in two phases in T. virginiana. While enclosed in the callosic walls of the tetrad, a basic pattern is established and this pattern is further consolidated after the liberation of spores from callose. The interval between late tetrad and early microspore stages is an important period for the spore wall growth, as it undergoes nearly 100% increase in thickness during this phase of development. This is unlike T. bracteata in which according to Mepham (1970), and Mepham and Lane (1970) the entire exine developed while the spores were still enclosed in the callosic walls. The tapetum plays an important role in the development of spore wall after the dissolution of callose wall. It acquires a secretory surface in

contact with the spore wall (Chapter 4) and disruption of this surface by treatments with colchicine results in the development of abnormally placed sporopollenin deposits in the tapetum (Chapter 5), supporting the view that plasmodium has the capacity to provide precursors for spore wall growth.

In the previous investigations on pollen development some attention has been paid to the cytoskeletal elements, particularly microtubules, during pollen wall development (Echlin and Godwin, 1968b; Heslop-Harrison, 1971c; see also Dickinson, 1976; Buchen and Sievers, 1981). These investigations were performed on conventionally-prepared thin sections which provide incomplete picture both with regards to microtubule preservation as well as limitations of thin section analysis. Freeze-substitution on the other hand offers an improved preservation of microtubules (see later) and when coupled with immunofluorescence technique can give a more complete picture of the appearance, spatial relationships and possible roles of microtubules.

A high population of microtubules occurs in the pre-pattern spore. During the period when the spore wall is being laid down, there is a substantial decline in their population, as seen in FS spores. Immunofluorescence preparations at the corresponding stage show diffuse fluorescence, indicating the presence of unpolymerized tubulin. Microtubules become frequent during late stages of tetrad development, after the

spore wall has become well-established and their population remains high until well after pollen mitosis. A recent spectrophotometric study of fluorescently labelled microtubules in Gasteria (Van Lammeren et al., 1985) also recorded a low population of microtubules during the tetrad stage. Unlike Tradescantia, the population of microtubules in Gasteria remains low until after pollen mitosis.

The role of the microtubules in the pre-pattern phase is not clear. They occur in high frequency (25-30um^{-1} in sections) and run transverse to the polar axis. It may well be that the high frequency of microtubules is somehow related to the establishment of polarity that determines the future growth. The spores at this stage are already polarized in the sense that an axis of elongation can be seen and the position of apertures is predetermined. The appearance of high frequency of microtubules in early pre-pattern phase may be instrumental in further establishing the polarity. Support for this conclusion also comes from immunofluorescence studies of Lilium (Dickinson and Sheldon, 1984) and Canna (unpublished data) where the mature pollen grains have oval and round shapes, respectively, and the microtubules at the tetrad stage are arranged radially between the spore surface and nuclear envelope, in spite of the fact that the shape of spore at tetrad stage is the same as in Tradescantia.

The population of microtubules declines in the late pre-pattern phase and they remain sparse during the establishment of exinous wall-pattern. The microtubules at this stage may show variable orientation in relation to each other, but their overall orientation remains transverse to the long axis of the spore. This contrasts with Lilium (Dickinson and Sheldon, 1984) and Canna (unpublished data) where radial microtubules occur during the phase when the spore wall is being laid down. Tradescantia also differs from Gasteria where according to Van Lammeren et al. (1985) 'individual microtubules run throughout the whole cytoplasm but sometimes they tend to be arranged parallel to the longitudinal axis'. Van Lammeren et al. do not describe the stage in relation to spore wall development, nor do they describe the common orientation of microtubules; hence it is difficult to compare Tradescantia with Gasteria. In view of the reduced numbers of microtubules during exine formation, it seems unlikely that they are directly involved in exine-pattern formation in Tradescantia. Results of colchicine treatments accord with this view. 12h of colchicine treatment removed most of the microtubules (see Chapter 5) and yet the spores that were allowed to grow in colchicine for longer durations developed exines not unlike the controls. The treated spores did show apertural areas with more compact bacula (see later) than in the controls, but the overall disposition of apertural and

non-apertural areas, structure of exine - the sexine and nexine layers, and the fused bacular heads did not appear different from the normal spores.

During the period when exine is being laid down and when the microtubules become infrequent in the FS preparation, the immunofluorescence preparations show a diffuse fluorescence, indicating that a reserve pool of unpolymerized tubulin is maintained. These changes coincide with the proliferation of endomembranes. The converse trends take place after the establishment of wall pattern; the microtubules become frequent and the diffuse immunofluorescence disappears, suggesting that the pool of unpolymerized tubulin is drawn upon for microtubule polymerization. Coincident with this change there is a decline in the population of endomembranes. It therefore seems plausible that the unpolymerized tubulin is associated with the cytoplasmic membranes. The long detergent treatments (1h) employed during the procedure almost certainly would have extracted any unbound tubulin that existed free in the cytosol. Attempts were made to localize this tubulin by gold-tagged second antibody, but so far without success.

During the interval between late tetrad and young microspore stages the spore undergoes a preferential expansion to metamorphose from a 3-sided spore into a prolate ellipsoid. The microtubules become frequent preceding this change in shape and it is surmised that they may participate in the change in spore shape.

Results of colchicine treatments support this interpretation. The treated spores fail to expand in a normal manner so that the 3-sided shape is retained even in late microspores.

Similar roles also seem indicated for the high frequency of microtubules at young microspore stage (no intine yet). By this stage, the spores have acquired their final shape, but the cell expansion continues. During the interval between young and late microspore stages the spores elongate almost 100% and the cortical microtubules remain oriented transverse to the polar axis, just as in other expanding cells (see Gunning and Hardham, 1982). The microtubules at young microspore stage may determine the direction of cell expansion. Unlike the normal spores, in colchicine-treated spores the cell expansion is general, further supporting the view that the microtubules determine the direction of cell expansion. Indeed the general expansion of treated spores may be responsible for the compact appearance of bacula at the apertural regions of treated spores. In normal spores, because of the absence of organized nexine layers at the apertural regions, the spore expansion results in a higher degree of stretching at the apertural regions than at the non-apertural regions and consequently the bacula become further spaced at the late microspore stage. In the drug-treated spores the 3-sided shape is retained and the cell expansion is general so that bacula at their apertural sites appeared more compact than normal.

Microtubules continued to be frequent in late microspore and bicelled pollen grains. By the late microspore stage the intine wall has developed and its microfibrils run predominantly transverse to the polar axis, as also known in the pollen grains of some other species (see Heslop-Harrison and Heslop-Harrison, 1982). The microtubules show a co-orientation with the intine wall microfibrils (considered to be cellulosic, see Sitte, 1953), suggestive of a role in the orientation of deposition. Such co-orientation is common in plant cells (see Gunning and Hardham, 1982; Robinson and Quader, 1982). It has not been possible to detect the precise stage of commencement of intine synthesis during young-late microspore transition. However, it seems likely that the synthesis commenced before the bacula at the apertural surfaces begin to become spaced; otherwise, since the nexine is thin and discontinuous, separation of bacula in the absence of an underlying intine would result in the rupture of the spore wall. The intine is developed asymmetrically, and becomes almost twice as thick at the apertural area than at non-apertural ones.

Channels traverse the intine wall and conceivably provide a route for transfer of material between the plasmodium and the interior of pollen grain. Channels are commonly found in the exine, as also in Tradescantia, but the reports of their occurrence in the intine are few. To the best of my knowledge, comparable

intine wall channels have been recorded only in T. paludosa (Fernández-Morán and Dahl, 1952) and Poa (Rowley et al., 1959).

The technique of freeze-substitution resulted in visualization of some novel features of microtubules which may be of general import. Such preparations have consistently shown more microtubules than in CF preparation. Because of their synchronous development, the microspores provide an advantage for quantitative studies of microtubules, since cell populations identical in terms of developmental stage, nuclear condition, size, and shape, can be processed in different ways and a reliable comparison can be made. The quantitative analysis performed at late microspore stage shows that the FS spores have at least twice the number of microtubules/um than CF spores. These data provides quantitative support to the observations of Howard and Aist (1979) and Mckerracher and Heath (1985) that conventional fixation causes loss of microtubules. Lower frequencies of microtubules in CF, as opposed to FS, have also been noted in other tissues such as the epidermal cells of the ovules of Datura and leaf of Triticum, and cells of the stamen hair of Tradescantia (data not presented in thesis).

Despite the differences in the frequency of microtubules in tissues processed by the two methods, the average length of the microtubules in Datura has been found to be similar, in the range of 2-4um (data

not presented here). Microtubules with 'closed' terminations (eg., Fig. 60) are of interest in this context. In a normal longitudinal profile, microtubule terminations usually appear 'open'. C-shaped terminations (in transverse profiles) have also been observed (Hardham and Gunning, 1978) and these have been considered to represent microtubules which are either growing or depolymerizing. The 'closed' terminations seen in FS Tradescantia pollen suggest that these microtubules may have become capped and hence perhaps structurally stabilized. Such terminations have also been noted in FS stamen hair cells of Tradescantia and in Datura ovule epidermal cells (data not shown here) but the morphology of terminations can differ.

The closed terminations were conspicuous where microtubules were joined 'end on' (Fig. 6.60) with each other. The aggregates gave the impression of consisting of relatively long microtubules. Their end on attachment is relevant to studies of the length of microtubules. Closed microtubule terminations could easily be overlooked and two or more microtubules attached end on (in Fig. 6.60, 2 or possibly 3 microtubules are seen joined end on to each other along one trajectory) could easily be misinterpreted as single microtubules. The problem may further be compounded if conventional procedures of electron microscopy are employed, since the closed terminations may be rendered indistinguishable. They have not been seen in any CF preparation of this investigation.

The discrepancy that while there were more microtubules in FS than in CF and yet the microtubule lengths appear predominantly similar can be resolved if it is envisaged that microtubules with closed terminations are structurally stabilized and that the conventional procedures only preserve the stabilized microtubules.

Freeze-substitution preserved microfilaments in developing spores and mature pollen grains of Tradescantia. Previous reports of microfilaments have been restricted to pollen tubes (Franke et al., 1972), germinating pollen (Condeelis, 1974), and sperm cells (Zhu et al., 1980) where roles in streaming and motility have been indicated. In Tradescantia occasional microfilaments were visualized through out the course of pollen development. However, during early stages of spore development and in later stages of bicelled pollen grain, the microfilaments occurred most extensively and were consistently recorded in the cell cortex. During spore development from early pre-pattern stage to early pattern stage microfilaments occurred as a delicate system in the plane of and underlying the plasma membrane. This is the period when cortical microtubules are reduced in number and when the basic pattern of the exine is formed. It may be that microfilaments rather than microtubules are involved in the formation of pollen exine patterning. The nature of these microfilaments remains to be elucidated. They could not

be detected using anti-actin or rhodamine-phallacidin (data no presented here), but such techniques involve chemical fixation which may destroy them.

The significance of cortical microfilaments that occur during the late bicelled pollen grain stage is not clearly understood. Cortical microtubules begin to become infrequent by this stage, but intine synthesis seems to continue and in still later stages the intine wall microfibrils were seen to have variable orientations. It may well be that the cortical microfilaments are involved in intracellular transport of vesicles containing intine wall material. Certainly, microfilament bundles occur consistently in the vicinity of dictyosomal vesicles which may be a possible sourse of material for intine development, as inferred in other species (see Knox, 1984a). Equally unclear is the role of microfilaments at the nuclear envelope of the vegetative cell. These microfilaments occur as small bundles that are associated with the nuclear envelope at certain places, and not all around the nucleus, as in certain animal cells (Franke, 1971). This is the stage when generative cell elongation is taking place and the microfilaments may help in spatial adjustments in the vegetative cell.

FIG. 6.1. An isobilateral tetrad with all four spores in an optical plane. The second set of cell plates have been laid down parallel to each other. The polar axis in the spores runs perpendicular to the plane of the micrograph. x 1,100.

Fig. 6.2. A tetrad with second set of cell plates at 90^{o} angle to each other. Spores in the lower half show their intervening cell plates whereas the cell plates between the upper two spores can not be seen in this plane of focus. The upper spore also shows clearly the polar axis (direction of double headed arrow) along which the predominant cell expansion takes place. White arrows show the perispore membrane. x 1,000

Fig. 6.3. A tetrad with second set of cell plates at approximately 45^{o} angle to each other. x 750.

Fig. 6.4. Aniline blue-induced callosic fluorescence is restricted to the peripheral wall of the tetrad and cell plate region. The figure shows an isobilateral tetrad and another with cell plates at right angles to each other. x 580.

Fig. 6.5. A tetrad close to the late tetrad stage. The peripheral callose wall has undergone complete dissolution by this stage, but the cell plates can still be seen. Vacuoles (arrows) have begun to develop by this stage. x 1,000.

Fig. 6.6. An early microspore. The spore has stretched from a 3-sided condition at the tetrad stage into a prolate ellipsoid. Large vacuoles (v) and the nucleus (n) can also be seen. x 820.

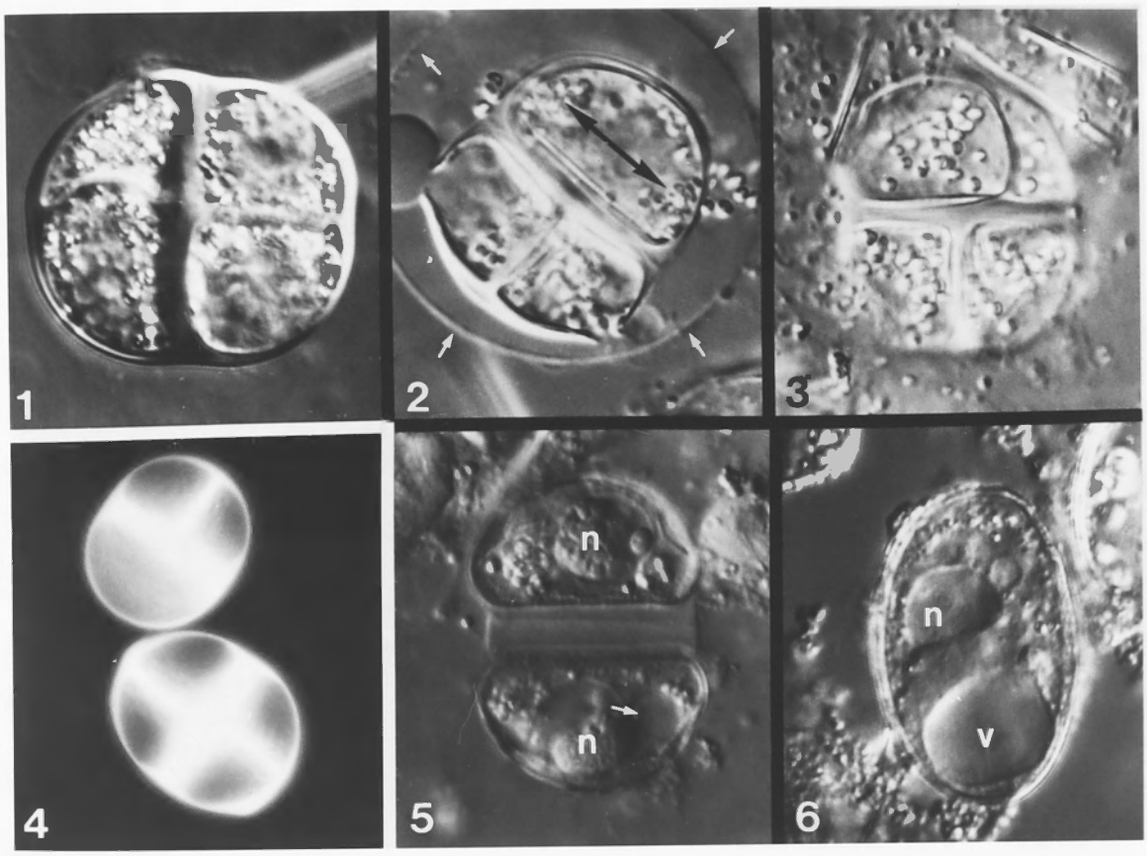
1
2
3
4
n
n
5
n
v
6

Figs. 6.7-7.13 are from CF spores.

Fig. 6.7. The presumptive non-apertural surface of a nascent spore showing the outer callosic wall (c), the plasma membrane and dense cytoplasm. Note the retraction of plasma membrane from the callose. x 81,000.

Fig. 6.8. The presumptive non-apertural surface of an early pre-pattern spore. Electron-dense primexine (p) and a short lamella (arrowheads), closely apposed to the plasma membrane can also be seen. Arrows indicate terminations of the lamellae. The callose wall (c) and the primexine are separated by an electron-lucent space. Loose fibrous material is visible in this space. x 75,000.

Fig. 6.9. The presumptive non-apertural surface of a pre-pattern spore. The callose wall (c), and electron-dense primexine (p) can be seen. The space between the two shows loose fibrous material. The lamellae (arrows), closely apposed against plasma membrane, have become more frequent and their terminations (arrows) appear indistinct. x 90,000.

Fig. 6.10. The Thiéry reaction stains the callose wall (c) and the primexine (p) only slightly, but the plasma membrane is stained densely. A median sectioned profile of a lamella (arrowheads) can also be seen, but it does not stain with the Thiéry reaction. The space between callose and primexine is not seen in this figure. x 60,000.

Fig. 6.11. Non-apertural surface of an early-pattern spore. The short lamellae seen in Figs. 6.8 and 6.9, have become extensive by this stage and a single lamella (arrowheads) can be seen embedded between the primexine and spore plasma membrane. The callose wall is not shown in the figure, but a part of the space between the callose and the primexine, containing loose fibrous material is visible. Primexine shows some dense patches (arrows), which presumably are the early probacula. The plasma membrane appears retracted from the lamella at some places. x 63,100.

Fig. 6.12. Non-apertural surface at a later stage than in Fig. 6.11. The primexine cannot be seen. The sexine (s), consisting of compact columnar probacula (arrowheads) is situated on a lamella (arrows) which can be seen in some places. Note the electron-lucent spaces between the plasma membrane and the probacula-bearing lamella. x 85,700.

Fig. 6.13. Non-apertural surface at the late pattern stage. The callose wall (c) still encloses the spores and the sexine (s) still shows compact probacula. The 'white line' (arrows) occurs at the apparent base of sexine (since nexine 1 can not be distinguished from sexine), and nexine 2 occurs bellow the white line. In some places electron-dense granular aggregates (arrowheads) occur between the spore wall and the plasma membrane. x 73,600.

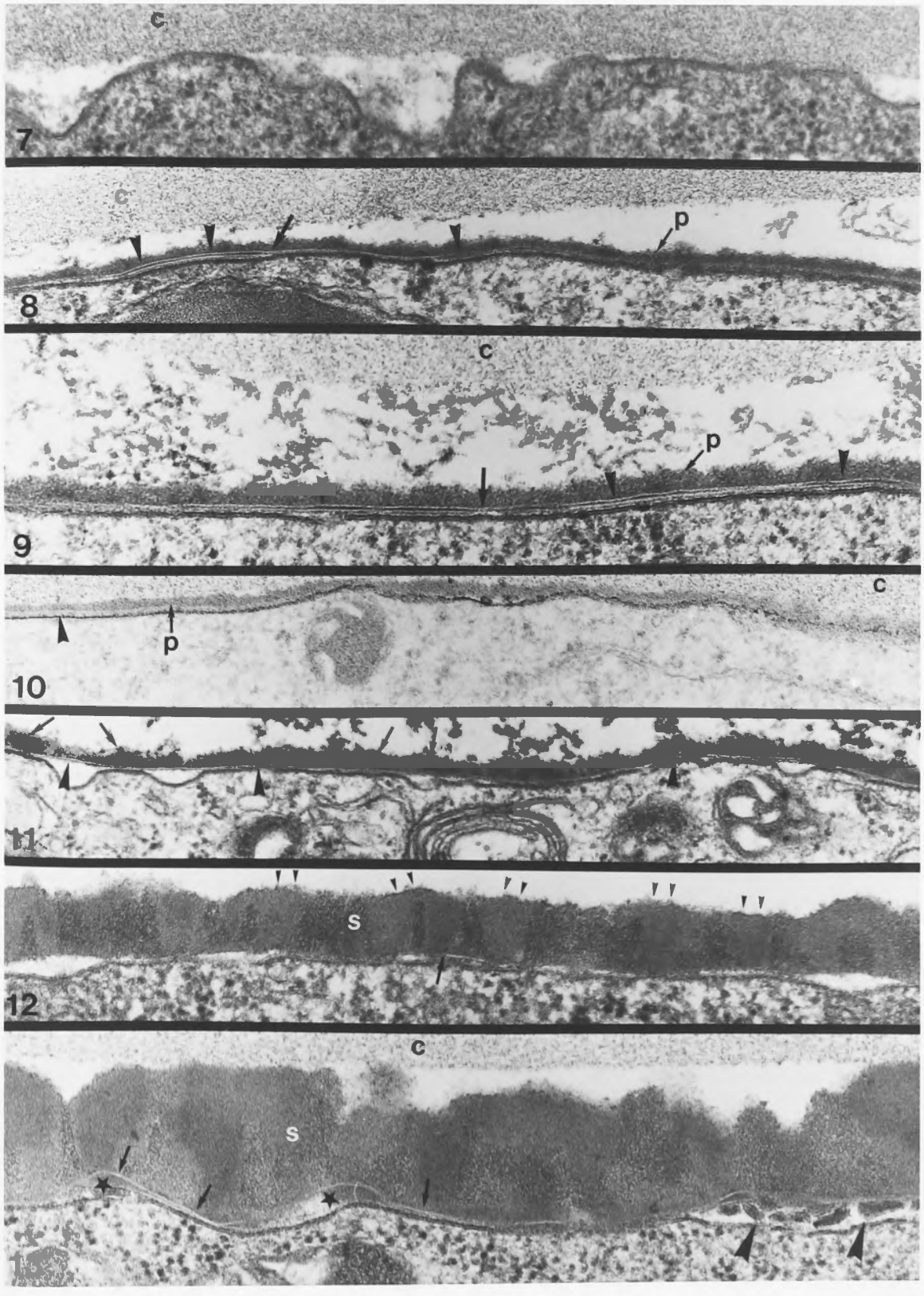
c
7
c
p
8
c
p
9
c
p
10
11
s
12
c
s
13

Figs. 6.14-6.19 are from CF spores.

Fig. 6.14. Non-apertural spore wall at late microspore stage. The sexine (s) consists of discrete bacula. Many bacula have fused at their heads. Nexine (n) can also be seen but the distinction between nexine 1 and 2 can not be made since the intervening 'white line' is indistinguishable. Channels (arrowheads) can be seen in the nexine. Intine (i) and cortical microtubules (arrows) are also visible. x 72,000.

Fig. 6.15. The Thiéry reaction imparts electron-density to the intine (i) wall layer (n, nexine; s, sexine). x 70,000.

Fig. 6.16. Pollen wall at the non-apertural regions at bicelled pollen stage. Two layers (1,2) can be seen in the intine (s, sexine). x 48,000.

Fig. 6.17. Apertural pollen wall at the bicelled pollen stage. The intine is much thicker than at the non-apertural regions (Fig. 6.16) and its two layers (1,2) are distinct. The nexine layers cannot be seen and the bacula are sparse and do not show fused heads as in Fig. 6.16. x 50,000.

Figs. 6.18,6.19. Non-apertural and apertural regions of pollen wall, respectively, at the time of pollen dehiscence. The channels (arrowheads) are seen in the nexine layers. The two layers (1,2) of intine have become much thicker than in previous stage. Electron-dense pollenkitt (arrows) occurs at the pollen surface and in the cavities of sexine (s, sexine). Both x 48,000.

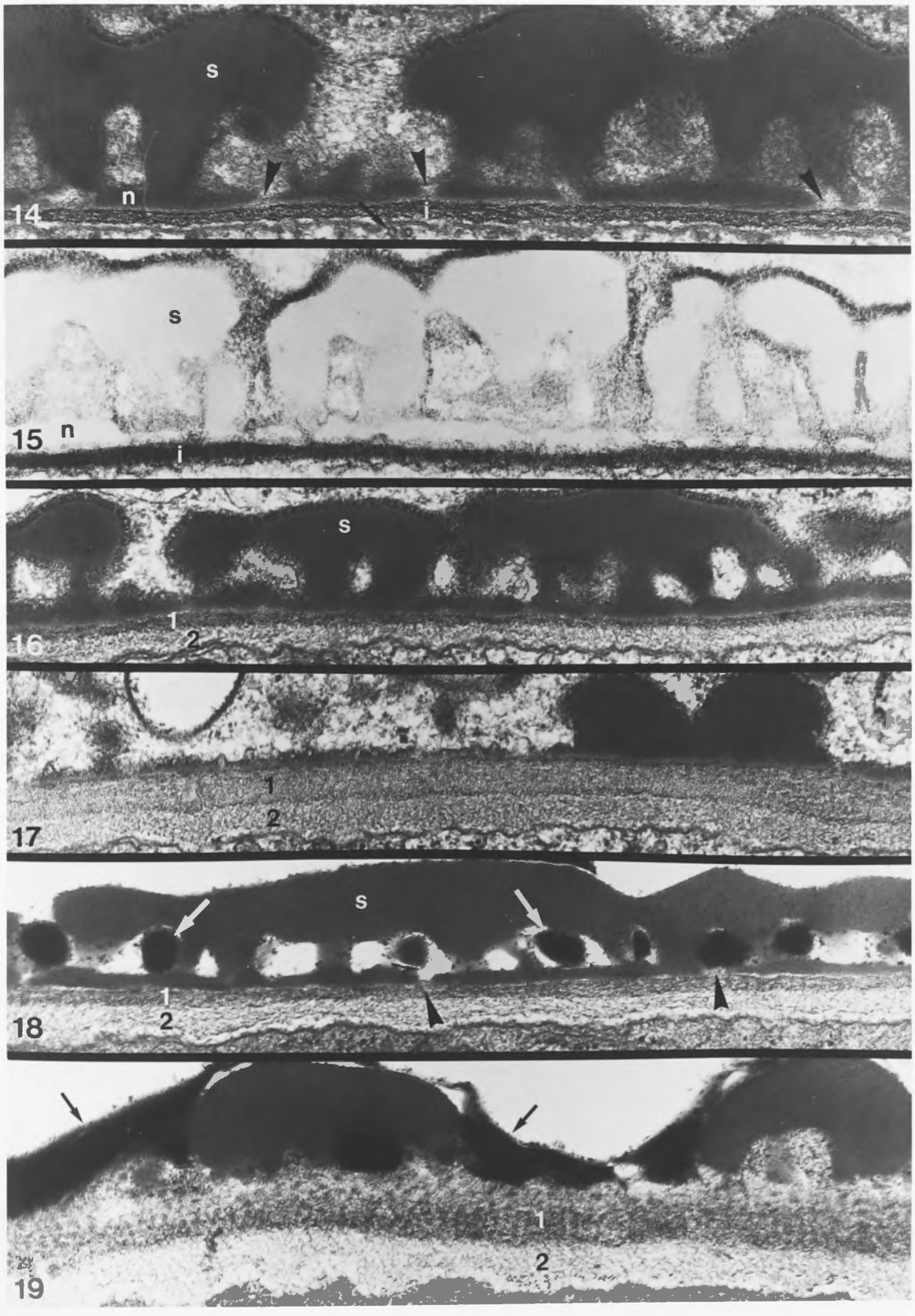
s
n
i
14
s
15
n
i
s
1
2
16
1
2
17
s
1
2
18
1
2
19

Figs. 6.20-6.27 are from FS spores.

Figs. 6.20,6.21. Spore surfaces at late pre-pattern stage. A region of lighter electron-density (star) lies between the spore surface and the callosic wall (c). A more or less continuous lamella (arrows) is situated outside the plasma membrane. Sometimes electron-dense blebs (arrowheads) can be seen at the lamella. The wavy outline of lamella is clearly visible. x 56,000 and 48,000, respectively.

Fig. 6.22. Non-apertural spore surface at early pattern stage. The figure shows the lamella (arrows), early probacula (small arrowheads) and the callose wall (c). The wavy outline of the lamella, the occurrence of electron-dense granular structures between the lamella and the plasma membrane, and the zone of lighter electron-density (star) at the inner surface of the callosic wall can also be seen. x 54,000.

Fig. 6.23. Non-apertural surface at slightly more advanced stage than in Fig. 6.22. The probacula are situated on the lamella (arrows). The lamella has become thicker than in Fig. 6.22. The spaces between the lamella and plasma membrane show more granular structures (arrowheads). The zone of lighter electron-density (star) can be seen at the inner side of callose (c). x 70,000.

Fig. 6.24. Non-apertural surface at the late pattern stage. A well-developed sexine (s) in which some bacular heads have fused (white arrowheads), and nexine 1 (n1) and 2 (n2) can be seen on outer and inner surfaces of the white line (white arrows). Note also the interfacial zone (star) containing granular structures (arrowheads; c, callose; arrows, microtubules). x 50,000.

Figs. 6.25,6.26. The non-apertural and apertural surfaces of the spore at late tetrad stage. The white line (white arrowheads) corresponding with the lamella can be seen between the nexine 1 and 2 layers. In apertural area a thin and discontinuous nexine 1 can be seen, but not nexine 2. The spore wall in non-apertural area is centered around the lamella, but in apertural region it develops directly over the plasma membrane and, correspondingly, the white line does not occur at such regions. Note also the differences in sexine at non-apertural and apertural surfaces. Microtubules (arrowheads) can also be seen. x 43,000 and 48,000, respectively.

Fig. 6.27. Spore wall at the boundary of apertural and non-apertural areas from a dividing late microspore. Nexine layer (arrowheads) can be seen at the boundary , but not at the apertural areas. Note also the gradual thickening of intine from the boundary region to the apertural region. Arrows indicate the channels in the intine. x 48,000.

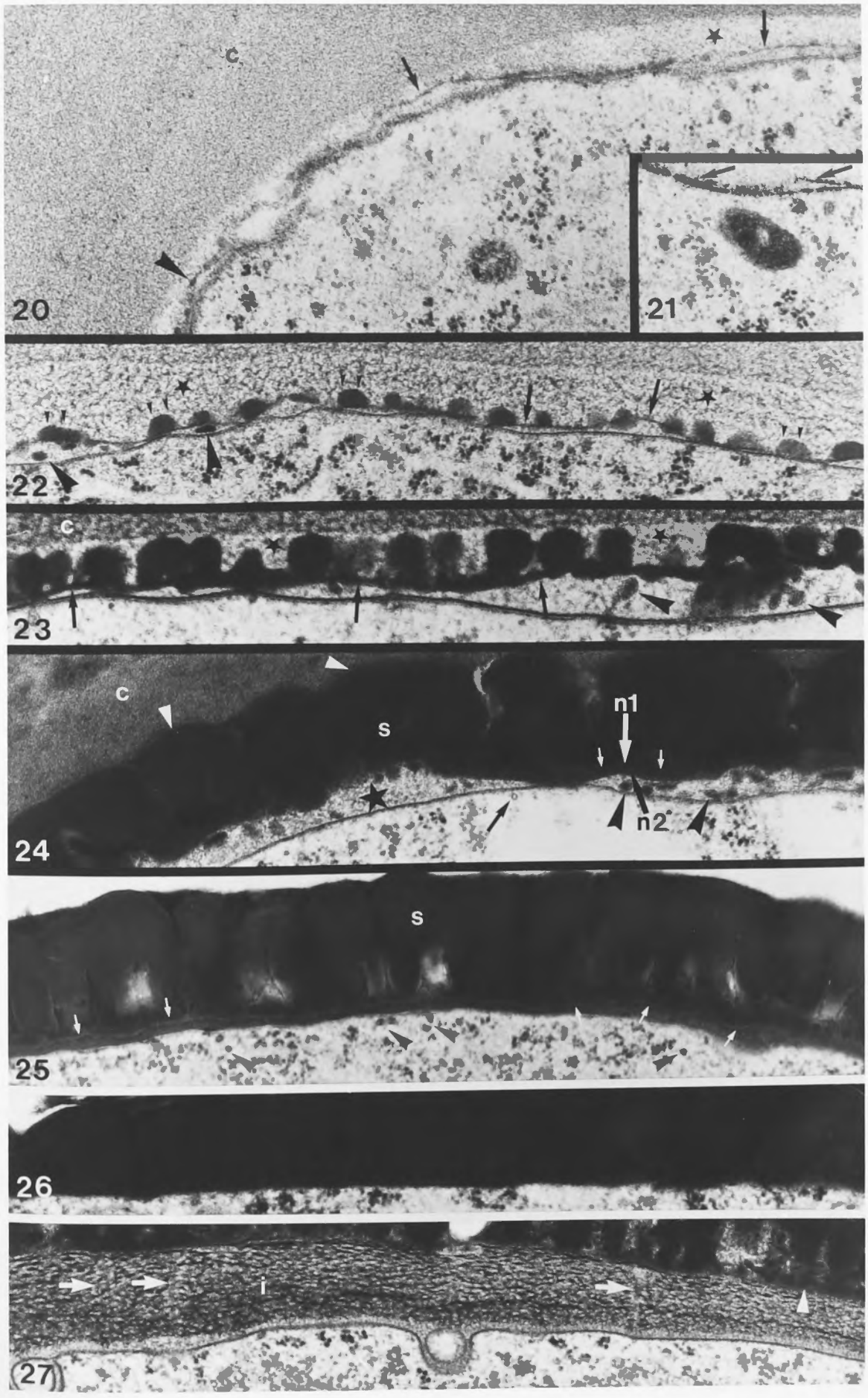
c
20
21
22
c
23
c
s
n1
n2
24
s
25
26
i
27

Fig. 6.28. The general ultrastructure of the spore cortex at late pre-pattern stage. The callose wall (c), primexine (arrows), the spaces between the two, and the myelin-like figures (m) are prominent. CF spore. x 24,000.

Fig. 6.29. Higher magnification view of spore cortex at late pre-pattern stage. Note the occurrence of multivesicular body (mvb). Vesicles similar to those in the mvb also occur at the spore surface. Arrows indicate the primexine (c, callose; d, dictyosomes; m, mitochondria). CF spore. x 60,000.

Fig. 6.30. A 1µm thick section of a ZnIO-impregnated spore at late pre-pattern stage. The callose wall and the primexine can not be seen in the figure as they do not show enough electron-density by the procedure. However, their presence was confirmed on the basis of images from adjacent thin sections which were stained with uranyl acetate and lead citrate. The figure does not show any particular spatial relationship between the electron-dense endomembranes and the presumptive apertural (a) regions (n, nucleus; na, presumptive non-apertural surfaces). x 11,000.

Fig. 6.31. A high magnification view of a part of thick ZnIO-impregnated spore to show the nuclear envelope (ne) with its pore complexes and the flat cisterna of endoplasmic reticulum showing nuclear pore-like structures (arrowheads). x 15,000.

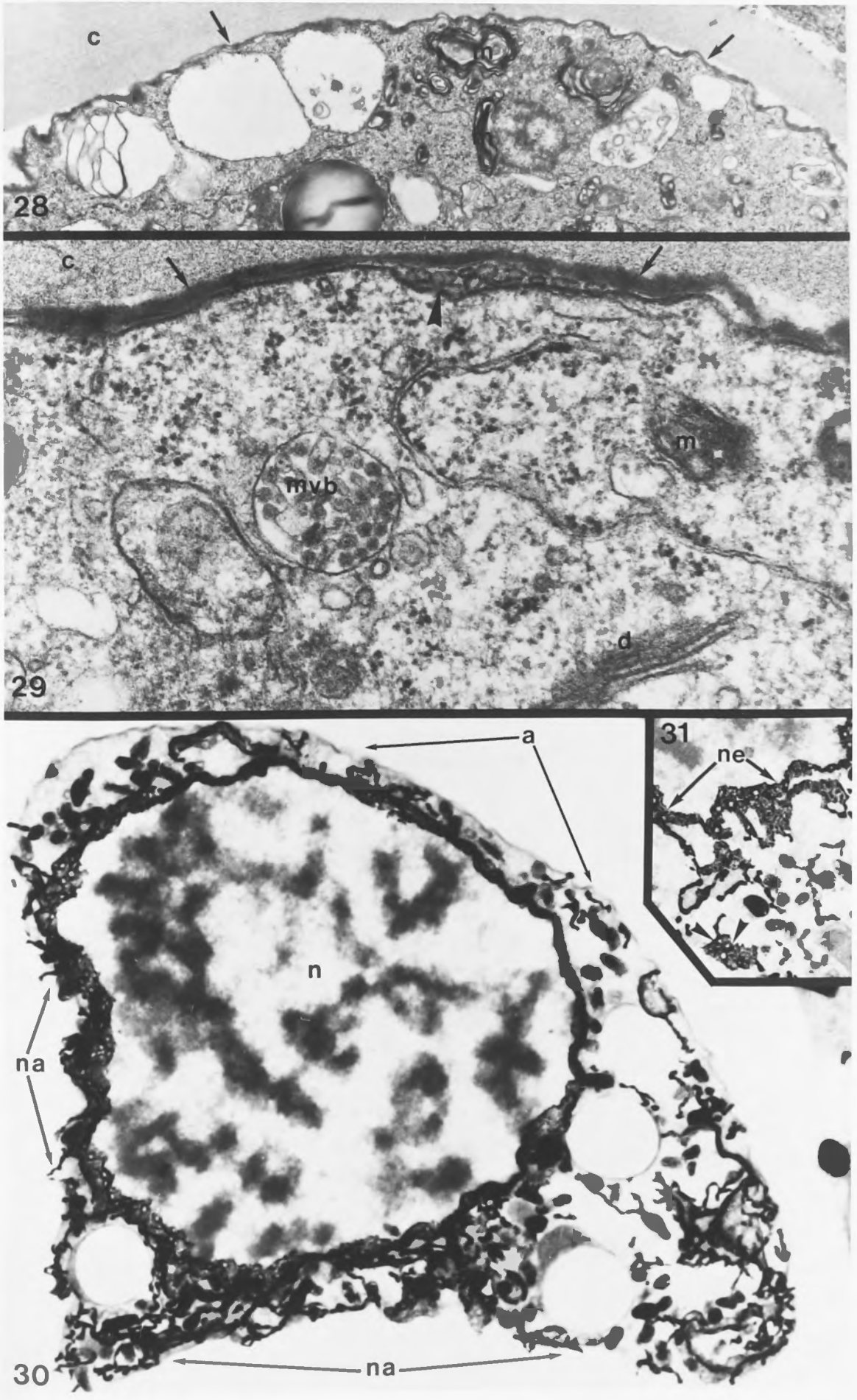
c
28
c
m
myb
d
29
a
31
ne
n
na
30
na

Figs. 6.32-6.34 are from FS spores.

Fig. 6.32. Grazing transverse section of an early pre-pattern spore. Numerous microtubules oriented perpendicular to the long axis of the spore can be seen. Stars show the pockets of partially-coated membranes which are shown at higher magnification in Fig. 6.37 (c, callose; m, mitochondria). x 9,700.

Fig. 6.33. High magnification view of the spore cortex at early pre-pattern stage. The callose wall (c) has become separated from the spore surface during sectioning (this is a common problem in FS tissues). Note several microtubules (large arrowheads) and the microfilaments (small arrowheads). x 48,000.

Fig. 6.34. Grazing section of a late pre-pattern spore showing the delicate system of microfilaments (arrowheads) in the spore cortex. x 70,000.

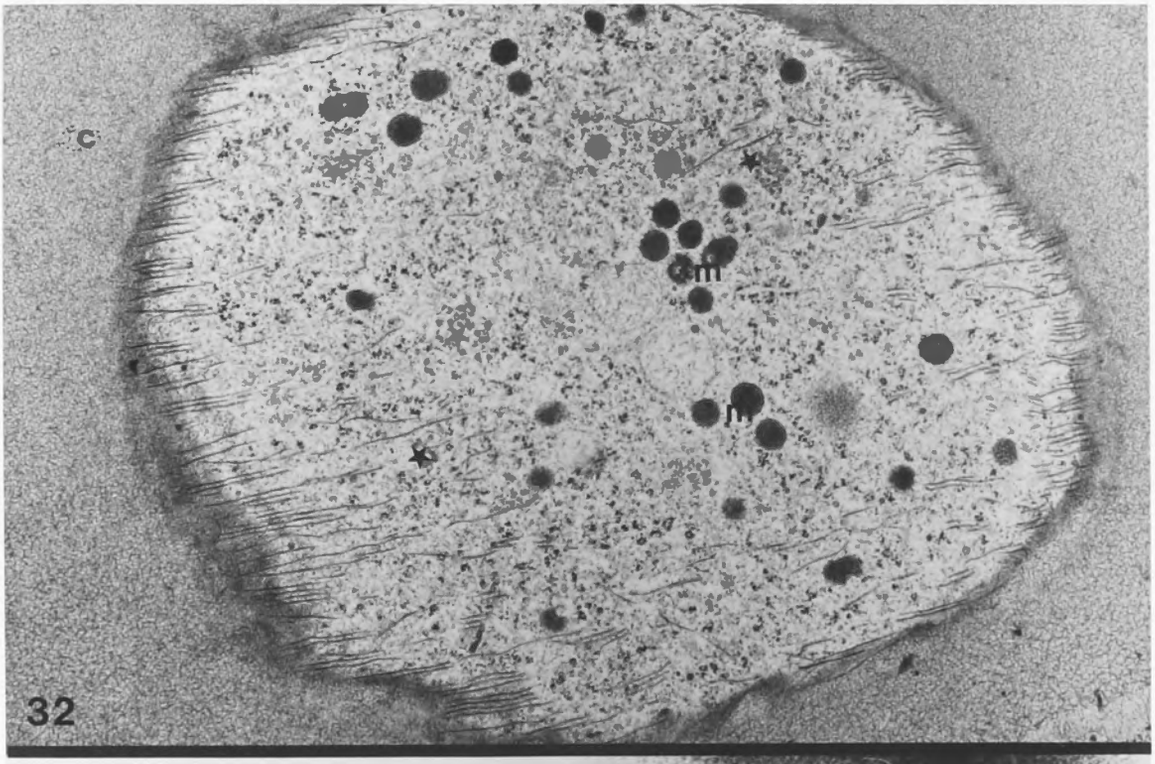
c
m
m
32

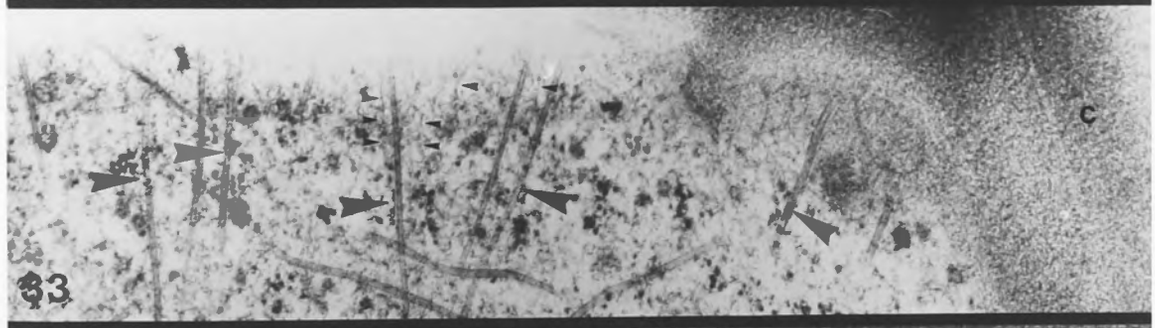
c
33

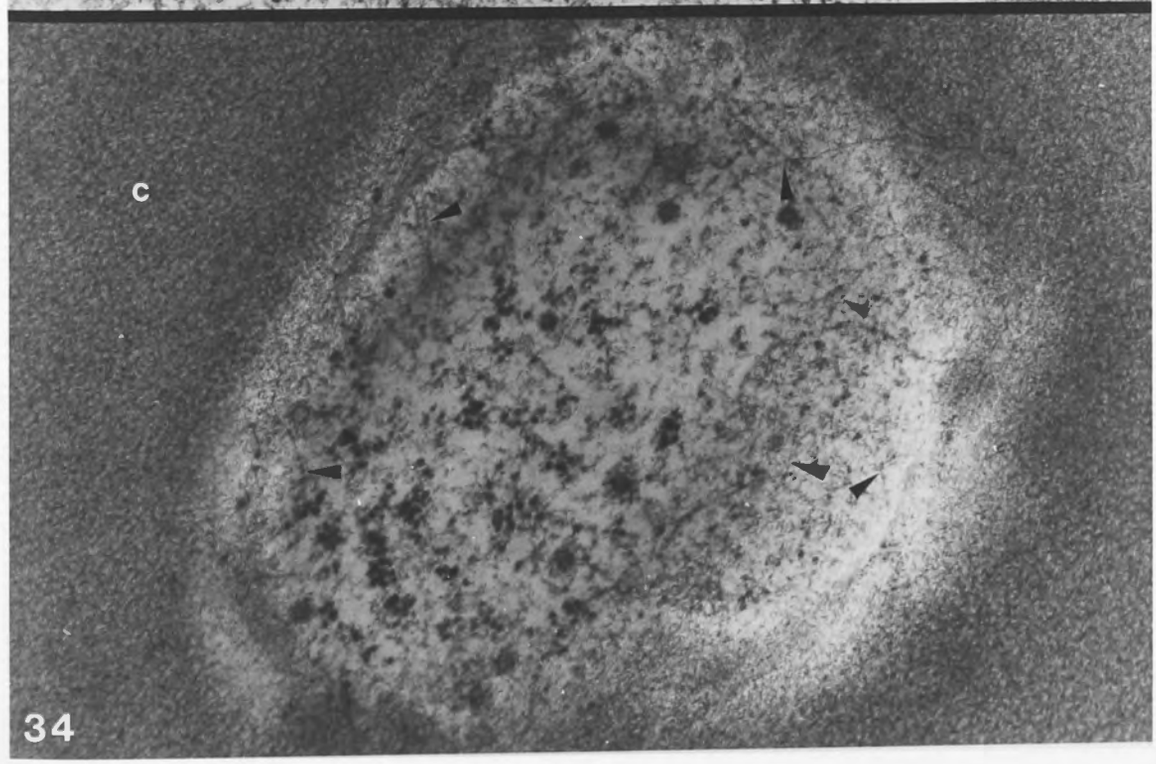
c
34

Figs. 6.35-6.38 are from FS spores.

Fig. 6.35. General ultrastructure of spore at late pre-pattern stage. The cortical microtubules have become infrequent and the stratification in callose (arrowheads) is just beginning. The plasma membrane shows occasional infolding, and the lamellae are not yet formed (d, dictyosomes; m, mitochondria; c, callose). x 48,000.

Fig. 6.36. High magnification view of a part of a spore to show the structure of a multivesicular body from a freeze-substituted preparation of a late pre-pattern spore. x 21,350.

Fig. 6.37. Late pre-pattern spore. A pocket of partially-coated membranes (star), helically arranged ribosomal aggregate (arrowhead) and a partially collapsed (freezing damage, see Chapter 2 for more comments) can be seen. The microtubules have become infrequent, but the stratification in callose has not yet occurred (c, callose). x 48,000.

Fig. 6.38. Oblique section of an early pattern spore showing the primary exine (pe), microtubules (arrowheads) and the cortical microfilaments (arrows). Many filaments can be seen underlying the plasma membrane. x 42,000.

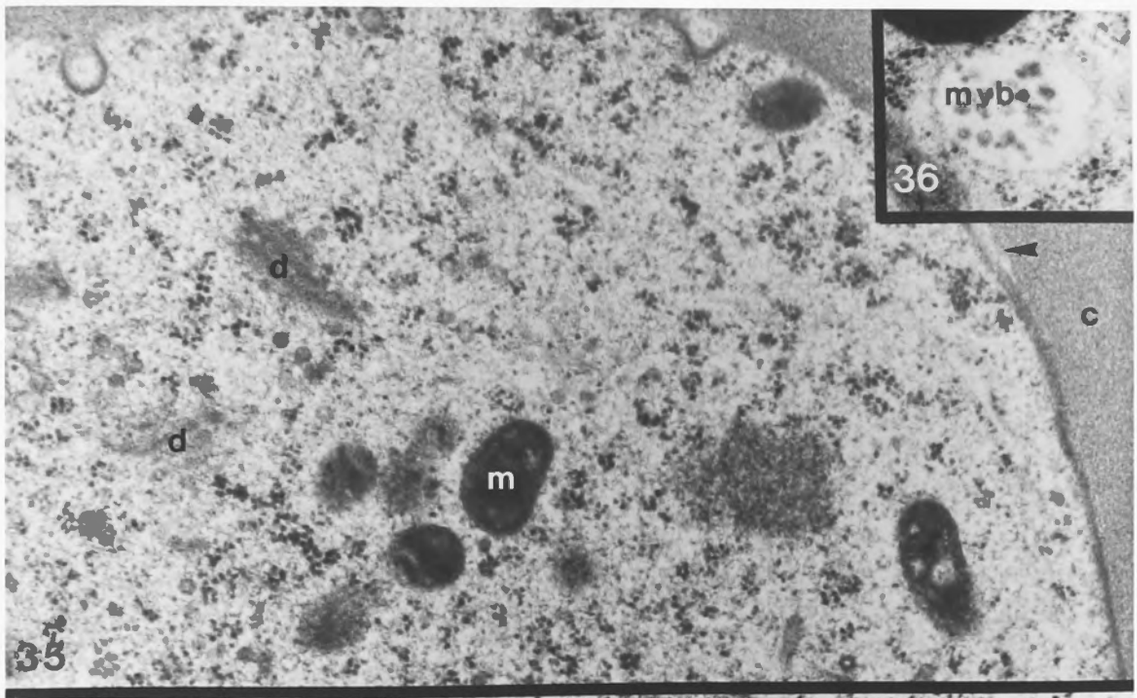
myb
36
d
d
m
c
35

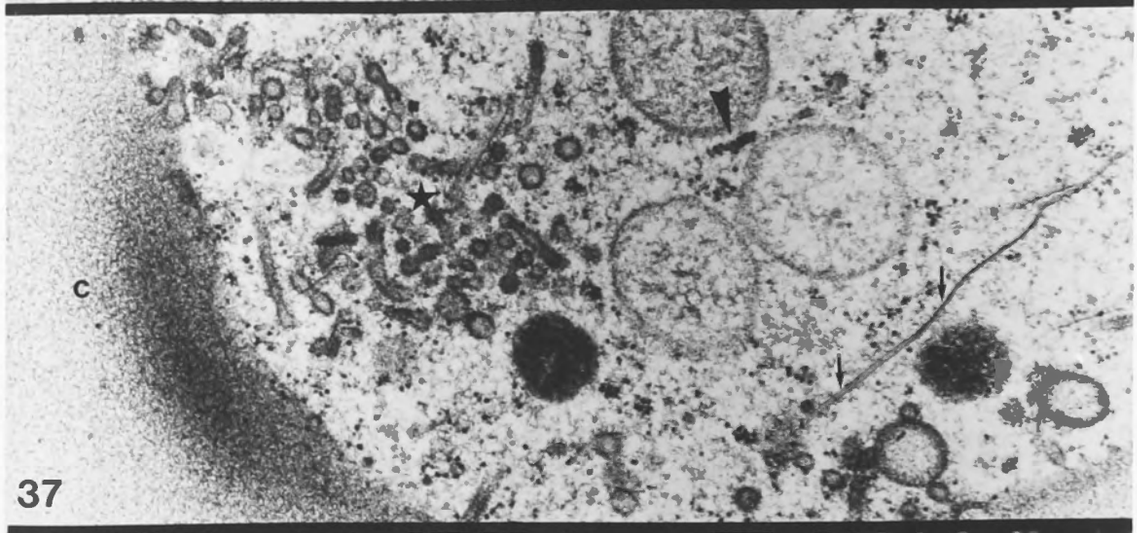
c
37

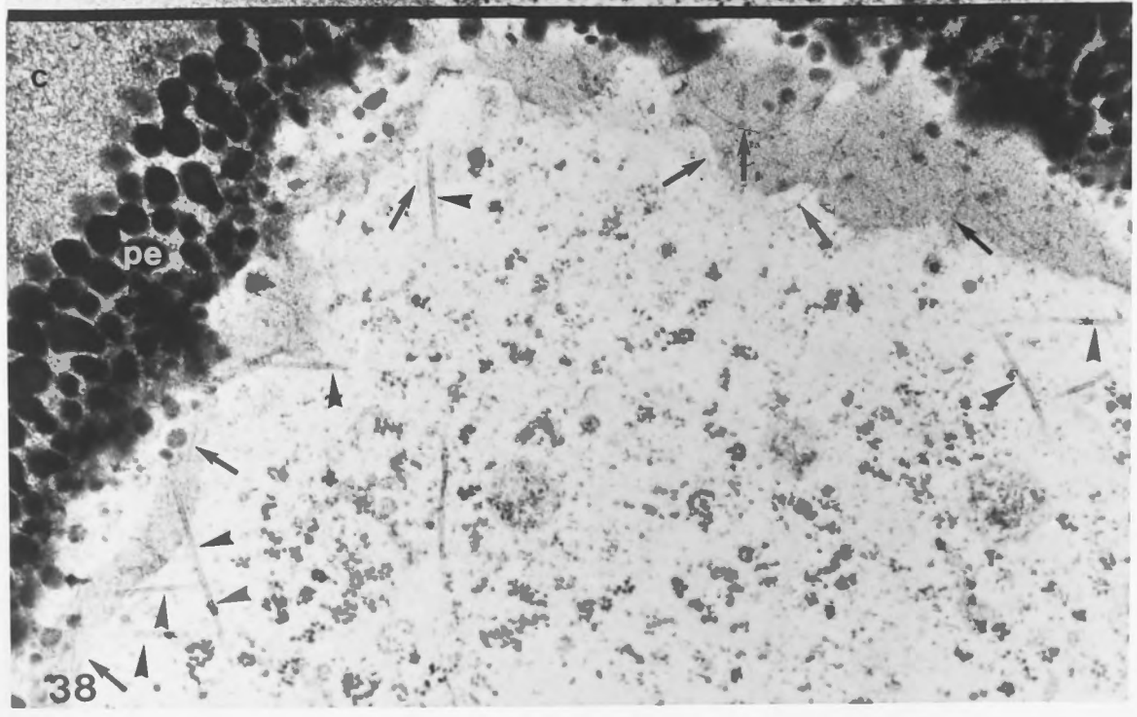
c
pe
38

Figs. 6.39-6.41 are from freeze-fracture replicas of unfixed, uncryoprotected spores.

Fig. 6.39. Replica of the late pre-pattern spore when the development of lamella has become extensive. The figure shows the non-apertural surface. Note the pattern of elevated areas of the lamella. White arrow indicates the direction of shadowing. x 34,000.

Fig. 6.40. Replica of the non-apertural surface at early pattern stage. The probacula (arrowheads) and the callose wall (c) can be seen. The surface pattern seen in Fig. 6.39 is still retained. White arrow indicates the direction of shadowing. x 28,800.

Fig. 6.41. Replicas of a early pattern spore that shows the cross-fractured edges. The probacula (arrowheads) do not show any preferential fracture plane, indicating the absence of membranes in them. The lamella is shown by arrows. Note the lack of any fibrous component in the spaces between the probacula (c, callose). x 30,000.

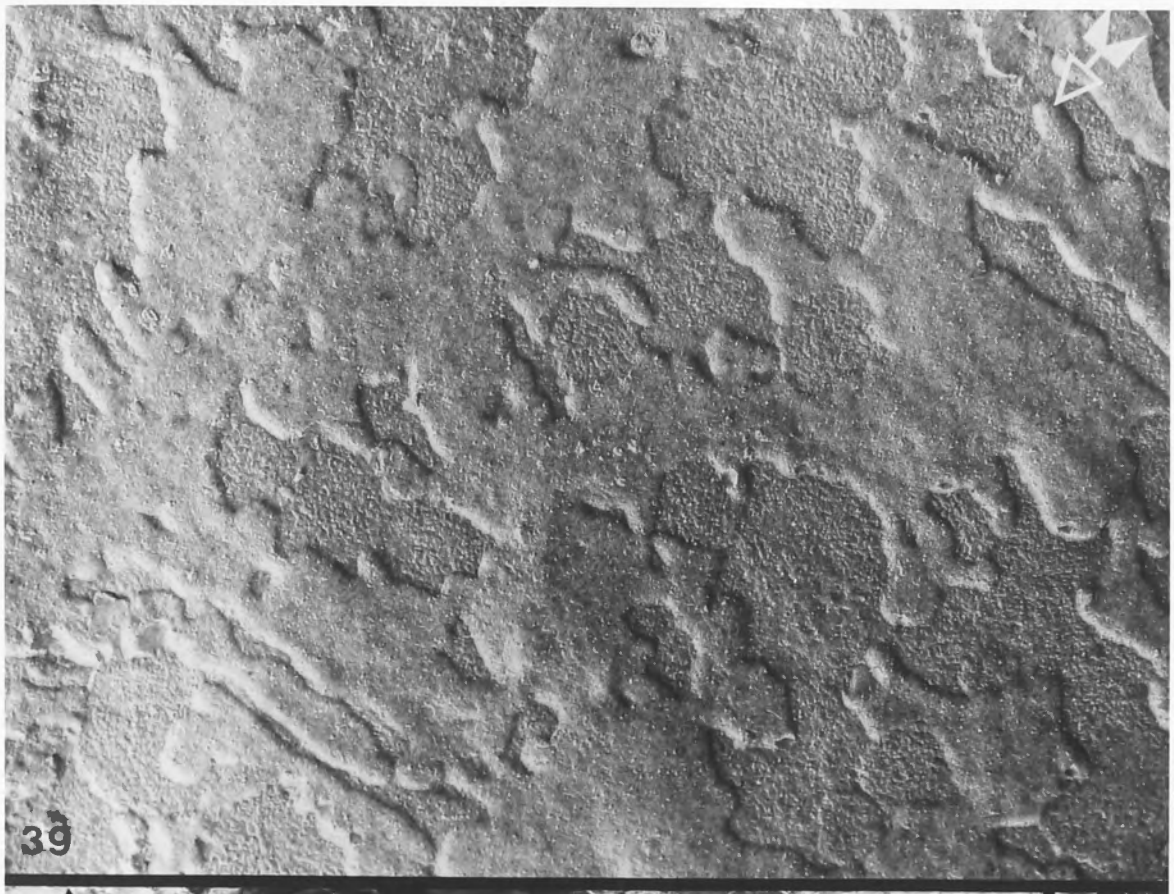

39

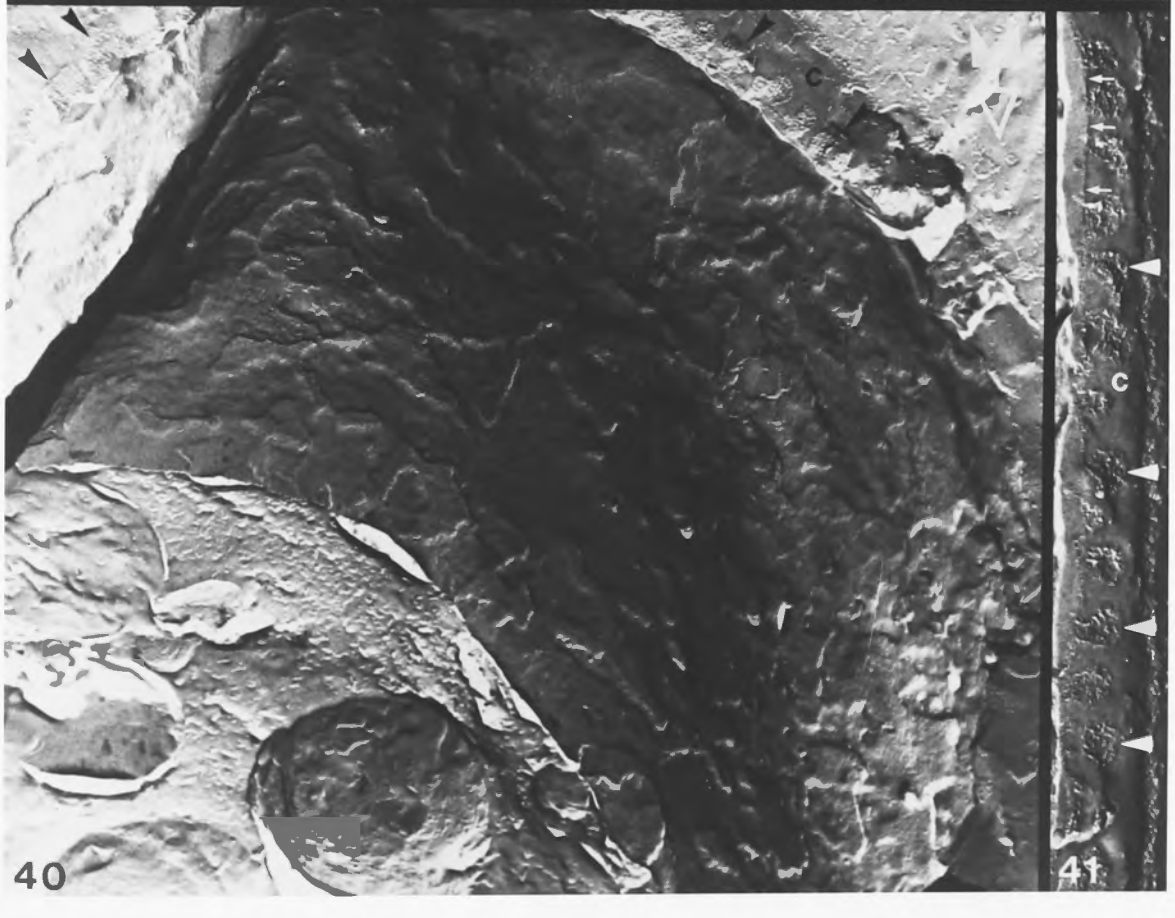

40

41

Figs. 6.42-6.47. Immunofluorescence and phase contrast micrographs of sectioned (Figs. 6.42-6.45) and permeabilized whole spore cells (Figs.6.46, 6.47), stained with FITC-labelled anti-tubulin. Generally, spore cells (s) at the early pattern period show diffuse fluorescence. Few microtubules (arrowheads) may also be seen, sometimes. Arrows indicate the fluorescence corresponding with microtubules in the tapetum (t; see Chapter 4 for details of tapetum). Figs. 6.42-6.46 x 1,200; 6.47 and 6.48 x 1,000.

Figs. 6.48-6.49. Immunofluorescence and phase contrast pair of a young microspore after its liberation from the tetrads. The microtubules can be seen running predominantly perpendicular to the polar axis. Both x 1,600.

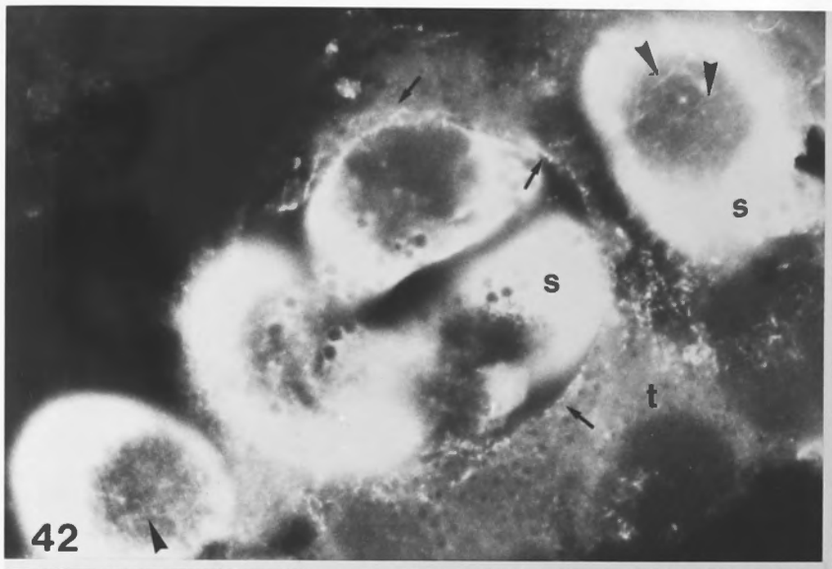

42

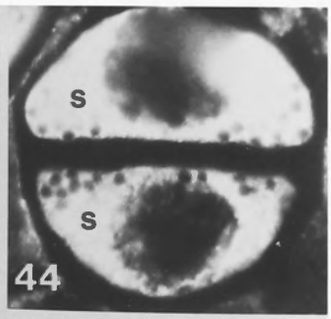

44

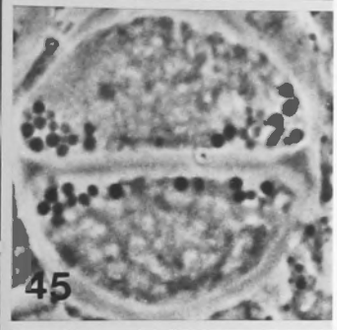

45

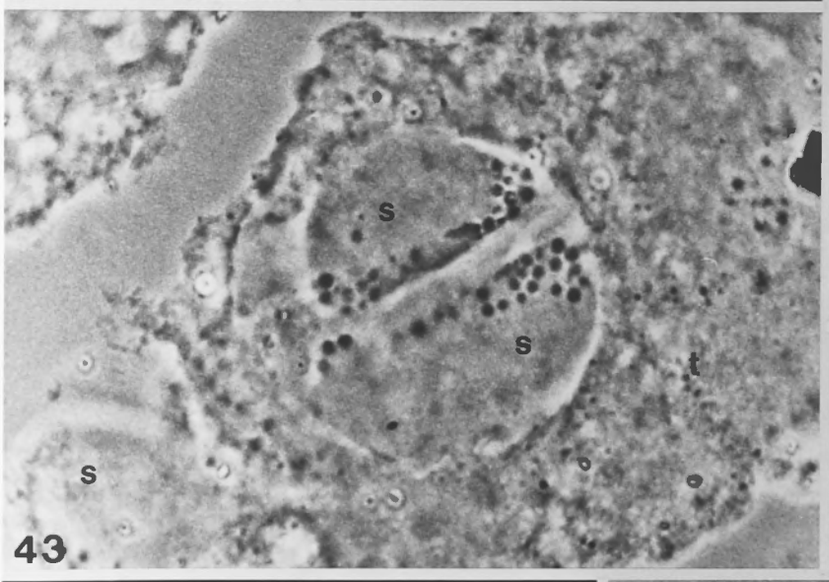

43

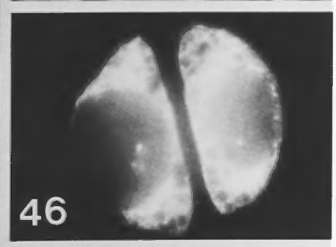

46

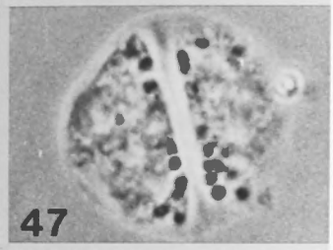

47

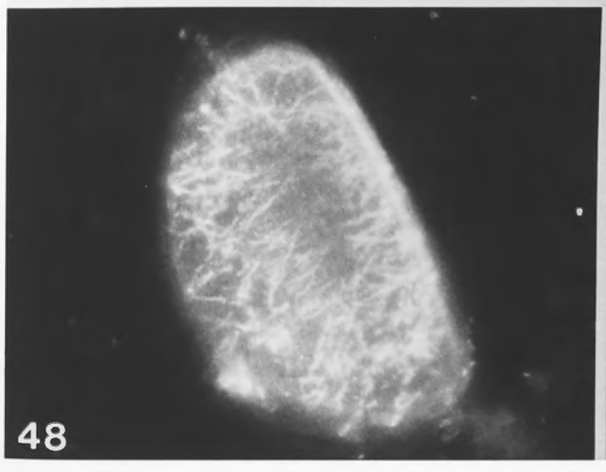

48

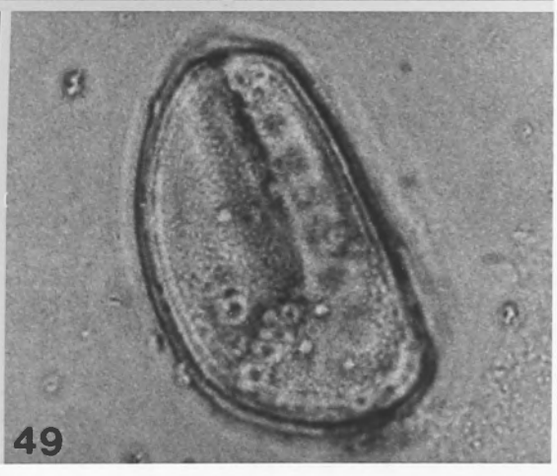

49

Fig. 6.50. A median transverse section of a freeze-substituted isobilateral tetrad. The peripheral callosic wall can not be seen at this stage, but the cell plates remain. The primary exine is well differentiated and shows clear apertural and non-apertural regions. The probacula are shorter and sparse at the apertures when compared with non-apertural surfaces. The spores show a 3-sided shape. Arrowheads indicate the corners where a well-developed interfacial zone occurs. x 2,600.

Fig. 6.51. A 1µm thick median transverse section of a ZnIO-impregnated spore at late tetrad stage (a, apertural area; na, non-apertural area; t, tapetum). x 7,150.

Fig. 6.52. A corner region from a freeze-substituted spore at late tetrad stage showing the interfacial zone (star). Arrows indicate oblique profiles of microtubules (w, primary exine). x 36,000.

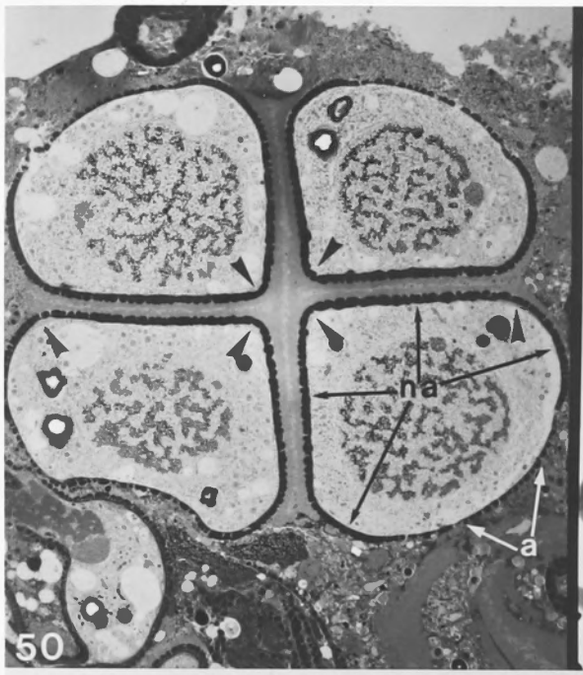

50

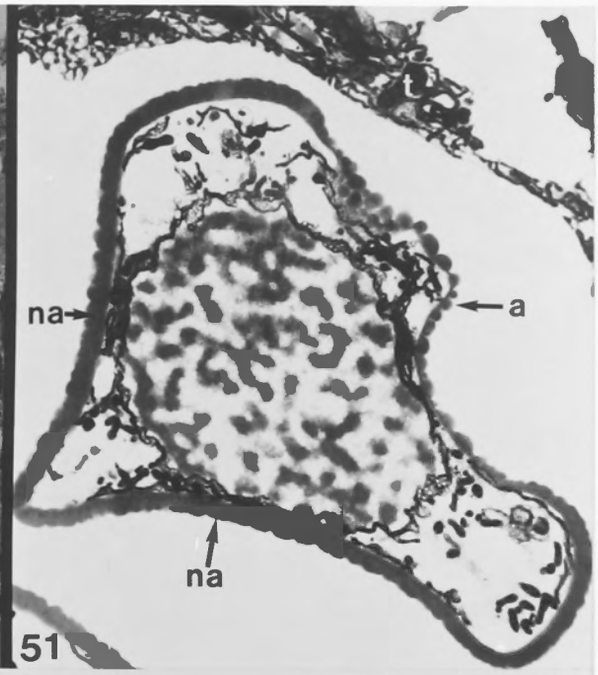

51

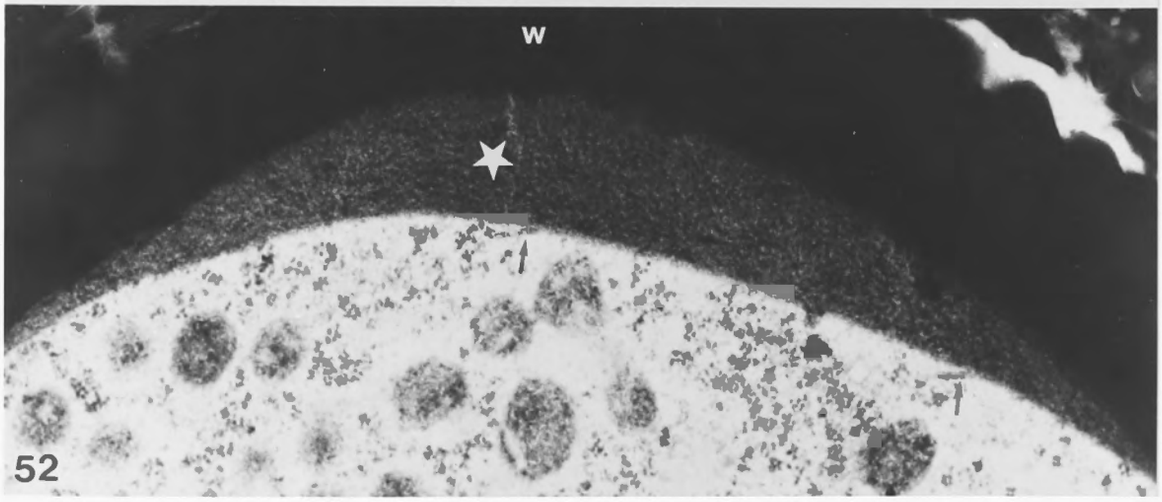

52

Fig. 6.53. A conventionally-processed late microspore. The microspores have attained their full size by this stage and intine is fairly well-developed. TTransverse sections of spores such as this one shows that by this stage the spores are ellipsoidal (a, apertural area; na, non-apertural area). x 3,000.

Fig. 6.54. lum thick section of a ZnIO-impregnated late microspore to show the distribution of electron-dense endomembranes. x 3,200.

Fig. 6.55. Grazing section of a freeze-substituted late microspore showing the co-oriented intine (i) wall microfibrils and microtubules (arrows). x 43,200.

Fig. 6.56. Grazing section of a conventionally-processed late microspore shows fewer microtubules and the microfibrillar nature of the intine (i) is not identifiable. x 42,630.

Fig. 6.57. A part of a tangential section of intine (i) at late microspore stage showing several channels. x 69,230.

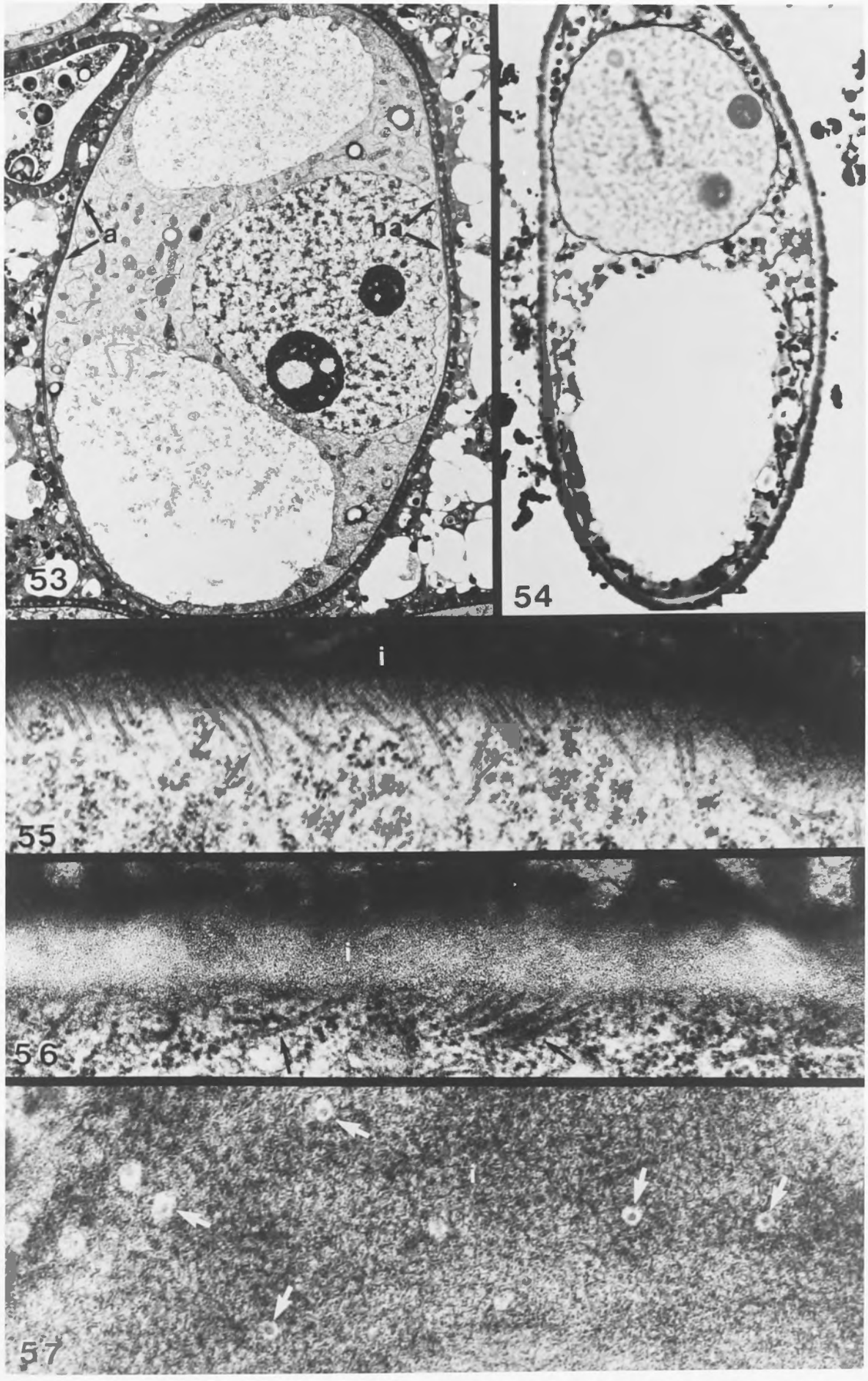
a
ha
53
54
i
55
i
56
i
57

Fig. 6.58. Grazing section of a freeze-substituted late microspore showing numerous cortical microtubules oriented perpendicular to the long axis of the microspore. High magnification views of this preparation revealed that 6 of the microtubules terminations were of the 'closed' type. x 30,600.

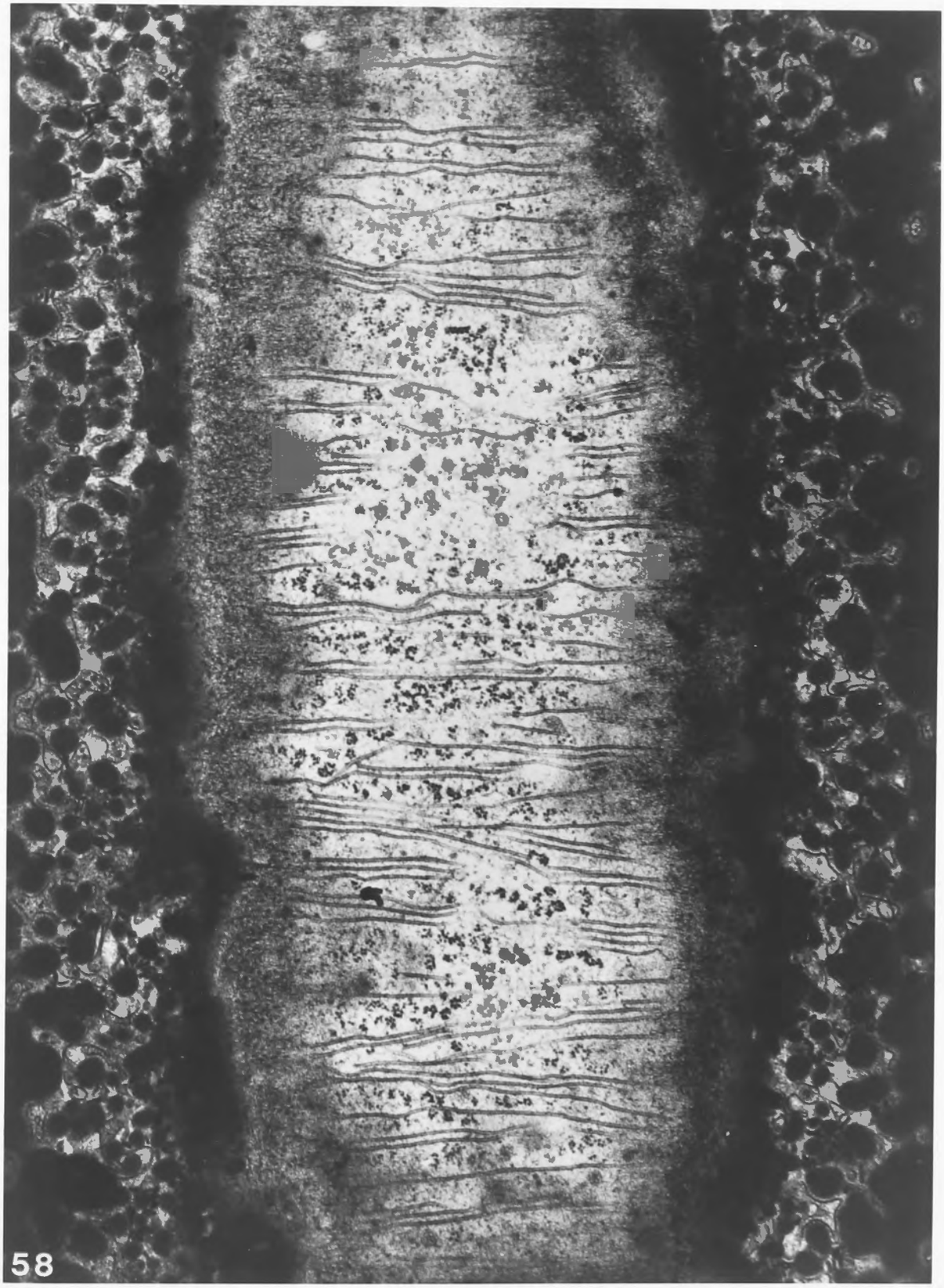
58

Fig. 6.59. Oblique section of a freeze-substituted microspore showing intine-like channels (white arrows) and the closed terminations (black arrows) in cortical microtubules. x 50,000.

Fig. 6.60. Stereopair of a part of the section in Fig. 6.59 to show the spatial relationship between cortical microtubules (arrows, closed terminations; arrowheads, intine channel). Tilt angle 15^{o}. x 59,480.

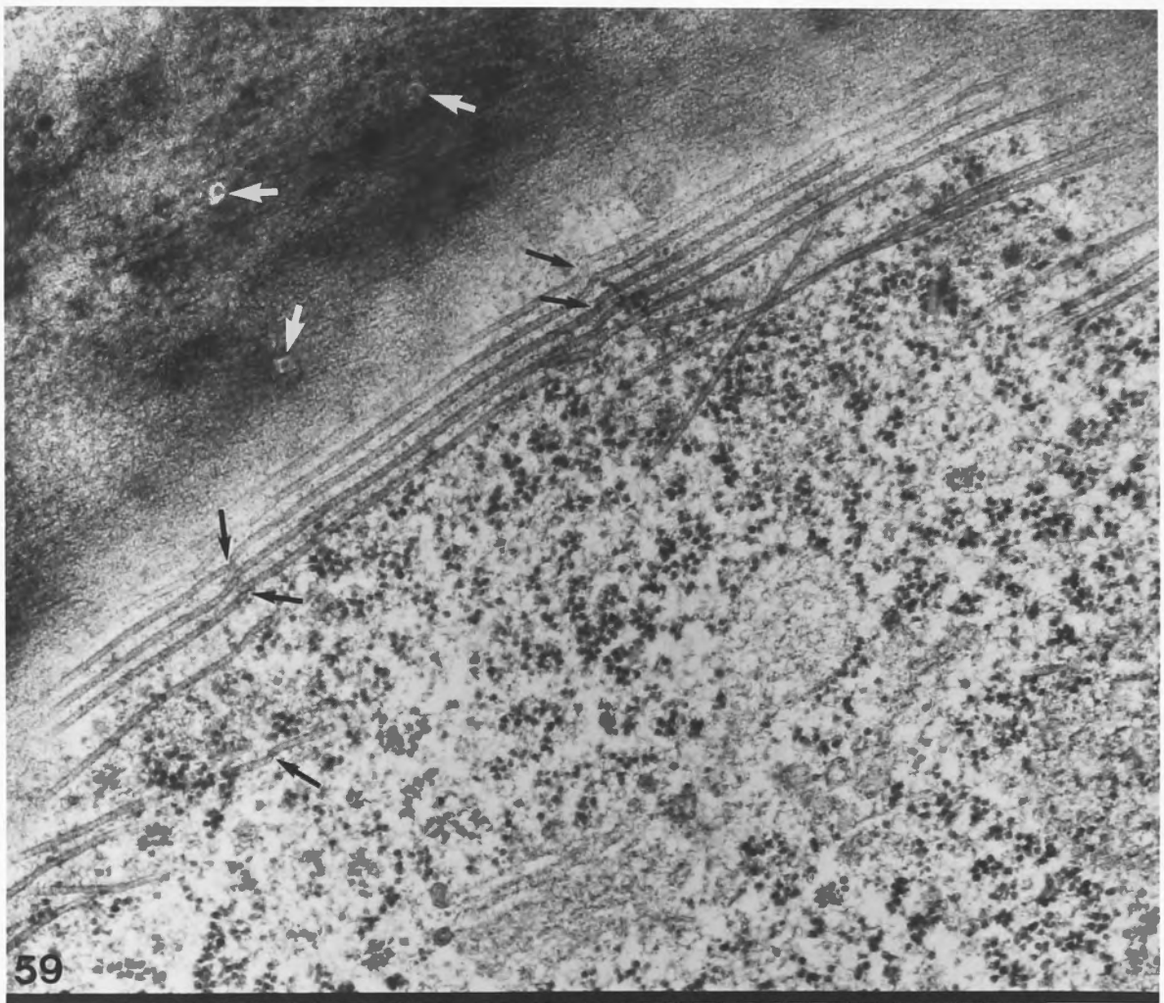

59

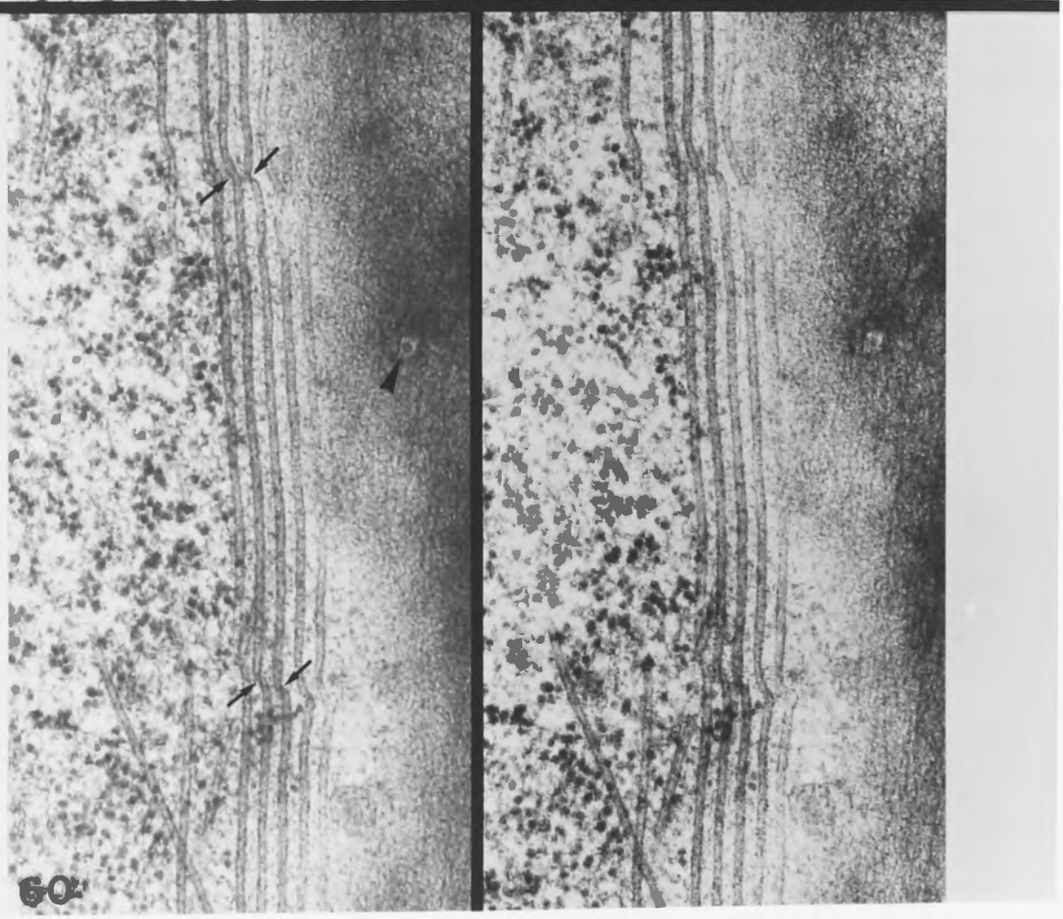

60

Figs. 6.61-6.64. Freeze-substituted bicelled pollen at a stage when generative cell is undergoing elongation. An extensive system of microfilaments (arrowheads) occurs in the vegetative cell at this stage. Microfilaments are seen located in the cell cortex (Figs. 6.61,6.62), sometimes in association with cortical microtubules, but largely independent and with no preferred orientations (i, intine). The microfilaments also occur in association with nuclear (n) envelope (Figs. 6.63,6.64). x 72,000; 61,330; 58,000; and 50,000, respectively.

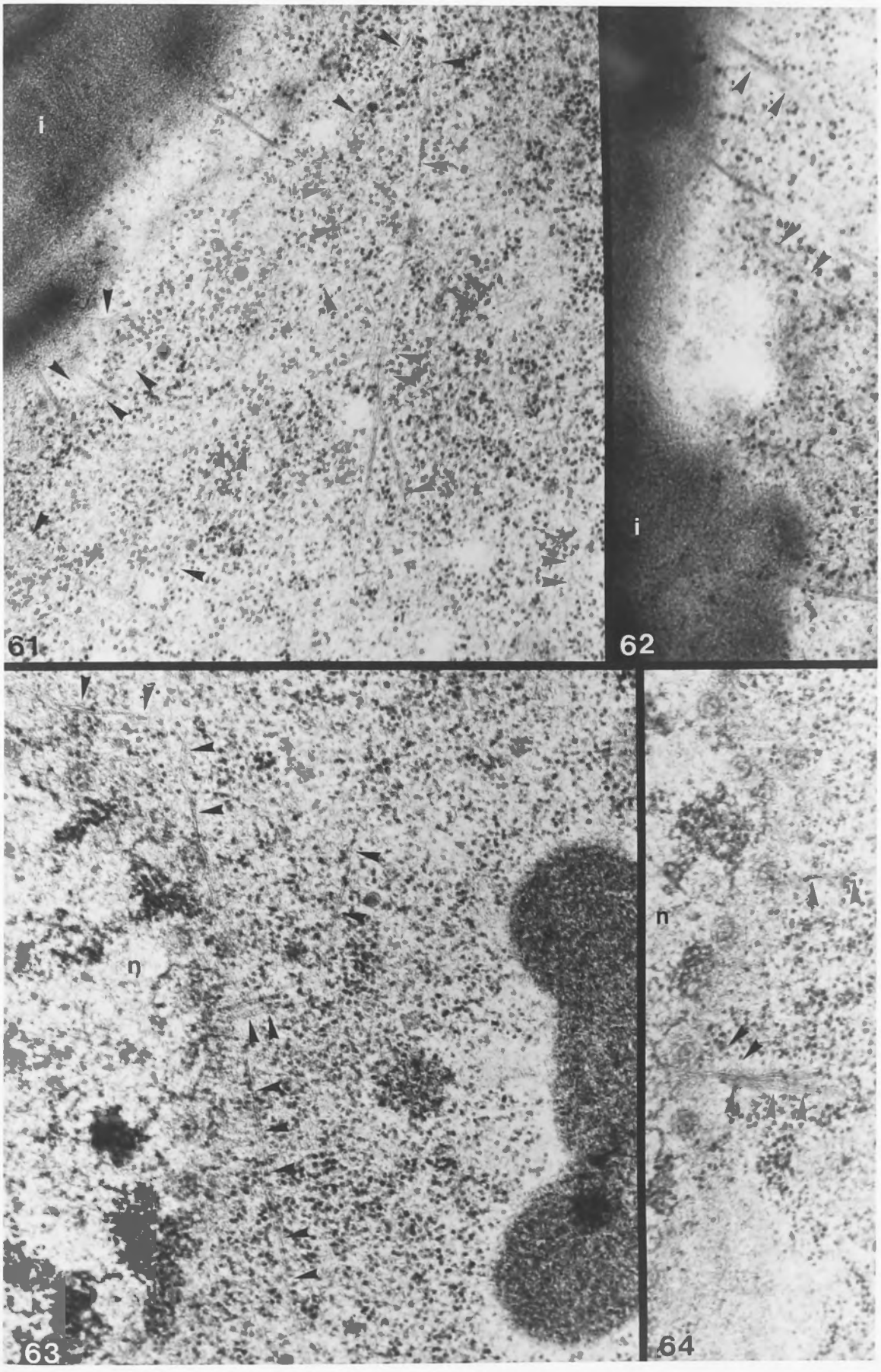
i
61
i
62
η
63
η
64

Figs. 6.65,6.66. Oblique section of a freeze-substituted bicelled pollen (Fig. 6.65) and the freeze-fracture replica image (Fig. 6.66) at corresponding stage. These images are obtained from pollen grains with elongating generative cells. Note the preferred orientation of intine (i) wall microfibrils, transverse to the long axis of the pollen grain (shown by double-headed arrow). x 70,000 and 80,000, respectively.

Figs. 6.67,6.68. Freeze-substitution and freeze-fracture replica images, respectively, of a dehisced pollen grain showing the loss of preferred orientation of intine wall microfibrils. Intine wall channels (arrows) can be seen in the freeze-fracture replica. x 50,200 and 60,000, respectively.

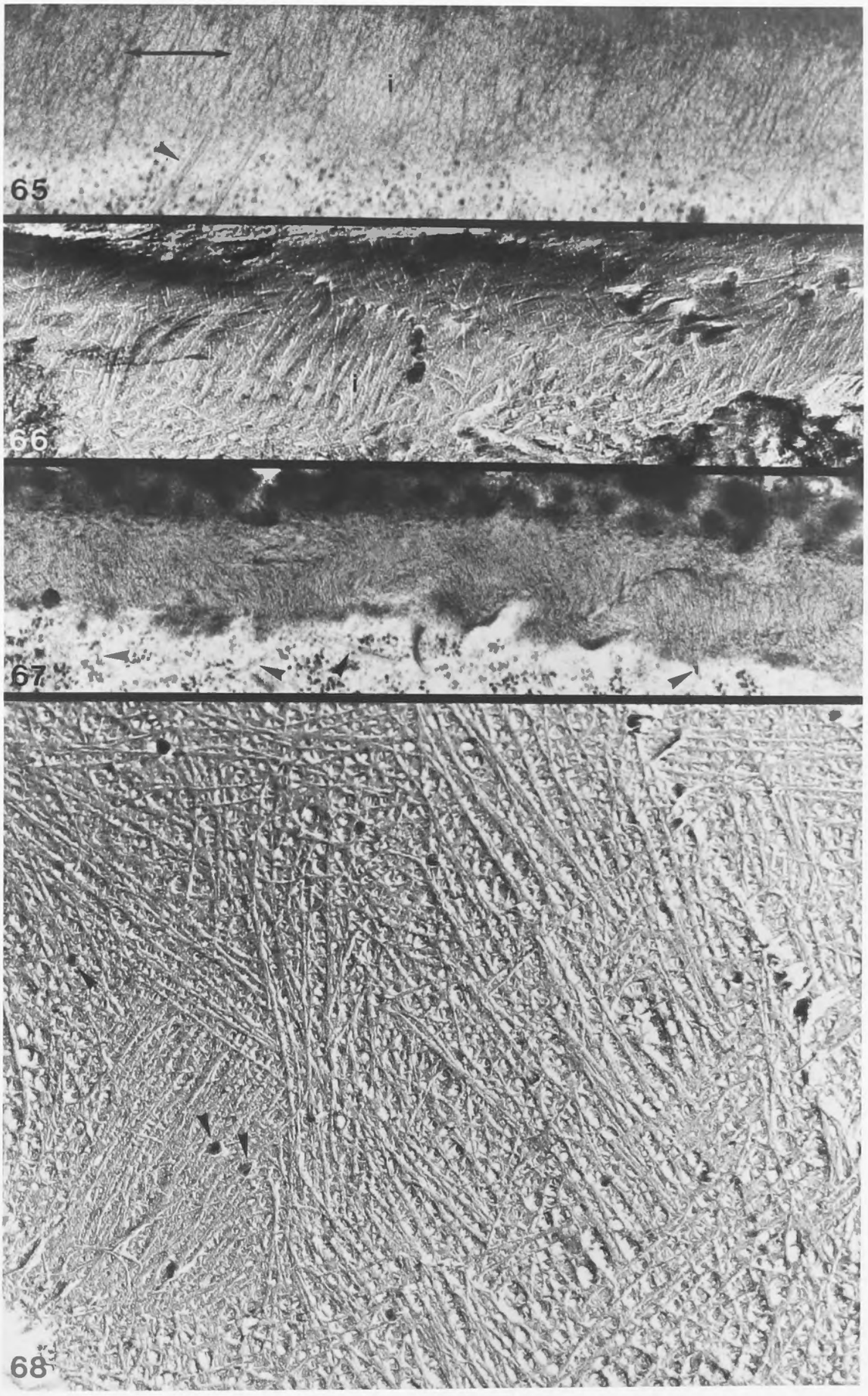
i
65
i
66
67
68

Figs. 6.69,6.70. Parts of a conventionally-processed pollen grain to show the general ultrastructural appearance. The pollen grains show an abundance of usual cell organelles. Rough endoplasmic reticulum (er) cisternae occur in close association with lipid bodies. x 12,500 and 18,460, respectively.

Fig. 6.71. Scanning electron micrograph of mature pollen grain from dehisced anthers. The apertural region has infolded (arrows) and hence can only be seen as a furrow that runs between the two poles of the pollen grain. Arrowheads show the discontinuities in the otherwise completely tectate exine at the non-apertural regions. x 1,900.


69
70
er
71

Figs. 6.72-6.75. Microspores which were subjected to colchicine solution from early tetrad stage (Figs. 6.72,6.73) and microspores from controls (Figs. 6.74,6.75). The treated microspores, seen here in transverse sections, have abnormal shapes and compact bacula in their apertural areas (a). Fig. 6.74 shows a transverse section of a normal microspore and Fig. 6.75 a longitudinal section. Note that in normal spores the shape is elliptical, unlike the treated ones. x 3,500; 4,500; 3,800; and 3,500, respectively.

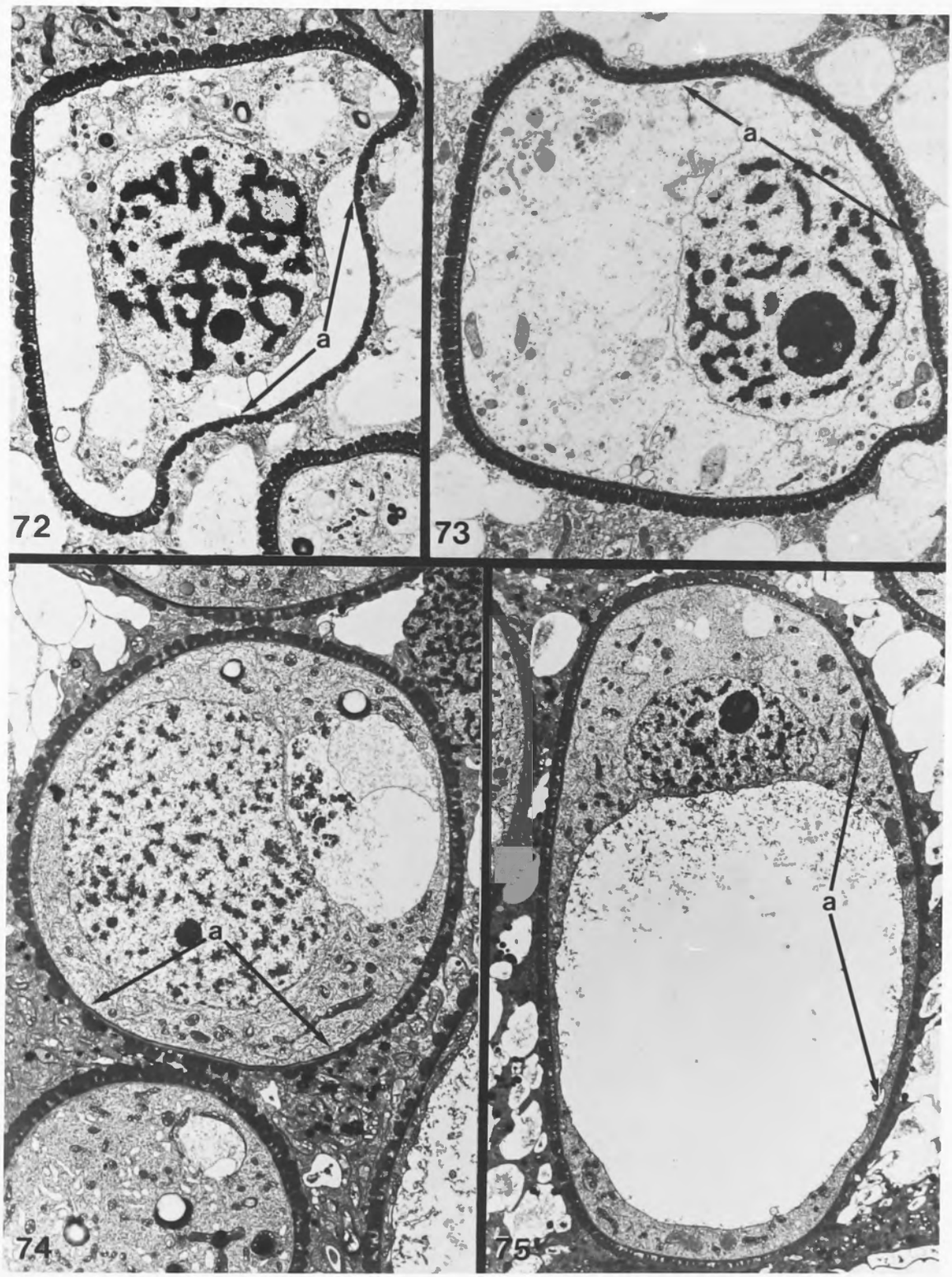
a
72
a
73
a
74
a
75

CHAPTER 7

DEVELOPMENT OF THE GENERATIVE CELL IN *TRADESCANTIA VIRGINIANA* L.

7.1. INTRODUCTION

The majority of angiospermic pollen grains at the time of anthesis consist of two cells: the larger vegetative cell which during pollen germination forms the pollen tube, and the smaller generative cell which is lodged within the vegetative cell and after gametogenesis forms two male gametes or sperm cells. The generative cell division is usually initiated after pollen germination when this cell has moved into the pollen tube, but can also occur in ungerminated pollen - the features are largely species specific (Brewbaker, 1967). As the forerunner of male gametes in higher plants, the generative cells were studied extensively by early cytologists (for reviews see Maheshwari, 1949; Steffen, 1963). Recent investigations have focused on the wall around the generative cell, the roles of microtubules in pollen mitosis (Burgess, 1970a), phragmoplasts and the formation of the hemispherical partitioning wall between the generative and vegetative cells (Heslop-Harrison, 1968d), the microtubular cytoskeleton in the generative cell (Sanger, and Jackson, 1971b; Cresti et al., 1984), the mitosis in the generative cell that produces the two male gametes (Burgess, 1970b; Karas and Cass, 1976) and the sperm cells (see McConchie et al., 1985 and the references cited therein).

Sax and Edmonds (1933) studied the development of generative cell in Tradescantia and claimed that the

position of the generative cell was predetermined at the time of meiosis. According to them the axis of the spindle of pollen mitosis (that results in the formation of the generative cell) developed at a 45^{o} angle to that of the previous meiotic divisions. Disputing this, Geitler (1935) asserted that while the position of the generative cell was fixed for a given species, there was no spatial relationship between the pollen mitosis and the meiotic divisions. One aim of the present investigation was to determine if there was any relationship between the two sets of divisions in Tradescantia virginiana. Continuing the ultrastructural investigation of pollen development of this species, the present Chapter describes the absence of a predetermined position of the generative cell, aspects of cellular connections between the cells of mature pollen grains, and the behaviour and role of microtubules as determined through the technique of freeze-substitution and administration of colchicine.

7.2. MATERIAL AND METHODS

Plants of Tradescantia virginiana L. 'Sydney hybrid' were grown and maintained as described in Chapter 4.

7.2.1. Light Microscopy

For light microscopic observations, anthers were isolated from buds and flowers at different stages, cut

at their apical ends with a sharp razor blade and their contents gently extruded in distilled water on a clean glass slide, mounted with a cover slip and observed and photographed on a Zeiss Photomicroscope III fitted with differential interference contrast optics.

7.2.2. Conventional Electron Microscopy

The procedure for conventional transmission electron microscopy was as described in Chapter 4. Observations were made on Hitachi H500 or H600 TEM at an accelerating voltage of 75 kV.

7.2.3. Freeze-Substitution

Spore cells were gently extruded out of freshly isolated unfixed anthers on to wire loops coated with a dry thin film of agar (2%) and processed as described in Chapter 3.

7.2.4. Cytochemistry

Callose was identified by mounting cells in a drop of 0.05% aniline blue (made in 0.067M phosphate buffer, pH 8.5) and observing with a Zeiss photomicroscope using mercury vapour lamp and UG1 as exciter and 51 as barrier filters. Controls were mounted in phosphate buffer. Calcofluor white M2R (0.01% aqueous solution) was also employed to localize wall constituents at the light microscopic level in pollen cells at appropriate stages of development using

UG1 and 41 filter combinations. Controls were mounted in distilled water.

To localize polysaccharides at the ultrastructural level, the Thiéry reaction (Thiéry, 1967) was employed. Thin sections were collected in plastic loops and processed in the same way as described in Chapter 3.

The endoplasmic reticulum was localized by the zinc-iodide-osmium tetroxide (ZnIO) impregnation method of Harris and Chrispeels (1980). This procedure has been described in Chapter 4. Thick (0.25-1.0 μm) and ultra-thin sections of the ZnIO-impregnated spore cells were cut. Ultra-thin sections were lightly stained with alcoholic uranyl acetate and lead citrate whereas thick sections were observed unstained with Hitachi H600 TEM at an accelerating voltage of 75 kV.

7.2.5. Freeze-Fracture Replicas

Freeze-fracture replicas of both fresh, and fixed and cryoprotected spores were prepared as described in Chapter 6.

7.2.6. Colchicine Treatment

Mature pollen grains from buds a day before anthesis were extruded onto a glass slide in a drop of 5×10^{-3}M aqueous colchicine solution, mounted with a cover glass and observed at hourly intervals up to 8h and then at 12, 24 and 36h with differential

interference contrast optics on a Zeiss Photomicroscope III. In between observations, the slide was maintained in a moist petri dish in darkness. Controls were run simultaneously in distilled water under identical conditions.

7.3. OBSERVATIONS

7.3.1. Early Spore

Ultrastructural aspects of early spore development in Tradescantia virginiana have been described in Chapter 6. Briefly, the meiotic cytokinesis is of the successive type. The spores are commonly arranged in isobilateral tetrads, indicating that the axes of the second set of meiotic spindles presumably were oriented parallel to each other. Tetrads are also met with in the same loculus with the second set of meiotic cell plates at right angles or 45^{o} to each other, indicating variations in the axes of meiotic spindles in such tetrads. The nuclei in the spores of a tetrad generally occupy a central position. Early free microspores may or may not show much vacuolation (Fig. 7.1). However, soon vacuoles develop at the poles (Fig. 7.2; in this investigation 'polar axis' refers to the axis of elongation), displacing the nucleus. In departure from previous observations no refractile granules were seen comparable to those described by Sax and Edmonds (1933). The young microspores do show several granules (Figs. 7.1,7.2) but

they are easily identifiable as starch grains in this species.

7.3.2. Premitotic Spores

Before pollen mitosis, an anther loculus shows two types of spores: 1. in which a large vacuole continues to occupy more than half the spore, with the nucleus at a polar location (Fig. 7.3); 2. the more common type, with two large vacuoles occupying the polar regions and the nucleus located in the middle, as in Fig. 7.4. The nucleus in the former type either lies on the polar axis, as in Fig. 7.3, or is appressed against the non-apertural wall, whereas in the latter type it occurs generally close to or appressed against the non-apertural wall (Fig. 7.4). The nucleus is never seen against the apertural wall. The non-apertural wall can be easily distinguished from the apertural wall, even at the light microscopic level, by the sparse distribution of the bacula at the apertural surface, compared with a more or less tectate exine at the non-apertural areas (Fig. 7.5). Earlier ultrastructural investigation (Chapter 6) has indicated that the extent and position of apertural and non-apertural areas is fixed and traceable to the surfaces in a tetrad even before their differentiation begins. In spores formed as two-by-two isobilateral tetrads with all four spores in one optical plane, the apertural wall always develops at the surfaces away from the cell plates, abutting the

peripheral callose wall. However, in the spores which arise from tetrads with cell plates at right angles or oblique to each other, the apertural area is smaller and develops mostly at lateral surfaces. The position of the apertural area in a free spore is a useful marker since it provides an indication of the geometrical arrangement of spores in the tetrad and hence information on the planes of meiotic division that might have occurred in the particular tetrad from which the spore is derived. On this basis, no correlation was found between the position of premitotic nucleus and the previous meiotic spindle axes, the above variations occurring in a single anther loculus.

By the time of commencement of pollen mitosis (Fig. 7.6), the spores have attained their full size. By this stage thee exine development is more or less complete, but the intine continues to develop until after pollen mitosis (Chapter 6). In spores where the nucleus is centrally located, the bulk of the cytoplasm also exists in the middle while in those with polar nuclei, the bulk of the cytoplasm also occupies the same pole. Reserve substances such as lipids and starch are sparse when compared with preceding stages of development (compare Fig. 7.1 with Figs. 7.3,7.4,7.6). As described in Chapter 6, numerous cortical microtubules were visualized, especially in freeze-substituted preparations, running perpendicular to the polar axis of the spores and co-oriented with the intine

wall microfibrils. Chapter 6 also emphasizes the superiority of the technique of freeze-substitution over conventional procedures for the preservation of cytoskeletal elements and in the present Chapter the attempt has been to lay emphasis on the details observed by way of freeze-substitution.

Spore nuclei corresponding with the onset of prophase show a condensation of chromatin material (Fig. 7.18). Special attention was paid to the question of whether a preprophase band of microtubules occurs, but none was found in conventional or freeze-substituted spores. However, in freeze-substituted preparations of spores at this stage microtubules were consistently visualized in the vicinity of, or associated with, the outer nuclear envelope (Figs. 7.18-7.20), presumably running parallel to the nuclear surface. Unfortunately, these observations could only be made in spores with the nucleus in the middle; the other types of spore, being fewer in a given anther, were not found without ice crystal damage. However, the nuclear envelope-associated microtubules showed two locations of predominant orientation although a degree of local variation was met. Microtubules associated with the lateral surfaces (in relation to the pollen axis) were fewer and showed a co-orientation with the cortical microtubules (Fig. 7.19); in other words, they run perpendicular to the polar axis of the microspores. However, those at the nuclear surfaces facing the spore

poles were more numerous and commonly ran along the polar axis (Fig. 7.20). Since the position of the generative cell is related to the position of the premitotic nucleus (Geitler, 1935), by extrapolation the orientation of these microtubules can also be described in relation to the axis of future mitotic spindle. Thus, the former population of microtubules run parallel, and the latter, perpendicular to the mitotic spindle. Some of these microtubules also showed an occasional microfilament associated with them. Nucleo-microtubular associations are transient and were not recorded in preceding or succeeding stages. They were also not seen in conventionally prepared spores of comparable stage. At this stage, the cortical microtubules remain unchanged, occurring along the entire length of the spore.

7.3.3. Pollen Mitosis

Irrespective of whether the nucleus is located at the pole or in the middle of the spore, the mitotic spindle is asymmetric i.e., shorter toward the mitotic pole where the generative cell is going to be formed (Figs. 7.21-7.23). A random analysis of thin sections at pollen mitosis revealed that most of the cell organelles become aligned at one pole of the spindle, the larger half, so that the future vegetative cell inherits almost all the plastids and a majority of other organelles. Figure 7.21 shows the aggregation of

organelles in one half of the spindle at late anaphase. Cortical microtubules could not be visualized in spores showing division figures. Cytokinesis takes place quickly, resulting in the formation of a cell plate, at first flat and soon curving. The cell plate grows in a centrifugal manner (Figs. 7.22,7.23) resulting in a hemispherical wall which separates the generative cell from the vegetative (Fig. 7.23). Fig. 7.24 shows this wall at higher magnification; note a few microtubules oriented perpendicular to the wall, presumably relics of the phragmoplast. The cell wall forms deltoid-shaped regions of attachment with the intine (Fig. 7.23).

7.3.4. Nascent Generative Cell

Most of the pollen grains show the generative cell existing in the middle of the spore and anchored to one side of the spore wall, invariably the non-apertural wall (Fig. 7.7). The shape being lenticular, the long axis of such generative cells coincides with that of the pollen. In spores presumed to have had polar premitotic nuclei, the generative cell was seen formed at a polar end of the spore (Figs. 7.25,7.33), but still at the non-apertural wall. The mid region of the partition wall in such cases is placed at approximately 45^{o} angle (Fig. 7.25), or perpendicular (Fig. 7.33) to the polar axis of the spore. The long axis of such generative cells was at 45^{o} angle, or perpendicular to that of the pollen.

By the time a generative cell wall is formed, cortical microtubules reappear along the entire spore plasma membrane and, as in premitotic spores, maintain a predominant orientation, transverse to the long axis of the spores (Figs. 7.26,7.27). The microtubules in the generative cells that are formed in the middle of the pollen grain show a predominant orientation, perpendicular to the long axis of the generative cell, which in this case coincides with the polar axis of the pollen. However, in the nascent polar generative cells, the cortical microtubules occur in two localized domains. Those close to the intine are predominantly co-oriented with the microtubules in the rest of the spore cell cortex i.e., in the vegetative cell (Fig. 7.26,7.27). In other words, the microtubules at the intinic surface, whether in the generative or in the vegetative cell, show a common orientation. This condition was consistently found, regardless of the orientation of the long axis, or the position of the generative cell at the pole or in a corner (at a pole). Fig. 7.26 shows a generative cell formed at 45^{o} angle to the polar axis with its own long axis at 45^{o} to that of the pollen, and yet the microtubules at the intinic surface show an orientation with regard to the polar axis of microspores and not the generative cell itself. The second domain of microtubular orientation is found at the newly formed partitioning wall that separates the generative cell from the vegetative cell. Here the MTs

are more variable in their orientation (Figs. 7.27,7.28). Most lie more or less parallel to this wall, perpendicular to the polar axis of the pollen grain, like those against the intine. A sub-population occurs perpendicular to the wall, perhaps being relics of the phragmoplast. At this stage, the microtubules also occur at the partition wall in the vegetative cell and with the same degree of variability (Figs. 7.27,7.28) as in the generative cell at this wall. The microtubules in the vegetative and generative cells at the edges of the new wall where it adjoins the intine, gently arch at the deltoid regions (Figs. 7.26,7.27) to become parallel to those associated with the intine.

Estimating the direction of previous meiotic spindles on the basis of the position of apertural areas failed to show a consistent relationship between the position of generative cell (and by inference the axis of the mitotic spindle) and the axis of meiotic spindles. For reasons mentioned before, such correlation can be clearly studied in pollen grains derived from isobilateral tetrads. Generative cells were formed at the middle, polar or corner positions in such spores as well as in spores derived from tetrads other than isobilateral.

7.3.5. Old Generative Cell

As is evident from the electron micrographs of the previous stages, freeze-substitution provides better

preservation of microtubules as well as general ultrastructure, when compared with conventional preparations. Freeze-substituted preparations continue to show more microtubules at this stage than in conventional preparations.

In older spores, the microtubules could not be visualized at the partition wall in the vegetative cell (Fig. 7.31). However, in the generative cells, the majority of the microtubules at the partition wall alter in orientation to become predominantly transverse to the long axis of the generative cell. Fig. 7.31 shows the microtubules at the partition wall of a polar generative cell. While this happens, the microtubules at the intinic surface maintain their orientation transverse to the polar axis of the pollen (Fig. 7.32). This change is only apparent in polar generative cells whose long axis does not match that of the spore as a whole (Fig. 7.31). Figure 7.31 also illustrates an image occasionally seen in cells that are freeze-substituted in the presence of osmium tetroxide. These cells show 'negative' staining of the membranes.

In most conventional preparations the generative cell outline appears wavy and the cell itself appears to be surrounded by two unit membranes (one being the plasma membrane of the vegetative cell and the other that of generative cell), enclosing an electron-lucent area (Fig. 7.29). Sometimes the preparations showed a wall of medium electron density between the two plasma

membranes. However, whether wall material is visible or not, the Thiéry reaction imparts electron density in this zone (Fig. 7.30), just as in the intine, indicating the presence of polysaccharides. The wall also shows a yellow, aniline blue-induced fluorescence, characteristic of callose. The fluorescence initially develops along the cell plate region (Fig. 7.11), but gradually as the generative cell undergoes detachment from the spore wall, the fluorescence spreads on all sides of the cell so as to completely surround the generative cell (Figs. 7.13,7.14). Callosic fluorescence disappears once the cell has become detached from the spore wall although the Thiery-positive material is retained. Calcofluor-induced fluorescence closely followed the pattern of callose (Fig. 7.12) and also disappeared after the detachment of the cell. Fig. 7.12 also shows calcofluor-induced fluorescence in the intine, where this fluorescence persisted throughout the course of development.

Unlike most conventional preparations, freeze-substituted generative cells show a smooth outline and the presence of a homogeneous non-fibrillar wall with medium electron density between the two membranes that surround these cells (Figs. 7.27,7.28). This feature of the wall remains unchanged throughout the course of its development (Figs. 7.43,7.45). In freeze-fracture replicas where the generative cell was cross-fractured no fibrillar component was visualized in the space

between the two membranes around the generative cell. Cytoplasmic continuities resembling plasmodesmata traverse the wall between the two cells (Fig. 7.31).

In conventional preparations the generative cell throughout the course of its development showed a much denser cytoplasm when compared with the vegetative cell (Figs. 7.29,7.35,7.36,7.38,7.40,7.46). However, such distinction was not found in freeze-substituted spores (Figs. 7.27,7.31,7.41-7.45). There is an abundance of ribosomes and a few well-differentiated, albeit smaller (when compared with those in the vegetative cell) mitochondria, and dictyosomes. There is a tendency to exclude plastids from this cell. In all the preparations examined, only one profile of a plastid was seen (Fig. 7.29). Thick sections (1 μm) of ZnIO-impregnated spores at this stage show that the endoplasmic reticulum in the generative cell is sparse (Fig. 7.33). Ultra-thin sections of ZnIO-impregnated spores revealed the occasional continuity between the ER systems of the generative and vegetative cells (Fig. 7.34), presumably through the plasmodesmata-like channels. However, the distension of the particular wall region that consistently occurs when the ZnIO technique is used precludes accurate assessment of the morphology of these channels. Presumably the image in Fig. 7.31 (freeze-substitution) is more faithful than that in Fig. 7.34.

7.3.6. Generative Cell Detachment

Subsequently, the polar vacuole(s) of the pollen begin to disappear (compare Fig. 7.7 with Figs. 7.8 and 7.9), the generative cell becomes detached from the pollen wall so that it now occupies a relatively deeper location in the vegetative cell (Fig. 7.8), and undergoes elongation (Fig. 7.9) and curvature so as to surround the vegetative cell nucleus almost completely at the time of anther dehiscence (Fig. 7.10). At the ultrastructural level, the generative cell detachment process was studied only in conventionally-fixed pollen. It was noticed in such preparations that with further development the outline of the generative cell gradually became more sinuate (Figs. 7.35,7.36,7.38,7.47). A comparison of detached generative cells processed by way of chemical fixation and freeze-substitution reveals that the irregular outline of the cell is an artifactual image. During its detachment from the spore wall a constriction develops at the lateral surfaces of the generative cell, close to the intine (Fig. 7.35). Gradual closing of the constriction area (Figs. 7.36,7.37) results in the separation of this cell from the intine. Microtubules were sometimes seen at the edges of the constriction zone. An accompanying migration of the vegetative cell cytoplasm in the areas formed due to the gradual narrowing of the constriction zone eventually displaces the detached generative cell from a peripheral to a deeper location in the vegetative

cell. Small remnants of the lateral walls of the generative cell persist at the intine after the generative cell has become detached. These serve as markers for determining the original position of the generative cell after the cell has become detached. No evidence was found for the active migration of the generative cell to the deeper parts of the vegetative cell cytoplasm. This was evident from the observation that after their detachment, various generative cells (whether from the middle or polar location) occupied a position in the vegetative cell that appeared more or less equidistant from the wall remnants at the intine.

7.3.7. Detached Generative Cell

Often during the detachment process the generative cell undergoes a change in shape so as to acquire a round (Fig. 7.38) or ellipsoidal (Fig. 7.40) outline by the time of its complete detachment. In conventional preparations the surface of the detached generative cell continues to appear sinuate, but this does not occur in freeze-substituted preparations.

After complete detachment, the cortical microtubules, still predominantly occur singly (Fig. 7.39), retaining their previous orientation in the round cells. Fig. 7.39 shows an oblique section through a round generative cell with microtubules running in oblique profiles in the surface protrusions. No microfilaments were recorded in the vegetative cell

cytoplasm at the generative cell wall, although sometimes occasional microtubules could be seen in freeze-substituted spores. The ER continuities and plasmodesmata-like channels between the generative and vegetative cells could no longer be visualized. However, the plasmodesmata-like channels continued to be visible in freeze-substituted preparations (Fig.7.45).

Generative cell elongation commences soon after detachment (Fig. 7.40-7.42); in fact the oval shape seen in many generative cells during later stages of cell detachment, could be considered as a mark of the early stages of cell elongation. In freeze-substituted oval generative cells, the microtubule population appeared to increase, as evident from a comparison between freeze-substituted generative cells at this stage, and the cell before its detachment (compare Fig. 7.31 with Figs. 7.39,7.44). Also, microtubule orientation changes, becoming parallel to the developing long axis of the generative cell itself (Fig. 7.44). In freeze-substituted preparations of polar generative cells, a pointed end was seen to develop facing the opposite pole of the pollen (Fig. 7.42). The microtubules occupy axial orientations in this region (Figs. 7.43,7.45). Such pointed regions were difficult to discern in conventionally prepared polar generative cells because of their irregular outline. Also such regions were not seen in generative cells that were formed in the middle

of the pollen grain (Fig. 7.41), indicating perhaps that whereas the polar generative cells elongate unilaterally toward the other pole of the pollen axis, the middle generative cells elongate more uniformly.

7.3.8. Elongated Generative Cell

Eventually, close to the time of anthesis, almost all the generative cells have undergone elongation to such an extent that the cells run along the entire length of the pollen (Figs. 7.9,7.46). So far, it has not been possible to freeze-substitute the mature elongate generative cells of the kind shown in Fig. 7.9. However, conventional preparations showed that the wall at this stage has become even more sinuous than in previous stages, with numerous regularly spaced folds (Fig. 7.47-7.49). The space between the two membranes around the generative cell often showed some vesicular inclusions (Fig. 7.48), probably representing poorly-preserved plasmodesmata-like channels. The freeze-fracture replicas (Figs. 7.50,7.51) of mature generative cells were consistent with the presence of plasmodesmata-like channels traversing the generative cell wall. In conventional preparations the continuity of ER between generative and vegetative cells could not be seen (Figs. 7.48,7.49). By this stage the microtubules have become organized into several bundles each consisting of 20-40 microtubules (Figs. 7.48,7.49), lying in the cortical regions between the surface

infoldings (Figs. 7.48,7.49). The microtubules continue to run in the peripheral cytoplasm along the long axis of the generative cell. Single microtubules seen in earlier stages in the cortical cytoplasm cease to exist by this time.

7.3.9. Colchicine Treatment

Colchicine treatments were employed to evaluate the role of axial microtubules seen in the mature, elongated generative cell. Mature pollen grains from dehisced anthers showed generative cells forming curved profiles around the vegetative nucleus. However, these pollen were unsuitable for treatment, since most of them germinated within 2-3 minutes of hydration. Pollen grains from buds at a day before anthesis also showed apparently mature, cylindrical and elongate generative cell, running almost the entire length of the pollen grains. These pollen grains did not germinate on hydration, and therefore could be used for experimental purposes. Such pollen grains were subjected to colchicine treatment. Fig. 7.9 is representative of the stage of the generative cell at the time of commencement of the treatment. 12h of treatment did not bring about any perceptible change in the shape or size of the generative cells. However, in spores subjected to 24h of treatment, the generative cells had lost their thin, cylindrical and elongate shape. They became much smaller in size with a clearly visible compact nucleus

(Figs. 7.15-7.17). In most pollen, they were seen lying in the vicinity of the vegetative nucleus (Figs.7.15,7.16), but in some pollen grains they also lost their position and were seen close to, or at the poles (Fig. 7.17). Unlike the drug-treated pollen, those from the control preparations continued to show the same morphology as seen in Fig. 7.9.

7.4. DISCUSSION

It is again evident that the technique of freeze-substitution offers superior preservation of cellular ultrastructure as compared to the conventional procedures. In the present investigation this is demonstrated with regard to the preservation of cortical microtubules as well as the transient nuclear envelope associated microtubules, the microfilaments occasionally seen in association with the microtubules, the cell wall, and the plasmodesmata-like connections. The superiority of this technique has earlier been emphasized in Howard and Aist (1979), Tiwari *et al.* (1984), McKerracher and Heath (1985), Lancelle *et al.* (1985) and in Chapter 6.

Attempts have been made in the past to determine if the position of the generative cell was predetermined in any way. Goebel (1933) erroneously reported that the position of the generative cell in gymnosperm pollen was fixed at the dorsal side and that in angiosperms, it was on the ventral side. Challenging this, Geitler (1935)

has cited cases of different angiospermic species with varying positions of generative cells. Among cytologists (Sax and Edmonds, 1933; Geitler, 1935; Sax and Husted, 1936; Brumfield, 1941; Maheshwari, 1949; Steffen, 1963) there has been a consensus that the position of the premitotic nucleus and the generative cell was constant for a given species and sometimes even for a genus. It is also held that the position and size of the generative cell is largely correlated with the position, axis and asymmetry of the mitotic spindle, notwithstanding few exceptions (see Maheshwari, 1949; Steffen, 1963). Sax and Edmonds (1933), and Sax and Husted (1936) working with Tradescantia (isobilateral tetrads and successive mode of meiotic cytokinesis) reported that the premitotic nucleus always adhered to the non-apertural wall in the middle of the spore axis and that the axis of the mitotic spindle developed at an angle of 45^{o} to the previous meiotic division. This view has, however, been contested by Geitler (1935) who believes that although the positions of the premitotic nucleus and generative cell are fixed for a given species, there is no correlation between the axes of the mitotic spindle and the previous meiotic spindle.

During the course of the present investigation several noteworthy observations were recorded which are related to the above points. In departure from Sax and Edmonds (1933), Geitler (1935) and Sax and Husted (1936), in T. virginiana the position of the premitotic

nucleus is not a constant one, for spores with polar or middle nuclei can be seen within the same loculus. These variations are encountered irrespective of whether the spore cells were produced in isobilateral tetrads or in those with cell plates at right angles or 45° to each other. The position of the generative cell, again at variance with Geitler (1935), is also variable in the sense that it can occur in a lateral, polar or corner position within the spores of a given loculus. However, its position appears to be correlated with that of the premitotic nucleus. Also, there is a definite relationship between the non-apertural wall and the generative cell; the generative cell was never seen at the apertural wall. In the spores that are formed in isobilateral tetrads, the generative cell does occur generally at a 45° angle to the previous meiotic divisions, but exceptions are found as spores originating in these tetrads can also have polar generative cells. In spores emanating from tetrads with cell plates oblique to or at right angles to each other the variations in the position of generative cell are more common, and all three locations can be found. The contention of Sax and Husted (1935) that external or internal environmental conditions could influence spatial relationships between the second set of meiotic spindles and the mitotic spindle does not seem to hold for the present species since variations occurred within the same loculus.

In most cases the nucleus is central at the tetrad stage and in premitotic spores, but its position prior to mitosis does not appear constant. The spores which are formed as isobilateral tetrads, where there are clear markers in the form of apertural and non-apertural wall directly traceable to the surfaces in the tetrads, can show the premitotic nucleus either in the middle or at a polar location in the cell. As also noted in some other species (Steffen, 1963; Mepham and Lane, 1970; Heslop-Harrison, 1972), development of vacuole(s) correlates with the change in nuclear position.

At the premitotic stage, microtubules were only found in the cortical regions of the cell, characteristic of cells at interphase (see Gunning and Hardham, 1982). Gradually, at the onset of prophase, they also appeared associated with the nuclear envelope. Similar microtubules have been previously described only in one species, Dactylorchis (Burgess, 1970a). They were not seen in other investigations (Angold, 1968; Heslop-Harrison, 1968d; Sanger and Jackson, 1971a) perhaps, as my experience suggests, because they were not preserved by the conventional procedures employed. In Dactylorchis, although no concentrated band of microtubules occurs, the microtubules were found for only about 5 um on either side of the nucleus, leading Burgess to compare them with a preprophase band. No concentrated band of microtubules was found in

T. virginiana. Rather, cortical microtubules occurred along the entire length of the pollen wall, as at interphase microspore stage, leading to the interpretation that they are not comparable to a preprophase band. Moreover, unlike the normal preprophase band, it is hard to correlate the directionality of nuclear envelope associated microtubules with the plane or angle of the future mitotic spindle, although in thin sections more microtubules were visualized running perpendicular to that axis. It may be that these microtubules are responsible for the finer adjustment of nuclear position prior to mitosis. They may also represent early stages of spindle formation, as in root tip cells (Wick and Duniec, 1983). Earlier reports on nuclear envelope associated microtubules (see Mineyuki and Furuya, 1985; McKerracher and Heath, 1985) have indicated the role of microtubules in the positioning and migration of the nucleus.

The mitotic spindle is asymmetric, as described earlier by Sax and Edmonds (1933), and the generative cell is formed at the non-apertural wall as a small lenticular cell. As is common in cells undergoing division (see Gunning and Hardham, 1982), cortical microtubules could not be seen in spores showing division figures. However, they reappeared after the completion of division. Microtubules in the generative cell at the surface adjacent to the intine showed a co-

orientation with the wall microfibrils and those of the vegetative cell. The co-orientation of the cortical microtubules parallel to the intine wall microfibrils, whether in generative or vegetative cell, is remarkably fixed and transcends the structural polarity of the generative cell itself. In commonly seen middle generative cells it is only incidental that these microtubules also run perpendicular to the long axis of the generative cell. This is illustrated by observations of the polar generative cells. These generative cells have their long axis perpendicular or at a 45^{o} angle to that of the spore, but microtubules at the intinic surfaces invariably run in the same direction as in the middle generative cells formed commonly. The co-orientation of these microtubules argues against the idea of the complete isolation of the generative cell from the latter (c.f. Heslop-Harrison, 1968d; Gorska-Brylass, 1970). Whatever influence governs the orientation of these microtubule arrays evidently pervades both cells. Indeed, the partitioning wall between the two cells is perforated by plasmodesmata-like channels, further strengthening the case that they can communicate (see later). Although predominantly co-oriented with cortical microtubules of the pollen wall, the microtubules at the partition wall of the generative cell initially show variable orientations, possibly correlated with the absence of cellulose microfibrils in this wall.

Gradually, when the generative cell has detached from the pollen wall, it comes to occupy a relatively deeper location in the vegetative cell cytoplasm. No evidence was found to suggest that the cell was motile. The words 'migration' or 'movement' used in this context (see Steffen, 1963; Oryol, 1969) are not apt. The change in generative cell position could at best be described as passive shift in position.

During its detachment, the cell shape changes from lenticular, first to round or ellipsoidal, and later to elongate. During its elongation, microtubules were found to run axially along the developing long axis of the cell. The microtubules may be a cytoplasmic determinant of the elongate shape. They can be seen in such orientations both in young elongating cells and in mature elongated cells. Detached polar generative cells show a pointed end formed at their surfaces which face the opposite pole of the pollen axis, with microtubules occurring in axial orientations in such regions, much as in the apices of the tip growing cells of fungi and pollen tubes. Such tips were not seen in generative cells that arose in the middle region, suggesting that in such cells, the cell elongation occurs uniformly.

In a mature elongated generative cell the axial microtubules have a shape maintenance role as evidenced by results of colchicine treatments. Earlier colchicine treatments of generative cells in Haemanthus by Sanger and Jackson (1970b) also suggested a shape maintenance

role for the axial microtubules. Although all mature generative cells are more or less central in the pollen, some generative cells were found to occupy a polar location in drug treated pollen grains. Ultrastructural investigations of drug-treated cells were not performed, but in the light of observations of unilaterally, tip growing, generative cells, it seems possible that the removal of microtubules may induce former polar generative cells to return to their original polar location.

Cresti et al. (1984) considered that the appearance and numerical augmentation of microtubules represented a sign that the generative cell was ready to undergo mitosis and, after pollen germination, to bring about 'the requisite polarity correlated with mobility' of the generative cell in the pollen tube. In T. virginiana microtubular augmentation is first detected during cell elongation and certainly much before the generative cell is ready to undergo division (which, incidently, takes place only in the pollen tube in this species), let alone pollen germination. Hence the above contention does not seem to hold for this species.

Although the generative cell is generally regarded as a cell, the presence of a wall around it has remained a contentious issue. A wall has been reported in Oenothera (Diers, 1963), Tradescantia paludosa (Maruyama et al., 1965), Dactylorchis (Heslop-Harrison,

1968d), Corylus, Loriodendron, Plantago, Lupinus, Coffea, Orchis, Allium gaditanum (Lombardo and Gerola, 1968), Endymion non-scriptus (Angold, 1968), Haemanthus (Sanger and Jackson, 1971a), Monotropa (Lutz and Sjolund, 1973), Gastilleria (Jensen et al., 1974), Allium cepa (Rodriguez-Garcia and Risueno, 1978), Tillandsia (Brighigna et al., 1981) Gibasis, Tradescantia blossfoldiana (Owens and Westmuckett, 1983) and Lilium longiflorum (Nakamura and Miki-Hiroshige, 1985). Electron micrographs of Clauhs and Grun (1977) on generative cells in Solanum also show a wall although the authors do not comment on this. On the other hand, the generative cells of following species are reportedly covered by two unit membranes, either appressed together or with an intervenning electron-lucent space: Orchis (Chardard, 1958), Lilium (Bopp-Hassenkamp, 1960), Quercus, Aquilegia, Ranunculus, Macranthus, Prosopis, Tradescantia paludosa, Parkinsonia, Hippeastrum, Ambrosis (Larson, 1963), Petunia (Croh, 1967), Delphynium, Campanula, Chrysanthemum, Euphorbia, Pelargonium (Lombardo and Gerola, 1968; Dunbar, 1973), Scilla (Gimènèz-Martin et al., 1969), Endymion non-scriptus (Burgess, 1970a), Saintpaulia (Ledbetter and Porter, 1970), Tradescantia bracteata (Mepham and Lane, 1970), Castilleia wightii (Jensen et al., 1974), Impatiens (Van Went, 1974), and Hordeum (Cass and Karas, 1975). In species such as Gossipium (Jensen et al., 1968), Trollius, Clematis (Roland, 1971), Petunia,

Nicotiana and Prunus (Cresti et al., 1984), the electron-lucent area between the two membranes has been shown to react positively in cytochemical tests for polysaccharides.

In some species, the presence of a wall is assumed although the furnished electron micrographs do not substantiate this assumption. A critical survey of the electron micrographs in Petunia (Sassen, 1964) Parnassia, Galium (Lombardo and Gerola, 1968), Endymion (Angold, 1968), Beta (Hoefert, 1969), Linum (Vazart, 1969), Epidendrum (Cocucci and Jensen, 1969), Haleocharis (Carniel, 1972) and Orthocarpus (Jensen et al., 1974) gives the impression that the authors have regarded the presence of a wide electron-lucent space as the indication of a wall.

In contrast with more recent reports, most of the earlier investigations on the generative cell wall were performed on permanganate-fixed tissue. It might appear that the fixative was not adequate for wall preservation, especially since the generative cell wall has been shown to contain callose (Gorska-Brylass, 1967, 1970; Heslop-Harrison, 1968d; Oryol, 1969; and present investigation) and pectins (Maruyama et al., 1965; Roland, 1971). Cellulose microfibrils, which do become stained with $KMnO_4$ (Deshpande, 1976), have not yet been demonstrated in this wall although some authors have considered the possibility of their existence (for example, see Roland, 1971). Inadequacy of permanganate

as a fixative certainly seems to be the case in Lilium, where Bopp-Hassenkamp (1960) reported the absence of a wall, while a recent investigation by Nakamura and Miki-Hiroshige (1985), employing a glutaraldehyde-osmium combination, demonstrated the presence of a wall. Larson (1963), using permanganate fixation, reported the absence of a wall in Tradescantia paludosa whereas Maruyama et al. (1965), also using permanganate fixation, reached the opposite conclusion for the same species. Contradictory results within the same species are also found in Orchis (see Chardard, 1958 and compare with Lombardo and Gerola, 1968, both investigations employed permanganate fixation). Investigations employing glutaraldehyde fixation have even been contradictory for the same species. For example, in Endymion non-scriptus Angold (1968) recorded the presence of a wall whereas Burgess (1970a) considered the wall to be absent.

Clearly, the idea that in some species a wall may exist, while in others the generative cell is only enveloped by two membranes (see Lombardo and Gerola, 1968; Owens and Westmuckett, 1983) is likely to be erroneous, merely reflecting poor preservation by conventional procedures for electron microscopy. In the present species, the wall material between the two membranes around the generative cell was present in very few conventional preparations. Most of the conventional preparations showed an irregularly distended, sinuous or

contorted, electron-lucent, vesicle-containing space between the two membranes. In freeze-substituted preparations, however, amorphous wall material of medium electron density was invariably present between the two smooth, apposed plasma membranes.

Gorska-Brylass (1970), based on her fluorescence microscope studies, proposed that the walled or wall-less conditions should not be considered as alternatives in different species, but as different developmental stages of the same cell. She concluded that the walled nature of the generative cell is a transient stage, occurring coincidently with the presence of callosic fluorescence. Since in all the species investigated so far, including the present species, the callose occurs only in the initial stages of generative cell formation, Gorska-Brylass argued that authors reporting the presence of a wall must be studying the callosic phase, whereas those reporting absence of a wall must be investigating later stages of generative cell development. In Hordeum (Cass and Karas, 1975) it is claimed that the converse sequence pertains: the walled stage follows a 'naked' stage. In I. virginiana, the callosic fluorescence was recorded in the generative cell wall until the time of its detachment from the pollen wall and yet, at electron microscopic level, the wall was not always present in conventionally prepared pollen at these stages. However, the technique of freeze-substitution revealed the wall consistently, before and after detachment.

Maruyama et al. (1965) considered the generative cell wall to be pectinaceous. Subsequent studies of Gorska-Brylass (1967,1970) and Heslop-Harrison (1968d) demonstrated that, at least initially, the wall has high amounts of callose. Although the presence of cellulose microfibrils has not yet been proved, Roland (1971) believed that some microfibrils do exist in this wall. In T. virginiana the freeze-substituted wall appears homogenous, even though the technique is capable of preserving wall microfibrils, as can be clearly seen by comparing the intine of pollen processed by way of conventional and freeze-substitution methods (Chapter 6). Furthermore, fluorescence induced by aniline blue, which preferentially stains β-1,3 glucans, confirmed the presence of callose in the wall. Similar transient aniline blue reactivity is also seen in young cell plates in other plant materials (for references see Gunning, 1982). However, calcofluor, which binds to β-1,3 and β-1,4 glucans (Maeda and Ishida, 1976; Takeuchi and Komamine, 1978), may stain callose and other wall components. The calcofluor induced fluorescence in the cell wall appeared at the same time as the callose and disappeared along with it, but the Thiery reaction continued to stain the wall in later stages of its development. It thus seems that the wall is composed of labile non-microfibrillar matrix substances with a high amount of callose initially. It is not known which cell, the generative or the

vegetative, produces the wall material. The cytoplasm of both cells contains dictyosomes and associated vesicles.

Heslop-Harrison (1968d) and Gorska-Brylass (1970) regarded the presence of a callosic wall around the generative cell as an insulation mechanism essential for the cell to be able to embark on an independent course of differentiation. Such a scheme precludes the existence of plasmodesmata or any other form of intercellular connections throughout the course of generative cell differentiation. However, subsequent observations have demonstrated the presence of intercellular connection in species such as Endymion (Burgess, 1970a) and Lilium (Nakamura and Miki-Hiroshige, 1985). Freeze-substitution and ZnIO techniques both reveal plasmodesmata-like connections in I. virginiana. It is noteworthy that in conventionally-prepared spores which did not show the wall material, the connections could only sometimes be identified and the space between the two membranes frequently showed membranous or vesicular inclusions, especially in the later stages. These inclusions are most likely the ill-preserved connections. After its detachment from the pollen wall, when the callosic fluorescence ceases to exist, the generative cell comes to occupy a deeper location in the vegetative cell cytoplasm and undergoes elongation. Despite its shift in position and subsequent free suspension in the vegetative cell,

freeze-substituted preparations as well as freeze-fracture replicas continued to show plasmodesmata-like channels.

As well as highlighting deficiencies in the preservation of details of ultrastructure of the generative cell surface by conventional means, freeze-substitution gives a different picture of overall morphology. Infoldings seen between microtubule bundles in conventional preparations are absent in frozen cells (both in freeze-substituted preparations or in freeze-fracture replicas of unfixed cells). This contrast suggests that the microtubule bundles withstand cell surface deformation that occurs during fixation and/or dehydration, thereby giving rise to the distribution of corrugations at the cell surface. Preliminary experiments on colchicine treatments also indicate that the microtubule cytoskeleton, rather than the cell wall, determines the shape of the generative cell. Drug treatment causes the cell to round up, reversing the shape change undergone during its development, when longitudinally-oriented microtubules appeared, first as a general array and later as discrete bundles. This is a case in which microtubules lie parallel to the direction of cell elongation, the explanation being that they evidently determine cell shape directly, rather than indirectly via regulation of the orientation of cell wall microfibrils. Whatever its biochemical nature, the non-microfibrillar wall around the

generative cell is readily deformable, indeed this may be a necessary property in relation to the future migration of the cell down the pollen tube after germination.

Fig. 7.1. A young free microspore showing a large nucleus (n) in the middle and few starch grains (arrowheads) at the two poles. x 1000.

Fig. 7.2. A young free microspore. The nucleus (n) remains in the middle and vacuoles (v) have begun to develop at the two poles. Few starch grains (arrowheads) can also be seen. x 950.

Fig. 7.3. A mature microspore with the nucleus (n) at one pole and a large vacuole (v) at another. x 680.

Fig. 7.4. A mature microspore with nucleus (n) in the middle adpressed against the non-apertural wall. Two large vacuoles (v) can be seen at the poles. x 720.

Fig. 7.5. Distinct apertural (a) and non-apertural (na) surfaces can be clearly distinguished in mature microspores. x 650.

Fig. 7.6. A mature microspore at mitotic prophase (n, nucleus; v, vacuoles). x 760.

Fig. 7.7. A bicelled pollen grain. The generative cell (g) is formed at the non-apertural wall as a lenticular cell (vn, vegetative cell nucleus). x 740.

Fig. 7.8. A bicelled pollen grain. The generative cell (g) has become detached from the pollen wall and lies within the vegetative cell (vn, vegetative cell nucleus). x 730.

Fig. 7.9. A bicelled pollen grain containing an elongated generative cell (arrows). The vegetative nucleus can not be seen in this plane of focus. x 680.

Fig. 7.10. A ripe dehisced bicelled pollen grain with generative cell (arrows) forming a curved profile around the vegetative cell nucleus (arrowhead). x 670.

Fig. 7.11. Aniline blue-induced callosic fluorescence is initially confined to the hemispherical partition wall between the generative (g) and vegetative cell. x 670.

Fig. 7.12. Calcofluor-induced fluorescence is visible in the partition wall as well as the intine (arrows; g, generative cell). x 680.

Figs. 7.13 and 7.14. Two different views of generative cell (g) showing that the callosic fluorescence gradually spreads to all surfaces of the generative cell and surrounds it completely. Both x 620.

Figs. 7.15 and 7.16. Two different planes of focus of a pollen grain that was treated with colchicine for 24h. Note the reduction in the size of the generative cell(g), which occupies a position close to the vegetative cell nucleus (vn). x 1400.

Fig. 7.17. A colchicine treated pollen grain with the generative cell (g) occupying a polar position (vn, vegetative cell nucleus). x 1220.

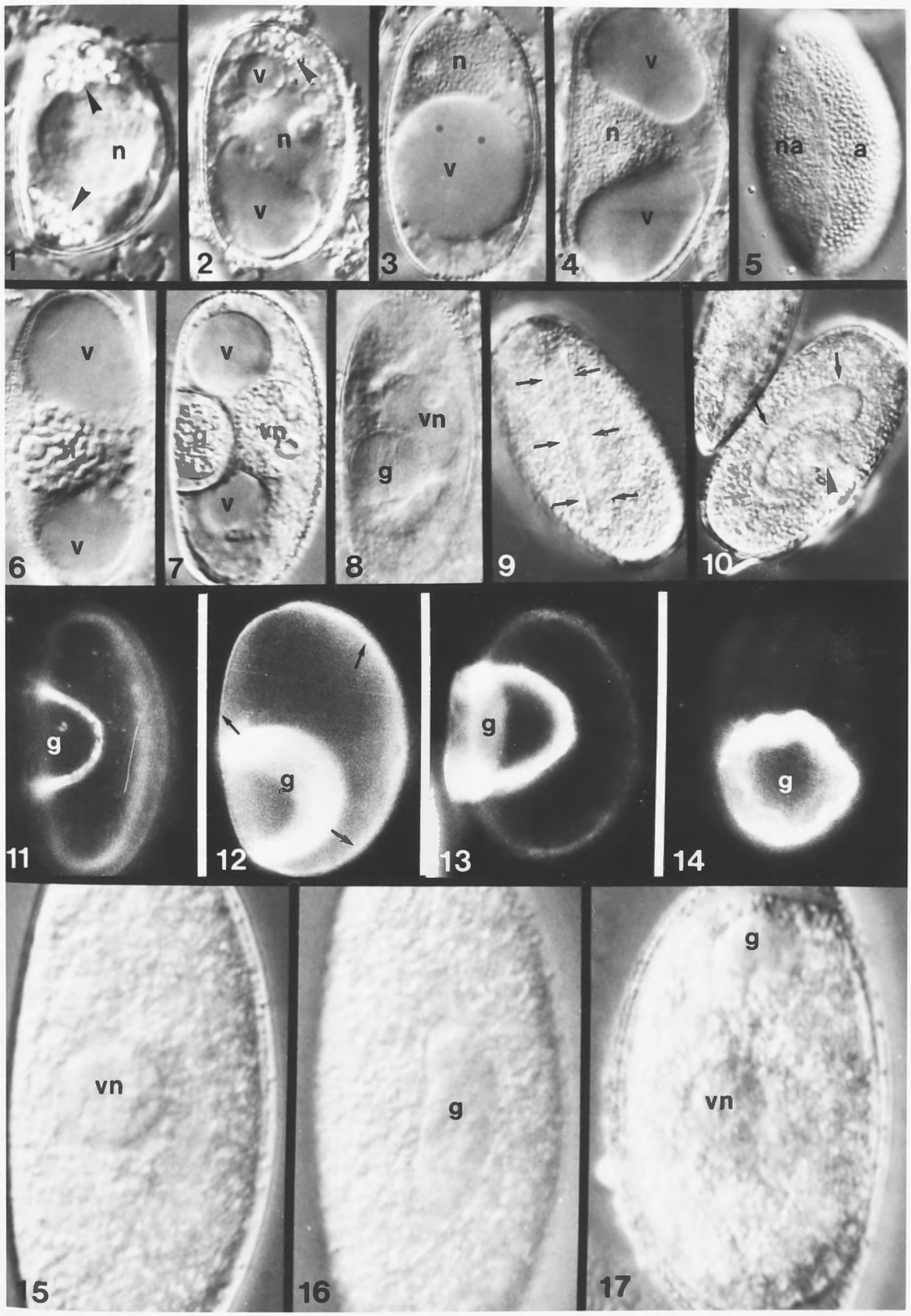
1
n
2
v
n
v
3
n
v
4
v
n
v
5
na
a
6
v
v
7
v
vn
v
8
vn
g
9
10
11
g
12
g
13
g
14
g
15
vn
16
g
17
g
vn

Figs. 7.18-7.20. Nuclear envelope associated microtubules in a spore at the onset of prophase, as seen in a freeze-substituted microspore. Fig. 7.19 shows the microtubules associated with the lateral surface (perpendicular to the pollen axis) of nucleus (n) and Fig. 7.20 shows the microtubules at the nuclear surfaces along the pollen axis. Arrowheads show the microfilaments that are seen in association with the microtubules. x 12,900; 43,100; and 32,380, respectively.

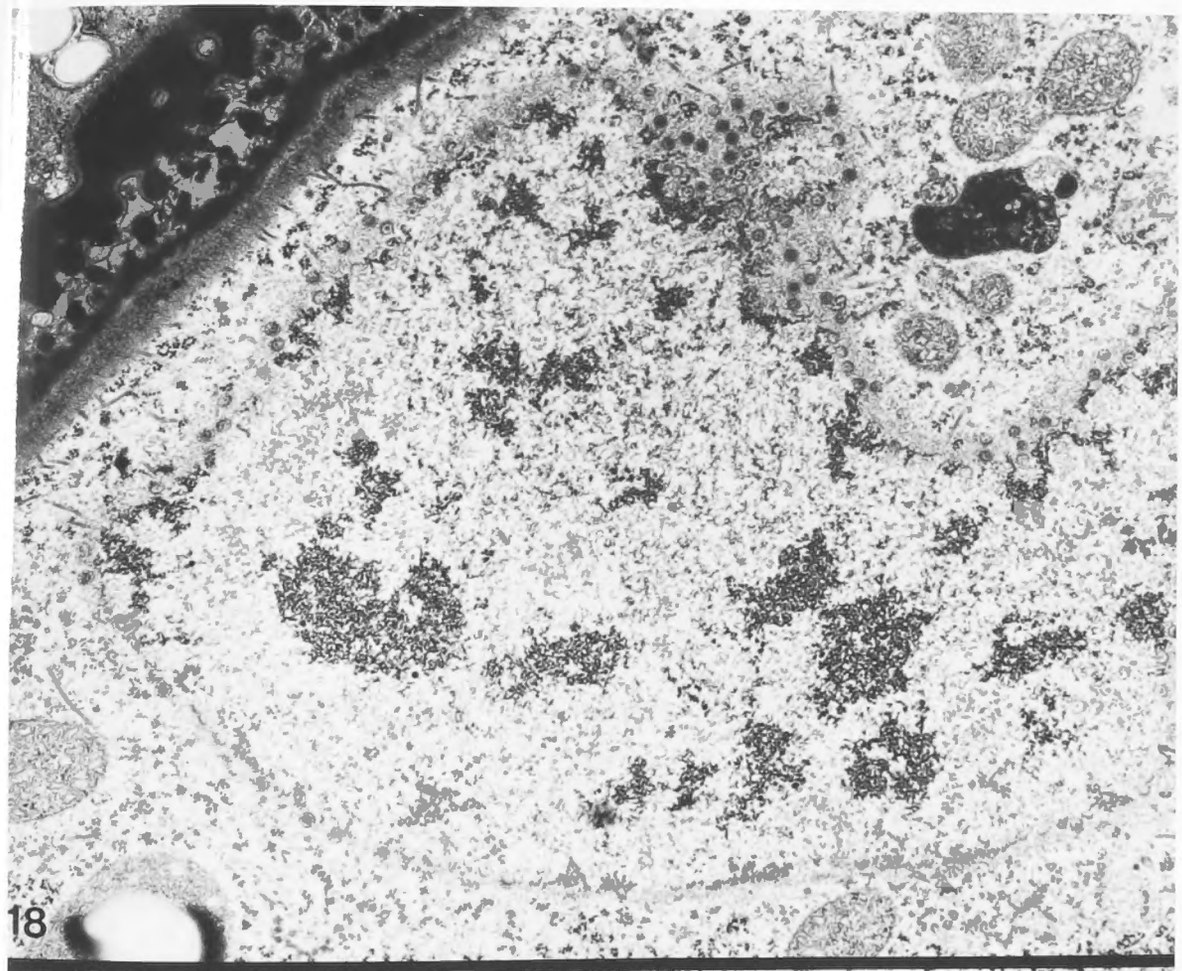

18

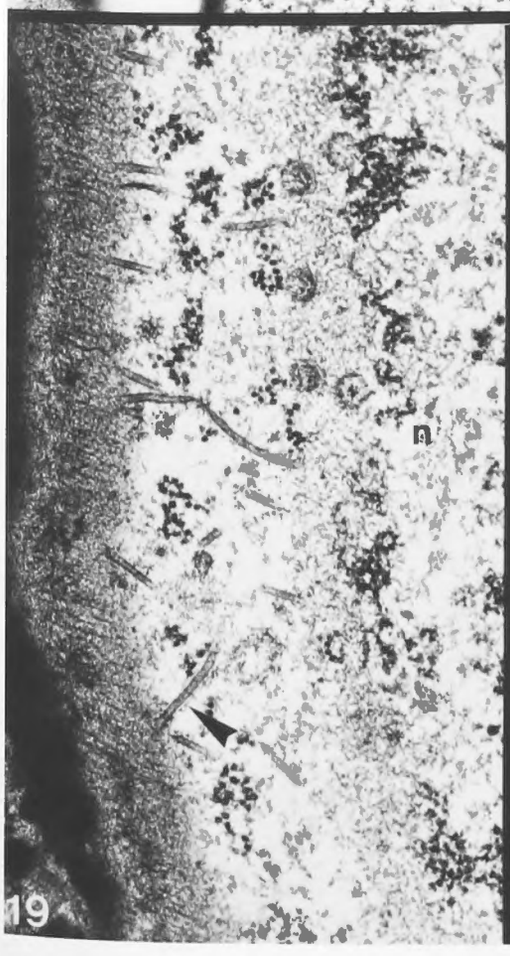

19

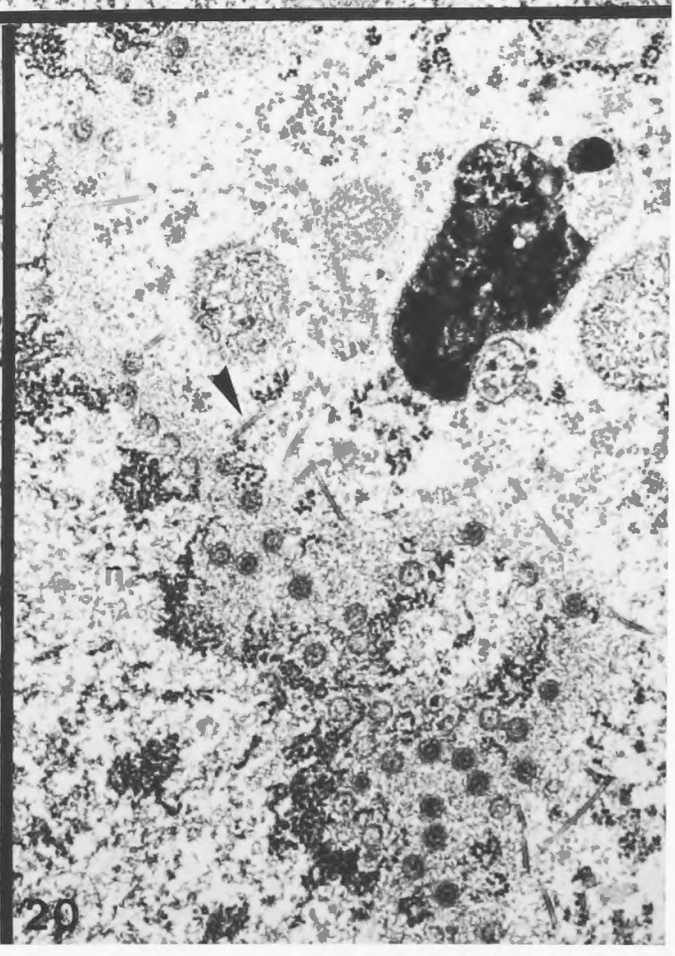

20

Fig. 7.21. Longisection of a microspore showing division figure. Most of the cell organelles are aggregated at the pole corresponding with the future vegetative cell. Arrows show the membranes and double headed arrow indicates the direction of polar axis. Conventional preparation. x 4,800.

Fig. 7.22. Early cytokinesis. The generative cell (lower half) develops at the non-apertural wall. Double headed arrow show the direction of polar axis (gn, generative cell nucleus; vn, vegetative cell nucleus). Conventional preparation. x 7,720.

Fig. 7.23. An early generative cell formed in the middle of a pollen grain (gn, generative cell nucleus; vn, vegetative cell nucleus; double headed arrow, polar axis). Conventional preparation. x 6430.

Fig. 7.24. A high magnification view of the newly-formed partition wall between generative (g) and vegetative (v) cells showing few microtubules (arrowheads). Conventional preparation. x 30,000.

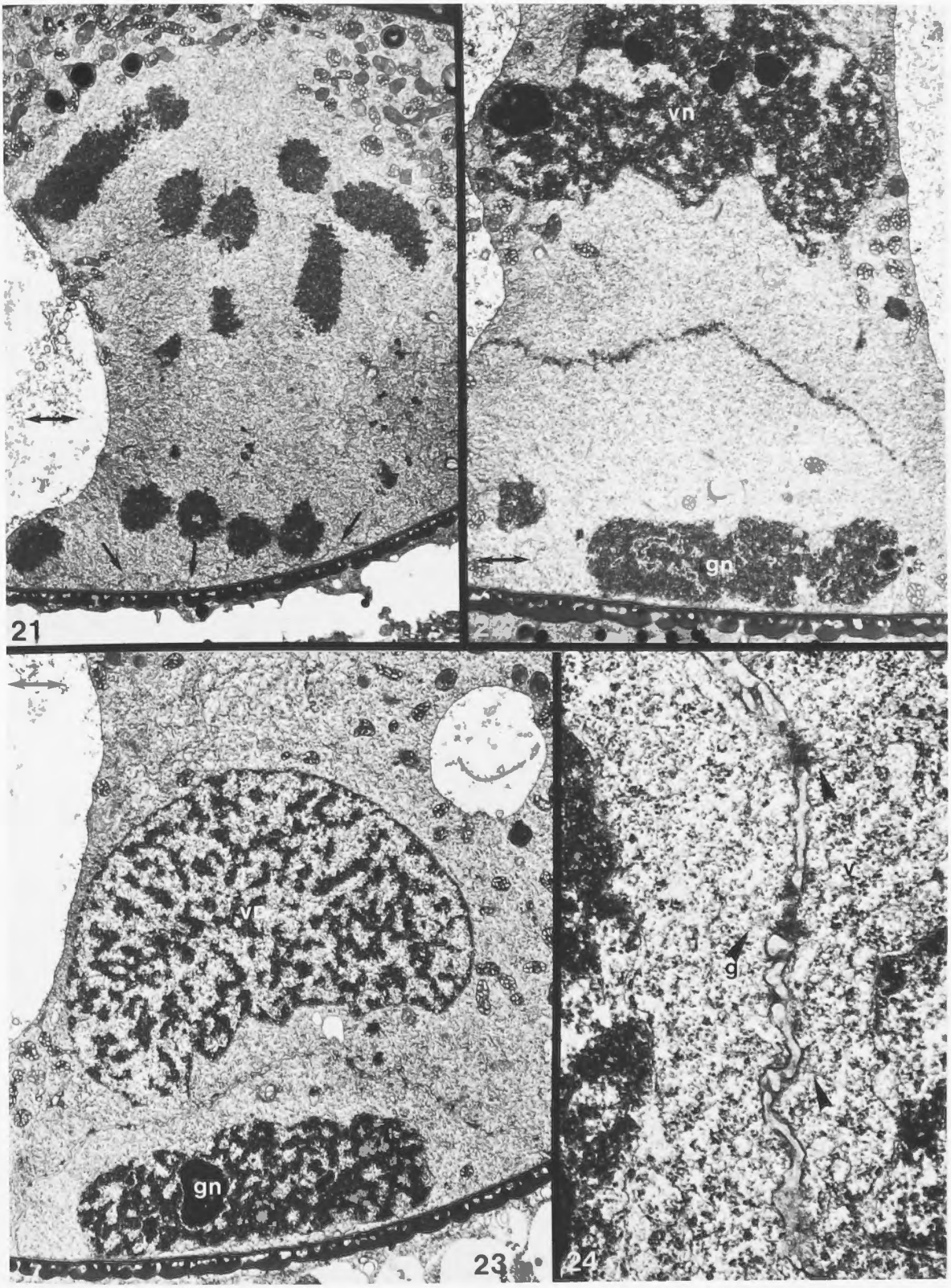
21
vn
gn
vr
gn
23
v
g
24

Fig. 7.25. Longisection of a freeze-substituted pollen grain showing the generative cell (g) formed in a corner at one pole of the pollen grain. Double headed arrows show the long axes (na, non-apertural region; v, vegetative cell). x 3,380.

Fig. 7.26. Higher magnification view of the generative cell from the microspore of Fig. 7.25. Note the wall material of medium electron density in the partition wall (arrows), the co-orientation of microtubules (arrowheads) at the intinic surfaces in the generative (g) and vegetative (v) cells, and the gentle arching of microtubules at the regions of attachment of partition wall with intine (i). Double headed arrows indicate the long axes. x 11,950.

Figs. 7.27 and 7.28. High magnification views of the partition wall at the site of its attachment to intine (i) and from the mid region. Note the orientation of the microtubules (arrowheads) at the partition wall in both the vegetative cell (v) and the generative cell (g), predominantly perpendicular to the long axis of pollen, except where they arch from the outer surface of the grain to the partition wall. Freeze-substituted preparation. x 30,000 and 42,290, respectively.

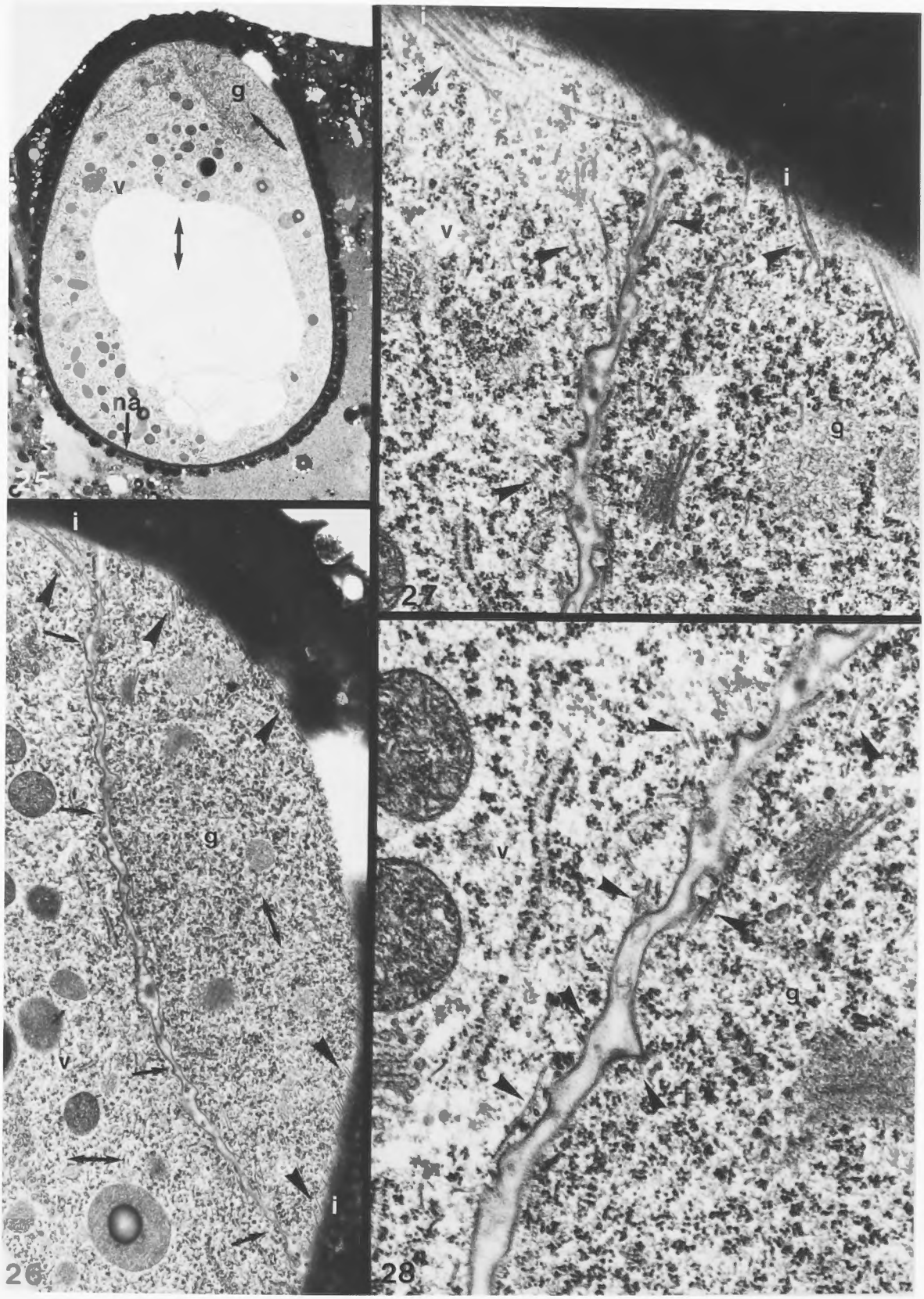
g
v
na
i
v
i
g
27
i
g
v
i
26
v
g
28

Fig. 7.29. A mature generative cell (g) before its detachment from the pollen wall. The partition wall (arrows) appears as sinuous electron-lucent area (p, plastid; double headed arrow, polar axis). Conventional preparation. x 7,330.

Fig. 7.30. The Thiéry reaction imparts electron density in the partition wall (arrows) and intine (arrowheads). Double headed arrow indicates the polar axis (vn, vegetative cell nucleus). x 5,620.

Fig. 7.31. The microtubules (long arrows) at the partition wall (small arrows) in a mature undetached generative cell (g) that occurs at 45^{o} angle to the long axis (double headed arrow) of pollen grain, exist singly or in small groups. They are oriented transverse to the long axis of the generative cell. The microtubules at the partition wall in the vegetative cell (v) can not be seen. Arrowhead shows a plasmodesmata-like channel. This preparation, freeze-substituted in the presence of osmium tetroxide, illustrates an example where the membranes show 'negative' staining. x 48,000.

Fig. 7.32. The orientation of the microtubules (arrows) in the generative cell (g) at the intinic surface (arrowheads) remains perpendicular to the long axis of the pollen (double headed arrow). The figure is from a generative cell that lay in the middle of the pollen grain (e, exine; gw, generative cell wall). Conventional preparation. x 40,000.

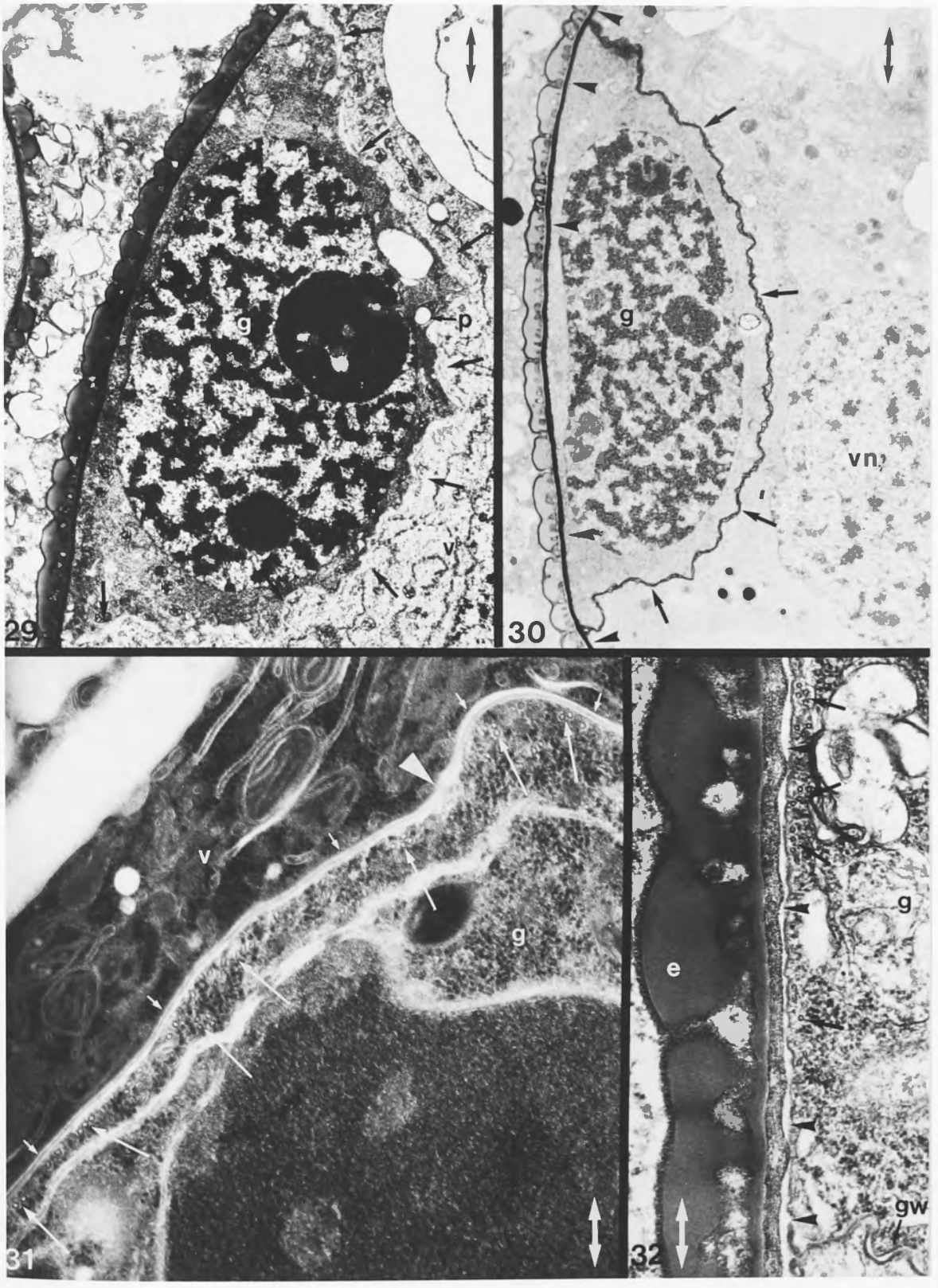
g
p
v
29
g
vn
30
v
g
31
e
g
gw
32

Fig. 7.33. A 1µm thick section of a ZnIO-impregnated pollen grain showing a polar generative cell (with long axis at 90^{o} angle to that of the pollen grain) showing electron-dense endomembranes. Double headed arrow show the polar axis (g, generative cell; vn, vegetative cell nucleus). x 6,000.

Fig. 7.34. Ultra-thin section of ZnIO-impregnated pollen grain showing the (electron-lucent) partition wall. The section was stained with uranyl acetate and lead citrate. The plasmodesmata-like channels (arrowheads) are stretched by distension of the space between the two cells, thus making it impossible to judge whether there is luminal continuity of endoplasmic reticulum from cell to cell (g, generative cell; v, vegetative cell). x 54,000.

Fig. 7.35-7.36. Two different stages of generative cell (g) detachment from the pollen wall. Note the constriction area (arrowheads) and the contorted cell outline. Conventional preparation. x 8,050 and 12,000, respectively.

Fig. 7.37. A higher magnification view of the constriction area (arrowheads) from Fig. 7.36. Conventional preparation. x 18,000.

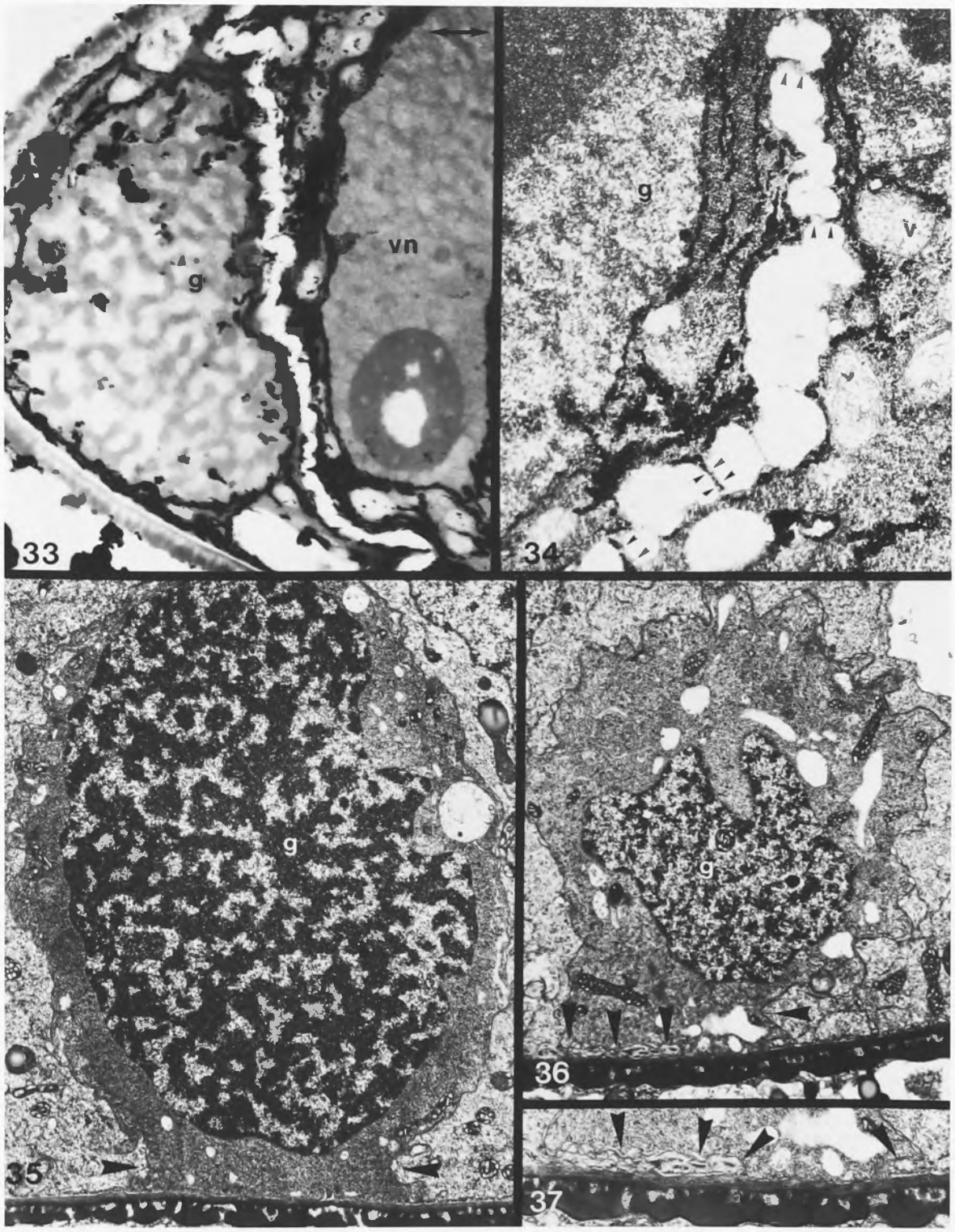
vn
g
33
g
v
34
g
35
g
36
37

Fig. 7.38. A completely detached generative cell (g) processed in conventional manner. The space between the two membranes around the generative cell continues to appear electron-lucent and its outline sinuate. The cell elongation has not commenced yet (v, vegetative cell). x 9,000.

Fig. 7.39. The microtubules (arrows) occupy the surface protrusions of the generative cell (g) shown in Fig. 7.38. Conventional preparation. x 34,900.

Fig. 7.40. A conventionally processed bicelled pollen grain showing the vegetative nucleus (vn) and the elongating generative cell (g; a, apertural wall; na, non-apertural wall). x 2,850.

Fig. 7. 41. A freeze-substituted bicelled pollen grain. This generative cell (g) was formed in the middle region of the pollen grain, as judged from the position of the wall remnants at the intine. Note the presence of a wall around the generative cell (v, vegetative cell).x 3,000.

Fig. 7. 42. A freeze-substituted bicelled pollen grain. The generative cell (g) was formed in a corner at the pole. Arrowheads show the pointed tip (incompletely sectioned here) which eventually grows towards the other pole of the pollen. The electron-lucent space in the wall region at the left hand side of the generative cell is a common problem in freeze-substituted materials (vn, vegetative cell nucleus). x 2,800.

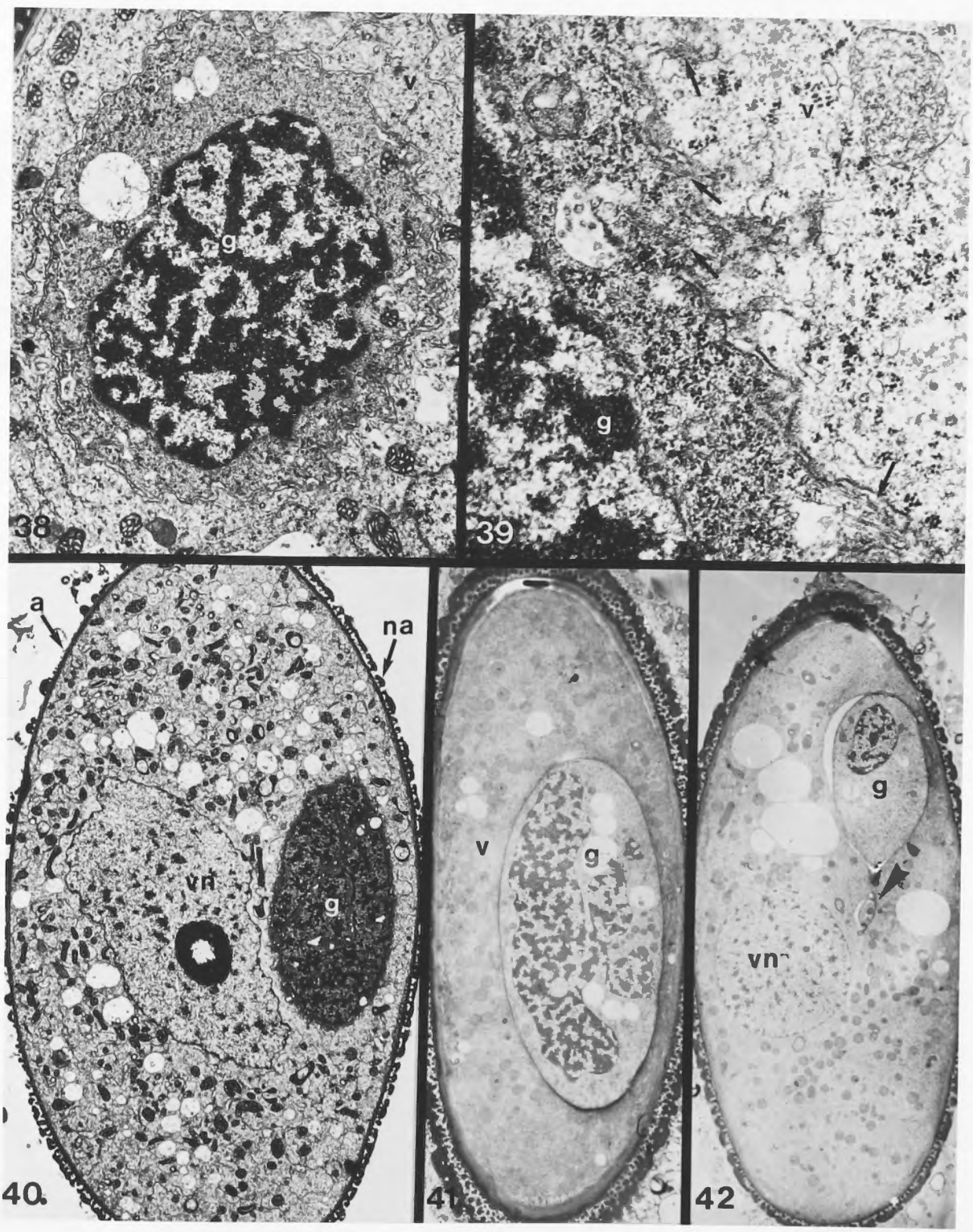
v
g
38
v
g
39
a
na
vn
g
40
v
g
41
g
vn
42

Fig. 7.43. The tip region of a polar generative cell (g) shows microtubules in axial orientations (arrows). The interface is sectioned obliquely, so that the plasma membranes and intervening wall can not be discerned (v, vegetative cell). Freeze-substituted preparation. x 83,300.

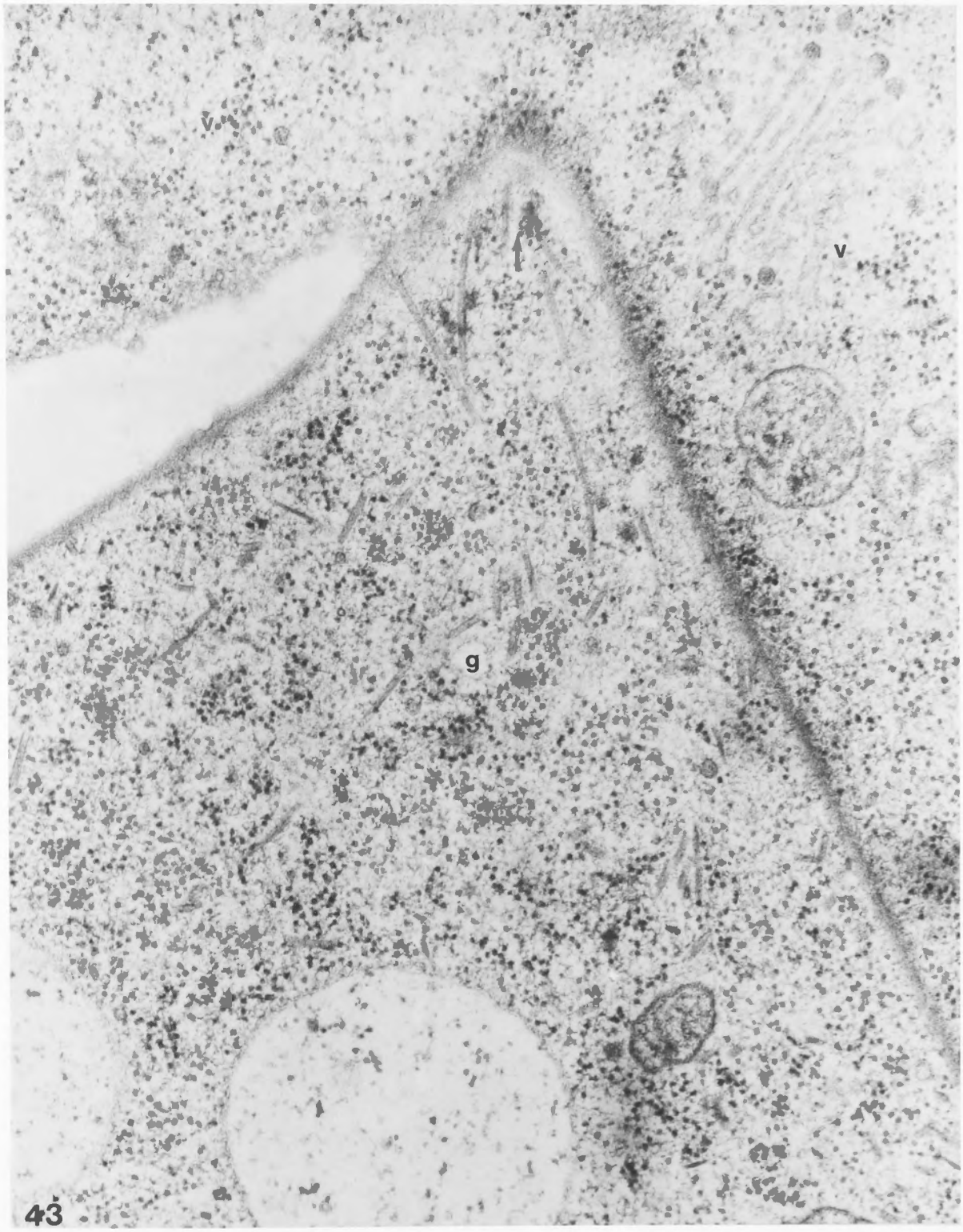

43

Fig. 7.44. Grazing section of a freeze-substituted generative cell (g) from the middle of a pollen grain. The cell represents the early stages of generative cell elongation. Note the orientation of the microtubules predominantly parallel to the long axis of the generative cell. Double headed arrow indicates the polar axis (v, vegetative cell). x 20,000.

Fig. 7.45. High magnification view of the tip region of a detached polar generative cell (g). Note the wall (arrows), side and face views of vesicle-bearing dictyosomes, face view of plasmodesmata (large arrowheads) and the axial orientation of the microtubules. Small arrowheads show a bundle of microfilaments in the vegetative cell (see Chapter 6 for more information on this aspect). freeze-substituted preparation. x 60,000.

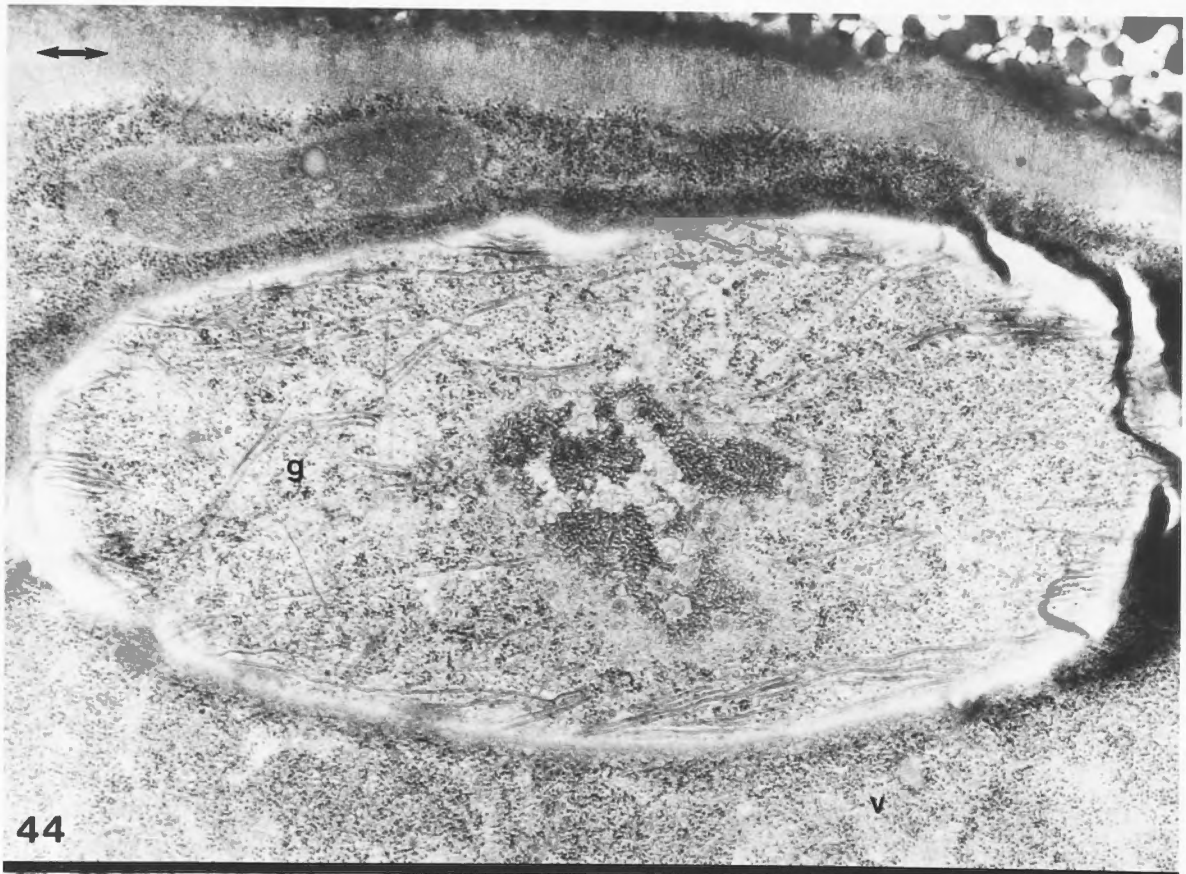

44

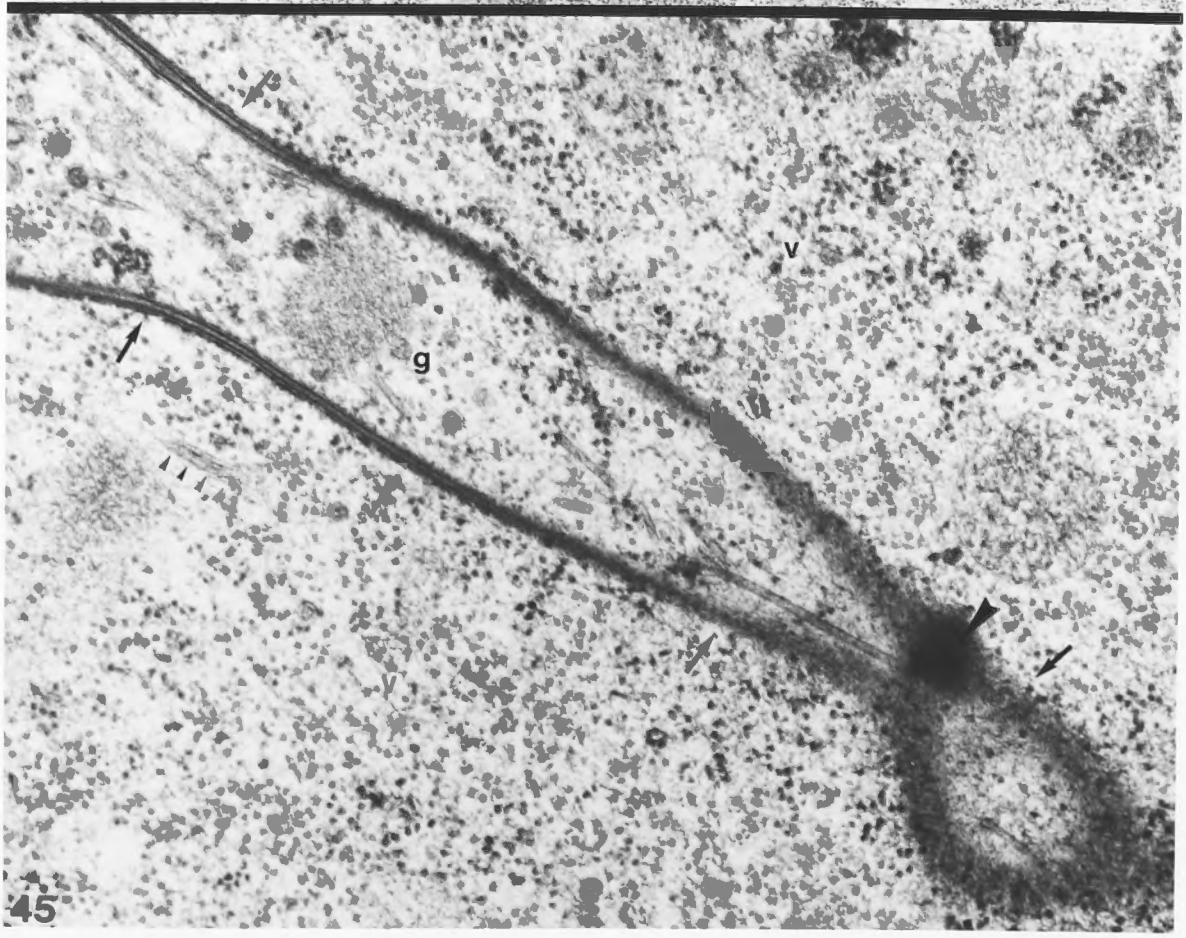

45

Fig. 7.46. Longisection of a conventionally-prepared bicelled pollen grain with elongate generative cell. Arrowheads indicate the boundary of generative cell (g). x 3,800.

Fig. 7.47. Transverse section of a conventionally prepared elongate generative cell (g). Note the folds (arrows) in generative cell outline. x 16,000.

Fig. 7.48. A part of the transverse section of a conventionally prepared elongate generative cell (g) showing microtubular bundles (large arrowheads) and some vesicular inclusions (small arrowheads) in the wall region. Arrows show the folds in generative cell outline (v, vegetative cell). x 50,000.

Fig. 7.49. A part of the longisection of a conventionally prepared elongate generative cell (g) showing microtubular bundles (arrowheads) running parallel to the long axis of generative cell. Note also the folds (arrows) in the wall region (v, vegetative cell). x 45,000.

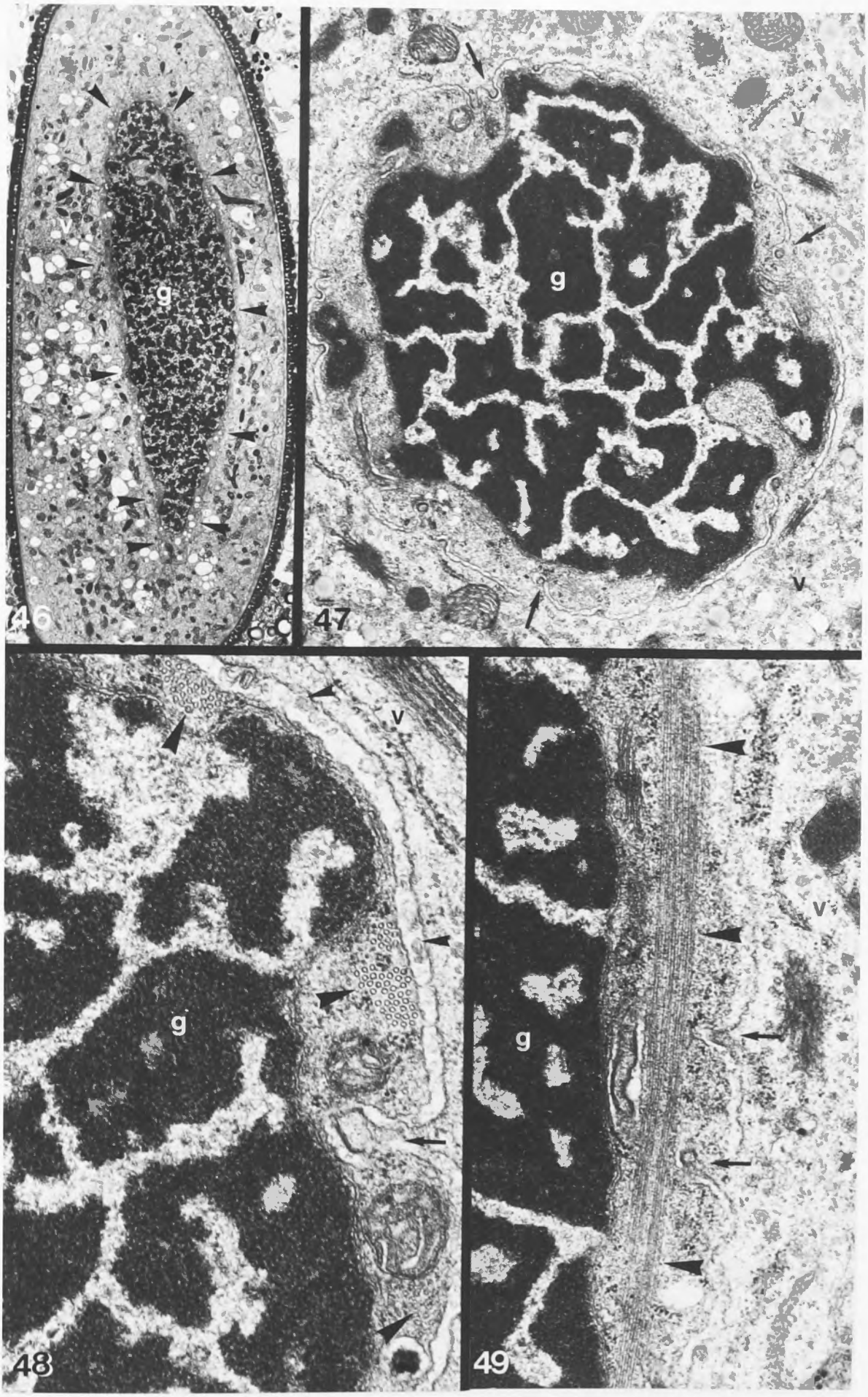
v
g
46
g
v
v
47
g
v
48
v
g
49

Fig. 7.50. Low magnification view of a freeze-etch replica of a mature pollen grain close to the time of dehiscence. By this time the generative cell (g) has become detached and has attained its final elongated shape. The vegetative nucleus is cross-fractured. The surface corrugations can be seen in the top part of generative cell. Such corrugations were not seen in replicas from unfixed pollen grains (photographs not included here). Fixed and cryoprotected. x 6,000.

Fig. 7.51. High magnification view of a freeze-etch replica of a pollen grain at the same stage as in Fig. 7.50. Note the presence of plasmodesmata-like channels (white arrows) and cell surface corrugation (cf. Fig. 7.47). Fixed and cryoprotected. x 40,000.

50

51

CONCLUDING REMARKS

Each chapter in this thesis includes a full discussion, so these "concluding remarks" merely draw together some of the lines of research that need to be followed up, building on the work described in Chapters 3-7.

The main work presented in the thesis is an integrated portrait of tapetum and pollen development from the young anther through to maturity. No comparable account exists in the literature, though obviously there have been very numerous studies of particular stages in selected species. It is clear that even though the information now available on Tradescantia is more detailed than for other species, there are still many gaps in knowledge. Projects that flow on from Chapters 3-7 fall into two categories: those concerned primarily with pollen development, and those of a more general relevance to plant cell biology.

In the first category, the discovery of a novel form of tapetum in Canna suggests a need for surveys to find out if there are other variations, or if the Canna type occurs in other taxa. The survey need not be at random. A logical basis for it is suggested in Chapter 3, where it is pointed out that very elongated anthers may not be capable of synchronising pollen and tapetal development in their locules. Invasive but non-syncytial tapetal cells could be a device that copes

with non-synchrony. It is already known that there are species with long anthers which do not have the Canna type of tapetum, but nevertheless species with elongated anthers (especially those in which a plasmodial tapetum has been recorded) should be high on the list of priorities in survey of the type envisaged.

Plasmodial tapeta offer unusual opportunities for studies of cell surface interactions and the behaviour of cytoskeleton. It would be desirable to perform more detailed investigations in other species to see how consistently the Tradescantia system is found. Already differences are known to exist at least in the timing of cell fusion in species with plasmodial tapetum. Also, physiological or electron microscopic cytochemical studies are needed to evaluate the role of calcium ions which have been generally considered to be a fusogenic agent.

Do variations exist in the constitution of sporopollenin in different species? The data presented in the thesis suggests the existence of an intrinsic 'order' in the constitution of sporopollenin. Colchicine experiments need to be extended to other species, for this may provide clues to the mechanism of formation of species-specific patterning of pollen exines in angiosperms.

The real or artifactual nature of primexine has to be determined in other species, such as Lilium. It would be desirable to study spore wall development in

other species by way of freeze-substitution. Freeze-substitution studies will also be needed to establish the prevalence of temporal and spatial relationships of microfilaments during pollen exine development. In this regard experiments with anti-actin drugs could be most useful.

Colchicine treatments have been used rather extensively in this work. It would be desirable to augment the information thus obtained by using more rapidly-acting and reversible drugs such as oryzalin, APM, IPC, etc. Some such experiments could involve semi-in-vitro approach, if systems could be developed for culture of young microspores in observation chambers.

The second category of project that arises from the thesis chapters is concerned more with plant cell biology in general. The value of freeze-substitution in the preservation of general ultrastructure and cytoskeleton has been pointed out in Chapters 6 and 7. The information obtained here provides a basis for extending freeze-substitution studies to monitor the cytoskeleton of other plant systems. Techniques need to be evolved whereby freeze-substitution could be routinely used for light microscopic immunocytochemistry of the cytoskeleton, as this is likely to provide more complete and reliable information on the behaviour and role of the constituent elements. For instance it would be valuable to combine freeze-substitution with immunogold labelling techniques.

Developing microspores constitute a potentially valuable model system for studying cytoskeletal regulation of wall (intine) deposition. Generally these cells develop in close synchrony thus offering a unique advantage over most other plant systems. Identical populations of discrete cells can be compared by different procedures or treatments. Besides, they develop from an intine-less to a walled (intine) condition, providing the advantages comparable to those presented by regenerating protoplasts for studies of wall development. The pollen grains therefore offer a natural system in which the mechanism of wall development and its regulation by the cytoskeleton can be followed. It is hoped that the microspores and pollen grains would be widely employed in such studies.

BIBLIOGRAPHY

Abadie, M., and M. Hideaux. 1979. L'anthère de Saxifraga cymbalaria L. ssp. huetiana (Boiss.) Engl. et Irmsch. en microscopie électronique (MEB et MET) I. Généralitiés. Ontogenèse des orbicules. Ann. Sci. Nat., Bot., Ser. 13, 1: 199-233.

Angold, R.E. 1968. The formation of the generative cell in the pollen grain of Endymion non-scriptus (L). J. Cell Sci. 3: 573-578.

Artschwager, E. 1947. Pollen degeneration in male sterile sugar beets with special reference to the tapetal plasmodium. J. agric. Res. 75: 191-197.

Atkinson, A.W., Jr., B.E.S. Gunning, and P.C.L. John. 1972. Sporopollenin in the cell wall of Chlorella and other algae: ultrastructure, chemistry, and incorporation of 14C-acetate studied in synchronous cultures. Planta 107: 1-32.

Audran, J.-C. 1981. Pollen and tapetum development in Ceratozamia mexicana (Cycadaceae): sporal origin of the exinic sporopollenin in cycads. Rev. Palaeobot. Palynol. 33: 315-346.

Banerjee, U.C. 1967. Ultrastructure of tapetal membranes of grasses. Grana Palynol. 7: 365-377.

Barak, L.S., and R.R. Yocum. 1981. NBD-phallacidin: synthesis of a fluorescent actin probe. Anal. Biochem. 110: 31-38.

Beer, R. 1905. On the development of the pollen grain and anther of some Onagraceae. Beih. Z. Bot. Centralbl. 19: 286-313.

Beer, R. 1911. Studies in spore development. Ann. Bot. 25: 199-215.

Bhandari, N.N. 1984. The microsporangium. In: Embryology of Angiosperms, Johri, B.M., Ed., pp. 53-121. Berlin: Springer-Verlag.

Blackmore, S., and S.H. Barnes. 1985. Cosmos pollen ontogeny: a scanning electron microscope study. Protoplasma 126: 91-99.

Bopp-Hassenkamp, G. 1960. Elektronenmikroskopische Untersuchungen an Pollenschlauchen zweier Liliaceen. Z. Naturforsch. 15B: 91-94.

Boyles, J. 1983. The use of primary amines to improve glutaraldehyde fixation. In: The Science of

Biological Specimen Preparation for Microscopy and Microanalysis, Revel, J.-P., Barnard, T., Haggis, G.H., Eds., pp. 7-21. AMF O'Hare (Chicago): Scanning Electron Microscopy, Inc.

Bradley, M.O. 1973. Microfilaments and cytoplasmic streaming: inhibition of streaming with cytochalasin. J. Cell Sci. 12: 327-343.

Breathnach, A.S., M. Gross, B. Martin, and C. Stolinski. 1976. A comparison of membrane fracture faces of fixed and unfixed glycerinated tissue. J. Cell Sci. 21: 437-450.

Brewbaker, J.C. 1967. The distribution and phylogenetic significance of binucleate and trinucleate pollen grains in the angiosperms. Am. J. Bot. 54: 1069-1083.

Brighigna, L., A.C. Fiordi, and M.R. Palandri. 1981. Ultrastructural investigations on the two-nucleate pollen grains of Tillandsia caput-medusae Morr. (Bromeliaceae). Am. J. Bot. 68: 1033-1041.

Brooks, J., and G. Shaw. 1978. Sporopollenin: a review of its chemistry, palaeochemistry and geochemistry. Grana 17: 91-97.

Brooks, M.H., J.S. Brooks, and L. Chien. 1966. The anther tapetum in cytoplasmic-genetic male sterile Sorghum. Am. J. Bot. 53: 902-908.

Brumfield, R.T. 1941. Asymmetrical spindle in the first microspore division of certain angiosperms. Am. J. Bot. 28: 713-722.

Buchen, B., and A. Sievers. 1981. Sporogenesis and pollen grain formation. In: Cytomorphogenesis in Plants, Kiermayer, O., Ed., pp. 350-376. Wien: Springer-Verlag.

Burgess, J. 1970a. Microtubules and cell division in the microspore of Dactylorchis fuschii. Protoplasma 69: 253-264.

Burgess, J. 1970b. Cell shape and mitotic spindle formation in the generative cell of Endymion non-scriptus. Planta 95: 72-85.

Carniel, K. 1972. Elektronenmikroskopische Analyse der Pollenentwicklung von Heleocharis palustris. Osterr. Bot. Z. 120: 223-234.

Cass, D.D., and I. Karas. 1975. Development of sperms cells in barley. Can. J. Bot. 53: 1051-1062.

Cerceau-Larrival, M.T., M. Abadie, L. Albertini, J.-C. Audran, A. Cornu, M.T. Cousin, L. Dan Dicko-Zafimahova, G. Duc, I.K. Ferguson, M. Hideaux, S. Nilsson, F. Roland-Heydacker, and A. Souvré. 1980-81. Relations sporophyte-gamétophyte: assise tapétale-pollen. Résultats préliminaires. Ann. Sci., Bot., Paris, 13 (2-3): 69-92.

Chardard, R. 1958. L'ultrastructure des grains de pollen d'Orchidées. Rev. Cytol. Biol. vég. 19: 223-235.

Chauhan, S.V.S., and S.P. Singh. 1966. Pollen abortion in male-sterile hexaploid wheat Norin having Aegilops ovata L. cytoplasm. Crop Sci. 6: 532-535.

Christensen, J. E., H. T. Horner, and N. R. Lersten. 1972. Pollen wall and tapetal orbicular wall development in Sorghum bicolor (Gramineae). Am. J. Bot. 59: 43-58.

Clauhs, R.P., and P. Grun. 1977. Changes in plastid and mitochondrion content during maturation of generative cells of Solanum. Am. J. Bot. 64: 377-383.

Clausen, P. 1927. Ueber das Verhalten des Antheren-Tapetums bei einigen Monokotylen und Ranales. Botan. Archiv 18: 1-27.

Cocucci, A., and W.A. Jensen. 1969. Orchid embryology: Pollen tetrads of Epidendrum scutella in the anther and on the stigma. Planta 84: 215-229.

Condeelis, J.S. 1974. The identification of F-actin in the pollen tube and protoplast of Amaryllis belladonna. Exptl. Cell Res. 88: 435-439.

Cresti, M., F. Ciampolini, and R.N. Kapil. 1984. Generative cell of some angiosperms with particular emphasis on their microtubules. J. Submicrosc. Cytol. 16: 317-326.

Croh, M. 1967. Fine structure of Petunia pollen germinated in vivo. Rev. Palaeobot. Palynol. 3: 197-203.

Davis, G. L. 1966. Systematic Embryology of the Angiosperms. New York: Wiley and Sons.

Deshpande, B. 1976. Observations on the fine structure of plant cell walls. I. Use of permanganate staining. Ann. Bot. 40: 433-437.

Dickinson, H.G. 1970a. Ultrastructural aspects of primexine formation in the microspore tetrad of Lilium longiflorum. Cytobiologie 1: 437-449.

Dickinson, H. G. 1970b. The fine structure of a peritapetal membrane investing the microsporangium of Pinus banksiana. New Phytol. 69: 1065-1068.

Dickinson, H.G. 1973. The role of plastids in the formation of pollen grain coatings. Cytobios 8: 25-40.

Dickinson, H.G. 1976. Common factors in exine deposition. In: The Evolutionary Significance of the Exine, Ferguson, I.K., Muller, J., Eds., pp. 67-89. London: The Linnean Society.

Dickinson, H.G., and L. Andrews. 1977. The role of membrane-bound cytoplasmic inclusions during gametogenesis in Lilium longiflorum. Planta 134: 229-240.

Dickinson, H. G., and P. R. Bell. 1973. The identification of sporopollenin in sections of resin embedded tissue by controlled acetolysis. Stain Technol. 48: 17-22.

Dickinson, H. G., and P. R. Bell. 1976. The changes in the tapetum of Pinus banksiana accompanying formation and maturation of the pollen. Ann. Bot. 40: 1101-1109.

Dickinson, H.G., and J. Heslop-Harrison. 1968. Common mode of deposition for the sporopollenin of sexine and nexine. Nature 220: 927-928.

Dickinson, H.G., and D. Lewis. 1973a. Cytochemical and ultrastructural differences between intraspecific compatible and incompatible pollinations in Raphanus. Proc. R. Soc. Lond. B 183: 21-38.

Dickinson, H.G., and D. Lewis. 1973b. The formation of the tryphine coating of the pollen grains of Raphanus, and its properties relating to the self-incompatibility system. Proc. R. Soc. Lond. B 184: 149-165.

Dickinson, H.G., and U. Potter. 1976. The development of patterning in the alveolar sexine of Cosmos bipinnatus. New Phytol. 76: 543-550.

Dickinson, H.G., and J.M. Sheldon. 1984. A radial system of microtubules extending between the nuclear envelope and the plasma membrane during early male haplophase in flowering plants. Planta 161: 86-90.

Diers, V.L. 1963. Elektronenmikroskopische Beobachtungen an der generativen Zelle von Oenothera hookeri Torr. et Gray. Z. Naturforsch. 18B: 562-566.

Dover, G.A. 1972. The organization and polarity of pollen mother cells of Triticum aestivum. J. Cell Sci. 11: 699-711.

Drahowzal, G. 1936. Beitrage zur morphologie und entwicklungsgeschichte der pollenkörner. Öst. bot. Z. 85: 241-269.

Dubey, D.K., and S.P. Singh. 1965. Mechanism of pollen abortion in three male sterile lines of flax (Linum usitatissimum L.). Crop Sci. 5: 121-124.

Ducker, S.C., J.M. Pettitt, and R.B. Knox. 1978. Biology of australian seagrasses: pollen development and sub-marine pollination in Amphibolis antarctica and Thalassodendron ciliatum (Cymodoceaceae). Aust. J. Bot. 26: 265-285.

Dunbar, A. 1973. Pollen ontogeny in some species of Campanulaceae. A study by electron microscopy. Bot. Notiser 126: 277-315.

Eames, A.J. 1961. Morphology of the Angiosperms. New York: McGraw-Hill.

Echlin, P. 1968. Development of the pollen grain wall. Ber. Dtsch. Bot. Ges. 81: 461-470.

Echlin, P. 1971a. The role of tapetum in microsporogenesis of angiosperms. In: Pollen: Development and Physiology, Heslop-Harrison, J., Ed., pp. 41-62. London: Butterworth.

Echlin, P. 1971b. Production of sporopollenin by the tapetum. In: Sporopollenin, Brooks, J., Grant, J. R., Muir, M., van Gijzel, P., Shaw, G., Eds., pp. 220-247. London: Academic Press.

Echlin, P., and H. Godwin. 1968a. The ultrastructure and ontogeny of pollen in Helleborus foetidus L. I. The development of the tapetum and Ubisch bodies. J. Cell Sci. 3: 161-174.

Echlin, P., and H. Godwin. 1968b. The ultrastructure and ontogeny of pollen in Helleborus foetidus L. II. Pollen grain development through the callose special wall stage. J. Cell Sci. 3: 175-186.

Edwardson, J.R. 1970. Cytoplasmic male-sterility. Bot. Rev. 36: 341-420.

Erdtman, G. 1966. Sporoderm morphology and morphogenesis. A collocation of data and suppositions. Grana Palynol. 16: 318-323.

Feder, N., and R.L. Sidman. 1958. Methods and principles of fixation by freeze-substitution. J. Biophys. Biochem. Cytol. 4: 593-602.

Fernández-Morán, H., and A.O. Dahl. 1952. Electron microscopy of ultrathin frozen sections of pollen grains. Science 116: 465-467.

Fisher, D. B., and T. L. Housley. 1972. The retention of water-soluble compounds during freeze-substitution and microautoradiography. Pl. Physiol. 49: 166-171.

Franke, W.W. 1971. Relationship of nuclear membranes with filaments and microtubules. Protoplasma 73: 263-292.

Franke, W.W., W. Herth, W.J. Van der Woude, and D.J. Morré. 1972. Tubular and filamentous structures in pollen tubes: possible involvement as guide elements in protoplasmic streaming and vectorial migration of secretory vesicles. Planta 105: 317-341.

Frankel, R., S. Izhar, and J. Nitsan. 1969. Timing of callase activity and cytoplasmic male sterility in Petunia. Biochem. Genet. 3: 451-455.

Fujiwara, K., and R. W. Link. 1982. The use of tannic acid in microtubule research. In: Methods in Cell Biology, Vol 24, The Cytoskeleton, Part A, Cytoskeletal Proteins, Isolation and Characterisation, Wilson, L., Ed., pp. 217-233. New York: Academic Press.

Geitler, L. 1935. Beobachtungen Über die erste Teilung im Pollenkorn der Angiospermen. Planta 24: 361-386.

Gicquaud, C., J. Gruda, and Pollender. J.-M. 1980. La phalloidine protège la F-actin contre les effets destructeurs de l'acide osmique et du permanganate. Eur. J. Cell Biol. 20: 234-239.

Gicquaud, C., and A. Loranger. 1981. La phalloïdine protège la F-actine contre les effets destructeurs de l'acide osmique. II. Protection par la phalloïdine de la F-actine traitée aux aldéhydes. Eur. J. Cell Biol. 24: 320-323.

Gimènèz-Martin, G., M.C. Risuèno, and J.F. Lopez-Saèz. 1969. Generative cell envelope in pollen grains as

a secretion system, a postulate. Protoplasma 67: 223-235.

Godwin, H. 1968. The origin of the exine. New Phytol. 67: 667-676.

Godwin, H., P. Echlin, and B. Chapman. 1967. The development of the pollen grain wall in Ipomoea purpurea L (Roth). Rev. Palaeobot. Palynol. 3: 181-195.

Goebel, K. 1887. Outlines of Classification and Special Morphology of Plants. English Translation. Oxford: Clarendon Press.

Goebel, K. 1905. Organography of Plants. Vol. II. Special Organography. English Translation. Oxford: Clarendon Press.

Goebel, K. 1933. Organographie der Pflanzen. III. Samenpflanzen. Jena: Gustav Fischer.

Goldman, R.D., B. Chojnacki, and M.-J. Yerna. 1979. Ultrastructure of microfilament bundles in baby hamster kidney (BHK-21) cells. The use of tannic acid. J. Cell Biol. 80: 759-766.

Gorczynski, T. 1934. Zytologische Analyse einiger Pollenentwicklungsvorgange bei der Apfelsorte "Schöner von Boskoop". Acta Soc. Bot. Pol. 11: 103-118.

Gorska-Brylass, A. 1967. Temporary callose wall in the generative cell of pollen grains. Naturwissenschaften 9: 230-231.

Gorska-Brylass, A. 1970. The 'callose stage' of the generative cells in pollen grains. Grana 10: 21-30.

Green, J.R. 1894. On the germination of the pollen grain and nutrition of the pollen tube. Ann. Bot. 8: 225-228.

Gunning, B.E.S. 1977. Transfer cells and their roles in transport of solutes in plants. Sci. Prog. Oxf. 64: 539-568.

Gunning, B. E. S., and A. R. Hardham. 1982. Microtubules. Ann. Rev. Plant Physiol. 33: 651-698.

Gunning, B.E.S., and S.M. Wick. 1985. Preprophase bands, phragmoplasts and spatial control of cytokinesis. J. Cell Sci. In press.

Gupta, S.C., and K. Nanda. 1972. Occurrence and histochemistry of anther tapetal membrane. Grana Palynol. 12: 99-104.

Gupta, S.C., and K. Nanda. 1983. Development of tapes in the pollen exine of Ipomoea (Convolvulaceae). Grana 22: 141-146.

Hardham, A., and B.E.S. Gunning. 1978. The structure of cortical microtubule arrays in plant cells. J. Cell Biol. 77: 14-34.

Harris, N., and M. J. Chrispeels. 1980. The endoplasmic reticulum of mung bean cotyledons: quantitative morphology of cisternal and tubular ER during seedling growth. Planta 148: 293-303.

Harris, N., K.J. Oparka, and D.J. Walker-Smith. 1982. Plasmatubules: an alternative to transfer cells? Planta 156: 461-465.

Hart, J. W., and D. D. Sabnis. 1976. Colchicine and plant microtubules: a critical evaluation. Curr. Adv. Pl. Sci. 26: 1095-1104.

Harvey, D.M.R. 1982. Freeze-substitution. J. Microsc. 127: 209-221.

Harvey, P.H., C.S. Levings, and E.A. Wernsman. 1972. The role of extrachromosomal inheritance in plant breeding. Adv. Agron. 24: 127.

Heslop-Harrison, J. 1957. The experimental modification of sex expression in flowering plants. Biol. Rev. 32: 38-90.

Heslop-Harrison, J. 1963. An ultrastructural study of pollen wall ontogeny in Silene pendula. Grana Palynol. 4: 7-24.

Heslop-Harrison, J. 1964. Cell walls, cell membranes and protoplasmic connections during meiosis and pollen development. In: Pollen Physiology and Fertilisation, Linskens, H. F., Ed., pp. 39-47. Amsterdam: North Holland Publ.

Heslop-Harrison, J. 1968a. Tapetal origin of pollen coat substances in Lilium. New Phytol. 67: 779-786.

Heslop-Harrison, J. 1968b. Pollen wall development. Science 161: 230-237.

Heslop-Harrison, J. 1968c. Wall development within the microspore tetrad of Lilium longiflorum. Can. J. Bot. 46: 1185-1192.

Heslop-Harrison, J. 1968d. Synchronous pollen mitosis and the formation of the generative cell in massulate orchids. J. Cell Sci. 3: 457-466.

Heslop-Harrison, J. 1969. An acetolysis resistant membrane investing tapetum and sporogenous tissue in the anthers of certain compositeae. Can. J. Bot. 47: 541-542.

Heslop-Harrison, J. 1971a. The pollen wall: structure and development. In: Pollen: Development and Physiology, Heslop-Harrison, J., Ed., pp. 75-98. London: Butterworths.

Heslop-Harrison, J. 1971b. Sporopollenin in a biological context. In: Sporopollenin, Brooks, J., Grant, P. R., Muir, M., van Gijzel, P., Shaw, G., Eds., pp. 1-30. New York, London: Academic Press.

Heslop-Harrison, J. 1971c. Wall pattern formation in angiosperm microsporogenesis. Symp. Soc. exp. Biol. 25: 277-300.

Heslop-Harrison, J. 1972. Sexuality of Angiosperms. In: Plant Physiology, A Treatise, Vol. VIC, Steward, F. C., Ed., pp. 133-289. New York: Academic Press.

Heslop-Harrison, J. 1975. The physiology of the pollen grain surface. Proc. R. Soc. Lond. B 190: 275-299.

Heslop-Harrison, J. 1980. Compartmentation in anther development and pollen wall morphogenesis. In: Cell Compartmentation and Metabolic Channelling, Nover, L., Lynen, F., Mothes, K., Eds., pp. 471-484. Amsterdam: Fischer, Jena and Elsevier/North-Holland Biomedical Press.

Heslop-Harrison, J., and H.G. Dickinson. 1969. Time relationships of sporopollenin synthesis associated with tapetum and microspores in Lilium. Planta 84: 199-214.

Heslop-Harrison, J., and Y. Heslop-Harrison. 1958. Long-day and auxin-induced male sterility in Silene pendula L. Port. Acta biol. 5: 79-94.

Heslop-Harrison, J., Y. Heslop-Harrison, R.B. Knox, and B. Howlett. 1973. Pollen-wall proteins: 'gametophytic' and 'sporophytic' fractions in the pollen walls of Malvaceae. Ann. Bot. 37: 402-412.

Heslop-Harrison, J., R.B. Knox, and Y. Heslop-Harrison. 1974. Pollen-wall proteins: exine-held fractions associated with the incompatibility response in Cruciferae. Theoret. Appl. Genet. 44: 133-137.

Heslop-Harrison, Y., and J. Heslop-Harrison. 1982. The microfibrillar component of the pollen intine: Some structural features. Ann. Bot. 50: 831-842.

Hesse, M. 1978. Entwicklungsgeschichte und Ultrastruktur von Pollenkitt und Exine bei nahe verwandten entomophilen und anemophilen Angiospermensippen: Ranunculaceae, Hamamelidaceae, Platanaceae und Fagaceae. Pl. Syst. Evol. 130: 13-42.

Hesse, M. 1980. Entwicklungsgeschichte und Ultrastruktur von Pollenkitt und Exine bei nahe verwandten entomophilen und anemophilen Angiospermensippen der Alismataceae, Liliaceae, Juncaceae, Cyperaceae, Poaceae und Araceae. Pl. Syst. Evol. 134: 229-267.

Hesse, M. 1981. Pollenkitt and viscin threads: their role in cementing pollen grains. Grana 20: 145-152.

Hobot, J.A., E. Caslemalm, W. Villiger, and E. Kellenberger. 1984. Periplasmic gel: new concept resulting from the reinvestigation of bacterial cell envelope ultrastructure by new methods. J. Bact. 160: 143-152.

Hoefert, L.L. 1969. Ultrastructure of Beta pollen. I. Cytoplasmic constituents. Am. J. Bot. 56: 363-368.

Horner, H.T., Jr. 1977. A comparative light- and electron-microscopic study of microsporogenesis in male-fertile and cytoplasmic male-sterile sunflower (Helianthus annuus). Am. J. Bot. 64: 745-759.

Horner, H.T., Jr., and C. Pearson. 1978. Pollen wall and aperture development in Helianthus annuus (Compositae: Heliantheae). Am. J. Bot. 65: 293-309.

Horner, H.T., Jr., and M.A. Rogers. 1974. A comparative light and electron microscopic study of microsporogenesis in Male-fertile and cytoplasmic male-sterile pepper (Capsicum annuum). Can. J. Bot. 52: 435-441.

Horvat, F. 1966. Contribution a la connaisance de l'ultrasrtucture des parois du pollen de Tradescantia paludosa L. Grana Palynol. 6: 416-434.

Howard, R. J., and J. R. Aist. 1979. Hyphal tip ultrastructure of the fungus Fusarium: improved preservation by freeze-substitution. J. Ultrastruct. Res. 66: 224-234.

Iqbal, S.J., and B.S. Weakley. 1974. The effects of different preparative procedures on the ultrastructure of the hamster ovary. I. Effects of various fixative solutions on ovarian oocytes and their granulosa cells. Histochemistry 38: 95-122.

Ito, S. 1974. Form and function of the glycocalyx on free cell surfaces. Phil. Trans. R. Soc. Lond. B 268: 55-66.

Izhar, S., and R. Frankel. 1971. Mechanism of male sterility in Petunia: The relationship between pH, callase activity in the anthers, and the breakdown of the microsporogenesis. Theoret. Appl. Genet. 41: 104-108.

Jensen, W.A., M.E. Ashton, and L.R. Heckard. 1974. Ultrastructural studies of the pollen of subtribe Castilleiinae, family Scrophulariaceae. Bot. Gaz. 135: 210-218.

Jensen, W.A., D.B. Fisher, and M.E. Ashton. 1968. Cotton embryogenesis: The pollen cytoplasm. Planta 81: 206-228.

Karas, I., and D.D. Cass. 1976. Ultrastructural aspects of sperm cell formation in rye: evidence for cell plate involvement in generative cell divison. Phytomorphology 26: 36-45.

Karnovski, M. J. 1971. Use of ferrocyanide-reduced osmium tetroxide in electron microscopy. Abstract, 11th Ann. Meeting Amer. Soc. Cell Biol. New Orleans, La.

Knoll, K. 1930. Über Pollenkitt und Bestaubungsart. Z. Bot. 23: 609-675.

Knox, R.B. 1971. Pollen-wall proteins: localization, enzymic, and antigenic activity during development in Gladiolus (Iridaceae). J. Cell Sci. 9: 209-237.

Knox, R.B. 1984a. The pollen grain. In: Embryology of Angiosperms, Johri, B.M., Ed., pp. 197-271. Berlin: Springer-Verlag.

Knox, R.B. 1984b. Pollen-pistil interactions. In: Encyclopedia of Plant Physiology, N.S. 17, Cellular Interactions, H.F. Linskens, J. Heslop-Harrison, Eds., pp. 508-608. Heidelberg: Springer-Verlag.

Knox, R.B., and J. Heslop-Harrison. 1969. Cytochemical localization of enzymes in the wall of the pollen grain. Nature 223: 92-94.

Knox, R. B., and J. Heslop-Harrison. 1970. A direct demonstration of the low permeability of the angiosperm meiotic tetrad using a fluorogenic ester. Z. Pflanzenphysiol. 62: 451-459.

Knox, R.B., J. Heslop-Harrison, and C.E. Reed. 1970. Localization of antigens associated with the pollen grain wall by immunofluorescence. Nature 225: 1066-1068.

Kress, J.W., and D.E. Stone. 1982. Nature of the sporoderm in monocotyledons, with special reference to the pollen grains of Canna and Heliconia. Grana 21: 129-148.

LaFountain, J.R., C.R. Zobel, H.R. Thomas, and C. Galbreath. 1977. Fixation and staining of F-actin and microfilaments using tannic acid. J. Ultrastruct. Res. 58: 78-86.

Lancelle, S.A., J.G. Torrey, P.K. Hepler, and D.A. Callaham. 1985. Ultrastructure of freeze-substituted Frankia strain HFPCcl3, the actinomycete isolated from root nodules of Casurina cunninghamiana. Protoplasma 127: 64-72.

Larson, D.A. 1963. Cytoplasmic dimorphism within pollen grains. Nature 200: 911-912.

Larson, D.A., and C.W. Lewis. 1963. Pollen wall development in Parkinsonia aculeata. Grana Palynol. 3: 21-27.

Laser, K.D., and N.R. Lersten. 1972. Anatomy and cytology of microsporogenesis in cytoplasmic male sterile angiosperms. Bot. Rev. 38: 425-454.

Ledbetter, M.C., and K.R. Porter. 1970. Introduction to the Fine Structure of Plant cells. New York: Springer-Verlag.

Lehrer, S.S. 1981. Damage to actin filaments by glutaraldehyde: protection by tropomyosin. J. Cell Biol. 90: 459-466.

Linskens, H.F. 1958. Physiologisce Unterzuchungen zur Reifeteilung. II. Mitteilung. Über die Anderung der Nukleinsaurengehaltes wahrend der Pollenmeiose und Pollenentwicklung von Lilium henryi. Acta bot. neerl. 7: 61-68.

Linskens, H.F. 1964. Pollen physiology. A. Rev. Pl. Physiol. 15: 255-271.

Lombardo, G., and L. Carraro. 1976. Tapetal ultrastructural changes during pollen development. III. Studies on Gentiana acaulis. Caryologia 29: 345-349.

Lombardo, G., and F.M. Gerola. 1968. Ultrastructure of the pollen grain and taxonomy. Giorn. Bot. Ital. 102: 353-380.

Luft, J. H. 1976. The structure and properties of the cell surface coat. Int. Rev. Cytol. 45: 291-382.

Lutz, R.W., and R.D. Sjolund. 1973. Development of the generative cell wall in Monotropa uniflora L. Pl. Physiol. 52: 498-500.

Madjd, A., and F. Roland-Heydacker. 1978. Sécrétions et dégénérescence des cellules du tapis dans l'anthère du Soja hispida Moench, Papilionaceae. Grana 17: 167-174.

Maeda, H., and N. Ishida. 1976. Specificity of binding of hexapyranosyl polysaccharides with fluorescent brightener. J. Biochem. 62: 276-278.

Maheshwari, P. 1949. The male gametophyte of angiosperms. Bot. Rev. 15: 1-75.

Maheshwari, P. 1950. An Introduction to the Embryology of Angiosperms. London: McGraw-Hill.

Marquardt, H., O.M. Barth, and U. Rahden. 1968. Zytophotometrische und elektronmikroskopische Beobachtungen über die Tapetumzellen in den Antheren von Paeonia tenuifolia. Protoplasma 65: 407-421.

Maruyama, K., H. Gay, and B.P. Kaufman. 1965. The nature of the wall between generative and vegetative nuclei in the pollen grain of Tradescantia paludosa. Am. J. Bot. 52: 605-610.

Mattsson, O. 1976. The development of dimorphic pollen in Tripogandra (Commelinaceae). In: The Evolutionary Significance of the Exine, Ferguson, I. K., Muller, J., Eds., pp. 163-183. London: The Linnean Society.

Maul, G.G., H.M. Maul, J.E. Slogma, M.W. Lieberman, G.S. Stein, B.Y.L. Hsu, and T.W. Borun. 1972. Time sequence of nuclear pore formation in phytohemagglutinin-stimulated lymphocytes and in HeLa cells during cell cycle. J. Cell Biol. 60: 192-201.

Maupin-Szamier, P., and T.D. Pollard. 1978. Actin filament destruction by osmium tetroxide. J. Cell Biol. 77: 837-852.

Maupin. P., and T.D. Pollard. 1983. Improved preservation and staining of HeLa cell actin filaments, clathrin-coated membranes, and other cytoplasmic structures by tannic acid-glutaraldehyde-saponin fixation. J. Cell Biol. 96: 51-62.

McConchie, C.A., S. Jobson, and R.B. Knox. 1985. Computer-assisted reconstruction of the male germ unit in pollen of Brassica campestris. Protoplasma 127: 57-63.

McKerracher, L.J., and I.B. Heath. 1985. Microtubules around migrating nuclei in conventionally-fixed and freeze-substituted cells. Protoplasma 125: 162-172.

Mepham, R. H. 1970. Development of the pollen grain wall: further work with Tradescantia bracteata. Protoplasma 71: 39-54.

Mepham, R. H., and G. Lane. 1968. Exine and the role of the tapetum in pollen wall development. Nature 219: 961-962.

Mepham, R. H., and G. Lane. 1969a. Role of the tapetum in the development of Tradescantia pollen. Nature 221: 282-284.

Mepham, R. H., and G. Lane. 1969b. Formation and development of the tapetal periplasmodium in Tradescantia bracteata. Protoplasma 68: 175-192.

Mepham, R.H., and G. Lane. 1970. Observations on the fine structure of developing microspores of Tradescantia bracteata. Protoplasma 70: 1-20.

Mineyuki, Y., and M. Furuya. 1985. Involvement of microtubules in nuclear positioning during apical growth in Adiantum protonemata. Pl. Cell Physiol. 26: 627-634.

Misset, M. T., and J. P. Gourret. 1984. Accumulation of smooth cisternae in the tapetal cells of Ulex europaeus L. (Papilionoideae). J. Cell Sci. 72: 65-74.

Mollenhauer, H. H., and J. D. Morré. 1976. Cytochalasin b, but not colchicine, inhibits migration of secretory vesicles in root tips of maize. Protoplasma 87: 39-48.

Nakamura, S., and H. Miki-Hiroshige. 1985. Fine-structural study on the formation of the generative cell wall and intine-3 layer in a growing pollen grain of Lilium longiflorum. Am. J. Bot. 72: 365-375.

Nakashima, H., and S. Hosokawa. 1974. Histochemical studies in the cytoplasmic male sterility of some crops. III. Distribution of 14-C assimilates in maize. Proc. Crop Sci. Soc. Jpn. 43: 1-7.

Nanda, K., and S.C. Gupta. 1977. Development of tapetal periplasmodium in Rhoea spathacea. Phytomorphology 27: 308-314.

O'Brien, T. P., and M. E. McCully. 1981. The Study of Plant Structure. Principles and Selected Methods. Melbourne: Termarcarphi Pty. Ltd.

Oross, J. W., and Thomson W. W. 1982. The ultrastructure of the salt glands of Cynodon and Distichlis (Poaceae). Amer. J. Bot. 69: 939-949.

Oryol, L.I. 1969. Polarity of microspores and movement of nuclei and of generative cell in Zea mays. Rev. Cytol. Biol. veg. 32: 37-42.

Owens, S. J., and H. G. Dickinson. 1983. Pollen wall development in Gibasis (Commelinaceae). Ann. Bot. 51: 1-15.

Owens, S.J., and A.W. Westmuckett. 1983. The structure and development of the generative cell wall in Gibasis karwinskyana, G. venustula and Tradescantia blossfeldiana (Commelinaceae). In: Pollen: Biology and Implications for Plant Breeding, Mulcahy, D.L., Ottaviano, E., Eds., pp. 149-157. New York: Elsevier Biomedical.

Pacini, E., and B. E. Juniper. 1979. The ultrastructure of pollen grain development in the olive (Olea europaea). 2. Secretion by the tapetal cells. New Phytol. 83: 165-174.

Pacini, E., and B. E. Juniper. 1983. The ultrastructure of the formation and development of the amoeboid tapetum in Arum italicum Miller. Protoplasma 117: 116-129.

Pankov, H. 1957. Über den Pollenkitt bei Galanthus nivalis L. Flora 146: 240-253.

Pease, D.C. 1973. Substitution techniques. In: Advanced Techniques in Biological Electron Microscopy, Koehler, J.K., Ed., pp. 35-66. Berlin: Springer-Verlag.

Pettitt, J. M. 1966. A new interpretation of the structure of the megaspore membrane in some gymnospermous ovules. J. Linn. Soc. (Bot.) 59: 253-263.

Pettitt, J. M., C. A. McConchie, S. C. Ducker, and R. B. Knox. 1984. Reproduction in seagrasses: pollen wall morphogenesis in Amphibolis antarctica and wall structure in filiform grains. Nord. J. Bot. 4: 199-216.

Picton, J. M., and M. W. Steer. 1981. Determination of secretory vesicle production rates by dictyosomes in pollen tubes of Tradescantia using cytochalasin D. J. Cell Sci. 49: 261-272.

Raj, A.Y. 1969. Histological studies in male-sterile and male-fertile Sorghum. Indian J. Genet. Pl. Breed. 28: 335-341.

Reynolds, E.S. 1963. The use of lead citrate at high pH as an electron-opaque stain in electron microscopy. J. Cell Biol. 17: 208-212.

Reznikova, S. A., and H. G. Dickinson. 1982. Ultrastructural aspects of storage lipid metabolism in the tapetum of Lilium hybrida var. enchantment. Planta 155: 400-408.

Rick, C.M. 1945. Genetics and development of nine male-sterile tomato mutants. Hilgardia 18: 599-633.

Risueno, M. C., G. Gimenez-Martin, J. G. Lopez-Saez, and M. I. R. Garcia. 1969. Origin and development of sporopollenin bodies. Protoplasma 67: 361-374.

Rittscher, M., and R. Wiermann. 1983. Occurrence of phenylalanine ammonia-lyase (PAL) in isolated tapetal cells of Tulipa anthers. Protoplasma 118: 219-224.

Robinson, D.G., and H. Quader. 1982. The microtubule-microfibril syndrome. In: The Cytoskeleton in Plant Growth and Development, C.W. Llyod, Ed., pp. 109-126. London: Academic Press.

Rodriguez-Garcia, M.I., and M.C. Risueno. 1978. Ultrastructural aspects of the first post-meiotic mitosis and cytokinesis in the pollen grain of Allium cepa L. 9th Int. Congress on Electron Microscopy, Vol. II, , pp. 428-429.

Roland, F. 1971. Characterization and extraction of the polysaccharides of the intine and the generative

cell wall in the pollen grains of some Ranunculaceae. Grana 11: 101-106.

Roland, J.-C. 1978. General preparation and staining of thin sections. In: Electron Microscopy and Cytochemistry of Plant Cells, Hall, J. L., Ed., pp. 1-63. Amsterdam: Elsevier North-Holland Biomed. Press.

Roland-Heydacker, F. 1979. Aspects ultrastructuraux de l'ontogénie du pollen et du tapis chez Mahonia aquifolium Nutt. Berberidaceae. Pollen et Spores 21: 259-278.

Rowley, J.R. 1959. The fine structure of the pollen wall in Commelinaceae. Grana Palynol. 2: 3-30.

Rowley, J.R., and A. Dunbar. 1967. Sources of membranes for exine formation. Svensk. bot. Tidskr. 61: 49-64.

Rowley, J. R., and J. J. Skvarla. 1974. Plasma membrane-glycocalyx origin of Ubisch body wall. Pollen et Spores 15: 441-448.

Rowley, J. R., and J. J. Skvarla. 1975. The glycocalyx and initiation of exine spinules on microspores of Canna. Amer. J. Bot. 62: 479-485.

Rowley, J.R., and D. Southworth. 1967. Deposition of sporopollenin on lamellae of unit membrane dimensions. Nature 213: 703-704.

Rowley, J.R., K. Muhlethaler, and A. Frey-Wyssling. 1959. A route for the transfer of materials through the pollen grain wall. J. Biophys. Biochem. Cytol. 6: 537-539.

Ryan, K. G. 1984. Membranes in the spindle of iris pollen mother cells during the second division of meiosis. Protoplasma 122: 56-67.

Sanger, J.M., and W.T. Jackson. 1971a. Fine structure study of pollen development in Haemanthus katherinae Baker. I. Formation of vegetative and generative cells. J. Cell Sci. 8: 289-301.

Sanger, J.M., and W.T. Jackson. 1971b. Fine structure study of pollen development in Haemanthus katherinae Baker. II. Microtubules and elongation of the generative cell. J. Cell Sci. 8: 303-315.

Sassen, M.M.A. 1964. Fine structure of Petunia pollen grain and pollen tube. Acta Bot. Neerl. 13: 175-181.

Sax, K., and H.W. Edmonds. 1933. Development of the male gametophyte in Tradescantia. Bot. Gaz. 95: 156-163.

Sax, K., and L. Husted. 1936. Polarity and differentiation in microspore development. Am. J. Bot. 23: 606-609.

Schraudolf, H. 1984. Ultrastructural events during sporogenesis of Anemia phyllitidis (L.) Sw. II. Spore wall formation. Beitr. Biol. Pflanzen 59: 237-260.

Seagull, R.W., and I.B. Heath. 1979. The effects of tannic acid on the in vivo preservation of microfilaments. Eur. J. Cell Biol. 20: 184-188.

Sheldon, J.M., and H.G. Dickinson. 1983. Determination of patterning in the pollen wall of Lilium henryi. J. Cell Sci. 63: 191-208.

Simpson, W.L. 1941. An experimental analysis of the Altmann technique of freezing-drying. Anat. Rec. 80: 173-189.

Sitte, P. 1953. Untersuchungen zur submikroskopischen Morphologies der Pollen und Sporenmembranen. Mikroskopie 8: 290-299.

Skvarla, J.J., and D.A. Larson. 1966. Fine structural studies of Zea mays pollen. I. Cell membranes and exine ontogeny. Am. J. Bot. 53: 1112-1125.

Skvarla, J.J., and J.R. Rowley. 1970. The pollen wall of Canna and its similarity to the germinal aperture of other pollen. Amer. J. Bot. 57: 519-529.

Southworth, D. 1973. Cytochemical reactivity of pollen walls. J. Histochem. Cytochem. 21: 73-80.

Southworth, D. 1974. Solubility of pollen exines. Am. J. Bot. 61: 36-44.

Southworth, D., and D. Branton. 1971. Freeze-etched pollen walls of Artemissia pycnocephala and Lilium humboldtii. J. Cell Sci. 9: 193-207.

Sporne, K. R. 1973. A note on the evolutionary status of tapetal types in dicotyledons. New Phytol. 72: 1173-1174.

Spurr, A.R. 1969. A low-viscosity epoxy resin embedding medium for electron microscopy. J. Ultrastruct. Res. 26: 31-43.

Steer, M. W. 1977. Differentiation of the tapetum in Avena. II. The endoplasmic reticulum and golgi apparatus. J. Cell Sci. 28: 71-86.

Steffen, K. 1953. Zytologische Untersuchungen an Pollenkorn und -slausch. Flora 146: 240.

Steffen, K. 1963. Male gametophyte. In: Recent Advances in the Embryology of Angiosperms, Maheshwari, P., Ed., pp. 15-40. Delhi: Int. Soc. Pl. Morpho.

Stieglits, H., and H. Stern. 1973. Regulation of β-1,3-glucanase activity in developing anthers of Lilium. Dev. Biol. 34: 169-173.

Takeuchi, Y., and A. Komamine. 1978. Composition of the cell wall formed by protoplasts isolated from suspension cultures of Vinca rosea. Planta 140: 227-232.

Thiéry, J.-P. 1967. Mise en evidence des polysaccharides sur coupès fines en microscopie électronique. J. Microscopie 6: 987-1018.

Thomas, D.D.S. 1978. Cytochalasin effects in plants and eurokaryotic microbial systems. In: Frontiers of Biology. Vol. 46. Cytochalasins, Biochemical and Biological Aspects, Tanenbaum, S.W., Ed., pp. 257-275. Amsterdam: North-Holland Publishing Co.

Tischler, G. 1908. Zellstudien an sterilen Bastardpflanzen. Archiv f. Zellforschung 1: 33-151.

Tischler, G. 1915. Periplasmodienbildung in den Antheren der Commelinaceen und Ausblicke auf das Verhalten der Tapetenzellen bei den Ubrigen Monocotylen. Jahrb. f. Wiss. Bot. 55: 52-90.

Tiwari, S. C., S. M. Wick, R. E. Williamson, and B. E. S. Gunning. 1984. Cytoskeleton and the integration of cellular function in cells of higher plants. J. Cell Biol. 99: 63s-69s.

Troll, W. 1928. Über Antherenbau, Pollen und Pollination bei Galanthus. Flora 123: 321-343.

Ubisch, G.W. 1927. Zur Entwicklungsgeschichte der Antheren. Planta 3: 490-495.

Van Der Pijl, L. 1964. Discussion. In Pollen Physiology and Fertilization. Ed. H.F. Linskens. pp. 72. Amsterdam: North-Holland.

Van Lammeren, A.A.M., C.J. Kiejzer, M.T.M. Willemse, and H. Kieft. 1985. Structure and function of the microtubular cytoskeleton during pollen development in Gasteria verrucosa (Mill.) H. Duval. Planta 165: 1-11.

Van Went, J.L. 1974. The ultrastructure of Impatiens pollen. In: Fertilization in Higher Plants, Linskens, H.F., Ed., pp. 81-88. Amsterdam: North-Holland.

Vasil, I.K. 1967. Physiology and cytology of anther development. Biol. Rev. 42: 327-373.

Vasil, I.K. 1973. The new biology of pollen. Naturwissenschaften 60: 247-253.

Vazart, B. 1969. Structure et evolution de la cellule gènèratrice du Lin, Linum usitatissimum L., au cours des premiers stades de la maturation du pollen. Rev. Cytol. Biol. veg. 32: 101-114.

Vithanage, H.I.M.V., and R.B. Knox. 1976. Pollen-wall proteins: quantitative cytochemistry of the origins of intine and exine enzymes in Brassica oleracea. J. Cell Sci. 21: 423-435.

Volkmann, D., and A.W.P. Czaja. 1981. Reversible inhibition of secretion in root cap cells of cress after treatment with cytochalasin B. Support for the membrane flow concept. Exptl. Cell Res. 135: 229-236.

Warmke, H.E., and M.A. Overman. 1972. Cytoplasmic male sterility in Sorghum. I. Callose behaviour in fertile and sterile anthers. J. Heredity 63: 103-108.

Waterkeyn, L. 1968. La paroi speciale callosique et les premiers depots de l'exine chez Ipomoea purpurea (L.) Roth. C. R. Acad. Sci., Paris 267: 56-58.

Wick, S. M., and J. Duniec. 1983. Immunofluorescence microscopy of tubulin and microtubule arrays in plant cells. I. Preprophase band development and concomitant appearance of nuclear envelope-associated tubulin. J. Cell Biol. 97: 235-243.

Wieland, T. 1977. Modification of actins by phallotoxins. Naturwissenschaften 64: 303-309.

Williams, E.G., and J. Heslop-Harrison. 1979. A comparison of RNA synthetic activity in the plasmodial and secretory types of tapetum during the meiotic interval. Phytomorphology 29: 370-381.

Williamson, R.E. 1985. Immobilisation of organelles and actin bundles in the cortical cytoplasm of the alga Chara corallina Klein ex. Wild. Planta 163: 1-8.

Willison, J.H.M., and R. Rajaraman. 1977. 'Large' and 'small' nuclear pore complexes: the influence of glutaraldehyde. J. Microsc. 109: 183-192.

Wodehouse, R.P. 1935. Pollen Grains. New York: McGraw-Hill.

Zavada, M. S. 1983. Pollen wall development of Zamia floridana. Pollen et Spores 25: 287-304.

Zenkteler, M. 1962. Microsporogenesis and tapetal development in normal and male sterile carrots (Daucus carota). Am. J. Bot. 49: 341-348.

Zhu, C., S.Y. Hu, L.Y. Xu, X.R. Li, and J.H. Shen. 1980. Ultrastructure of sperm cell in mature pollen grain of wheat. Sci. Sin. 23: 371-376.